

THE UNIVERSITY
of EDINBURGH

This thesis has been submitted in fulfilment of the requirements for a postgraduate degree (e.g. PhD, MPhil, DClinPsychol) at the University of Edinburgh. Please note the following terms and conditions of use:

This work is protected by copyright and other intellectual property rights, which are retained by the thesis author, unless otherwise stated.
A copy can be downloaded for personal non-commercial research or study, without prior permission or charge.
This thesis cannot be reproduced or quoted extensively from without first obtaining permission in writing from the author.
The content must not be changed in any way or sold commercially in any format or medium without the formal permission of the author.
When referring to this work, full bibliographic details including the author, title, awarding institution and date of the thesis must be given.

Subversion of host cellular processes by the melioidosis pathogen, *Burkholderia pseudomallei*

Charles W. Vander Broek



PhD Genetics and Genomics of Animal Disease Resistance
Roslin Institute
University of Edinburgh
2015

Lay Summary

Burkholderia pseudomallei is a bacterium that causes severe disease in humans. The disease often results in death and is very difficult to treat which is why *Burkholderia pseudomallei* is classified as a bioterrorism agent. The bacteria is able to get inside of your cells where it can multiply and avoid detection by the immune system. To enter and survive inside your cells, *Burkholderia pseudomallei* assembles a complex molecular machine on its surface, which works similarly to a syringe. The syringe injects proteins into your cells, reprogramming them help with the bacteria's life cycle. Using the proteomics technique iTRAQ, we identified two new proteins, called effectors, that the *Burkholderia pseudomallei* syringe injects into your cells. We then used molecular biology techniques to explore which human proteins these new effectors interact with and what these interactions may do to human cells. The reason that this research is important is that it is possible that in the future we can use the identified proteins to design vaccines or design drugs to prevent the reprogramming of your cells, lowering the burden of disease.

Abstract

Burkholderia pseudomallei is an intracellular pathogen and the causative agent of melioidosis, a severe disease of humans and animals. One of the virulence factors critical for early stages of infection is the *Burkholderia* secretion apparatus (Bsa) Type 3 Secretion System (T3SS), a molecular syringe that injects bacterial proteins, called effectors, into eukaryotic cells where they subvert cellular functions to the benefit of the bacteria. Although the Bsa T3SS itself is known to be important for host cell invasion, intracellular replication, and virulence, only a few genuine effector proteins have been identified and the complete repertoire of proteins secreted by the system has not yet been fully characterized.

The aims of this study are twofold. The first is to expand the repertoire of known effector proteins using modern proteomics techniques. The second is to explore the function of a subset of effector proteins to better understand their interaction with host cells.

Isobaric Tags for Relative and Absolute Quantification (iTRAQ), a gel-free quantitative proteomics technique, was used to compare the secreted protein profiles of the Bsa T3SS hyper-secreting mutants of *B. pseudomallei* with the isogenic parent strain as well as a mutant incapable of effector protein secretion. This study provides one of the most comprehensive core secretomes of *B. pseudomallei* described to date and identified 26 putative Bsa-dependent secreted proteins that may be considered candidate effectors. Two of these proteins, BprD and BapA, were validated as novel effector proteins secreted by the Bsa T3SS of *B. pseudomallei*. To determine the possible function of two effector proteins, BipC and BapA, a yeast two-hybrid system was used to identify host cell proteins the effectors interact with. The proteins were screened against a library of human proteins for interactions. BapA interacted with 2 proteins while BipC interacted with 14. Both BapA and BipC were shown to interact with human C1QBP, a mitochondrial protein involved in inflammation, immunity and autophagy.

Finally, the Bsa T3SS protein BipC was characterised in its ability to interact with actin. This study is the first evidence that BipC has the ability to bind to filamentous actin, but not monomeric actin. This binding is direct and no intermediate proteins are required for the interaction. Ectopic expression of BipC in eukaryotic cells caused cytoskeletal rearrangements consistent with an actin-binding protein.

The core secretome represents a substantial resource of targets that will be mined for improved diagnostic assays and vaccines. Diagnostics that will detect early stages of disease to allow for more effective antimicrobial intervention are currently lacking. Furthermore, there is scope to design diagnostic assays with dual use such as to detect both melioidosis and infection of cystic fibrosis patients with the closely related opportunistic pathogen *B. cepacia*. The description of novel T3SS effector proteins is also of considerable value since T3SS proteins are often potent B- and T- cell antigens representing promising components of sub-unit vaccines. Such effector proteins commonly modulate cellular processes such as phagocytosis, inflammasome activation and cell cycle progression, hence the function of the predicted T3SS effectors will provide a series of future research opportunities.

Declarations

I, Charles W. Vander Broek, have read and understood The University of Edinburgh guidelines on plagiarism and declare that the work presented in this thesis is the result of my own original research, except where I indicate otherwise by proper use of quotes and references.

I confirm that:
(a) that the thesis has been composed by the myself, and
(b) either that the work is the my own, or, if the I have been a member of a research group, that I have made a substantial contribution to the work, such contribution being clearly indicated, and
(c) that the work has not been submitted for any other degree or professional qualification except as specified, and
(d) that any included publications are the my own work, except where indicated throughout the thesis and summarised and clearly identified on the declarations page of the thesis.

Signed:_____ Date:_____

Acknowledgements

I received a huge amount of help and support throughout the writing of this thesis as well as during the research it contains from a great many people. I will start by thanking my supervisor, the brilliant and supportive Dr. Jo Stevens. Over the last four years she has patiently offered unwavering guidance to me and anyone else who stepped through her door. I could not have asked for a better mentor. I must also thank my second supervisor, Professor Mark Stevens whose careful input played a critical role in the planning and outcome of this research. Dr. Kevin Chalmers provided was an incredible resource during the planning and writing of the iTRAQ section of this thesis. He also provided Jo and I with some brilliant coffee break stories. Nina, Hamimah, Kate, Seb and Steffi, the many hours spent in the lab were always something I looked forward to thanks to you. I was also lucky enough to share the lab module with Seema, Cosmin, Prerna, Robin and Christina all of whom were wonderfully supportive of me. Of course there were people outside of my work life to whom I owe equal thanks. To my partner Laura, thank you for being so supportive and putting up with my near disappearance during the writing of this thesis. And of course I must thank my wonderful family who have encouraged me and supported me at every turn throughout my life. To those many people whom I owe my gratitude, but I have not mentioned here. You know who you are and many of you are my closest friends and played vital roles in my success. Thank you so much.

Contents

1 Introduction **1**
1.1 Melioidosis 1
1.1.1 Epidemiology 1
1.1.2 Clinical Symptoms and Treatment 2
1.1.3 Related Species of Importance 4
1.1.4 Genomics 7
1.1.5 Pathogenesis 7
1.1.6 Animal Models of Infection 11
1.2 Type 3 Secretion System 12
1.2.1 Structure 12
1.2.2 Energising Secretion 18
1.2.3 Needle Tip and Translocators - Sensing Host Contact . . 19
1.2.4 Regulation of the T3SS 22
1.2.5 T3SS Signals and Chaperones 22
1.3 Bsa T3SS Effector Proteins 25
1.3.1 CHBP/Cif (BPSS1385) - Confirmed Bsa Effector 25
1.3.2 BopB/FolE (BPSS1514) - Hypothetical Bsa Effector . . . 26
1.3.3 BopC (BPSS1516) - Confirmed Bsa Effector 26
1.3.4 BprD (BPSS1521) - Hypothetical Bsa Effector 26
1.3.5 BopA (BPSS1524) - Hypothetical Bsa Effector 27
1.3.6 BopE (BPSS1525) - Confirmed Bsa Effector 28
1.3.7 BapB-C (BPSS1526-7) - Hypothetical Bsa Effectors 29
1.3.8 BapA (BPSS1528) - Hypothetical Bsa Effector 29
1.3.9 Unidentified Effector Proteins 30
1.4 Aims and Objectives 31

2 Materials and Methods **32**
2.1 Bacterial Strains, Plasmids and Culture Media 32
2.2 Molecular Methods 32

2.2.1 PCR and Ligations 32
2.2.2 Electrocompetent Cells and Transformations 33
2.2.3 *B. pseudomallei* Mutagenesis 34
2.2.4 Complementation of the Δ*bsaP* Mutant 36
2.2.5 Cloning of Candidate Effectors to Express c-Myc Epitope Fusion Proteins 36
2.3 General Protein Methods 36
2.3.1 Preparation of Bacterial Supernatants 36
2.3.2 Protein Precipitation 37
2.3.3 SDS-PAGE and Immunoblotting 38
2.3.4 Preparation of Glutathione S-Transferase-Fusion Proteins 39
2.3.5 Pull-Down Assays With Eukaryotic Cell Lysates 41
2.4 iTRAQ Quantitative Proteomics 44
2.4.1 iTRAQ Experimental Design 44
2.4.2 Protein Digestion and Peptide Fractionation 44
2.4.3 Peptide Concentration 44
2.4.4 iTRAQ Labelling 44
2.4.5 SCX Fractionation and Salt Cuts 45
2.4.6 Mass Spectrometry 45
2.4.7 Quantification and Bioinformatic Analysis 46
2.5 *Saccharomyces cerevisiae* Strains 47
2.6 *S. cerevisiae* Molecular Methods 48
2.6.1 *S. cerevisiae* DNA and Protein Extraction 48
2.6.2 *S. cerevisiae* Transformations 48
2.6.3 Cloning of Yeast Two-Hybrid Bait Proteins 49
2.7 Yeast Two-Hybrid 50
2.7.1 Yeast Two-Hybrid Media and Controls 50
2.7.2 Yeast Two-Hybrid Bait–Library Mating 51
2.7.3 Identification of Interacting Library Plasmids 52
2.8 BipC Methods 52
2.8.1 Actin Binding Using GSH-linked Sepharose Beads 52
2.8.2 Pyrene Actin Polymerisation 52
2.8.3 Actin Depolymerisation 54
2.8.4 Actin Sedimentation 55
2.8.5 Transfections and Immunofluorescence 56
2.9 Statistical Analysis 57
2.10 General Software Used in This Study 58

3 Quantitative Proteomic Analysis of Bsa T3SS Effector Proteins Using iTRAQ 59

3.1 Introduction . . . 59
3.2 Results . . . 62
3.2.1 Bioinformatic Prediction of Bsa T3SS Effector Proteins . . 62
3.2.2 Optimisation of Sample Precipitation Methods . . . 62
3.2.3 Chemical Induction of the Bsa T3SS . . . 63
3.2.4 Construction and Characterization of Hyper-secreting *Bsa* Mutants . . . 68
3.2.5 Characterization of the Core *B. pseudomallei* Secretome Under Standard Laboratory Conditions . . . 76
3.2.6 Identification of the Potential Bsa Effector Repertoire . . 80
3.2.7 Validation of iTRAQ Data by Analysis of the Secretion of Epitope-Tagged Candidate Effector Proteins . . . 86
3.3 Discussion . . . 92

4 Identification of Effector Protein Interacting Partners 96

4.1 Introduction . . . 96
4.2 Results . . . 99
4.2.1 Investigation of BipC-Protein Interactions Using Pull-Downs and Mass Spectrometry . . . 99
4.2.2 Generation of Strains and Validation of the Yeast Two-Hybrid System . . . 106
4.2.3 Yeast Two-Hybrid Screen of BipC, BprD and BapA . . . 113
4.2.4 Confirmation of Yeast-Two Hybrid Results . . . 124
4.2.5 Independent Validation of Protein Interactions . . . 128
4.3 Discussion . . . 134

5 Functional Characterisation of the Bsa T3SS Translocon Protein BipC138

5.1 Introduction . . . 138
5.2 Results . . . 142
5.2.1 BipC Directly Binds Actin . . . 142
5.2.2 BipC Polymerises Actin and Co-localises With the Actin Cytoskeleton in HeLa Cells . . . 148
5.2.3 BipC is Secreted Independently of the Bsa T3SS . . . 151
5.3 Discussion . . . 158

6 General Discussion **161**
6.1 Impact of This Study 161
6.2 Future Work 163
6.2.1 iTRAQ Analysis of the Bsa T3SS Secretome 163
6.2.2 Yeast-Two Hybrid Screen of BapA, BipC and BprD . . . 164
6.2.3 Investigation of the Interaction Between BipC and Actin 165
6.2.4 Closing Statement 165

Bibliography **166**

7 Supplemental **I**
7.1 *Galleria mellonella* Infections I
7.2 Y2H Colony PCRs III
7.3 Strains, Plasmids, Primers and Antibodies IV
7.4 Publications XV

List of Figures

1.1 **Transmission and outcome of infection with *B. pseudomallei*.** 3
1.2 **The two chromosomes of *B. pseudomallei* K96243.** 6
1.3 **The intracellular life of *B. pseudomallei*.** 9
1.4 **Overview of T3SSs from animal- and plant-pathogenic bacteria.** 13
1.5 **The 3-D structure of the *Salmonella* T3SS as determined by cryo-EM.** 14
1.6 **The assembly of the T3SS in *Yersinia*.** 16
1.7 **Predicted structure of the *B. pseudomallei* Bsa T3SS.** 17
1.8 **The *B. pseudomallei* K96243 *bsa* T3SS gene locus.** 23

3.1 **Comparison of the Use of Strataclean Beads and TCA for precipitating proteins from *S. flexneri* bacterial supernatants.** . . . 64
3.2 **Comparison of PRMM, TCA and TCA with DOC for precipitating proteins from *S. flexneri* bacterial supernatants.** 65
3.3 **Attempts at chemical induction of the *B. pseudomallei* 10276 Bsa T3SS.** 67
3.4 **Amino acid sequence alignment of *B. pseudomallei* K96243 BsaP with Salmonella InvE and Shigella MxiC 'gatekeeper' proteins.** 69
3.5 **Mutagenesis of the bacterial chromosome by double homologous recombination using the suicide vector pDM4.** 70
3.6 **PCR confirmation of deletion of the *bsaP* gene in *B. pseudomallei* 10276Δ*bsaP* strain.** 72
3.7 ***B. pseudomallei* 10276 Bsa T3SS mutants used in this study.** . . 73
3.8 ***B. pseudomallei* 10276 and mutant strain secreted protein profiles.** 74
3.9 **Western blot analysis of the expression and secretion of BopE and BipD proteins by *B. pseudomallei* 10276 and mutant strains.** 75

3.10 **Work flow for analysis of *B. pseudomallei* secreted proteins by iTRAQ.** . . . 77
3.11 **Western blots of 3 biological replicates before and after pooling for iTRAQ labelling.** . . . 79
3.12 **Density plot constructed with R software (R Core Team, 2015) illustrating the distribution of the median normalised iTRAQ ratios.** . . . 81
3.13 **Venn diagram of the core secretome of *B. pseudomallei*.** . . . 82
3.14 **Proteins with high iTRAQ protein abundance ratios are enriched in hyper-secreting *B. pseudomallei* strains and encoded within the Bsa T3SS locus.** . . . 83
3.15 **Constitutive expression of the effector protein BopE by the plasmid pBHRT causes T3SS-independent secretion of BopE in *B. pseudomallei* 10276.** . . . 88
3.16 **Leaky secretion of constitutively expressed BopE in *B. pseudomallei* 10276 *bsaZ*::pDM4 is not caused by bacterial cell lysis.** 89
3.17 **Western blot analysis of the effect of IPTG on expression and secretion of the known *B. pseudomallei* Bsa T3SS effector protein BopE expressed as c-Myc tagged fusion protein.** . . . 90
3.18 **Western blot analysis of the expression and secretion of putative *B. pseudomallei* Bsa T3SS effector proteins expressed as c-Myc tagged fusion proteins.** . . . 91

4.1 **The yeast two-hybrid system for identifying protein-protein interactions.** . . . 98
4.2 **Pull-downs using A549 cell lysates and GST-fusion proteins bound to GSH-linked sepharose beads visualised by silver staining.** . . . 101
4.3 **Pull-downs using murine splenic lysates and GST-fusion proteins bound to UltraLink Biosupport beads visualised by silver staining.** . . . 102
4.4 **α-actin immunoblot of proteins pulled-down from murine splenic lysates by GST-BipC and GST-BopE.** . . . 103
4.5 **Comparison of the amino acid sequence of BipC expressed by pGBKT7.** . . . 107
4.6 **Comparison of the amino acid sequence of BapA expressed by pGBKT7.** . . . 108

4.7 **Comparison of the amino acid sequence of the C-terminus of BapA expressed by pGBKT7.** 109
4.8 **Comparison of the amino acid sequence of BprD expressed by pGBKT7.** 110
4.9 **Western blot showing expression of BapA, BprD and BipC fusion proteins in *S. cerevisiae* AH109.** 112
4.10 **Auto-activation of *S. cerevisiae* containing pGBKT7-BapA or pGBKT7-BipC.** 114
4.11 **Auto-activation of *S. cerevisiae* containing pGBKT7-BprD.** . . 115
4.12 **Validation of Y2H media stringency.** 116
4.13 **Microscope images of *S. cerevisiae* AH109 zygotes.** 119
4.14 **Positive *S. cerevisiae* colonies resulting from the BapA Y2H screen.** 120
4.15 **Positive *S. cerevisiae* colonies resulting from the BipC Y2H screen.** 121
4.16 **Example of a PCR screen from *S. cerevisiae* colonies containing pGBKT7-BipC after mating**. 122
4.17 **Testing the bait proteins PAWR and C1QBP for auto-activation.** 125
4.18 **Testing BapA interaction with PAWR and C1QBP in a clean *S. cerevisiae* AH109 background.** 126
4.19 **Testing BipC interaction with PAWR and C1QBP in a clean *S. cerevisiae* AH109 background.** 127
4.20 **Coomassie stained gel of BipC-GST and BapA-GST fusion proteins used in pull-down assays.** 129
4.21 **Validation of BipC-C1QBP interaction using protein pull-downs.**130
4.22 **Validation of BipC-PAWR interaction using protein pull-downs.**131
4.23 **Validation of BapA-C1QBP interaction using protein pull-downs.**132
4.24 **Validation of BapA-PAWR interaction using protein pull-downs.**133

5.1 **Entry of host cells by *Salmonella* and *Shigella* via T3SS induced actin rearrangement**. 140
5.2 **Amino acid alignment of BipC (*B. pseudomallei*) with SipC (*Salmonella*) and IpaC (*Shigella*).** 143
5.3 **Pull-down assay using GST-BipC and murine splenic lysates.** 144
5.4 **Direct binding of rhodamine-labelled actin by GST-BipC.** . . 146
5.5 **Testing BipC interaction with Actin in a clean *S. cerevisiae* AH109 background.** 147
5.6 **Co-sedimentation assay of GST-BipC with actin.** 149

5.7 **Investigation of BipC-Actin interaction using protein pull-downs.** 150
5.8 **Polymerisation of pyrene-actin by *B. pseudomallei* GST-BipC.** 152
5.9 **F-actin depolymerisation in the presence of GST-BipC.** 153
5.10 **Confocal microscope images of HeLa cells eptopically expressing Myc tagged BipC.** 154
5.11 **Western blot analysis of the *B. pseudomallei* Bsa T3SS effector/translocator protein BipC expressed as a c-Myc tagged fusion protein.** 156
5.12 **Western blot of BipC secretion using EPEC as a surrogate host.** 157

7.1 **Infection of *Galleria mellonella* larvae using *B. pseudomallei* and *bsa* T3SS mutants.** II
7.2 **Colony PCR screen of *S. cerevisiae* containing pGBKT7-BipC after mating (gels 1-5).** III

List of Tables

2.1 **Pyrene actin polymerisation assay control reactions used to set gain.** 53
2.2 **Pyrene actin polymerisation assay example.** 54
2.3 **Pyrene actin depolymerisation assay example.** 55
2.4 **Actin sedimentation assay reactions.** 56

3.1 **Candidate Bsa T3SS effector proteins identified by iTRAQ.** . . 85

4.1 **Proteins identified as possible BipC-interacting partners using pull-downs and mass spectrometry analysis.** 105
4.2 **Human proteins identified as interacting parters for BapA and BipC by Y2H screening.** 123

7.1 **Strains and plasmids used in this study.** IV
7.2 **Primers used in this study.** X
7.3 **Antibodies used in this study.** XIV

Chapter 1

Introduction

1.1 Melioidosis

1.1.1 Epidemiology

Originally described in drug addicts in Rangoon in the early 20th century by Alfred Whitmore (Whitmore, 1913), *Burkholderia pseudomallei*, formerly *Pseudomonas pseudomallei* (Yabuuchi *et al.*, 1992), is a facultative intracellular pathogen (Pruksachartvuthi *et al.*, 1990) that is the causative agent of melioidosis, or Whitmore's disease. It is a rod shaped bacterium that is motile, oxidase-positive and Gram-negative, but with a staining pattern that resembles a safety pin in appearance (Dance *et al.*, 1989). Melioidosis is not host specific, causing disease in humans, a wide range of other mammals, as well as birds and reptiles (Reviewed in (Titball *et al.*, 2008)). Despite the fact that *B. pseudomallei* is an important human pathogen, it is considered a saprophyte and is found in the soil and water in Northern Australia and Southeast Asia (Brook *et al.*, 1997, Draper *et al.*, 2010). Clinical cases of melioidosis have also been reported in Northeastern Brazil, on the Indian sub-continent, Africa, China, the Caribbean and Mexico (Rolim *et al.*, 2005, Vidyalakshmi *et al.*, 2007), (Reviewed in Currie *et al.* (2008), Birnie *et al.* (2015)).

Infection with *B. pseudomallei* is usually associated with environmental exposure and can occur through breaks in the skin, inhalation or ingestion (Reviewed in (Cheng and Currie, 2005)). Up to 85% of cases of *B. pseudomallei* infection in Thailand occur during the rainy season (Currie and Jacups, 2003). Infection with the bacteria has been linked to extreme weather events such as cyclones, and due to an increase in *B. pseudomallei*-related pneumonia after such events, it is thought that this may be caused by bacteria being aerosolized

from surface water and soil and then inhaled (Currie and Jacups, 2003). It is also thought that melioidosis can be caused by ingestion. In a mouse model of infection the bacteria is able to colonize the stomach after oral inoculation (Goodyear *et al.*, 2012). *B. pseudomallei* is the leading cause of community-acquired bacteraemia in Thailand with an incidence of melioidosis reported to be 12.7 cases per 100,000 people (Limmathurotsakul *et al.*, 2010). In Northern Australia, *B. pseudomallei* causes 32% of septicaemia-related pneumonia, more than any other community-acquired bacterial infection (Douglas *et al.*, 2004).

1.1.2 Clinical Symptoms and Treatment

In the majority of cases, the incubation period for melioidosis is between 1 and 21 days (Ngauy *et al.*, 2005). About 50% of melioidosis cases affect people with diabetes and other important risk factors include lung disease, cystic fibrosis and excessive alcohol consumption (Currie *et al.*, 2010). There are varied clinical presentations of *B. pseudomallei* infection ranging from skin infections to pneumonia and septic shock (Figure 1.1) (Currie *et al.*, 2010). In one study of melioidosis in Northern Australia, the most common presentations were pneumonia, genitourinary tract infection and skin infection (Currie *et al.*, 2010). In the same study of 540 cases of melioidosis, 298 of the patients developed bacteraemia of which 58 died (Currie *et al.*, 2010). Even with modern medical care the mortality of patients diagnosed with melioidosis remains high with a mortality rate of over 40% in Northeast Thailand and 14% in Northern Australia (Currie *et al.*, 2010, Limmathurotsakul *et al.*, 2010).

One interesting aspect of melioidosis infection is its ability to reactivate after remaining latent for years following a primary infection. The longest reported period between infection and reactivation occurred in a World War II veteran who manifested symptoms 62 years after exposure (Ngauy *et al.*, 2005). Patients who survive an initial infection with *B. pseudomallei* have a 13% chance of recurrence over the following 10 years (Maharjan *et al.*, 2005). Of recurrent cases, 75% are caused by the same strain indicating a relapse (Maharjan *et al.*, 2005). In one patient with chronic asymptomatic melioidosis, the genome of the single infecting strain of *B. pseudomallei* was sequenced twelve years apart (Price *et al.*, 2013). The sequencing indicated that over the twelve year period the *B. pseudomallei* strain underwent host adaptation resulting in the loss of over 221 genes, including genes involved in lipopolysaccharide biosynthesis (Price *et al.*, 2013). It is not uncommon for melioidosis patients to be infected

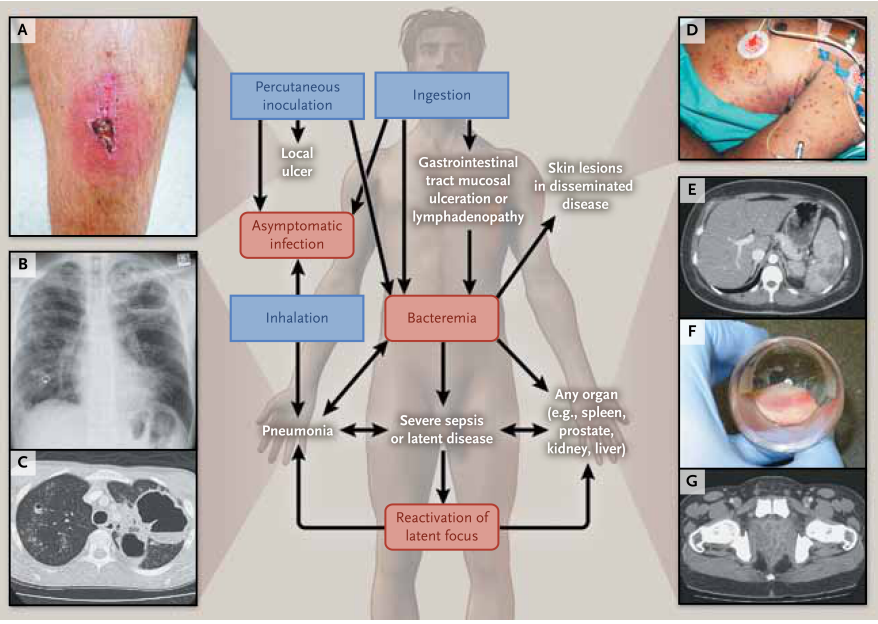


Figure 1.1: Transmission and outcome of infection with *B. pseudomallei*. The routes of infection for *B. pseudomallei* are through cuts or breaks in the skin, inhalation or ingestion (indicated by the blue boxes). Clinical presentations of melioidosis are varied and range from mild skin infections, genito-urinary infections, organ abscesses and pneumonia. Figure taken from Wiersinga *et al.* (2012).

by more than one strain of *B. pseudomallei* concurrently with 5 out of 18 patients having 2 or more strains upon hospitalization (Pitt *et al.*, 2007).

Isolation of *B. pseudomallei* from patients by culture is still the primary method of diagnosis which is usually carried out using Ashdown's selective agar (Peacock, 2006). Because bacterial culture methods with *B. pseudomallei* may not be available in all locations, it is likely that the incidence of melioidosis may be under-reported (Limmathurotsakul *et al.*, 2010).

Treatment of melioidosis often requires supportive therapy as well as administration of antibiotics as there is currently no approved vaccine for melioidosis (Reviewed in Cheng and Currie (2005)). *B. pseudomallei* is highly resistant to many antibiotics including cephalosporins, penicillins, rifamycins, aminoglycosides, quinolones and macrolides making it very difficult to treat (Reviewed in Cheng and Currie (2005)). Recommended antibiotic treatment includes ceftazidime, imipenem or meropenem with co-trimoxazole (Reviewed in Cheng and Currie (2005)). Because of the high mortality rate, the resistance to a large number of antibiotics, the ability to be cultured easily as well as disseminated as an aerosol and spread into the environment, *B. pseudomallei* has been classified as a schedule 5 organism in the UK and as a class B bioterrorism agent by the US Centres for Disease Control and Prevention (Reviewed in Cheng and Currie (2005), (Rotz *et al.*, 2002)).

1.1.3 Related Species of Importance

The genus *Burkholderia*, originally defined by Yabuuchi *et al.* (1992), now contains over 40 species of bacteria including the human pathogens *B. pseudomallei*, *Burkholderia mallei* and the *Burkholderia cepacia* complex of species (Reviewed in (Compant *et al.*, 2008)). Members of the genus *Burkholderia* are found in a range of environments from soil and water to animals and humans, and species are used for their ability to assist with bioremediation and plant growth promotion (Reviewed in (Coenye and Vandamme, 2003) and Compant *et al.* (2008)). *Burkholderia* are primarily pathogens of plants, but some species are animal and human pathogens, with two clinically relevant species being *B. pseudomallei* and *B. mallei* (Reviewed in (Compant *et al.*, 2008)). In addition, the *B. cepacia* complex is known for causing severe opportunistic infections in cystic fibrosis patients (Reviewed in (Drevinek and Mahenthiralingam, 2010)).

B. mallei, the causative agent of glanders, is an obligate pathogen unable to survive outside its host with restricted host range (Yabuuchi *et al.*, 1992, Srinivasan *et al.*, 2001). Glanders is an infection of equids which can also be trans-

mitted to humans (Srinivasan *et al.*, 2001). Symptoms of glanders in equids include nasal discharge, enlargement of lymph nodes and the presence of nodules and ulcers on the extremities, as well as fever and emaciation (Srinivasan *et al.*, 2001, Khan *et al.*, 2013). Glanders was a major disease in horses in the past, but has been largely eradicated in the West, though there are signs it may be re-emerging (Srinivasan *et al.*, 2001, Khan *et al.*, 2013). In humans, *B. mallei* causes a disease similar to melioidosis and because of its similarities to *B. pseudomallei*, *B. mallei* is also listed as a schedule 5 organism in the UK and a class B bioterrorism agent by the US CDC (Van Zandt *et al.*, 2013, Rotz *et al.*, 2002).

Burkholderia thailandensis is a bacterium that is considered non-pathogenic to humans and has been used as an alternative model system for *B. pseudomallei* and *B. mallei* in some studies as it contains many homologues of virulence factors from these pathogenic species (Brett *et al.*, 1998, Haraga *et al.*, 2008, Moore *et al.*, 2004, Yu *et al.*, 2006). *B. thailandensis* was originally differentiated from *B. pseudomallei* in soil samples by its ability to assimilate L-arabinose, a function which *B. pseudomallei* lacks (Wuthiekanun *et al.*, 1996). It was shown that clinical samples from melioidosis patients never contained bacteria with the ability to assimilate L-arabinose (*B. thailandensis*) (Wuthiekanun *et al.*, 1996). However, there has been a reported case of non-fatal *B. thailandensis* infection in Thailand in a 16-year-old man that sustained injury causing heavy inoculation of the bacteria as the result of a motorcycle accident (Lertpatanasuwan *et al.*, 1999). Another reported case of non-fatal *B. thailandensis* infection was in a 2 year old male in the United States after a car accident left the child submerged under water for 2 minutes allowing bacteria to enter his lungs (Glass *et al.*, 2006a). Importantly, while it has been shown that *B. thailandensis* can be used as a model system to study the virulence associated T3SS of *B. pseudomallei*, because *B. thailandensis* is less pathogenic to humans, study of the Bsa T3SS in the native organism is still warranted (Haraga *et al.*, 2008).

Other similar species include *Burkholderia humptydooensis* which is also able to assimilate L-arabinose and is found in the waters of Northeastern Australia (Gee *et al.*, 2008, 2014) and *Burkholderia oklahomensis*, which is a pathogenic *B. pseudomallei*-like strain found in soil in the United States. It was initially isolated from a leg wound of a farmer in Oklahoma and also having caused disease in an automobile accident victim in Georgia (Glass *et al.*, 2006b, McCormick *et al.*, 1977, Nussbaum *et al.*, 1980).

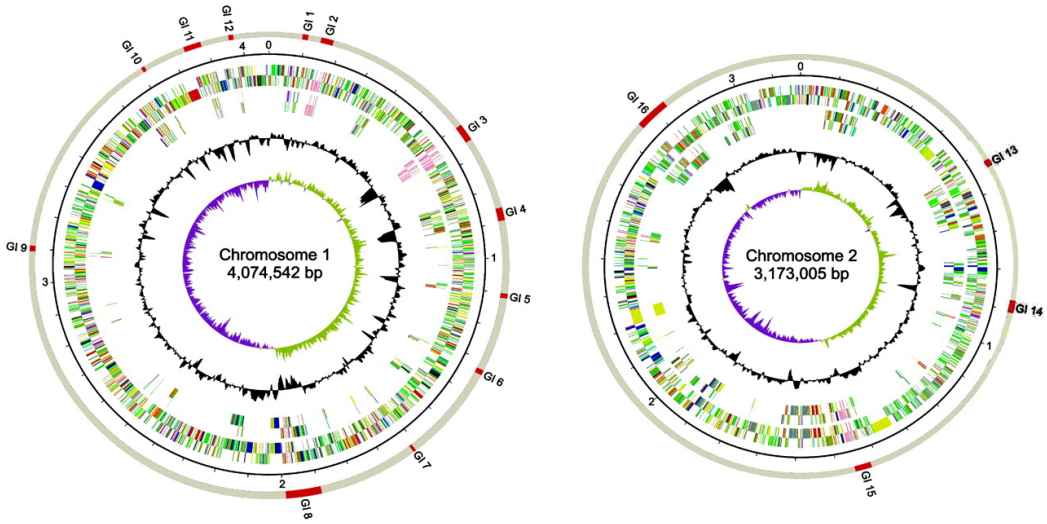


Figure 1.2: The two chromosomes of *B. pseudomallei* K96243. Chromosome 1 is comprised of 4.07 Mb and contains many housekeeping genes while chromosome 2 is comprised of 3.17 Mb and contains genes that are associated with adaptation to changing environments. The genome contains 16 genomic islands that are thought to be the product of horizontal gene transfer. The outside ring depicts the locations of the 16 genomic islands in red. The second ring in shows a scale bar in Mb. The 3rd ring shows annotated coding sequences colour coded as follows: dark blue, pathogenicity/adaptation; black, energy metabolism; red, information transfer; dark green, surface-associated; cyan, degradation of large molecules; magenta, degradation of small molecules; yellow, central/intermediary metabolism; pale green, unknown; pale blue, regulators; orange, conserved hypothetical; brown, pseudogenes; pink, phage plus IS elements; gray, miscellaneous. The 4th, 5th and 6th rings depict: additional coding sequences compared to the sequenced *B. mallei* strain ATCC 2944; the percentage of G + C content plot; (G–C)/(G + C) deviation plot (>0%, olive; <0%, purple). Figure taken from Holden *et al.* (2004).

1.1.4 Genomics

The genome of the *B. pseudomallei* reference strain K96243 is large for a bacterium (7.2 Mb) and consists of two circular chromosomes (Figure 1.2) (Holden *et al.*, 2004). Chromosome one (4.07 Mb) encodes mostly housekeeping genes, while chromosome two (3.17 Mb) encodes largely genes that are expressed in response to different environments the bacteria may encounter, including many of the known virulence factors (Holden *et al.*, 2004). Full genome comparisons of almost 100 strains of *B. pseudomallei* identified 86% of genes as being conserved and present in all strains (Sim *et al.*, 2008). The other 14% of genes were considered accessory genes, and disproportionally represented genes present in strain K96243 genomic islands (GIs) (14 of 16 GIs were represented by accessory genes) and were associated with clinical isolates (Sim *et al.*, 2008). The GIs in *B. pseudomallei* are highly variable between strains. A study of five clinical *B. pseudomallei* strains identified a total of 71 GIs distributed between the strains, with at least half being unique to the strain in which they were identified (Tuanyok *et al.*, 2008). The variability in these regions is largely due to horizontal gene transfer and *B. pseudomallei* has one of the highest rates of lateral gene transfer as compared to the mutation rates of any other bacterial species measured (Pearson *et al.*, 2009). Interestingly, large differences in the genomes of *B. pseudomallei* can be correlated with the geographic distribution of the strains in the endemic regions of Northern Australia and Northeast Thailand (Vesaratchavest *et al.*, 2006).

1.1.5 Pathogenesis

B. pseudomallei has many factors associated with its ability to cause disease including the production of surface polysaccharides, quorum sensing, flagella, pili, intracellular motility (BimA), as well as Type 2, 3 and 6 secretion systems (Reviewed in Galyov *et al.* (2010)).

B. pseudomallei produces four types of surface polysaccharides identified as types I-IV O-PS. Type I O-PS produces an –3)–2-O-acetyl–6-deoxy-β-D-*manno*-heptopyranose-(1- capsule that is similar to that of *Neisseria meningitides* and *Haemophilus influenza* (Reckseidler *et al.*, 2001). The capsule has been shown to provide resistance to complement (Reckseidler-Zenteno *et al.*, 2005). It was shown that the LD50 for a capsular mutant was over 1000 fold higher than that of wild type *B. pseudomallei* in an animal model of infection (Reckseidler *et al.*, 2001). Type II O-PS forms the *B. pseudomallei* lipopolysaccharide which

is required for full virulence in hamster, guinea pig and rat models of melioidosis (DeShazer *et al.*, 1998). The importance of type I and II O-PS in virulence is further demonstrated by the ability of antibodies to the two types of O-PS to provide passive protection to mice infected intraperitoneally with 10^4 CFU of *B. pseudomallei* (Jones *et al.*, 2002). Type III and IV O-PS are less well characterised, but of the two only type IV O-PS is required for full virulence in a murine model of melioidosis (Sarkar-Tyson *et al.*, 2007).

The intracellular life of *B. pseudomallei* is shown in Figure 1.3. *B. pseudomallei* is a facultative intracellular pathogen capable of survival in both phagocytic and non-phagocytic cell lines (Jones *et al.*, 1996). Internalization of *B. pseudomallei* can be inhibited by cytochalasin D, which is an actin polymerization inhibitor (Jones *et al.*, 1996). This indicates the importance of actin cytoskeletal rearrangement in uptake of *B. pseudomallei*. Once in the cytosol a bacterium needs to be able to survive the antimicrobial peptides produced by the host cell. *B. pseudomallei* was shown to be resistant to antimicrobial peptides, showing a statistically significant increase in growth rate when exposed to one antimicrobial peptide, the defensin human neutrophil peptide 1 (HNP–1), which is commonly found in the granules of neutrophils (Jones *et al.*, 1996). *B. pseudomallei* also appears to interfere with host cell synthesis of inducible nitric-oxide synthase preventing the production of reactive nitrogen species, which likely helps the bacteria to survive the intracellular environment of the macrophage (Utaisincharoen *et al.*, 2006).

The mechanisms by which *B. pseudomallei* escape the host cell are still unclear, but it has been suggested it may be related to intracellular motility and the fusion of host cells into multinucleated giant cells (MNGC) (Kespichayawattana *et al.*, 2000). *B. pseudomallei* has been shown to induce MNGC formation when internalized in macrophages as well as in non-phagocytic cell lines (Kespichayawattana *et al.*, 2000). MNGCs are formed by the fusion of macrophages or monocytes and have been associated with infections by pathogens such as *Mycobacterium tuberculosis* and HIV (Brodbeck and Anderson, 2009). Intracellular motility is required for the formation of MNGCs by *B. pseudomallei* (French *et al.*, 2011). *B. pseudomallei* has the ability to polymerize host cell actin at one pole to create actin-based motility through a mechanism involving the bacterial protein BimA (Stevens *et al.*, 2005). Other intracellular bacteria including *Shigella flexneri* and *Listeria monocytogenes* are known to polymerize actin at one pole in order to spread directly from cell to cell, but these bacteria do not induce MNGC formation (Kespichayawattana *et al.*,

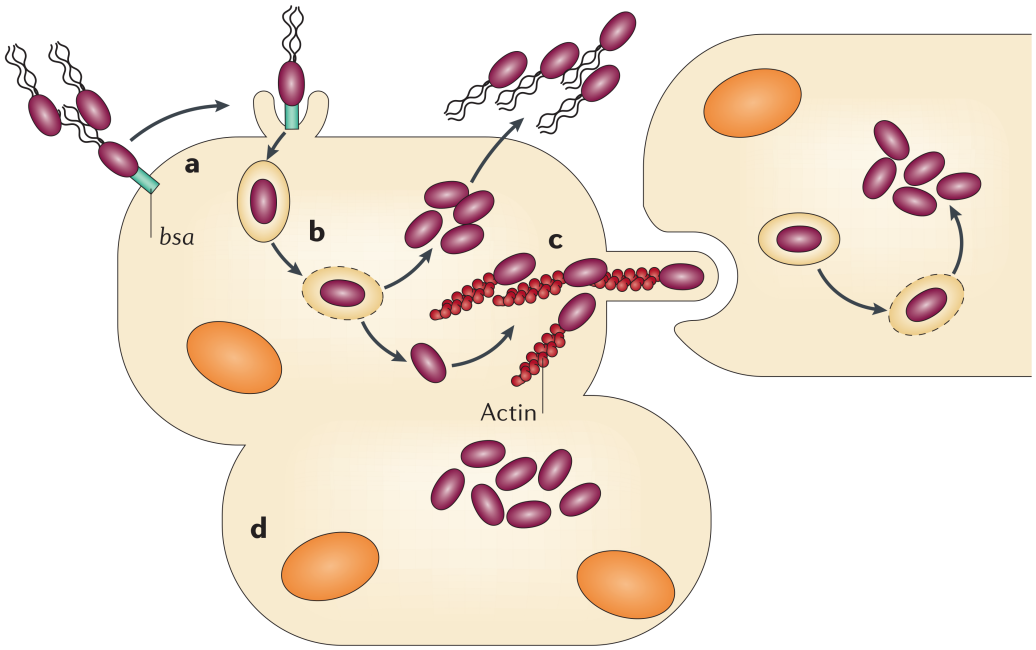


Figure 1.3: The intracellular life of *B. pseudomallei*. Upon contact with a host cell, *B. pseudomallei* become internalized (a), escape the endocytic vacuole (b), polymerize actin at one pole creating actin-based motility (c) and cause membrane fusion forming multinucleated giant cells (MNGC). Figure taken from Wiersinga *et al.* (2006).

2000). Another bacterial factor involved in MNGC formation is LfpA, which drives infected RAW 264.7 cells towards an osteoclast-like phenotype (Boddey *et al.*, 2007). MNGCs are important *in vivo*, and are not just an *in vitro* experimental artefact, because they can be found in the tissues of infected humans and animals (Wong *et al.*, 1995). It is speculated that the fusion of host cells in this way may be a mechanism for cell-to-cell spreading while evading the host immune system (Kespichayawattana *et al.*, 2000).

Secretion systems play a role in almost all steps of the *B. pseudomallei* infection cycle and allow the transport of bacterial proteins across the inner and outer bacterial membranes. The Type 2 secretion system (T2SS) allows transport of proteins into the surrounding environment, while the Type 3 (T3SS) and Type 6 secretion systems (T6SS) inject proteins directly into the cytoplasm target host cells (Reviewed in Costa *et al.* (2015)). The *B. pseudomallei* T2SS is responsible for the secretion of 48 proteins including 12 proteases and the deubiquitinase TssM (Burtnick *et al.*, 2014). TssM inhibits the activation of NF-κB and TssM mutants are attenuated in a murine model of inhalation melioidosis (Tan *et al.*, 2010). Yet T2SS mutants display no attenuation of virulence in mice inoculated intraperitoneally indicating further work is needed for a full understanding of the importance of the T2SS in *B. pseudomallei* (Burtnick *et al.*, 2014).

The ability of *B. pseudomallei* to invade cells has also been linked to the *Burkholderia* Secretion Apparatus (Bsa) Type 3 Secretion System (T3SS) (Stevens *et al.*, 2003). The Bsa T3SS is also required for efficient escape of the bacterium from the endocytic vesicle following uptake (Stevens *et al.*, 2002). The Bsa T3SS is similar to that of the Inv/Mxi-Spa T3SS found in *Salmonella* Spp. and *S. flexneri* which is required in these bacteria for invasion and escape from the endocytic vacuole into the cytosol of the host cell (Stevens *et al.*, 2002). In *B. pseudomallei*, it has also been shown that escape from the vacuole is required for MNGC formation which is further supported by a loss of MNGC formation when a deletion mutation is made deactivating the Bsa T3SS (Burtnick *et al.*, 2008). The Bsa T3SS is discussed in more depth in the next section.

The T6SS is a mechanism Gram-negative bacteria use to transport a protein across the cell envelope and into a target eukaryotic or bacterial cell (Bingle *et al.*, 2008). *B. pseudomallei* K96243 encodes six T6SSs in its genome (Burtnick *et al.*, 2011). The bacterial T6SS resembles the T4 bacteriophage tail in structure with the hexameric Hcp protein polymerizing to form the tube-like structure and VgrG proteins forming the cell-puncturing device at the tip of the secre-

tion system (Bingle *et al.*, 2008). A recent study showed that a mutation in the *hcp1* gene of the T6SS–5 of *B. pseudomallei* K96243 ablated the ability of the bacteria to induce MNGCs whilst maintaining the ability to enter cells, escape into the cytosol and display actin-based motility in RAW 264.7 macrophages (Burtnick *et al.*, 2011). The same study also demonstrated that the *hcp1* mutant had lowered virulence in a Syrian hamster model of melioidosis indicating its importance *in vivo* (Burtnick *et al.*, 2011). It has also been shown that VgrG-5 is required for formation of MNGCs (Toesca *et al.*, 2014, Schwarz *et al.*, 2014). The regulation of the T6SS–5 of *B. pseudomallei* is itself regulated by BsaN, which also regulates effector protein secretion in the Bsa T3SS (Chen *et al.*, 2011).

1.1.6 Animal Models of Infection

In order to better investigate the pathogenesis of *B. pseudomallei in vivo*, a number of animal models of infection have been developed. The most frequently used animal model of melioidosis is the murine model of infection using BALB/c or C57BL/6 (Reviewed in Titball *et al.* (2008), Warawa (2010)). BALB/c mice are more susceptible to *B. pseudomallei* and represent an acute model of infection, while C57BL/6 mice are comparatively more resistant and represent a chronic model of disease (Leakey *et al.*, 1998). Both the strain of *B. pseudomallei* used and the route of infection determine the median lethal dose, which ranges from <10 to 10^6 CFU over a period from 10 to 65 days (Reviewed in Titball *et al.* (2008), Warawa (2010)). Large numbers of bacteria are recovered from the liver and spleen of infected animals, which reflects human septicaemic disease (Reviewed in Titball *et al.* (2008)).

While mice are the primary surrogate model used for melioidosis, there are a range of other models used less frequently. Syrian hamsters have been used as an infection model of *B. pseudomallei* and are extremely sensitive to the bacterium, with a median lethal dose at 48 hours of <10 CFU (Brett *et al.*, 1997). In order to conduct research in a model that is more physiologically relevant, models of melioidosis in non-human primates, generally rhesus macaques (*Macaca mulatta*), have also been described (Yingst *et al.*, 2014).

There are also well described models of melioidosis in invertebrates. For example, the wax moth larvae (*Galleria mellonella*) infection model has been shown to be sensitive enough to differentiate between *B. pseudomallei* strains shown to be virulent or avirulent in mice (Wand *et al.*, 2011). *B. pseudomallei* has been shown to be intracellular in the haemocytes of infected wax moths (Wand *et al.*, 2011). Invertebrate models such as the wax moth larvae may help

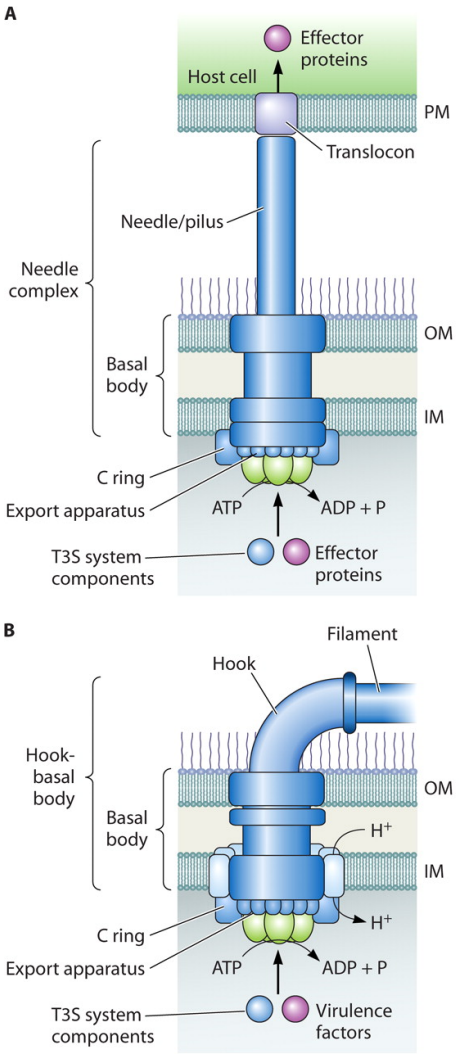
to reduce the use of animals in early stages of pathogenesis research.

1.2 Type 3 Secretion System

Type 3 secretion systems (T3SSs) span the bacterial inner and outer membranes forming a "molecular syringe" which allows Gram-negative bacteria to export proteins called effectors from the bacterial cytoplasm into a target eukaryotic cell (Reviewed in (Galán *et al.*, 2014)). T3SSs have been shown to be important for virulence in many bacteria including pathogenic *Escherichia coli, Salmonella, Shigella, Yersinia* and *Burkholderia* (Galan and Curtiss, 1989, Maurelli *et al.*, 1985, Gemski *et al.*, 1980, Jarvis *et al.*, 1995, Stevens *et al.*, 2002). The *B. pseudomallei* genome encodes three T3SSs. T3SSs-1 and -2 share homology with Hrp2 family of T3SSs found in plant pathogens (Winstanley *et al.*, 1999, Rainbow *et al.*, 2002). Indeed, *B. pseudomallei* T3SS-1 and -2 mutants are attenuated in a tomato plant model of infection (Lee *et al.*, 2010). Though T3SSs-1 and -2 were shown to be dispensable in a Syrian hamster model of infection (Warawa and Woods, 2005), a more recent study found that T3SS-1 was required for full virulence in a respiratory murine model of melioidosis (D'Cruze *et al.*, 2011a). T3SS-3, also known as the *Burkholderia* Secretion Apparatus (Bsa) T3SS, is similar to the Inv-Spa (*Salmonella* pathogenicity island (SPI)-1) and Mxi-Spa T3SSs of the animal pathogens *Salmonella* spp. and *S. flexneri*, respectively (Stevens *et al.*, 2002). The Bsa T3SS is required for full virulence in both murine and Syrian hamster models of infection (Stevens *et al.*, 2004, Warawa and Woods, 2005, Gutierrez *et al.*, 2015). T3SSs-2 and -3 are present in the genomes of *B. mallei* and *B. thailandensis*, whereas T3SS-1 is absent from both (Rainbow *et al.*, 2002).

1.2.1 Structure

The core structure of the T3SS is well conserved and is similar to that of the bacterial flagella system (Figure 1.4:A-B)(Young *et al.*, 1999, Kubori *et al.*, 1998, Gophna *et al.*, 2003). It is thought that the flagella and the T3SS evolved from a similar ancestor, but the T3SS has been the product of a large amount of horizontal gene transfer (Gophna *et al.*, 2003). T3SSs are separated into seven different families named after the archetype system in each family, each with slight differences in structure and host cell target, with multiple types of T3SS present in some bacterial species (Figure 1.4:C-D)(e.g. plant or animal) (Reviewed in Büttner (2012)).



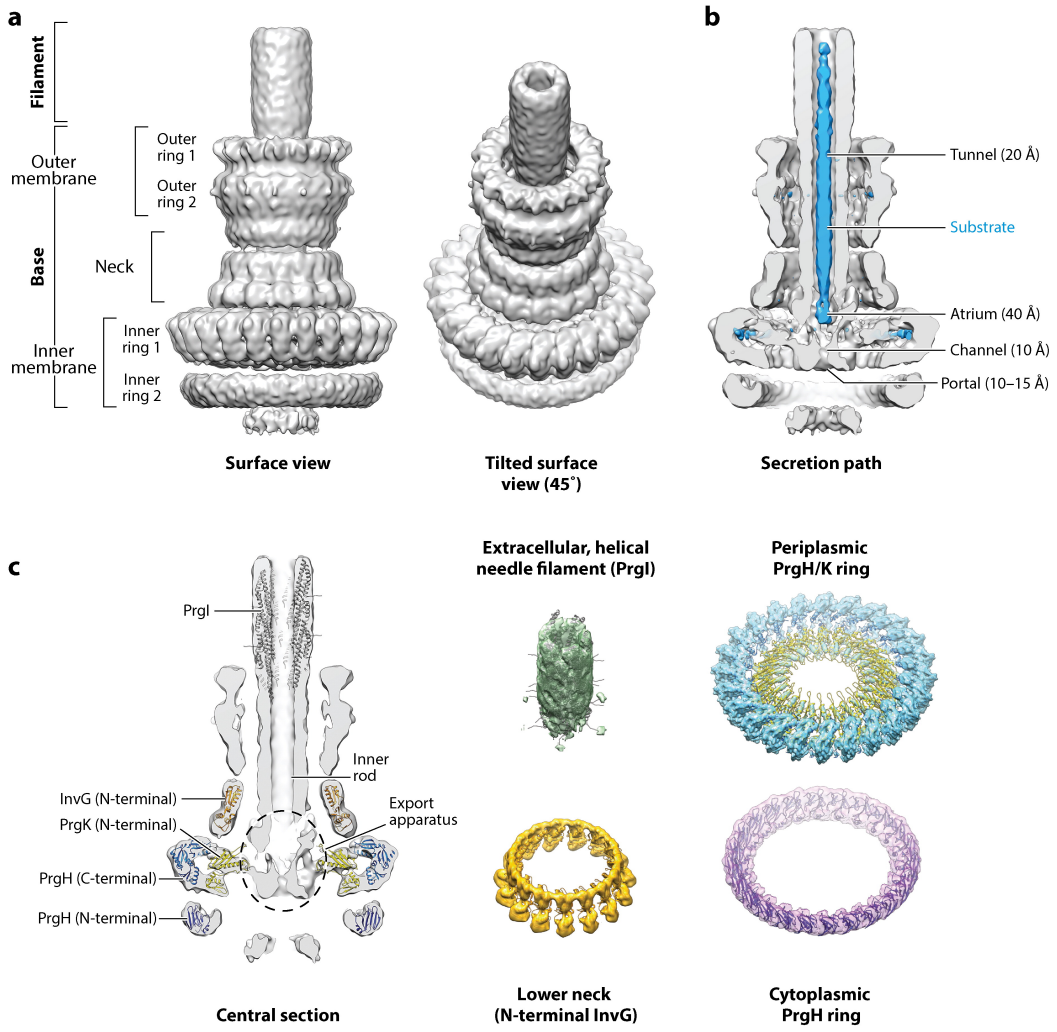
C

Families of translocation-associated T3S systems	Bacterial species that usually contain this T3S system
Ysc	*Yersinia* spp.
Inv-Mxi-Spa	*Salmonella* spp. (encoded by SPI-1) *S. flexneri*
Ssa-Esc	*Salmonella* spp. (encoded by SPI-2) EPEC (encoded by LEE)
Eiv-Epa	*E. coli* (encoded by ETT2)
Hrp1	*P. syringae* *Erwinia* spp.
Hrp2	*Xanthomonas* spp. *R. solanacearum*
Chlamydiales	*Chlamydia* spp.
Rhizobiales	*Rhizobium* spp.

D

Bacterial species	Families of T3S systems
Salmonella spp.	Inv-Mxi-Spa (SPI-1) Ssa-Esc (SPI-2)
Enterohaemorrhagic *E. coli*	Eiv-Epa and Ssa-Esc (LEE)
Yersinia pestis *Yersinia pseudotuberculosis* *Yersinia enterocolitica* serotype 3	Ysc Ssa-Esc
Yersinia enterocolitica biotype 1B	Ysc Inv-Mxi-Spa (Ysa-T3S system)
Burkholderia pseudomallei	2 x Hrp2 Inv-Mxi-Spa
Xanthomonas axonopodis pv. *phaseoli*	Hrp2 Inv-Mxi-Spa
Xanthomonas albilineans	No Hrp-type T3S system Inv-Mxi-Spa (SPI-1)
Vibrio parahaemolyticus	Ysc Hrp2
Burkholderia spp.	Inv-Mxi-Spa 2 x Hrp2

Figure 1.4: Overview of T3SSs from animal- and plant-pathogenic bacteria. (A) The translocation-associated T3SS functions similar to a molecular syringe, allowing injection of bacterial proteins into the cytoplasm of a target host cell. (B) The flagellar T3SS has an extracellular hook and is involved in bacterial motility. (C) A list of the different families of translocation-associated T3SSs from bacterial pathogens of plants or animals. (D) Examples of bacterial species and their corresponding translocation-associated T3SSs (note some species contain multiple systems). Figure taken from Büttner (2012).



Galán JE, et al. 2014.
Annu. Rev. Microbiol. 68:415–38

Figure 1.5: The 3-D structure of the *Salmonella* T3SS as determined by cryo-EM. (a) Surface views of the T3SS showing base comprised of the membrane spanning inner and outer membrane rings connected by a neck, and the filament forming the extracellular "needle". (b) Section view showing the path an unfolded effector protein (substrate) takes through the needle complex. (c) Component view of the T3SS. Figure taken from Galán *et al.* (2014).

In recent years the structure of the *Salmonella* T3SS has been solved using cryo-EM (Schraidt and Marlovits, 2011). The structure of the *Salmonella* T3SS (Reviewed by Galán *et al.* (2014)) consists of inner and outer membrane rings connected by a rod, the extracellular needle and a secreted translocation pore which spans the target cell membrane (Figure 1.5). Assembly of the T3SS appears to be hierarchical and is the subject of multiple recent reviews (Büttner, 2012, Diepold and Wagner, 2014). Based on evidence from *Yersinia* and *Salmonella*, it appears construction of the T3SS begins with the formation of the outer-membrane/structural ring (Secretin) and independently the inner-membrane export machinery, which are then linked by YscJ (*Yersinia*) or PrgK (*Salmonella*), followed by assembly of the ATPase/C-ring and the formation of the mature needle complex (Figure 1.6) (Diepold *et al.*, 2010, 2011, Wagner *et al.*, 2010).

Only a few structural proteins in the *B. pseudomallei* Bsa T3SS have been studied. Figure 1.7 shows the predicted location of each of the structural components of the Bsa T3SS. BsaZ(BPSS1534) is a structural component with homology to SpaS of *Salmonella* (Stevens *et al.*, 2002). SpaS is a component of the inner membrane complex and has been shown to undergo autocleavage causing a switch between secretion of structural components to secretion of the needle complex and translocator proteins (Zarivach *et al.*, 2008). Mutations in *bsaZ* caused delays in escape from the phagosome and reduced intracellular survival in J774.2 cells (Stevens *et al.*, 2002, Burtnick *et al.*, 2008). *bsaZ* mutants have also been shown to be attenuated in murine (Stevens *et al.*, 2004, Burtnick *et al.*, 2008) and Syrian hamster (Warawa and Woods, 2005) models of melioidosis. The *bsaZ* mutant phenotype is thought to be due to its inability to secrete effector and translocator proteins such as BopE and BopC (Stevens *et al.*, 2003, Muangman *et al.*, 2011).

Another component of the inner membrane ring of the *B. pseudomallei* Bsa T3SS that has been described is BsaQ (BPSS1543), which is homologous to InvA from *Salmonella* (Sun *et al.*, 2005). InvA is required for the formation of the mature T3SS in *Salmonella* as well as secretion of effector proteins (Kubori *et al.*, 2000). *bsaQ* mutants displayed a similar phenotype to *bsaZ* mutants in that they are delayed in phagosome escape resulting in reduced intracellular survival (Muangsombut *et al.*, 2008). The *bsaQ* mutants are unable to secrete BopE or BipD into the supernatants and showed defects in cell invasion (Muangsombut *et al.*, 2008).

A third inner membrane component, BsaM (BPSS1547), is homologous to

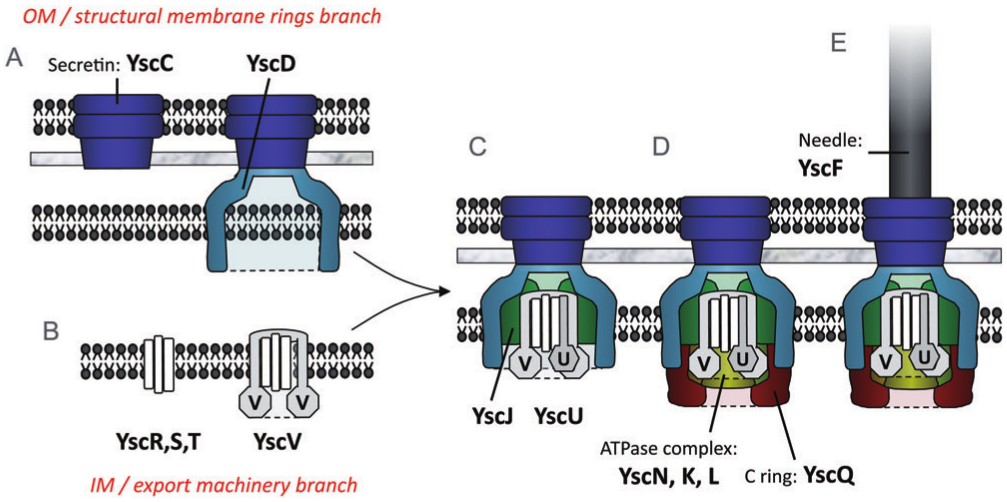


Figure 1.6: The assembly of the T3SS in *Yersinia*. Assembly of the outer membrane/structural rings (A) and the inner membrane export machinery (B) appear to happen simultaneously in two separate branches. The recruitment of YscJ by both complexes allows the two structures to merge (C). Finally, the ATPase-C ring is added to the base of the injectisome (D), followed by secretion and assembly of the needle (E). Figure taken from Diepold *et al.* (2011).

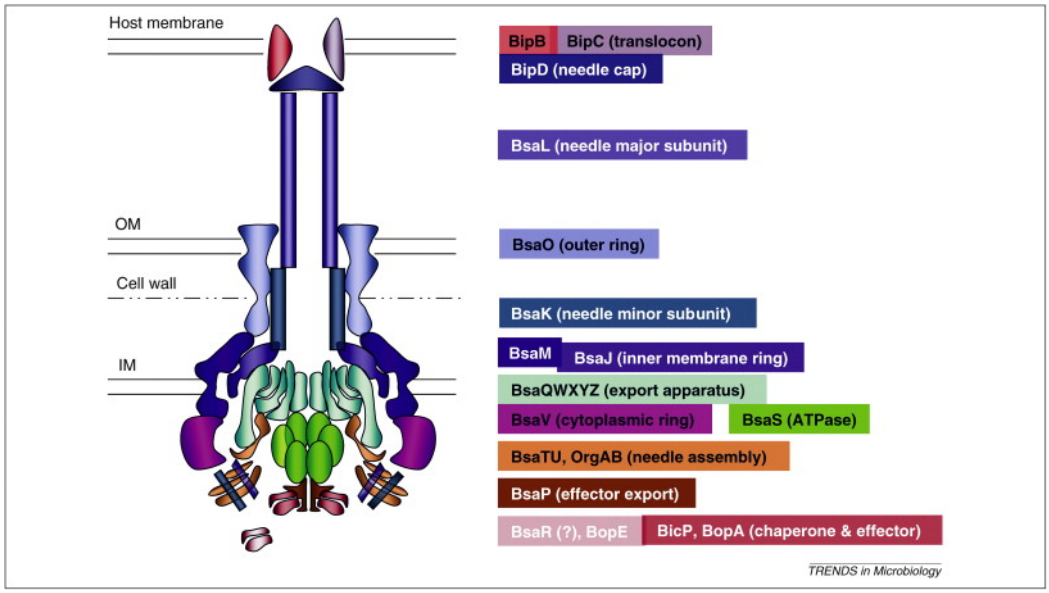


Figure 1.7: Predicted structure of the *B. pseudomallei* Bsa T3SS. Each of the proteins of the Bsa T3SS are mapped onto their predicted location corresponding to homologous proteins within *Salmonella*. Figure taken from Sun and Gan (2010).

Salmonella PrgH, which forms the inner membrane ring of the *Salmonella* T3SS and is required for secretion of effector proteins (Kubori *et al.*, 2000, Marlovits *et al.*, 2004). A *B. pseudomallei bsaM* mutant was shown to induce lower levels of NF-κB in HEK 293T cells when compared to WT, but similar levels to a *bsaS* mutant (Teh *et al.*, 2014). The *bsaM* mutant was shown to activate NF-κB at time points corresponding to a delayed escape from the phagosome suggesting it has similar effects to the other *bsa* T3SS structural knockouts (Teh *et al.*, 2014).

BsaU (BPSS1539) is homologous to InvJ from *Salmonella* which is the "molecular ruler" which determines the length of the T3SS needle (Kubori *et al.*, 2000). Mutation of *bsaU* in *B. pseudomallei* resulted in a delay in phagosome escape and reduced virulence in a BALB/c intranasal mouse infection model (Pilatz *et al.*, 2006). The mutant was also deficient in its ability to secrete BopE and BipD into the supernatant (Pilatz *et al.*, 2006).

The protein BsaL (BPSS1548) has had its crystal structure solved and was shown to have a similar structure to MxiH (*Shigella*) and PrgI (*Salmonella*), which form the external needle structure (major needle subunit) of the T3SS (Zhang *et al.*, 2006, Wang *et al.*, 2007, Barrett *et al.*, 2008). The Nod-like receptor NLRC4 recognises T3SS minor needle component proteins from a range of Gram-negative bacteria, including BsaK (BPSS1549) from *B. pseudomallei*, activating an innate immune response through casapase-1 (Miao *et al.*, 2010, Zhao *et al.*, 2011, Bast *et al.*, 2014). A *B. pseudomallei bsaK* mutant was highly attenuated in an intranasal murine model of melioidosis (Bast *et al.*, 2014).

1.2.2 Energising Secretion

Proteins are secreted in an unfolded state due to the narrow width of the needle channel which is around 2–3 nm in *S. flexneri* (Blocker *et al.*, 2001, Radics *et al.*, 2014). This was proven by cryo-EM imaging of a substrate which was engineered to become trapped in the secretion channel (Radics *et al.*, 2014). The ATPase at the base of the secretion system has been shown to dissociate proteins from their chaperones and also is thought to be involved in unfolding of the protein (Akeda and Galán, 2005). The source of energy for exporting proteins is the subject of some debate. It has been shown in the flagellar T3SS of *Yersinia* and *Salmonella* that secretion can take place in the absence of the ATPase (Wilharm *et al.*, 2004, Erhardt *et al.*, 2014). This evidence, combined with a study which showed flagellar T3S was halted in the absence of a proton gradient, has led to the hypothesis that the ATPase is primarily for unfolding and proton motive force energises secretion of the unfolded substrate (Paul *et al.*,

2008). A *B. pseudomallei bsaS* (BPSS1541) mutant was shown to be unable to secrete the known effector protein BopE (Gong *et al.*, 2015). The mutant also showed a reduction of intracellular survival in RAW 264.7 cells and was attenuated in BALB/c mice infected intranasaly, demonstrating that the ATPase is required for Bsa T3SS function (Gong *et al.*, 2015).

1.2.3 Needle Tip and Translocators - Sensing Host Contact

Upon host cell contact, the translocators of the T3SS are inserted into the host cell membrane forming a pore through which effector proteins may pass. *Shigella* was shown to lyse red blood cells (RBC) by inserting the translocators IpaB and IpaC into the RBC membrane forming a 25 angstrom pore (Blocker *et al.*, 1999). Secretion of the translocator proteins is regulated by the needle tip protein. A *Shigella* tip protein mutant, *ipaD*, constitutively secreted the translocators, IpaB and IpaC (Picking *et al.*, 2005). Immunofluorescence staining for IpaD of *Shigella*, demonstrates the presence of the protein on the surface of the bacteria in the absence of a host cell membrane, which was further confirmed by electron microscopy (Espina *et al.*, 2006). The needle tip protein probably acts to sense host cell contact, stopping early secretion of translocators (Espina *et al.*, 2006). In the same study it was shown that antibodies to the tip protein disrupted the haemolysis of sheep erythrocytes indicating IpaD's functional importance in the insertion of the translocator complex into eukaryotic cell membranes as well as regulating effector secretion (Espina *et al.*, 2006).

Continuing with *Shigella* as an example, growth in the bile salt deoxycholate (DOC) causes IpaB to be present at the tip of the needle in a manner which correlates to DOC binding IpaD (Olive *et al.*, 2007, Stensrud *et al.*, 2008). The authors suggest this may correspond to *Shigella* sensing bile salts as it passes through the human GI tract and is an initial step in "priming" the T3SS (Stensrud *et al.*, 2008). The final step in secretion of the translocation pore was shown to be dependent on *Shigella* interacting with liposomes to induce IpaC secretion (Epler *et al.*, 2009). When cultured in the presence of liposomes, IpaC localised to the bacterial surface and was secreted into the supernatant as shown by electron microscopy and Western blot (Epler *et al.*, 2009). This agrees with earlier evidence that cholesterol is bound by translocation components (*Salmonella* SipB and *Shigella* IpaB), is important for entry into host cells and is required for efficient translocation of effector proteins into host cells (Lafont *et al.*, 2002, Hayward *et al.*, 2005).

BipD (BPSS1529)

BipD (BPSS1529) is the needle tip protein of the Bsa T3SS. It is homologous to SipD (*Salmonella*), IpaD (*Shigella*) and LcrV (*Yersinia*). The crystal structure of BipD was solved (Erskine *et al.*, 2006, Knight *et al.*, 2006, Roversi *et al.*, 2006, Johnson *et al.*, 2007, Pal *et al.*, 2010) and the 3-dimensional structure is highly similar to IpaD of *Shigella* (Johnson *et al.*, 2007) and *Salmonella* SipD (Espina *et al.*, 2007). It was demonstrated that the structure of BipD, as well as IpaD and SipD, is dependant on pH changes (Markham *et al.*, 2008). Interestingly when cultured in a more acid pH of 4.5, *B. thailandensis* secretes larger amounts of BipD as well as BopE (Jitprasutwit *et al.*, 2010). The same study also described distinct forms of BipD in *B. pseudomallei* and *B. thailandensis*, but one *B. thailandensis* strain carried a *B. pseudomallei*-like BipD, possibly due to a shared environmental reservoir (Jitprasutwit *et al.*, 2010).

Needle tip proteins are of interest because of their potential as subunit vaccines. Most notably the needle tip protein LcrV (V antigen) from *Yersinia pestis*, especially when combined with the Fraction 1 (F1) protein, is a an effective vaccine that has been tested in human clinical trials (Reviewed by Williamson (2009)). Vaccination of mice with the *Shigella* needle tip protein IpaD, along with the translocator IpaB, induces high levels of protection upon subsequent challenge (Martinez-Becerra *et al.*, 2012, Heine *et al.*, 2013, Martinez-Becerra *et al.*, 2013).

In *B. pseudomallei*, it was initially described that convalescent serum from a melioidosis patient reacted specifically with recombinant GST-BipD (Stevens *et al.*, 2002). $CD4^+$ T cells taken from mice infected with an attenuated strain of *B. pseudomallei* showed specificity for BipD (Haque *et al.*, 2006). Similarly, human monocyte-derived dendritic cells from healthy *B. pseudomallei* seropositive donors were pulsed with purified BipD after which CD4+ T cells were able to recognise the recombinant protein (Tippayawat *et al.*, 2011). BipD mutants in *B. pseudomallei* strains 10276 and 576 were significantly attenuated in a BALB/c intranasal murine infection model when compared to WT, demonstrating the importance of BipD *in vivo* (Stevens *et al.*, 2004). Multiple attempts have been made to use BipD as a recombinant subunit vaccine in a BALB/c murine intraperitoneal model of infection, but in both studies the vaccine showed no protection when the mice were challenged (Stevens *et al.*, 2004, Druar *et al.*, 2008).

BipB (BPSS1532)

BipB (BPSS1532) shares 46% amino acid identity with the translocator protein SipB from *Salmonella*. A *B. pseudomallei* K96243 *bipB* insertion mutant showed reduced invasion and cell-to-cell spread in HeLa cells and a reduced ability to form MNGCs in J774A.1 cells. *In vivo* in BALB/c mice infected intranasaly, the *bipB* mutant was greatly attenuated and showed a phenotype similar to that of the BipD mutant (Suparak *et al.*, 2005, Stevens *et al.*, 2004). This is likely due to the inability of the T3SS to function correctly without the formation of the translocation pore. The N-terminal region of BipB was tested as a protective antigen for *B. pseudomallei* infection in mice, but showed no protection (Druar *et al.*, 2008).

BipC (BPSS1521)

BipC (BPSS1531) is a homologue of the translocators SipC from *Salmonella* and IpaC from *Shigella*. SipC has been shown to interact with SipB to form the translocon pore (Myeni *et al.*, 2013). Beyond their role as a translocator protein, SipC and IpaC also function as effector proteins within the eukaryotic cell. SipC has actin nucleation activity and bundles F-actin (Hayward and Koronakis, 1999). The ability of SipC to nucleate and bundle F-actin as well as form the translocation pore, are all dependant on the C-terminal 209 amino acids of the 409 amino acid protein (Hayward and Koronakis, 1999, Chang *et al.*, 2005, Myeni and Zhou, 2010). Actin bundling appears to be important for cell invasion, as *Salmonella* containing a mutated form of *sipC* that is unable to bundle actin, but still able to act as a translocon, was less invasive than WT *Salmonella* (Myeni and Zhou, 2010). SipC has also been shown to bind to host Syntaxin6 and thereby recruit LAMP1 to the *Salmonella* containing vacuole (SCV), helping to stabilise its membrane (Madan *et al.*, 2012). Interestingly, the protein SipA enhances SipC's ability to nucleate and bundle F-actin (McGhie *et al.*, 2001), but a homologue of SipA is not present in *B. pseudomallei*.

The C-terminal and N-terminal regions of BipC were separately tested as a protective antigen for *B. pseudomallei* infection in mice, but neither antigen showed any protection (Druar *et al.*, 2008). These results agreed with previously reported unpublished results from other studies (J. Hill, M. W. Wood & E. E. Galyov, unpublished observations). In another study, a *B. pseudomallei* K96243 *bipC* insertion mutant showed reduced cell adhesion and invasion of A549 cells when compared to the WT strain (Kang *et al.*, 2015). This *bipC*

mutant also showed a delay in escape from the phagosome leading to a delay in formation of actin tails and intracellular replication (Kang *et al.*, 2015). The mutant was also attenuated in BALB/c mice infected intraperitoneally when compared to WT (Kang *et al.*, 2015). While this shows the importance of BipC in virulence, both *in vivo* and *in vitro*, it does not separate BipC's role as a translocator necessary for a functioning T3SS, from roles it may have as an effector protein. More work is needed to determine whether BipC, similar to SipC and IpaC, may play a secondary role.

1.2.4 Regulation of the T3SS

The regulation of the *bsa* T3SS has been elucidated by Sun *et al.* (2010) (Figure 1.8). At the top of the regulatory hierarchy is the gene *bspR* (BPSL1105), which, when disrupted caused a greatly reduced level of expression in genes in the *bsa* T3SS locus as shown by microarray and real time PCR (Sun *et al.*, 2010). *bspR* signals through the membrane bound regulator *bprP* (BPSS1553) which controls expression levels of both structural and secreted components of the *bsa* T3SS (Sun *et al.*, 2010). *bprP* further signals through *bsaN* (BPSS1546) and it's co-activator, the chaperone *bicA* (BPSS1533), controlling transcription of the known effectors *bopE* and *bopA*, as well as the genes *bicP* (BPSS1523) and *bprB-D* (BPSS1520-22) (Sun *et al.*, 2010, Chen *et al.*, 2014). *bsaN* also relays the regulation signal to the virulence-associated Type 6 secretion system and virulence factors such as *bimA* and *virAG* (Sun *et al.*, 2010, Chen *et al.*, 2014).

The presence of genes allowing for the ability to assimilate arabinose was noticed to be one of the differences between virulent *B. pseudomallei* and avirulent *B. thailandensis* (Smith *et al.*, 1997, Moore *et al.*, 2004). It was later shown that by expressing the *B. thailandensis* arabinose assimilation operon in *B. pseudomallei*, virulence in a Syrian hamster model was reduced (Moore *et al.*, 2004). There was also a down-regulation of *bsa* T3SS genes, notably the T3SS regulator *bsaN* (Moore *et al.*, 2004). Interestingly *bprP*, the regulator of *bsaN* and the structural components of the *bsa* T3SS, was not repressed in the presence of the arabinose assimilation operon (Moore *et al.*, 2004).

1.2.5 T3SS Signals and Chaperones

Type 3 secretion signals are located at the N-terminus of a protein, are not cleaved and do not share sequence homology with each other (Michiels and Cornelis, 1991, Schesser *et al.*, 1996). In *Yersinia*, it was shown that as little

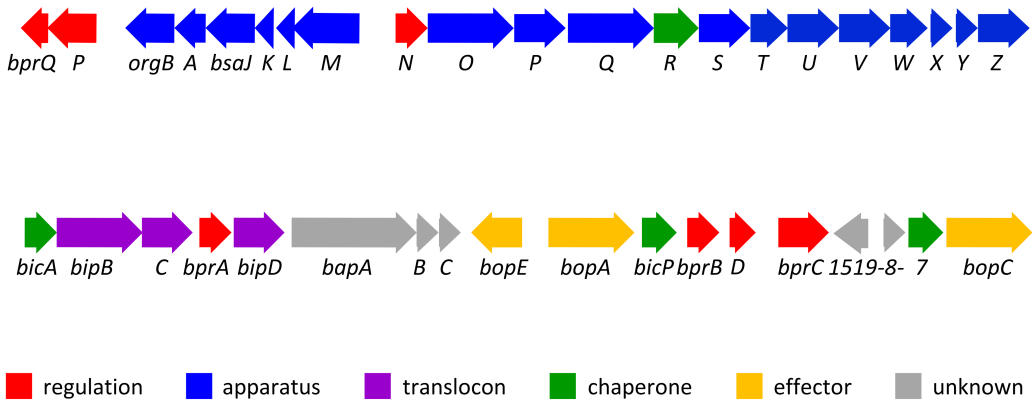


Figure 1.8: The *B. pseudomallei* K96243 *bsa* T3SS gene locus. The locus ranges from *bopC* (BPSS1516) to *bprQ* (BPSS1554). The Bsa T3SS comprises of regulators (red), structural components (blue), translocators (purple), chaperones (green), effectors (yellow) and genes with unknown function (grey). Figure taken from Chen *et al.* (2014).

as 15 amino acids of the N-terminus of YopE fused to calmodulin-dependant adenylate cyclase were enough for secretion into the supernatant (Sory *et al.*, 1995). Interestingly, substituting the alanines at position 2 and 15 in the YopE secretion signal with glutamic acid, did not affect secretion (Anderson and Schneewind, 1997). Even shifting the reading frame did not prevent the secretion of YopE, which the authors suggested may indicate a secretion signal located in the mRNA of the effector protein (Anderson and Schneewind, 1997). A second important signal in the N-terminal region of T3S effector proteins is the chaperone binding domain (CBD) which is required for the specific secretion of effector proteins (Lee and Galán, 2003, Ehrbar *et al.*, 2003, Lee and Galán, 2004, Ehrbar *et al.*, 2006, Abe *et al.*, 1999) as well as for their stability in the bacterial cytoplasm (Frithz-Lindsten *et al.*, 1995, Abe *et al.*, 1999). By determining the crystal structure of an effector protein bound to its chaperone, it is known that T3S chaperones in *Yersinia* and *Salmonella* bind the N-terminal amino acids of their effector protein, just after the T3S signal, but before any functional domains, and maintain the bound effector protein in a partially unfolded state that may be more competent for secretion (Stebbins and Galán, 2001, Birtalan and Ghosh, 2001).

The T3S signal also appears to be promiscuous between systems, allowing secretion of effector proteins from bacteria in an unrelated host bacterium containing a T3SS (Rossier *et al.*, 1999, Hovis *et al.*, 2013). This is even true of less similar T3SSs, as shown by the ability of the Hrp Plant T3SS of *Xanthomonas* to secrete the mammalian effector protein YopE of *Yersinia* (Rossier *et al.*, 1999). Maybe because of the similarity between the two, virulence associated T3SS effectors can be secreted by the bacterial flagellar T3SS system in *Yersinia* and *Salmonella* (Young and Young, 2002, Warren and Young, 2005, Lee and Galán, 2004, Ehrbar *et al.*, 2006). It is only through interaction with the appropriate chaperone that specific secretion through one system is achieved. Removal of the ability of SopE in *Salmonella* to bind it's chaperone InvB, caused secretion through both the flagellar and SPI-1 virulence associated T3SS (Lee and Galán, 2004, Ehrbar *et al.*, 2006)

B. pseudomallei has 4 putative Bsa T3SS chaperones, though little work concerning their function has been performed. The protein encoded by the gene BPSS1517 is a putative chaperone and has been shown to interact with the downstream effector protein BopC (BPSS1516) (Muangman *et al.*, 2011). Another putative chaperone, BicA (BPSS1533) has been shown to be required for the secretion of the known effector protein BopE (Sun *et al.*, 2010). Two hy-

pothetical chaperones, BicP (BPSS1523) and BsaR (BPSS1542) have not been studied to date.

1.3 Bsa T3SS Effector Proteins

The role of the T3SS is to deliver an array of effector proteins into the target cell to subvert host cell functions. The function of different effector proteins is extremely varied, ranging from blocking apoptosis (*E. coli* NleH), prevention of phagocytosis (*Yersinia* YopH), cytotoxic activity (*Pseudomonas aeruginosa* ExoU) and disruption of the actin cytoskeleton (*Salmonella* SopE) (Hemrajani *et al.*, 2010, Persson *et al.*, 1997, Sato *et al.*, 2003, Hardt *et al.*, 1998). The location of the genes encoding effector proteins within *bsa* T3SS locus are depicted in Figure 1.8. *B. pseudomallei* encodes three effector proteins known to be secreted by the Bsa T3SS (CHBP, BopC and BopE) as well as six hypothetical T3SS effectors (BopA, BapA, BapB, BapC, BprD and BopB) (Reviewed in Sun and Gan (2010)).

1.3.1 CHBP/Cif (BPSS1385) - Confirmed Bsa Effector

CHBP (BPSS1385) is a homologue of cell cycle inhibiting factor (Cif) in *E. coli*. Cif and CHBP are able to deamidate NEDD8 causing cell cycle arrest (Nougayrède *et al.*, 2001, Cui *et al.*, 2010). CHBP has been shown to cause cell cycle arrest when expressed in *B. thailandensis*, but until recently it had yet to be demonstrated that CHBP is secreted in a Bsa-dependent manner by *B. pseudomallei* (Cui *et al.*, 2010).

In a recent study, we determined that CHBP is present in 76.7% (33/43) of the available *B. pseudomallei* genomes (Pumirat *et al.*, 2014). A Western blot assay used to probe for the presence of the CHBP protein in *B. pseudomallei* clinical isolates from the endemic region detected CHBP in 46.6% (7/15) isolates (Pumirat *et al.*, 2014). It was also shown that CHBP is not secreted under standard growth conditions, but wild type (WT) *B. pseudomallei* was able to secrete CHBP into U937 cells, whereas the *bsaQ* mutant was unable to (Pumirat *et al.*, 2014). A *B. pseudomallei* K96243 *chbP* insertion mutant showed a reduction in the ability to form plaques in HeLa cells at 24 hours and lower cytotoxicity at 6 hours as assessed by LDH release assays (Pumirat *et al.*, 2014). Both of these phenotypes were complemented when *chbP* was expressed on a plasmid indicating the phenotype was due to disruption of the *chbP* gene and not due to

unexpected polar effects of the insertion mutation (Pumirat *et al.*, 2014).

1.3.2 BopB/FolE (BPSS1514) - Hypothetical Bsa Effector

BopB (BPSS1514) or FolE, is annotated to be a GTP cyclohydrolase I and was thought to be a candidate effector protein (Stevens *et al.*, 2004). Yet a *bopB* mutant did not display a significantly reduced time to death when compared to WT *B. pseudomallei* in a BALB/c intraperitoneal infection (Stevens *et al.*, 2004). Similarly, mutation of *bopB* did not affect invasion and intracellular replication within cells (Chen *et al.*, 2014). Expression of *bopB* is co-regulated with the other effectors of the *bsa* T3SS by BsaN, but the role BopB plays in infection is still unknown (Chen *et al.*, 2014).

1.3.3 BopC (BPSS1516) - Confirmed Bsa Effector

BopC (BPSS1516) is a 509 amino acid protein with no high sequence homology to proteins from other species besides *B. mallei*. It is encoded just before the T3SS locus along with BPSS1517, which has been shown to be a chaperone for BopC (Muangman *et al.*, 2011). BopC was detected in the supernatants of WT *B. pseudomallei* 10276, but not in supernatants of a *bsaZ* insertion mutant, indicating that BopC is secreted by the Bsa T3SS (Muangman *et al.*, 2011). The first 20 amino acids of BopC fused to the beta-lactamase gene TEM1, was also shown to be sufficient for translocation into HeLa cells in a T3SS-dependant manner (Muangman *et al.*, 2011).

A *B. pseudomallei* K96243 *bopC* mutant was hindered in its ability to invade A549 cells (Muangman *et al.*, 2011). Another study demonstrated that the mutation in *bopC* reduced levels of intracellular survival when compared to WT bacteria (Srinon *et al.*, 2013). It was also shown by staining for co-localisation with LAMP–1 that the *bopC* mutant showed a delayed escape from the phagosome in J774A.1 cells compared to WT, which likely explains the difference in intracellular survival (Srinon *et al.*, 2013).

1.3.4 BprD (BPSS1521) - Hypothetical Bsa Effector

BprD (BPSS1521) has no known homology to proteins outside of *B. pseudomallei* and the closely related *Burkholderia* species.. It is labelled as a putative regulator of the *bsa* T3SS, though a knockout of the *bpr* operon (*bprB,C,D*) showed no effect on the expression of genes in the *bsa* T3SS (Sun *et al.*, 2010). Also,

it is regulated by BsaN along with the known effector proteins BopA, BopC and BopE (Sun *et al.*, 2010). The gene expression of *B. pseudomallei* was analysed from the lungs, livers and spleens of BALB/c and C57BL/6J mice by microarray and *bprD* emerged as being highly over expressed in all tissues in both strains of mice (Chirakul *et al.*, 2014). A mutation in *bprD* increased the expression of the downstream gene in the same operon, *bprC*, which regulates expression of the T6SS-1 (Chirakul *et al.*, 2014). BALB/c mice infected intraperitoneally with the *bprD* mutant had a shorter time to death when compared to WT *B. pseudomallei*, which the authors point out may be due to the up-regulation of the T6SS-1 (Chirakul *et al.*, 2014).

1.3.5 BopA (BPSS1524) - Hypothetical Bsa Effector

BopA (BPSS1524) shares 23% homology with IcsB from *Shigella* (Cullinane *et al.*, 2008). It has been predicted to contain a Rho GTPase inactivation domain (RID) similar to that found in VcRtxA (*Vibrio cholera*) and other MARTX toxins which indirectly inactivate Rho GTPases (Pei and Grishin, 2009). IcsB, along with its chaperone IpgA, are important for *Shigella's* ability to escape LC3 positive phagosomes once inside the host cell, and this activity is dependent on IcsBs cholesterol binding domain (Kayath *et al.*, 2010, Campbell-Valois *et al.*, 2015). BopA also contains a functional cholesterol-binding domain (Kayath *et al.*, 2010). The *B. pseudomallei* homologue of IpgA is BicP, which co-purifies with BopA and helps to prevent its degradation, indicating that it is the chaperone for BopA (Kayath *et al.*, 2010).

While BopA has not been proven to be secreted by the Bsa T3SS in *B. pseudomallei*, BopA from *B. mallei* has been shown to be secreted in a surrogate *E. coli* host. By fusing the first 58 amino acids of BopA from *B. mallei* ATCC 23344, which contain the T3S signal, to the *Yersinia enterolitica* phospholipase YplA, the fusion protein was secreted by EPEC E2348/69, but not its isogenic *escN* mutant, which contains a non-functional secretion system (Whitlock *et al.*, 2008).

BopA is important to the intracellular survival of *B. pseudomallei* in phagocytic cells (Cullinane *et al.*, 2008). A *bopA* mutant in *B. pseudomallei* K96243 displayed reduced intracellular survival and an increased localisation with GFP-LC3, an indicator of autophagy stimulation, in RAW 264.7 cells (Cullinane *et al.*, 2008). This reduction in intracellular survival was eliminated when cells were treated with wortmannin, indicating the reduction was due to autophagy (Cullinane *et al.*, 2008). Another study demonstrated that BopA is

important for escape from the phagosome and the increased co-localisation of LC3 with bacteria was due to the inability of the bacteria to escape the phagosome allowing for recruitment of LC3 (Gong *et al.*, 2011).

A B. *mallei* ATCC 23344 *bopA* mutant had a decrease in intracellular survival in J774A.1 cells (Whitlock *et al.*, 2008). Interestingly, in the murine alveolar macrophage cell line MH-S, the same *B. mallei bopA* mutant exhibited increased intracellular survival when compared to the WT strain, indicating that different cell types may rely on different mechanisms to clear *B. mallei* (Whitlock *et al.*, 2009).

BALB/c mice infected intraperitoneally with a *B. pseudomallei* 576 *bopA* insertion mutant were significantly delayed in time to death when compared to the WT strain (median = 32 days vs. 20 days respectively) (Stevens *et al.*, 2004). BALB/c mice infected intranasaly with a *B. mallei* ATCC 23344 *bopA* insertion mutant showed a delayed time to death compared to the WT strain (median = 5 days vs. 7.5 days respectively). No bacteria were recovered from the lung tissue of animals infected with the *bopA* mutant while 10^8 bacteria were recovered from the lungs of animals infected with WT *B. mallei* (Whitlock *et al.*, 2009). In mice immunized with recombinant BopA and challenged intranasaly with *B. mallei* ATCC23344 and *B. pseudomallei* 1026b, the BopA vaccine protected 100% and 60% respectively of animals 21 days post infection (Whitlock *et al.*, 2010).

1.3.6 BopE (BPSS1525) - Confirmed Bsa Effector

BopE (BPSS1525) is the best characterised of the *B. pseudomallei* effector proteins. BopE shares 16% homology to the guanine nucleotide exchange factor (GEF) SopE from *Salmonella*. BopE was shown to be secreted by the Bsa T3SS in *B. pseudomallei* 10276 in a manner dependent on the structural protein BsaZ (Stevens *et al.*, 2003). Similarly, deletion of another structural component *bsaQ* in *B. pseudomallei* K96243, was shown to inhibit secretion of BopE into the supernatant (Muangsombut *et al.*, 2008). BopE is important for invasion of non-phagocytic cells, as a *B. pseudomallei bopE* insertion mutant was impaired in its ability to invade HeLa cells (Stevens *et al.*, 2003). Also, expression of BopE on a plasmid in HeLa cells caused the formation of actin rearrangements (Stevens *et al.*, 2003). Using fluorescence spectrometry, it was demonstrated that purified BopE, similar to SopE, is a functional guanine nucleotide exchange factor for both Rac1 and Cdc42, but with about 10 fold lower activity than SopE (Stevens *et al.*, 2003). This lower activity may be explained by differences in the catalytic domains, as the SopE catalytic domain stays in an open confor-

mation, while BopE adopts a closed conformation that must open upon interaction with Cdc42 to allow for GEF activity (Upadhyay *et al.*, 2008).

HEK 293T cells transfected with plasmids expressing BopE and casapase–1, resulted in the increased activation of casapase–1 and –7 (Bast *et al.*, 2014). When the active site of the transfected BopE was mutated, levels of activation of caspase–1 and –7 returned to basal levels indicating BopE's GEF activity is required for the activation of casapase–1 and –7 (Bast *et al.*, 2014). However, when *B. pseudomallei* E8 was used to infect murine macrophages, a mutation in BopE caused only slight differences in casapase–1 processing and does not seem to play a major role in infection (Bast *et al.*, 2014). This may be due to redundancy in other effector proteins.

In a murine model of melioidosis, BALB/c mice infected intraperitoneally with *B. pseudomallei* 10276 containing an insertion mutation in *bopE* did not show a significant increase in median time to death when compared to WT (21 days vs. 20 days respectively) (Stevens *et al.*, 2004). Immunisation of mice with a live attenuated mutant of *B. pseudomallei* induced $CD4^+$ and $CD8^+$ T cells specific for BopE (Haque *et al.*, 2006). Using the sera from healthy patients that are seropositive for *B. pseudomallei*, $CD4^+$ T cells were able to recognize BopE (Tippayawat *et al.*, 2011).

1.3.7 BapB-C (BPSS1526-7) - Hypothetical Bsa Effectors

Little work has been done on the putative effector proteins BapB (BPSS1527) and BapC (BPSS1526). BapC is homologous to IagB from *Salmonella* (Stevens *et al.*, 2002). IagB is thought to be a lytic transglycosylase involved in the breakdown of the bacterial peptidoglycan layer, allowing connection of the inner and outer membrane components of the secretion system, though this function has not formally shown (Zahrl *et al.*, 2005). A *bapC* mutant showed no significant attenuation in a Syrian hamster model of melioidosis (Warawa and Woods, 2005). BapB is homologous to IacP from *Salmonella*(Stevens *et al.*, 2002). IacP has been shown to be important for *Salmonella* invasion into host cells by playing a role in regulating SopA, SopB and SopD secretion(Kim *et al.*, 2011). The role of BapB in *B. pseudomallei* has not been explored.

1.3.8 BapA (BPSS1528) - Hypothetical Bsa Effector

BapA (BPSS1528) has no known homology to proteins outside of *B. pseudomallei* and the closely related *Burkholderia* species. A *bapA* mutant in *B. pseu-*

domallei 1026b showed no attenuation in a Syrian hamster model of infection (Warawa and Woods, 2005). There has been no other published work on this protein.

1.3.9 Unidentified Effector Proteins

It can be hypothesized that there are more Bsa T3SS effectors to be characterized. There are at least 21 effectors secreted by the T3SS of Enteropathogenic *E. coli* (EPEC) (Reviewed in (Dean and Kenny, 2009)) and 25–30 effectors secreted by *S. flexneri* (Reviewed in Parsot (2009)), and some of these effector proteins are encoded outside of the T3SS genetic locus. With so many uncharacterised and hypothetical effector proteins associated with the Bsa T3SS, it is clear that more research is required to understand importance these proteins may play in *B. pseudomallei* infection.

1.4 Aims and Objectives

Aims

The aim of this research is to identify novel effector proteins secreted by the *B. pseudomallei* Bsa T3SS and choose one or two effector proteins for further characterisation of the role of these effector proteins in pathogenesis.

Objectives

The following objectives have been set out in order to accomplish the aims of this research;

1. To dysregulate the *B. pseudomallei* Bsa T3SS creating mutants which hyper-secrete effector proteins under standard laboratory conditions.

2. To use quantitative proteomics to identify Bsa T3SS effector proteins secreted by *B. pseudomallei* WT, a mutant lacking a functional T3SS and hyper-secreting mutants.

3. To choose a subset of novel effector proteins identified by the study and use a yeast two-hybrid system to identify human proteins with which they interact.

4. To use relevant biochemical assays and confocal microscopy to further characterise the function of effector proteins.

Chapter 2

Materials and Methods

2.1 Bacterial Strains, Plasmids and Culture Media

Bacterial strains and plasmids are listed in Table 7.1. Bacteria were routinely cultured at 37°C on LB agar (Miller) or LB broth (Lennox), except for during sucrose counter selection when 15% sucrose LB agar plates (10 g/L tryptone, 5 g/L yeast extract, 150 g/L sucrose, 15 g/L agar, water to 1 L, pH 7.4) were incubated at 28°C. Antibiotic selection was performed at the following concentrations unless otherwise stated: ampicillin (Amp) 100 μg/ml, kanamycin (Kan) 50 μg/ml, chloramphenicol (Cm) 34 μg/ml, and tetracycline (Tet) 15 μg/ml. Isopropyl-β-D-thiogalactopyranosid (IPTG) was used at a final concentration of 0.5 mM where appropriate. Unless otherwise stated all chemicals were purchased from Sigma Aldrich (Dorset, UK). Eukaryotic tissue culture was performed at 37°C in the presence of 5% CO_2. HeLa cells were cultured in Dulbecco's Modified Eagle Medium (DMEM, Gibco) supplemented with 10% heat-inactivated fetal calf serum (FCS), 1% L-glutamine, 100 units/ml penicillin and 100 μg/ml streptomycin.

2.2 Molecular Methods

2.2.1 PCR and Ligations

All gel electrophoresis was performed using 1% tris-acetate-EDTA (TAE) agarose gels. Gel extraction kits (Qiagen), polymerase chain reaction (PCR) purification kits (Qiagen), and Miniprep plasmid purification kits (Qiagen) were used according to the manufacturer's instructions. Primers, purchased from Sigma Aldrich (Dorset, UK), are listed in Table 7.2. Unless otherwise stated,

the standard PCR was composed of: 0.4 U of Phusion polymerase (Thermo Scientific), 1x Phusion GC buffer, 1 μM of each primer , 2.5% dimethyl sulfoxide (DMSO), 200 μM deoxynucleotides (dNTPs), and 10–500 ng of template DNA in a total volume of 20 μl. The reaction conditions used were 98°C for 2 minutes, followed by 30 cycles of (98°C for 10 seconds, 72°C for 1–3 minutes) and one cycle of 72°C for 10 minutes.

PFU polymerase (0.8 U, Promega) was used to amplify regions flanking the *bsaP* gene with 1x PFU buffer, 1 μM of primers bsaP1/bsaP2 or bsaP3/bsaP4, 2.5% DMSO, 200 μM dNTPs, and *B. pseudomallei* 10276 genomic DNA in a total volume of 20 μl. The reaction conditions used were 97°C for 3 minutes, followed by 30 cycles of (97°C for 30 seconds, 68°C for 2.5 minutes) and one cycle of 68°C for 30 minutes. PCR products were then purified using gel electrophoresis and a gel extraction kit. To amplify the ligated bsaP1/bsaP2 and bsaP3/bsaP4 fragments, 0.8 U of PFU polymerase (Promega) was used with 1x PFU buffer, 1 μM of primers bsaP1 and bsaP4, 2.5% DMSO, 200 μM dNTPs, and the ligated product of bsaP1/bsaP2 and bsaP3/bsaP4. The reaction conditions used were 97°C for 3 minutes, followed by 30 cycles of (97°C for 30 seconds, 68°C for 3.5 minutes) and one cycle of 68°C for 30 minutes. PCR products were then purified using gel electrophoresis and a gel extraction kit.

Ligations were performed using 1 U of T4 DNA ligase (Promega), 1x ligation buffer, and 100–300 ng of each of the fragments of DNA to be ligated. Reactions were incubated for 30 minutes at room temperature or at 4°C overnight.

All sequencing of plasmids and PCR products was carried out by Sanger sequencing performed by Source BioScience (Lanarkshire, UK).

2.2.2 Electrocompetent Cells and Transformations

To prepare electrocompetent *E. coli* S17–1 *λpir*, overnight cultures were grown to an OD_{600} of 0.4±0.05 and then chilled on ice for 20 minutes. The cells were centrifuged four times at 3220 relative centrifugal force (RCF) for 10 minutes at 4°C and after each spin the supernatant was discarded and the cells were washed with either sterile water (washes 1 and 2) or 10% glycerol (washes 3 and 4) pre-chilled to 4°C. Individual aliquots were placed in a dry ice-ethanol bath for snap freezing. The cells were stored at –80°C until use.

Transformations of XL1-Blue (Agilent) and One Shot PIR1 (Invitrogen) *E. coli* were performed according to manufacturer's instructions. S17–1 *λpir E. coli* were electroporated with pDM4 constructs using a 0.2 cm cuvette at 2.5 kV, 25

μF, and 200 Ω. Bacteria were recovered in SOC media (0.5% yeast extract, 2% tryptone, 10 mM NaCl, 2.5 mM KCl, 10 mM $MgCl_2$, 10 mM $MgSO_4$, 20 mM glucose) shaking at 200 revolutions per minute (RPM) for 2 hours at 37°C followed by inoculation and overnight growth on LB plates containing the appropriate antibiotics. The resulting resistant colonies were confirmed by re-streaking onto LB plates containing the appropriate antibiotic, overnight growth, and colony PCR. Colonies containing the correct size insert were stored as glycerol stocks at –80°C.

Transformations of *B. pseudomallei* were performed using a method that requires no chilling as previously described (Choi *et al.*, 2006). Overnight cultures were centrifuged three times at 16,000 RCF for 2 minutes in a microcentrifuge and after each spin the bacteria were washed with sterile 300 mM sucrose. To 50 μl of bacteria, 2 μl of intact plasmid (about 1.5 μg) was added. Using a 0.1cm cuvette an electroporation was performed at 1.8 kV, 25 μF, and 200 Ω. Bacteria were recovered in SOC media shaking at 200 RPM for 2 hours at 37°C followed by inoculation and overnight growth on LA plates containing the relevant selective antibiotics.

2.2.3 *B. pseudomallei* Mutagenesis

The 10276 Δ*bsaP* in-frame deletion mutant was made using allelic exchange and the *sacB* containing positive-selection suicide vector pDM4 essentially as previously described (Logue *et al.*, 2009). DNA fragments upstream and downstream of *bsaP* (BPSS1544) were amplified by PCR from *B. pseudomallei* 10276 genomic DNA using primer pairs *bsaP-del*-1/*bsaP-del*-2 and *bsaP-del*-3/*bsaP-del*-4 which contain a *Spe*I and *Bgl*II restriction site respectively. The resulting DNA fragments were separated by electrophoresis on a 1% agarose gel, gel purified, and combined using PCR-ligation-PCR (Ali and Steinkasserer, 1995). In brief, the two fragments were phosphorylated to combine the bsaP1/bsaP2 and bsaP3/bsaP4 fragments using 20 U of T4 polynucleotide kinase (Promega), with 1x kinase buffer, 1 mM ATP, and 150 ng of each of the bsaP1/bsaP2 and bsaP3/bsaP4 fragments. The reaction was incubated at 37°C for 30 minutes followed by a 5 minute deactivation at 70°C. The two fragments were ligated together and amplified by PCR. The product was run on a 1% agarose gel and a band of the correct size was cut out and gel purified.

A-tailing was performed to add an adenosine to the blunt-ended PCR product using 3.5 U of Taq polymerase (Invitrogen), 1x Taq buffer, 1.5 mM $MgCl_2$, 1 mM ATP, and 50–100 ng of blunt ended DNA. The reaction was in-

cubated at 70°C for 30 minutes then purified with a PCR purification kit. The fragment was then was then ligated into pGEM-T resulting in the plasmid pGEM-T-Δ*bsaP*. The plasmid was transformed into XL1-Blue *E. coli* according to the manufacturers instructions and the bacteria were plated onto LB plates containing Amp. pGEM-T-Δ*bsaP* was isolated from the Amp resistant colonies using a miniprep kit and the insert was sent for Sanger sequencing (Source Bioscience) using T7-Forward and SP6 primers. A restriction digest was performed with *Spe*I and *Bgl*II on pGEM-T-Δ*bsaP* and the *Spe*I and *Bgl*II digested fragment containing the 10276 *bsaP* deletion was ligated into similarly digested pDM4, resulting in pDM4-Δ*bsaP*. To propagate larger amounts of pDM4-Δ*bsaP,* the plasmid was transformed into TOP 10 PIR1 cells (Life Technologies, Paisley, UK), a higher copy number strain, according to manufacturer's instructions, and then plated onto LB plates containing Cm. The pDM4-Δ*bsaP* plasmid was isolated with a miniprep kit and transformed into *E. coli* S17–1 *λpir* conjugal donor with selection for Cm resistance.

pDM4-Δ*bsaP* was introduced into *B. pseudomallei* strain 10276 by conjugation with *E. coli* S1–17 *λpir*. Conjugation between *B. pseudomallei* strain 10276 and *E. coli* S1–17 *λpir* was performed as previously described (Stevens *et al.*, 2002). In brief overnight cultures were grown of *E. coli* S1–17 *λpir* containing pDM4-Δ*bsaP* and *B. pseudomallei* strain 10276. The following day, the OD_{600} was measured and cultures were used if their absorbance was between 0.6 and 0.8. If the absorbance was too high, the cultures were sub-cultured into fresh media and grown for a further 2–3 hours until the OD_{600} was in the correct range. The following mixtures were then set up in universals containing 5 ml of filter sterilised 10 mM $MgSO_4$: a) 500 μl S1–17 *λpir* pDM4-Δ*bsaP,* b) 500 μl S1–17 *λpir* pDM4-Δ*bsaP* + 500 μl *B. pseudomallei* 10276 WT. The mixtures were gently mixed and run through sterile 0.22 μm nylon filters. The filters were removed and placed on a LB plate, bacteria side up, and incubated overnight at 37°C. The filter was then placed in 500 μl of sterile LB broth, vortexed for 15 seconds, and dilutions of the turbid solution were plated onto LB plates with Cm (50 μg/ml) and Kan (50 μg/ml) to select for B. *pseudomallei* with pDM4-Δ*bsaP* integrated into the chromosome by homologous recombination. Colonies were re-patched onto LA plates containing Cm (50 μg/ml) and Kan (50 μg/ml) to confirm resistance. Overnight cultures of the Cm resistant (Cm^r) colonies were cultured in LB broth without selection to allow for a second round of homologous recombination to take place, either restoring the full length *bsaP* gene, or resulting in *bsaP* deletion. To select for double

recombinants lacking pDM4-Δ*bsaP,* the overnight cultures were plated, 100 μl of neat, 10^{-1}, and 10^{-2} dilutions, onto 15% sucrose plates lacking NaCl and cultured at 28ºC for three days. Chromosomal deletion of *bsaP* was confirmed in sucrose resistant/Cm^s colonies by colony PCR and the resulting strain designated 10276 Δ*bsaP*, where the *bsaP* gene has been replaced by an in-frame start-stop (atg-taa) cassette.

2.2.4 Complementation of the Δ*bsaP* Mutant

For complementation of the Δ*bsaP* mutant the 10276 *bsaP* sequence was amplified by PCR using the forward primer *bsaP-exp-F* containing a *Cla*I restriction site and a ribosome-binding site and the reverse primer *bsaP-exp-R* containing a *Hind*III restriction site. The PCR fragment was cloned into pBHR1 (MoBiTec, 2B Scientific Ltd., Oxford, UK) to create pBHR1-*bsaP*. The plasmid was purified and transformed into *B. pseudomallei* 10276 Δ*bsaP* using the fast sucrose method of electroporation, creating strain 10276 Δ*bsaP*-p*bsaP*.

2.2.5 Cloning of Candidate Effectors to Express c-Myc Epitope Fusion Proteins

The coding region for candidate effectors based on the *B. pseudomallei* K96243 genome sequence were amplified from *B. pseudomallei* 10276 genomic DNA by PCR with a 5′ forward primer containing a ribosome-binding site and a 3′ reverse primer encoding an in-frame c-Myc tag followed by a stop codon. Each primer also contained a restriction site suitable for directional insertion into the vector pME6032. Plasmids were transformed into *E. coli* and the inserts sequenced. Purified plasmids were then transformed into *B. pseudomallei* 10276, 10276 *bsaZ*::pDM4, 10276 *bipD*::pDM4 and 10276 Δ*bsaP*.

2.3 General Protein Methods

2.3.1 Preparation of Bacterial Supernatants

Preparation of *B. pseudomallei* supernatants was performed by centrifuging overnight cultures of *B. pseudomallei* or the appropriate derivatives at 3220 RCF for 10 minutes at 4ºC, followed by disposal of the supernatant and resuspension of the bacteria in fresh LB to an OD_{600} of 1.0. Of the bacterial suspension, 1 ml was added to a new culture of 10 ml of fresh LB with the

appropriate antibiotics and IPTG, if needed, or the appropriate media. If required a sample was removed from the culture for serial dilutions and growth on LA plates to determine the starting bacterial count in a sample. The culture was incubated for 6 hours shaking at 225 RPM at 37°C. At the end of the 6 hours, if required, another sample was removed for dilutions and grown on LA plates for a final bacterial count. The sample was chilled on ice for 15 minutes and then centrifuged at 3220 RCF for 20 minutes at 4°C. The supernatant was collected and centrifuged a second time at 3220 RCF for 20 minutes at 4°C. The supernatant was passed through a 0.2 μm low protein binding cellulose acetate membrane filter (Millipore, Watford, UK) and stored at –20°C until use. For the investigation of induction conditions the bacteria were incubated in one of the following media: Lennox LB, LB with 0 mM NaCl, LB with 320 mM NaCl, trypticase soy broth (17 g/L enzymatic digest of casein, 3 g/L enzymatic digest of soybean meal, 5 g/L NaCl, 2.5 g/L K_2HPO_4, 2.5 g/L dextrose, pH 7.3), and LB containing 10 mM EGTA.

To prepare *S. flexneri* supernatants, overnight cultures of *S. flexneri* were centrifuged at 3220 RCF for 10 minutes at 4°C followed by disposal of the supernatant and re-suspension of the bacteria in fresh LB to an OD_{600} of 1.0. Of the bacterial suspension, 3 ml was added to a new culture of 20 ml of fresh LB. The culture was incubated for 4 hours shaking at 225 RPM at 37°C. The sample was chilled on ice for 15 minutes and then centrifuged at 3220 RCF for 20 minutes at 4°C. The supernatant was passed through a 0.2 μm low protein binding membrane filter cellulose acetate membrane filter and stored at –20°C until use.

2.3.2 Protein Precipitation

Proteins precipitation using a pyrogallol red-molybdate methanol (PRMM) solution was performed as previously described (Caldwell and Lattemann, 2004). In brief, equal volumes of bacterial culture supernatant and PRMM solution (0.5 mM pyrogallol red (Alfa Aesar), 0.16 mM sodium molybdate, 1.0 mM sodium oxalate, 50 mM succinic acid, 20% MeOH, pH to 2.0 w/HCl) were thoroughly mixed and the pH was adjusted to 2.8$\pm$0.1 with HCl. The samples were then precipitated at room temperature for one hour followed by overnight at 4°C. The resulting purple-blue precipitate was centrifuged at 3220 RCF, 4°C for 1 hour and the supernatant was discarded. The pellet was washed twice with acetone pre-chilled to –20°C and allowed to air dry. The protein pellet was then solubilised in freshly made 50 mM ammonium bicar-

bonate. Proteins were quantified using a Direct Detect Infrared Spectrometer (Millipore, Watford, UK) or with a bicinchoninic acid (BCA) protein assay kit (Pierce) using Quick Start bovine serum albumin (BSA, BioRad) to prepare a standard curve. Protein samples were stored at –20°C until use.

Trichloroacetic acid (TCA) precipitation was performed with and without deoxycholate (DOC). If DOC was used in the precipitation, DOC was added to the bacterial culture supernatant to a final concentration of 0.02% (w/v) and incubated at 4°C for 30 minutes. TCA precipitation was carried out by adding 100% TCA to bacterial culture supernatant to a final concentration of 10–15% followed by overnight incubation at 4°C. The samples were then centrifuged four times at 3220 RCF for 15 minutes at 4°C and the first three spins were followed by a wash with acetone pre-chilled to –20°C. After the final spin the supernatant was removed and the pellet was allowed to air dry, and then suspended in an appropriate volume of Laemmli buffer (0.2% bromophenol blue, 20% glycerol, 100 mM Tris pH 8.8, 4% SDS, 2% β-mercaptoethanol). Proteins were stored at –20°C until use.

Protein purification using Stratagene beads was performed by adding Stratagene beads at a ratio of 1:1000 v/v to bacterial culture supernatant and then mixed and incubated for 15 minutes with shaking at room temperature followed by centrifugation at 3220 RCF for 5 minutes. The beads were washed with phosphate-buffered saline (PBS), followed by another centrifugation to remove the PBS. The beads were then suspended in Laemmli buffer and heated to 90°C for 5 minutes followed by storage at –20°C until use.

2.3.3 SDS-PAGE and Immunoblotting

Proteins were separated using sodium dodecyl sulphate polyacrylamide gel electrophoresis (SDS-PAGE). Equal volumes of protein samples and Laemmli buffer were mixed and heated to 90°C for 5 minutes. Samples were separated on Any kD™ Mini-PROTEAN TGX gels (Bio-Rad, Hemel Hempstead, UK) or 4-12% TGX gels (Novex) in Tris-Glycine running buffer. Proteins were visualised by Coomassie staining. To visualize proteins by Coomassie staining, gels were submerged in Coomassie staining solution (0.25 g/L Coomassie Blue G–250, 45% MeOH, 10% acetic acid) for 1 hour, washed twice for 15 minutes in destaining solution (45% MeOH, 10% acetic acid), followed by further destaining in deionised H_2O overnight.

Western blots were used to visualise proteins of interest. Proteins were transferred onto a nitrocellulose or PVDF membrane using the Trans-Blot

Turbo semi-dry transfer system (Bio-Rad, Hemel Hempstead, UK) or a Trans-blot SD semi-dry transfer system (Bio-Rad). A list of all antibodies used in this study are listed in Table 7.3. α-BopE (Stevens *et al.*, 2003), α-BipD (Stevens *et al.*, 2004), or α-cMyc (Insight Biotechnology, Wembley, UK) rabbit polyclonal antibodies were used at 1 μg/ml. For detection by infrared fluorescence, goat-α-rabbit IgG (H+L) (DyLight^{TM} 800 Conjugate) was used at a 1:10,000 dilution (Cell Signalling Technology, Hitchin, UK). Blots were visualised using an Odyssey Infrared Imaging System (LI-COR Biosciences, Cambridge, UK) according to the manufacturer's instructions. Images were captured and analysed using Image Studio Lite (LI-COR Biosciences, Cambridge, UK). The membrane was then blocked for 1 hour in tris-buffered saline tween (TBS-T, 0.1% tween 20) with 5% BSA followed by three 15 minute washes in TBS-T. The membrane was then incubated with 1 μg/ml of primary antibodies, α-BopE (Stevens *et al.*, 2003) or α-BipD (Stevens *et al.*, 2004) rabbit polyclonal antibodies for 1 hour. The membrane was washed once for 15 minutes in TBS-T followed by two 5 minute washes in TBS-T and then incubated for 1 hour with horseradish peroxidase (HRP) linked goat α-rabbit IgG used at a 1:10,000 dilution (Invitrogen). The membrane was then washed one time for 15 minutes in TBS-T and then four times for 5 minutes in TBS-T. Enhanced chemiluminescence (ECL) reagent (GE Healthcare) was used according to manufacturer's instructions and the blot was visualized using the G-Box imaging system (Syngene) or following exposure to film (GE Healthcare).

2.3.4 Preparation of Glutathione S-Transferase-Fusion Proteins

To prepare the glutathione (GSH)-linked sepharose beads, 400 μl of GSH-linked sepharose 4B beads (GE healthcare) 50% v/v in PBS (137 mM NaCl, 2.7 mM KCl, 10 mM Na_2HPO_4, 2 mM KH_2PO_4) were centrifuged at 16,000 RCF in a microcentrifuge for 1 minute, the supernatant was removed, and the beads were re-suspended in 1 ml of sterile PBS. The wash was repeated 4 times and after the final spin a re-suspension volume of 200 μl was used. The washed GSH-linked sepharose beads were stored at 4^{o}C for up to two weeks until use.

To create proteins with N-terminal glutathione S-transferase (GST)-fusions, genes encoding proteins of interest were cloned into the vector pGEX-4T-1. The vector was transformed into *E. coli* Rosetta BL21 (Novagen). XL1-Blue *E. coli* containing pGEX-BipC, pGEX BapA, pGEX-SipC, pGEX-BimA, pGEX-

BopE or empty pGEX were inoculated into 5 ml of LB containing Amp and grown overnight shaking at 37°C. The following day 5 ml of the bacterial culture was used to inoculate 250 ml of LB containing Amp which was then incubated for 3 hours shaking at 37°C. The culture was then removed from the incubator and allowed to cool for 20 minutes to room temperature and IPTG was added to a final concentration of 0.5 mM followed by incubation for 3 hours at 37°C. Due to solubility concerns, for GST-BapA 2 mM IPTG was used and the culture was induced overnight shaking at 16°C. The bacteria were collected by centrifuging the culture at 3,220 RCF and removing the supernatant. The remaining bacterial pellet was lysed at 4°C with 5 ml of Bug Buster master mix (Merck Millipore) rocking for 1 hour or until the solution became clear. The insoluble fraction was removed by centrifuging at 10,000 RCF for 10 minutes at 4°C and discarding the pellet. Washed GSH-linked sepharose beads (200 μl 50% v/v in PBS) were added to the bacterial lysate which was then incubated at 4°C for 1 hour with agitation. The beads were centrifuged at 3,220 RCF for 5 minutes at 4°C, the supernatant was discarded and the beads were transferred to a microcentrifuge tube. The beads were then washed 8 times with 1 ml of ice cold NP–40 lysis buffer using a microcentrifuge at 16,000 RCF for 1 minute and discarding the supernatant after each wash. The beads were then re-suspended in an equal volume of cold sterile PBS (about 100 μl) and either used immediately for a pull-down or were stored at 4°C for up to 2 weeks before use.

When necessary, to elute the GST-fusion proteins from the GSH-linked sepharose beads, the beads were re-suspended in 200 μl of elution buffer (20 mM reduced GSH, 50 mM Tris, pH 8.0) in a microcentrifuge tube and incubated for 1 hour at room temperature with agitation. To remove the sepharose beads, the microcentrifuge tube was centrifuged at 16,000 RCF and the supernatant containing the eluted protein was transferred to a new microcentrifuge tube. The elution was performed 2 more times and the three sets of supernatants were combined. The solution was dialysed three times in 1000 volumes of PBS for a minimum of 2 hours each time to remove the detergents and salts from the eluted protein. The dialysed protein was concentrated using a 10 kD cut-off spin column centrifuged at 16,000 RCF for 30 minutes or until the final volume was about 200 μl. The protein concentrations where determined using the Bradford assay (Pierce Scientific). Proteins were aliquoted and stored at –80°C until use.

To bind proteins eluted from GSH-linked sepharose beads to UltraLink Bio-

support resin (Thermo Scientific), 0.02 g of UltraLink resin and 40 μl of 3 M sodium citrate was added to 200 μl of eluted GST-fusion protein. After incubation for 1 hour at room temperature with agitation, ten bead volumes of quench solution (3 M ethanolamine, pH 9.0) was added followed by an incubation for 2.5 hours with agitation at room temperature. The mixture was centrifuged for 10 minutes at 3,220 RCF, supernatants were discarded and 10 bead volumes of PBS was added followed by another 15 minute incubation at room temperature with agitation. The mixture was centrifuged for 10 minutes at 3,220 RCF, supernatants were discarded, and 1 ml of 1 M NaCl was added. After 15 minutes incubation with agitation at room temperature, the mixture was centrifuged for 10 minutes at 3,220 RCF, supernatants were discarded and 10 bead volumes of PBS was added followed by another 15 minute incubation at room temperature with agitation. This wash step was repeated one more time after which the beads were stored at 4^{o}C until use.

2.3.5 Pull-Down Assays With Eukaryotic Cell Lysates

HeLa Cell Lysate Pull-Downs

To confirm interactions seen in the yeast two-hybrid (Y2H) system with the proteins of interest (BipC and BapA) as well as to test BipC-actin interactions in the absence of polymerisation buffer, pull-downs were performed with GST-fusion proteins and HeLa cell lysates. HeLa cells were grown until confluent in a 150 mm flask. The flask was immediately placed on ice and the culture media was remove and, the cells were washed with ice cold sterile PBS. Cells were then lysed in 1.5 ml of ice cold sterile NP–40 lysis buffer (20mM Tris, pH 8; 150 mM NaCl, 20 μM leupeptin, 1 mM PMSF, 1 mM NaF, 1 mM B-glycerophosphate, 2 mM sodium orthovanadate, 2 mM EDTA, 10% glycerol, 1% NP–40) and a sterile cell scraper was used to disrupt the adherent cells. After 10 minutes of lysis, the liquid in the culture flask was removed and placed into a pre-chilled sterile 1.5 ml microcentrifuge tube. The cell lysates were incubated at 4^{o}C for a further 30 minutes with agitation followed by centrifugation at 16,000 RCF for 20 minutes in a microcentrifuge pre-chilled to 4^{o}C. The pellet was discarded and to clear the lysates, 50 μl of washed sepharose beads 50% v/v in PBS chilled to 4^{o}C were added to the supernatant and incubated for 30 minutes at 4^{o}C rotating. The lysate bead mixture centrifuged for 1 minute at 16,000 RCF in a microcentrifuge and the supernatants were collected. The supernatants were either used immediately for a pull-down, or were stored at

–80°C until further use.

To perform the pull down experiment, 100 μl of beads bound to bacterial proteins 50% v/v in PBS was added to 1 ml of cleared HeLa cell lysates in a microcentrifuge tube which was incubated overnight at 4°C rotating. The beads were then collected by spinning at 16,000 RCF in a microcentrifuge and were washed 8 times with ice cold NP–40 buffer in a similar fashion. One final spin was performed, the supernatant was removed, and 50 μl of 2x Laemmli buffer was added. The beads were then boiled at 95°C for 5 minutes to denature the proteins, and then stored at –20°C until use in downstream applications. To probe the pull downs for the proteins of interest, PAWR and c1QBP, 5–10 μl of the bead and Laemmli buffer mixture was loaded onto a 4–15% TGX gel for SDS-PAGE in duplicate. One gel was stained using Coomassie brilliant blue to visualise all proteins. From the other gel, proteins were transferred onto a nitrocellulose membrane, and a Western blot was performed with rabbit α-PAWR and rabbit α-C1QBP primary antibodies and goat α-rabbit 800 DyLight secondary antibody. The Western blots were visualised using the Odyssey imaging system.

A549 Cell Lysate Pull-Downs

To prepare lysates of A549 cells, 75 mm flasks containing confluent A549 cells were washed with PBS and then treated with typsin for 3 minutes to detach the adherent cells. Cells were collected in a 15 ml falcon tube and washed once with PBS followed by incubation in 5 ml of 2x NP–40 at room temperature for 5 minutes. Insoluble material was removed by centrifuging for 10 minutes at 3,220 RCF.

Lysates were incubated with GST-BopE, GST-BipC and GST bound to GSH-linked sepharose beads for 1 hour at room temperature with agitation followed by five washes in ice cold PBS after which 50 μl of 2x Laemmli buffer was added. The beads were then boiled at 95°C for 5 minutes to denature the proteins, and then stored at -20°C until use in downstream applications. Proteins were visualised by SDS-PAGE using a 4–15% TGX gel followed by Coomassie or silver staining (Pierce Scientific).

Murine Splenic Lysate Pull-Downs

Pull-downs with murine splenic lysates (MSLs) were performed using dilutions of 10 x polymerisation buffer (G-Mg buffer supplimented with 1 x

K50MEI buffer). G-Mg buffer (2 mM Tris – pH 8, 0.5 mM DTT, 0.2 mM ATP, 0.1 mM $MgCl_2$, 0.01% NaN_3) and K50MEI buffer (500mM KCl, 10Mm $MgCl_2$, 10 mM EGTA, 100 mM imidazole – pH 7.0) were pre-prepared and stored at -20°C until use. Spleens from BALB/c or C57BL/6J mice were stored at -80°C until use. To prepare MSLs, the spleens were thawed on ice and then rinsed briefly in ice-cold 1 x polymerisation buffer. Up to four spleens were placed in a pre-chilled glass universal or beaker. To the spleens, 1 ml of ice-cold 1 x polymerisation buffer with protease inhibitors (1 mM PMSF, 1 μg/ml pepstatin A, 10 μg/ml leupeptin, 1 μg/ml aprotinin) was added per spleen. The spleens were homogenized using a tissue homogenizer ensuring the resulting mixture did not heat up. The homogenate was transferred to a plastic falcon tube and was centrifuged at 3,220 RCF for 15 minutes at 4°C to remove the large insoluble material. The remaining supernatant was transferred to an ultracentrifuge tube and centrifuged at 100,000 RCF at 4°C for 2 hours to remove remaining the insoluble material. The supernatant was collected and aliquoted into chilled microcentrifuge tubes and stored at -80°C until use.

To perform pull downs with the MSLs, a 500 μl aliquot of MSLs was defrosted on ice. It was diluted to a final volume of 2 ml with 1 x polymerisation buffer and $CaCl_2$ was added to a final concentration of 100 μM followed by thorough mixing. The GST-fusion proteins of interest (BopE, BimA, BipC, SipC and GST) bound to GSH-linked sepharose beads were added to microcentrifuge tubes containing 200 μl of MSL in polymerisation buffer followed by incubation for 1 hour at room temperature with agitation. The sepharose beads were then washed 5 times with ice-cold PBS by centrifuging at 16,000 RCF and removing the supernatant. To the beads, 10 μl of 2x Laemelli buffer was added, the samples were boiled for 5 minutes at 95°C and stored at -20°C until use. Proteins were analysed by SDS-PAGE using a 4-12% TGX gel. The proteins were then visualised by Coomassie blue staining of Silver staining. For immunoblotting, proteins were transferred to PVDF membranes and visualised using rabbit α-Cdc42, rabbit α-Rac1 and goat α-actin primary antibodies followed by goat α-rabbit or rabbit α-goat HRP-linked secondary antibodies. The antibodies were detected using ECL followed by film exposure.

2.4 iTRAQ Quantitative Proteomics

2.4.1 iTRAQ Experimental Design

Bacterial culture supernatants of *B. pseudomallei* 10276, 10276 *bsaZ::*pDM4, 10276 *bipD::*pDM4, and 10276 Δ*bsaP* were generated in three independent experiments. Equal amounts of protein from each replicate were combined creating a single pooled sample for each strain. These samples were sent to Dundee Cell Products where they were enzymatically digested, peptides were labelled using isobaric tag for relative and absolute quantitation (iTRAQ) reagents, and then pooled and submitted to liquid chromatography and tandem mass spectrometry (LC MS/MS) in three technical replicates as follows.

2.4.2 Protein Digestion and Peptide Fractionation

Protein samples were prepared for MS analysis using a protocol adapted from Boisvert *et al.* (2010). Following protein quantification, samples were reduced in 10 mM dithiothreitol (DTT) and alkylated in 50 mM iodoacetamide prior to boiling in loading buffer, and then separated by one-dimensional SDS-PAGE (4–12% Bis-Tris Novex mini-gel, Invitrogen) and visualized by colloidal Coomassie staining (Novex, Invitrogen). The entire protein gel lanes were excised and cut into 10 slices each. Every gel slice was subjected to in-gel digestion with trypsin overnight at 37ºC (Boisvert *et al.*, 2010). The resulting tryptic peptides were extracted using formic acid (FA, 1%) and acetonitile (ACN), lyophilized in a speedvac and resuspended in 1% formic acid.

2.4.3 Peptide Concentration

To determine the concentration of the peptides, the dried samples were resuspended in 100 mM triethylammonium bicarbonate (TEAB) 1 M ACN. To determine the volume of sample needed for an even protein load across all samples, 1 μl was injected onto an LTQ Velos Mass Spectrometer (Thermo Fisher Scientific, MA, USA) and the total ion current (TIC) trace was used.

2.4.4 iTRAQ Labelling

Samples were labelled according to the manufacturer's instructions using an iTRAQ Reagents Multiplex kit - 4 plex (AB Sciex UK Ltd., Warrington, UK). To each vial of labelling reagent (labels- 114, 115, 116 & 117), 70 μl ethanol was

added, after which they were vortexed and centrifuged. A single vial of label was added to a single vial of sample and mixed. The samples used with each label were: 10276 *bsaZ*::pDM4–114, 10276 WT–115, 10276 *bipD*::pDM4–116, and 10276 Δ*bsaP*–117. Samples were incubated with shaking at room temperature for 1 hour, after which 100 μl of water was added and incubated for a further hour. The 4 vials of labels/samples were pooled into one vial and then dried under vacuum. Samples were desalted using a standard method.

2.4.5 SCX Fractionation and Salt Cuts

To a Millipore (Watford, UK) C18 ziptip, 10 μl Poros HS resin (Life Technologies, Paisley, UK) was added and washed with 3 x 25 μl Buffer A (35% ACN, 0.1% FA). Samples were re-suspended in Buffer A and loaded onto the resin, washed with 3 x 25 μl Buffer A, and eluted with 2 x 25 μl of each of 11 salt cuts ranging from 5 mM to 800 mM NaCl. A final elution was performed using 2 x 25 μl 50% isopropanol, 0.4% ammonium hydroxide. Samples were centrifuged and speed vacuumed until dry. Samples were re-suspended in 1% FA and pooled as six samples containing the salt cuts as follows: JS–1 (5 mM, 10 mM, 20 mM), JS–2 (50 mM), JS–3 (100 mM), JS–4 (15 0mM), JS–5 (200 mM), JS–6 (250 mM, 300 mM, 400 mM, 80 mM).

2.4.6 Mass Spectrometry

Peptides were separated using an Ultimate 3000 RSLC nanoflow LC system (Thermo Fisher Scientific, MA, USA). With a constant flow of 5 μl/minute, 15 μl of sample was loaded onto an Acclaim PepMap100 nanoViper C18 trap column (100 μm inner-diameter, 2 cm) (Thermo Fisher Scientific, MA, USA). After trap enrichment, peptides were eluted onto an Acclaim PepMap RSLC nanoViper, C18 column (75 μm, 15 cm) (Thermo Fisher Scientific, MA, USA) with a linear gradient of 2–45% solvent B (80% ACN with 0.08% FA) over 125 minutes with a constant flow of 300 nl/minute. The high-performance liquid chromatography (HPLC) system was coupled to a linear ion trap Orbitrap hybrid mass spectrometer (LTQ-Orbitrap Velos) (Thermo Fisher Scientific, MA, USA) via a nanoelectrospray ion source (Thermo Fisher Scientific, MA, USA). The spray voltage was set to 1.2 kV and the temperature of the heated capillary was set to 250°C. Full-scan MS survey spectra (m/z 335–1800) in profile mode were acquired in the Orbitrap with a resolution of 60,000 after accumulation of 1,000,000 ions. The ten most intense peptide ions from the preview scan

in the Orbitrap were fragmented sequentially by higher-energy collisional dissociation (HCD) (two-step (6%) normalised collision energy (NCE), 40%; and activation time, 0.1 ms) prior to analysis in the Orbitrap after accumulation of 50,000 ions. Maximal filling times were 500 ms for the full scans and 200 ms for the MS/MS scans.. Precursor ion charge state screening was enabled, and all unassigned charge states as well as singly charged species were rejected. The lock mass option was enabled for survey scans to improve mass accuracy (Olsen *et al.*, 2005). Data were acquired using the Xcalibur software (Thermo Fisher Scientific, MA, USA).

2.4.7 Quantification and Bioinformatic Analysis

The raw mass spectrometric data files obtained for each experiment were collated into a single dataset using Proteome Discoverer (Thermo Fisher Scientific, MA, USA) and the Mascot search engine (www.matrixscience.com) using a translated *B. pseudomallei* K96243 genome as a reference for protein identification. Enzyme specificity was set to that of trypsin, allowing for cleavage N-terminal to proline residues and between aspartic acid and proline residues. Other parameters used were: (i) variable modifications, methionine oxidation, protein N-acetylation, gln pyro-glu; (ii) fixed modifications, cysteine carbamidomethylation; (iii) database: *B_pseudomallei_* K96243_20120601; (iv) iTRAQ labels: standard iTRAQ 4-plex quant method with labels 114–117; (v) MS/MS tolerance: FTMS- 10 ppm, FTMS/MS- 0.06 Da; (vi) minimum peptide length, 6; (vii) maximum missed cleavages, 2; (viii) false discovery rate, 1%. Peptide ratios were calculated for samples using the 10276 *bsaZ*::pDM4–114 label as the denominator. Protein ratios were normalised using the overall median ratio for all quantified proteins in each sample based on the assumption the abundance of a majority of secreted proteins remain unchanged in each condition. Proteins were selected as potential T3SS effector protein candidates if they had at least 2 unique peptides used in quantification with a MASCOT peptide score of over 21, which corresponds to the threshold value for a 95% confidence level (a 1 in 20 chance that the match is random), and a "high" iTRAQ ratio in at least one strain, which we defined as a value greater than 1.5 X inner quartile range (IQR). When n = complete set of ratios over 10276 *bsaZ*::pDM4 for all quantified proteins in a given sample, IQR is defined as:

$$IQR = Q_3 - Q_1$$

where

$$Q_3 = (\frac{3(n+1)}{4})^{th}term$$

and

$$Q_1 = (\frac{(n+1)}{4})^{th}term$$

2.5 *Saccharomyces cerevisiae* Strains

Saccharomyces cerevisiae strains were grown at 30°C on either yeast extract peptone dextrose (YPD) agar, YPD broth (20 g/L peptone (oxoid), 10 g/L yeast extract, glucose at 2% final concentration, water to 1 L, pH 6.5). If selection was required, yeast strains were instead grown in either SD agar (6.7 g/L yeast nitrogen base without amino acids, 20 g/L agar (Invitrogen), glucose at 2% final concentration, amino acid supplements (Clontech), water to 1 L, pH 5.8) or synthetic defined (SD) broth (6.7 g/L yeast nitrogen base without amino acids, glucose at 2% final concentration, amino acid supplements (Clontech), water to 1 L, pH 5.8). The amino acids were added in the following concentrations: L-adenine hemisulfate salt 20 mg/L, L-arginine HCl 20 mg/L, L-histidine HCl monohydrate 20 mg/L, L-isoleucine 30 mg/L, L-leucine 100mg/L, L-lysine HCl 30 mg/L, L-methionine 20 mg/L, L-phenylalanine 50 mg/L, L-threonine 200 mg/L, L-tryptophan 20 mg/L, L-tyrosine 30 mg/L, L-uracil 20 mg/L, L-valine 150 mg/L. The amino acids Trp, Leu, Ade and His were excluded from SD media where appropriate to select for plasmids encoding the amino acids. The nomenclature for SD media lacking an amino acid is SD/-(amino acid). For example, SD media lacking Trp, Leu, Ade and His is written SD/-Trp/-Leu/-Ade/-His. Kan was used at a final concentration of 50 μg/ml in all yeast media. X-α-Gal (Clontech) was dissolved at 20 mg/ml in DMF and stored at –20°C in the dark. For blue/white colony screening 200 μl of X-α-Gal was spread onto 10 cm SD plates and allowed to dry before streaking of yeast strains.

2.6 *S. cerevisiae* Molecular Methods

2.6.1 *S. cerevisiae* DNA and Protein Extraction

To extract DNA from yeast, 20 μl of 0.02 M NaOH was added to a PCR tube along with a partial colony of *S. cerevisiae* (until cloudy). The yeast suspension was then boiled in a PCR cycler at 99°C for 10 minutes to lyse the yeast. The resulting yeast lysates were were stored at –20°C until use as a template at a 1:20 final concentration in PCR reactions.

Extraction of plasmids from yeast grown in liquid or on solid media was performed using the Zymoprep yeast plasmid miniprep II kit (Zymo Research) according to the manufacturers instructions. The kit uses zymolase to lyse the yeast and plasmids were eluted from the spin columns with DNAase free water.

Yeast glycerol stocks were made by suspending a colony of yeast in 200 μl of sterile water, vortexing thouroughly, and then adding 200 μl of sterile 50% PBS/glycerol. Glycerol stocks were stored at –80°C until later use.

To extract protein from yeast, 5 ml cultures were grown shaking overnight at 30°C. The cultures were then centrifuged at 1,000 RCF, the supernatant was discarded, and the pellet was resuspended in 2 ml of YeastBuster protein extraction reagent containing 1 x tris(hydroxypropyl)phosphine (THP) and 25 U/ml Benzonase Nuclease (Merck Millipore). After a 30 minute incubation, or until the solution was clear, an equal volume of 2x RSTB was added to the lysates and the mixture was heated at 95°C for 10 minutes. Protein extracts were stored at –20°C until their use in downstream applications.

2.6.2 *S. cerevisiae* Transformations

Plasmids were transformed into *S. cerevisiae* AH109 using a protocol similar to that described in Gietz and Woods (2002). A single colony about 2 mm in size of the *S. cerevisiae* AH109 strain to be transformed was inoculated into 5 ml of YPD broth, or the appropriate dropout media, and was grown overnight shaking at 30°C . The following day, the yeast culture was centrifuged at 1,000 RCF, the supernatant was discarded, and the pellet was resuspended in 1 ml of sterile water and added to a 1.5 ml microcentrifuge tube. The yeast was centrifuged again at full speed in a microcentrifuge (16,000 RCF) for 30 seconds and the supernatant was discarded. Single stranded herring sperm carrier DNA (10 mg/ml, Clontech) was pre-boiled at 99°C for 5 minutes then

immediately put into an ice bath. Reagents were added to the pellet in the following order with mixing after each addition: 240 μl of filter sterilized PEG BioUltra 3,500 (Sigma) 50% w/v in water, 36 μl 1.0 M LiAc, 10 μl chilled herring sperm carrier DNA, 1 μg plasmid DNA (containing the insert of interest), sterile water to a total of 360 μl of liquid added to the yeast pellet (about 60–70 μl depending on plasmid concentration). The transformation mixture was then incubated in a 42°C water bath for 3 hours after which it was pelleted in a microcentrifuge at 16,000 RCF for 30 seconds. The supernatant was discarded and the pellet was resuspended in 1 ml of sterile water by disrupting with the pipette tip and vortexing thoroughly. The re-suspended yeast was spread onto SD plates lacking the appropriate amino acids using 100 μl of neat and a 10^{-1} dilution and then incubated overnight at 30°C. Resulting colonies were re-streaked onto SD plates lacking the appropriate amino acids and incubated overnight at 30°C. Colonies were confirmed to contain the correct plasmid by colony PCR and glycerol stocks were made.

2.6.3 Cloning of Yeast Two-Hybrid Bait Proteins

Primers were designed to amplify each gene of interest, BprD (BPSS1521), BapA(BPSS1528), and BipC(BPSS1531), in their full length adding an *Nde*I restriction site using the forward primer and a *Bam*HI restriction site using the reverse primer. Genes were amplified from *B. pseudomallei* 10276 genomic DNA. The standard PCR cycle conditions were used and the product was run on a 1% agarose gel, imaged, and the band corresponding to the correct size was cut out and purified. The DNA fragments were then quantified and then both the fragments and the plasmid pGBKT7 were submitted to a double digest using *Nde*I and *Bam*HI at 27°C for 1 hour. The digested products were run on a 1% agarose gel, the correct sized bands were cut out, and gel purified. A ligation was performed with T4 DNA ligase overnight at 4°C and the ligation product was transformed into XL1-Blue *E. coli*. After 2 hours of recovery shaking at 37°C, the *E. coli* was plated onto LA plates containing Kan and grown overnight at 37°C. Colonies were selected and re-streaked onto Kan containing LA plates to confirm resistance to the antibiotic. The resulting colonies were grown overnight shaking at 37°C in LB containing Kan. Plasmids for each of the proteins of interest (pGBKT7-*bprD*, pGBKT7-*bapA*, pGBKT7-*bipC*) were extracted from the overnight cultures using a mini-prep kit and then sent for Sanger sequencing using the T7 Forward and 3' DNA-BD. Sequences were compared to that of *B. pseudomallei* K96243 using Blast P and plasmids which

showed no amino acid differences to K96243, or other strains of *B. pseudomallei*, were chosen for use in the Y2H testing and the corresponding strains of XL1-Blue *E. coli* were stored at –80ºC as glycerol stocks.

The pGBKT7 plasmids (pGBKT7-*bprD*, pGBKT7-*bapA*, pGBKT7-*bipC*) were transformed into *S. cerevisiae* AH109 and colonies containing the plasmids were selected by inoculation onto SD/-Trp plates. Colonies were confirmed to contain the correct plasmid by colony PCR. To ensure the proteins of interest were being expressed in *S. cerevisiae* AH109, protein extracts were made and were run on a 4–15% TGX gel by SDS-PAGE. The proteins were transfered to a nitrocellulose membrane and visualized by Western blot using a rabbit α-c-Myc primary antibody and a goat α-rabbit secondary antibody. Colonies showing bands at the correct size were stored at –80ºC as glycerol stocks until use in Y2H testing.

In order to test for auto activation of the Y2H reporter genes by the bait proteins, the *S. cerevisiae* AH109 strains containing pGBKT7-*bprD*, pGBKT7-*bapA*, pGBKT7-*bipC* were plated onto both SD/-Trp/X-α-Gal and SD/-Trp/-Ade/-His/X-α-Gal and grown for 2–3 days at 30ºC. Colonies were compared to controls and checked for growth on each media as well for presence or absence of blue colony color. The size of colonies on SD/-Trp/X-α-Gal were also compared to colonies of *S. cerevisiae* AH109 pGBKT7 that were plated simultaneously to test for toxicity of the bait protein to the yeast.

2.7 Yeast Two-Hybrid

2.7.1 Yeast Two-Hybrid Media and Controls

The three putative proteins of interest submitted to Y2H screening were BprD (BPSS1521), BapA(BPSS1528), and BipC(BPSS1531). Yeast two hybrid was performed using the Matchmaker GAL4 Two-Hybrid System 3 (Clontech) essentially as the manufacturer described.

In order to confirm batches of SD amino acid drop out media used in Y2H screening were stringent and to ensure the Y2H system was performing as expected, control strains of yeast were made and tested. The control plasmids pGBKT7–53 and pGBKT7-Lam were transformed into *S. cerevisiae* AH109 and colonies containing the plasmids were selected by inoculation onto SD/-Trp plates. The control plasmid pGADT7-T was provided by the manufacturer (Clontech) and was plated onto SD/-Leu plates. Control strains were pro-

duced by mating the following combinations of plasmid containing strains using the small scale mating procedure according to the manufacturer's instructions (Clonetech): Positive control: *S. cerevisiae* AH109 pGBKT7–53 and *S. cerevisiae* Y187 pGADT7-T, Negative control: *S. cerevisiae* AH109 pGBKT7-Lam and *S. cerevisiae* Y187 pGADT7-T. Colonies containing both plasmids were selected by inoculation onto SD/-Trp/-Leu plates and glycerol stocks were made for later use. The control strains were then used to test the stringency of the Y2H SD drop out media by looking for growth and blue colony colour on SD/-Trp/-Leu/X-α-Gal and SD/-Trp/-Leu/-Ade/-His/X-α-Gal.

2.7.2 Yeast Two-Hybrid Bait–Library Mating

The library used in the Y2H screen was a Mate and Plate universal human normalised library in the yeast strain *S. cerevisiae* Y187 (Clontech, Catalogue number 630480, Lot number 1312192A). The manufacturer states that the library represents genes transcribed in a range of human tissues designed to offer nearly complete human gene coverage. Genes are amplified as cDNA from which high abundance transcripts are normalised using a duplex-specific nuclease to increase the relative quantity of lower abundance transcripts. The normalised cDNA is then cloned into pGADT7 for use in library screening. Quality control data pertaining to the library include: titer: $\geq$5 x 10^7 cfu/ml, number of independent clones: 1.84 x 10^7, average cDNA size: 1.43 kb, cDNA size range: 0.5–2.9 kb. The *S. cerevisiae* AH109 strains containing the genes of interest were mated with the library according to the manufacturers instructions. In brief, overnight cultures of the *S. cerevisiae* AH109 strains were mixed and incubated, each with a single aliquot of library shaking at 45 RPM at 30°C. After 24 hours the culture was checked for the formation of zygotes using a light microscope (40X). If mating occurred, the yeast cultures were pelleted at 1000 RCF for 10 minutes, washed once with sterile water, and resuspended in 10 ml of sterile water. A small amount of culture was plated onto SD/-Trp, SD/-Leu,and SD/-Trp/-Leu as a control for the number of colonies screened and the remaining culture was plated on SD/-Trp/-Leu/-Ade/-His plates (100 μl per plate). Colonies were incubated at 30°C for 10 days. The plates were checked at days 5 and 10 and any resulting colonies were re-streaked onto SD/-Trp/-Leu/-Ade/-His plates which were grown for 3 days at 30°C. In order to separate plasmids colonies were re-streaked on SD/-Trp/-Leu/-Ade/-His plates and grown twice more. Colonies were then streaked onto SD/-Trp/-Leu/-Ade/-His/X-α-Gal plates to check for a blue colour change and

glycerol stocks were made for each colony.

2.7.3 Identification of Interacting Library Plasmids

In order to determine what library plasmid each of the colonies contained a colony PCR was performed using the T7 Forward and 3′ DNA-AD primers which are specific for the library plasmid. The resulting product was run on a 1% agarose gel and inserts of different sizes were cut out, gel purified, and sent for Sanger sequencing (Source BioScience) using the T7 Forward primer. To confirm the interactions were not due to secondary library plasmids in the yeast strains, plasmids were extracted from the mated yeast strain using a mini prep kit and were transformed into *S. cerevisiae* AH109 containing the pGBKT7-bait protein. The strains were plated onto SD/-Trp/-Leu/-Ade/-His/X-α-Gal and SD/-Trp/-Leu/X-α-Gal plates. The library plasmids of interest were also checked for auto activation by transforming them into *S. cerevisiae* AH109 and inoculating the transformed strain onto SD/-Leu/X-α-Gal and SD/-Leu/-Ade/-His/X-α-Gal.

2.8 BipC Methods

2.8.1 Actin Binding Using GSH-linked Sepharose Beads

To investigate the ability of proteins of interest to directly bind actin, GSH-linked sepharose beads bound to GST, GST-BimA, GST-SipC, or GST-BipC were combined with 1 x polymerisation buffer containing 1 μM rhodamine-labelled actin on a glass microscope slide. The beads were immediately visualised using a Zeiss LSM 710 Scanning Laser Confocal Microscope using an excitation of 535 nm and an emission of 585 nm. If a protein is able to bind actin, it creates a high concentration of the rhodamine-labelled actin at the surface of the sepharose bead, which appears as a red ”halo” around the clear bead in microscope images.

2.8.2 Pyrene Actin Polymerisation

A 1 mg aliquot of pyrene-labelled actin was suspended in 50 μl of deionised water. A wide-bore tip was used to transfer the actin to a chilled bijou containing 2.495 ml G-buffer (2 mM Tris - pH 8, 0.5 mM DTT, 0.2 mM ATP, 0.1 mM $CaCl_2$, and 0.01% NaN_3), the mixture was briefly vortexed, and the actin was

incubated on ice in the dark for 1 hour to de-polymerise. The actin was then transferred to a polycarbonate ultracentrifuge tube and was ultracentrifuged at 100,000 RFC for 2 hours at 4°C to pellet any nucleation centres. The top 80% of the supernatant was transferred to a chilled bijou and stored on ice in the dark until use. The concentration of actin was determined using a Bradford assay (Pierce Scientific) and the molar concentration was determined. Monomeric actin used in polymerisation assays at a final concentration of 2-3 μM.

All assays were run in black opaque 96-well plates and run with a kinetic cycle where data was collected every 30 seconds for up to 1 hour using a FLUOstar Omega plate reader (BMG Labtech). Samples were excited with a wavelength of 365 nm and emission was data was collected at a wavelength of 407 nm. For each preparation of pyrene-labelled actin, the polymerisation capabilities were first determined and a gain was assigned and use in all subsequent reactions. To set the gain, reactions were set up in a 96 well plate as listed in 2.1 below. The reactions were allowed to polymerise in the dark for 1 hour, before measuring and using the value from Well 3 as the gain.

Table 2.1: Pyrene actin polymerisation assay control reactions used to set gain.

Reagent	**Well 1**	**Well 2**	**Well 3**
50 mM Tris pH 7.5	100 μl	90 μl	80 μl
20 μM pyrene actin	0 μl	10 μl	10 μl
10x polymerisation buffer	0 μl	0 μl	10 μl

The actin polymerisation assay was performed using recombinant proteins as controls, including GST-WASP-VCA (Cytoskeleton, VCG03) and bovine Arp2/3 (Cytoskeleton, RP01). GST-WASP-VCA was suspended in 500 μl of water at a final concentration of 1 mg/ml (Rmw is 43 kDa, so final concentration was 23 μM). The GST-WASP-VCA diluted to 10 μM, aliquoted in 10 μl aliquots, and was stored at -80°C until use. The working concentration for GST-WASP-VCA in the actin polymerisation assay was 100 nM.

The Arp2/3 complex was prepared by suspending in 10 μl of water and 10 μl of Arp2/3 buffer (20 mM Tris pH 7.5, 25 mM KCl, 1 mM MgCl2, 0.1 mM ATP and 1 mM DTT) The resulting solution had a concentration of 2.5 mg/ml (Rmw is 224 kDa, so final concentration was 11 μM) and was stored at -80°C

Table 2.2: Pyrene actin polymerisation assay example.

Reagent	**Well 1**	**Well 2**	**Well 3**	**Well 4**	**Well 5**	**Well 6**	**Well 7**
50 mM Tris pH 7.5	90 μl	80 μl	79 μl	79 μl	78 μl	70 μl	70 μl
10 μM VCA	– – –	– – –	1 μl	– – –	1 μl	– – –	– – –
1.3 μM Arp2/3	– – –	– – –	– – –	1 μl	1 μl	– – –	– – –
1 um GST	– – –	– – –	– – –	– – –	– – –	10 μl	– – –
GST-X	– – –	– – –	– – –	– – –	– – –	– – –	10 μl
20 μM pyrene actin	10 μl	10 μl	10 μl	10 μl	10 μl	10 μl	10 μl
10x polymerisation buffer	– – –	10 μl	10 μl	10 μl	10 μl	10 μl	10 μl
Total	100 μl	100 μl	100 μl	100 μl	100 μl	100 μl	100 μl

in 2 μl aliquots. The Arp2/3 complex was used at 13 nM in polymerisation assays. Assays were set up as in Table 2.2. The 10x polymerisation buffer was added last using a multichannel pipette so that all wells received the buffer at the same time. The plate was immediately loaded into the plate reader and after and initial shaking sequence, readings were taken ever 30 seconds for 1 hour. The assay was performed in three independent replicates with three measurements per replicate. Data was plotted in Excel. The rates of polymerization were calculated as the rise in fluorescence units per second during the linear phase of polymerization. The mean rates of polymerization for each protein were analysed by pairwise Student t tests using R software and P values of $\leq$0.05 were taken as significant.

2.8.3 Actin Depolymerisation

To asses the ability of BipC to stabilise actin filaments, an actin depolymerisation assay was performed. An aliquot of pyrene actin was thawed and converted to Mg-Actin. This conversion was done by incubating the actin suspended in G-buffer at 1 mg/ml with 125 μM EGTA and 50 μM $MgCl_2$ for 10 minutes at room temperature. The Mg-actin was then polymerised by adding

500 μl of G-Mg buffer and 110 μl of 10 x polymerisation buffer and incubating at room temperature in the dark for 2-4 hours. The depolymerisation assay was set up in a 96 well black opaque plate with each well containing 10 μl of F-actin (final concentration 2.3 μM) and 90 μl G-Mg buffer, plus or minus 2.5 μM GST-X protein. As controls, GST, phalloidin and MeOH were used and the gain was set using a well containing 10 μl of F-actin, 16 μl of H_2O and 74 μl of G-Mg buffer. The assay was set up as in Table 2.3. All assays were run in black opaque 96-well plates and run with a kinetic cycle where data was collected every 30 seconds for up to 1 hour using a FLUOstar Omega plate reader (BMG Labtech). Samples were excited with a wavelength of 365 nm and emission was data was collected at a wavelength of 407 nm. The assay was performed in three independent replicates with three measurements per replicate. Data was plotted in Excel.

Table 2.3: Pyrene actin depolymerisation assay example.

Reagent	**Well 1**	**Well 2**	**Well 3**	**Well 4**	**Well 5**	**Well 6**	**Well 7**
F-actin	– – –	10 μl	10 μl	10 μl	10 μl	10 μl	– – –
G-Mg buffer	100 μl	74 μl	74 μl	74 μl	74 μl	74 μl	74 μl
GST	– – –	– – –	10 μl	– – –	– – –	– – –	– – –
GST-X	– – –	– – –	– – –	10 μl	– – –	– – –	– – –
H_2O	– – –	16 μl	6 μl	6 μl	0.85 μl	0.85 μl	36 μl
phalloidin633	– – –	– – –	– – –	– – –	15.15 μl	– – –	– – –
MeOH	– – –	– – –	– – –	– – –	– – –	15.15 μl	– – –
Total	100 μl	100 μl	100 μl	100 μl	100 μl	100 μl	100 μl

2.8.4 Actin Sedimentation

To perform an actin sedimentation assay, rhodamine actin was first polymerised. In a microcentrifuge tube, 180 μl of sterile water containing 4 ug/μl rhodamine actin, 0.05 μM $MgCl_2$, and 0.125 μM EGTA was allowed to incubate for 10 minutes at room temperature in the dark to form Mg-actin. To the

mixture, 20 μl of 10x polymerisation buffer was added and was incubated for 2 hours at room temperature in the dark to polymerise the G-actin into F-actin. F-actin was used at a final concentration of 0.4 ug/μl in reaction mixtures listed in Table 2.4.

Table 2.4: Actin sedimentation assay reactions.

Negative Control	**GST**	**BimA**	**SipC**	**BipC**
10 ug F-actin	10 ug F-actin	10 ug F-actin	10 ug F-actin	10 ug F-actin
– – – – – –	1 μM protein	1 μM protein	1 μM protein	1 μM protein
59 μl G-Mg buffer	59 μl G-Mg buffer	59 μl G-Mg buffer	59 μl G-Mg buffer	59 μl G-Mg buffer
dH_2O to 100 μl	dH_2O to 100 μl	dH_2O to 100 μl	dH_2O to 100 μl	dH_2O to 100 μl

The reaction was incubated at room temperature for 30 minutes in the dark and then the F-actin was centrifuged at 100,000 RCF for 1 hour at 20°C to sediment the F-actin (Beckman Coulter TLA100.1 rotor was used at 53,000 RPM). The soluble fraction (monomeric G-actin fraction) was carefully removed into a fresh microcentrifuge tube and a suitable volume of 6 x Laemelli buffer was added. The pellet (filamentous F-actin fraction) was re-suspended in a suitable volume of 6x Laemelli buffer and transferred to a fresh microcentrifuge tube. The F-actin and G-actin were then both heated for 5 minutes at 95°C and the proteins were separated by 10% SDS-PAGE followed by visualisation using Silver staining (Pierce Scientific).

2.8.5 Transfections and Immunofluorescence

In order to investigate the effects of eptopically expressed BipC in eukaryotic cells, HeLa cells were transfected with the constitutive eukaryotic expression vector pRK5-myc-BipC, which adds an in-frame N-terminal Myc tag to the protein. The plasmid pEGFP which encodes enhanced green fluorescent protein (EGFP) was used as a control. HeLa cells were seeded at a density of 2 x 10^5 cells per well into 6-well plates containing glass cover slips and were grown overnight in DMEM at 37°C in the presence of 5% CO_2. Transfections were using Lipofectamine 2000 (Invitrogen) according to the manufacturers protocol

and 4.0 μg of plasmid per well. The transfected HeLa cells were grown for 48 hours in DMEM at 37ºC in the presence of 5% CO_2 after.

To visualise the Myc-tagged BipC, the transfected cells were fixed in 4% paraformaldehyde dissolved in PBS (pH 7.4) for 1 hour at room temperature. The cells were washed twice with PBS and permeabilised using 1 ml of 0.5% Triton X-100 dissolved in PBS for 15 minutes at room temperature. Cells were washed twice with PBS and then blocked for 30 minutes at room temperature with blocking buffer (PBS containing 0.5% bovine serum albumin w/v , 0.02% NaN_3 w/v, filtered using a 0.2 μm syringe filter). In order to detect the Myc-BipC, cover slips were incubated with 500 μl of rabbit α-c-Myc primary antibody (0.5 μl/ml, Santa Cruz) at 37ºC for 1 hour. The cover slip was washed 3 times with PBS followed by incubation with 500 μl of goat α-rabbit 488 secondary antibody (2 mg/ml, Molecular Probes) diluted in blocking buffer (1:200) for 1 hour. The cover slips were washed 3 times with PBS and incubated with 500 μl of phalloidin 568 (2 mg/ml, Invitrogen) for 15 minutes. The cover slip was washed six times with PBS, one time with waster and was mounted on a glass slide using Prolong Gold (5 μl, Invitrogen). The slides were visualised using a Zeiss LSM 710 Scanning Laser Confocal Microscope.

2.9 Statistical Analysis

Statistical analysis is also described in the methods sections in which it was used. For the iTRAQ experiment, proteins were selected as potential T3SS effector protein candidates if they had at least 2 unique peptides used in quantification with a MASCOT peptide score of over 21, which corresponds to the threshold value for a 95% confidence level (a 1 in 20 chance that the match is random, P value of =0.05), and a "high" iTRAQ ratio in at least one strain, which we defined as a value greater than 1.5 X inner quartile range.

To analyse actin polymerisation data, the fluorescence data was first plotted in Excel. The rates of polymerization were calculated as the rise in fluorescence units per second during the linear phase of polymerization. A pairwise Student t tests was performed using R software and P values of $\leq$0.05 were taken as significant.

2.10 General Software Used in This Study

Management of data sets as well as graphing of BipC-Actin polymerisation was performed in Excel (Microsoft). The following open source software was used throughout the research. For calculation of cut off values, statistical analysis the R software ((R Core Team, 2015)) was used. The thesis was written using the LaTeXsoftware (https://latex-project.org/). For image management the GNU Image Manipulation Program (GIMP) 2.0 (https://www.gimp.org/) was used. Inkscape (https://inkscape.org/en/) was used to create vector based graphic diagrams. Database searches for nucleotide and protein similarity was performed using NCBI BLAST (http://blast.ncbi.nlm.nih.gov/Blast.cgi) (Madden, 2013).

Chapter 3

Quantitative Proteomic Analysis of Bsa T3SS Effector Proteins Using iTRAQ

3.1 Introduction

The genome of *Burkholderia pseudomallei* encodes three Type III Secretion Systems (T3SS). T3SS-1 and T3SS-2 are more similar to plant pathogen-like secretion systems (Rainbow *et al.*, 2002) and are not required for virulence in a Syrian hamster model of infection (Warawa and Woods, 2005). One more recent study shows that T3SS-1 may be more important than previously thought, as a system knockout is attenuated in a murine respiratory model of melioidosis (D'Cruze *et al.*, 2011b). The T3SS-3, known as the *Burkholderia* Secretion Apparatus (Bsa) T3SS, has been shown to be important for non-phagocytic cell entry (Stevens *et al.*, 2003), escape of the endosome (Stevens *et al.*, 2002), and virulence in murine (Stevens *et al.*, 2004, Gutierrez *et al.*, 2015) and Syrian hamster models of infection (Warawa and Woods, 2005). There are only two effectors known to be secreted by the Bsa T3SS; BopE, a guanine nucleotide exchange factor (Stevens *et al.*, 2003), and BopC, a protein of unknown function involved in intracellular survival (Muangman *et al.*, 2011, Srinon *et al.*, 2013). By comparison to other T3SSs it can be hypothesized that with only three known secreted effector proteins in the *B. pseudomallei* Bsa T3SS, there are many more effectors to be characterized. For example there are at least 21 effectors secreted by the T3SS of Enteropathogenic *E. coli* (EPEC) (Reviewed in (Dean and Kenny, 2009)) and 25–30 effectors secreted by the T3SS of *Shigella flexneri* (Reviewed in Parsot (2009)).

One of the problems facing T3SS effector protein discovery is the tight regulation of the T3SS under laboratory conditions, with different T3SSs responding to very different environmental cues such as temperature and calcium ion concentration (*Yersinia*) (Forsberg and Wolf-Watz, 1988), the dye Congo Red (*Shigella*) (Parsot *et al.*, 1995), extracellular amino acids and serum proteins (*Yersinia*) (Lee *et al.*, 2001), bile salts (*Shigella*) (Olive *et al.*, 2007) and calcium restriction/depletion (*Chlamydia*) (Jamison and Hackstadt, 2008). The *B. pseudomallei* Bsa T3SS has been shown to be stimulated by salt stress (Pumirat *et al.*, 2009, 2010), and in the closely related species *B. thailandensis*, pH stimulated the Bsa T3SS (Jitprasutwit *et al.*, 2010). Yet, stimulating the T3SS system in such a way may not result in sufficient levels of effector secretion for less sensitive detection methods, illustrated by detection of BopE by western blot (Pumirat *et al.*, 2010), but not by 2D SDS-PAGE (Pumirat *et al.*, 2009).

To override the tight control of the T3SS, one solution employed in the study of other Gram-negative bacteria (for example *Citrobacter rodentium* and EPEC) was to generate mutations of T3SS components that dysregulate the system, thereby creating a hyper-secretion phenotype (Deng *et al.*, 2010, 2012). Although some genes involved in transcriptional control of the Bsa T3SS were recently identified (Sun *et al.*, 2010), little is known about the post-translational regulation of the system and what environmental signals may activate it. In one study the gene encoding the Bsa T3SS needle cap protein of *B. pseudomallei*, *bipD*, was interrupted and showed increased secretion of the effector BopE by western blot analysis (Stevens *et al.*, 2003).

One group of T3SS proteins that have been shown in many systems to be involved in the control of effector and translocator secretion are the so-called 'gatekeeper' family of proteins, InvE/MxiC/SepL/YopN-TyeA of *Salmonella/Shigella/E. coli/Yersinia*, respectively (Reviewed in Büttner (2012)). Investigation of these proteins has given insight into the temporal regulation of their respective T3SSs. Although deletion of all of these proteins causes an increase in levels of secreted effectors there are also differences between them. Deletion of *invE* (Kubori and Galán, 2002) and *sepL* (Kresse *et al.*, 2000, Deng *et al.*, 2004, 2005) cause a reduction in secreted levels of translocators, deletion of *mxiC* (Botteaux *et al.*, 2009) has no effect on their levels, and deletion of *yopN* (Forsberg *et al.*, 1991, Iriarte *et al.*, 1998) increases levels of secreted translocators. The closest homologue to this family of proteins in *B. pseudomallei* is the uncharacterised protein BsaP (BPSS1544), but its function has not been determined experimentally.

Upon generation of bacterial supernatants containing potential T3S effector proteins, there is still the task of identifying the T3SS proteins in a complex mixture with a large number of other non-Type 3 secreted proteins. In the past methods such as 2D gel electrophoresis have been used (Pumirat *et al.*, 2009), but suffer from low resolution in complex protein samples and a tendency to pick out only the most highly abundant proteins (reviewed in Rabilloud and Lelong (2011)). A recent unpublished study used 2D gel proteomics to attempt to identify *B. pseudomallei* Bsa T3SS effector proteins (M. Stevens and K. Brown, personal communication). *B. pseudomallei* K96243 and 10276 supernatants were prepared by culturing bacteria in LB to stationary phase at room temperature, subculturing into pre-warmed LB (37°C), and then incubating for 6 hours shaking at 37°C. Secreted proteins were precipitated by trichloroacetic acid (TCA) precipitation and analysed using 2D gel electrophoresis. Spots were cut out of the gel and analysed by trypsin digest and mass spectrometry (MS). The study failed to identify BopE in the bacterial supernatants. The study did however identify BopC and BipD in the supernatants. Because the effector protein BopE is secreted by WT *B. pseudomallei* at very low levels under standard laboratory culture conditions, the inability to detect BopE could be due to sub-optimal precipitation of the secreted proteins or could be due to the gel-based proteomics method used.

Because of the lack of sensitivity, depth and reproducibility, 2D gel proteomics is being replaced by gel-free MS methods (Reviewed in Wasinger *et al.* (2013)). Indeed, recent secretomics studies have used gel-free relative quantitative proteomic techniques as a sensitive way to determine proteins that are secreted in a T3SS-dependent manner (Sikora *et al.*, 2011, Deng *et al.*, 2010, 2012). Two common methods of gel-free quantitative proteomics are Stable Isotope Labelling of Amino Acids (SILAC) and Isobaric Tags for Relative and Absolute Quantification (iTRAQ) (Reviewed in Elliott *et al.* (2009)). SILAC uses a medium containing isotopically labelled amino acids which are incorporated into proteins as they are translated *in situ*, which can then be differentiated using MS (Ong *et al.*, 2002). In order to use SILAC, bacterial mutants that lack the ability to synthesise the chosen labelled amino acids need to be generated (Ong *et al.*, 2002). The alternative and more tractable method iTRAQ consists of binding isobaric tags of different molecular weights to the processed peptides immediately prior to analysis by MS (Wiese *et al.*, 2007). iTRAQ also allows for multiplexing of up to eight samples to be compared simultaneously (Reviewed in Elliott *et al.* (2009)).

3.2 Results

3.2.1 Bioinformatic Prediction of Bsa T3SS Effector Proteins

Recently there has been a focus on the possibility of predicting effector proteins using a bioinformatics approach. There have been a number of publications in close proximity using different algorithms to try to detect effector proteins (Arnold *et al.*, 2009, Lower and Schneider, 2009, Samudrala *et al.*, 2009, Yang *et al.*, 2010, Wang *et al.*, 2011). These studies use features from experimentally proven effector proteins such as N-terminal secretion sequence (T3S signal) to try to inform predictions (Reviewed in McDermott *et al.* (2011)). When used to predict effectors in *B. pseudomallei*, the programs show inconsistency and predict candidate effector proteins that are known to be secreted by alternative secretion systems or fail to identify known effector proteins. For example, the validated Bsa T3SS effector proteins BopE and BopC were subjected to the 3 different web portals for prediction. BopE or BopC were predicted as not being secreted by the T3SS using Effective (www.effectors.org). Similarly, SIEVE (http://cbb.pnnl.gov/portal/tools/sieve.html) predicted neither protein, BopE or BopC, was secreted by the T3SS. Modlab (http://gecco.org.chemie.uni-frankfurt.de/T3SS_prediction/T3SS_prediction.html) predicted BopE was secreted by the T3SS, BopC was not. While the ability to predict T3SS effectors using bioinformatics has been effective for identifying known effector proteins in model organisms (Reviewed in McDermott *et al.* (2011)), the most recent programs are still lacking in their ability to correctly identify effectors in *B. pseudomallei* and a better understanding of T3SS signals may still needed for comprehensive and accurate prediction. Because of the current inconsistencies of a bioinformatics approach, effector discovery and especially validation, still requires a lab based approach.

3.2.2 Optimisation of Sample Precipitation Methods

Before proceeding with the generation of bacterial supernatants for analysis by proteomics methods, it was important to optimise methods for generation and precipitation of the proteins in the bacterial culture supernatants. The method was first optimised in a containment level 2 laboratory using *Shigella flexneri* as a model organism, as it is known the *S. flexneri* T3SS is induced by addition of the dye Congo red (Parsot *et al.*, 1995). Cultures of *S. flexneri* were incubated overnight with shaking at 37°C. The overnight cultures were

centrifuged and re-suspended to an OD_{600} of 0.5 in fresh LB media containing 20 μM Congo Red. From the adjusted culture, 1 ml was added to 9 ml of LB media containing 20 μM Congo Red which was then incubated at 37°C for 4 hours with agitation. The supernatants were collected by centrifugation and filtered through a 0.2 μm low protein binding cellulose acetate syringe filter.

Proteins were first precipitated using TCA and Strataclean beads (hydroxylated silica particles which bind protein, Agilent Technologies). Of the precipitated proteins, half the total volume was analysed by SDS-PAGE and visualised by staining with Coomassie blue. Interestingly, there was little noticeable difference between the supernatant proteins cultured in the presence or absence of Congo red when precipitated with Strataclean Beads, while a difference was apparent in the lanes containing protein precipitated using TCA (Figure 3.1). Congo Red had no noticeable effect on the bacterial whole cell lysates. The lane containing bacterial supernatants precipitated using TCA had considerably more overall protein than the Strataclean bead lanes.

To test whether precipitation could be further improved, proteins were next precipitated from *Shigella* supernatants using one of three methods: Pyrogallol Red-Molybdate-Methanol (PRMM), TCA or TCA plus 2% sodium deoxycholate (TCA+DOC) as described in Chapter 2 (Caldwell and Lattemann, 2004, Bensadoun and Weinstein, 1976). Of the total volume of each precipitation, 1/ 50^{th} was analysed by SDS-PAGE and visualised by staining with Coomassie blue. When comparing the different secretion methods, the amount of protein present in the PRMM- and TCA-DOC-treated lanes were greater than that in the lane containing the TCA alone-treated sample (Figure 3.2). A blank LB sample was also precipitated and analysed to test for background proteins/peptides in the yeast extract used to prepare the media. No proteins were present in the LB sample above the dye front on the gel. PRMM was chosen as the precipitation method for all further experiments. This was advantageous because it does not contain detergents making it more compatible with downstream applications such as MS.

3.2.3 Chemical Induction of the Bsa T3SS

In order to generate high levels of Bsa T3SS effector proteins in the supernatants, initial studies sought to chemically induce the system by changing the composition of the culture media. Because previous reports have identified salt stress in *B. pseudomallei* as inducing the Bsa T3SS (Pumirat *et al.*, 2009, 2010), this condition, as well as calcium limited (EGTA) media, were tested

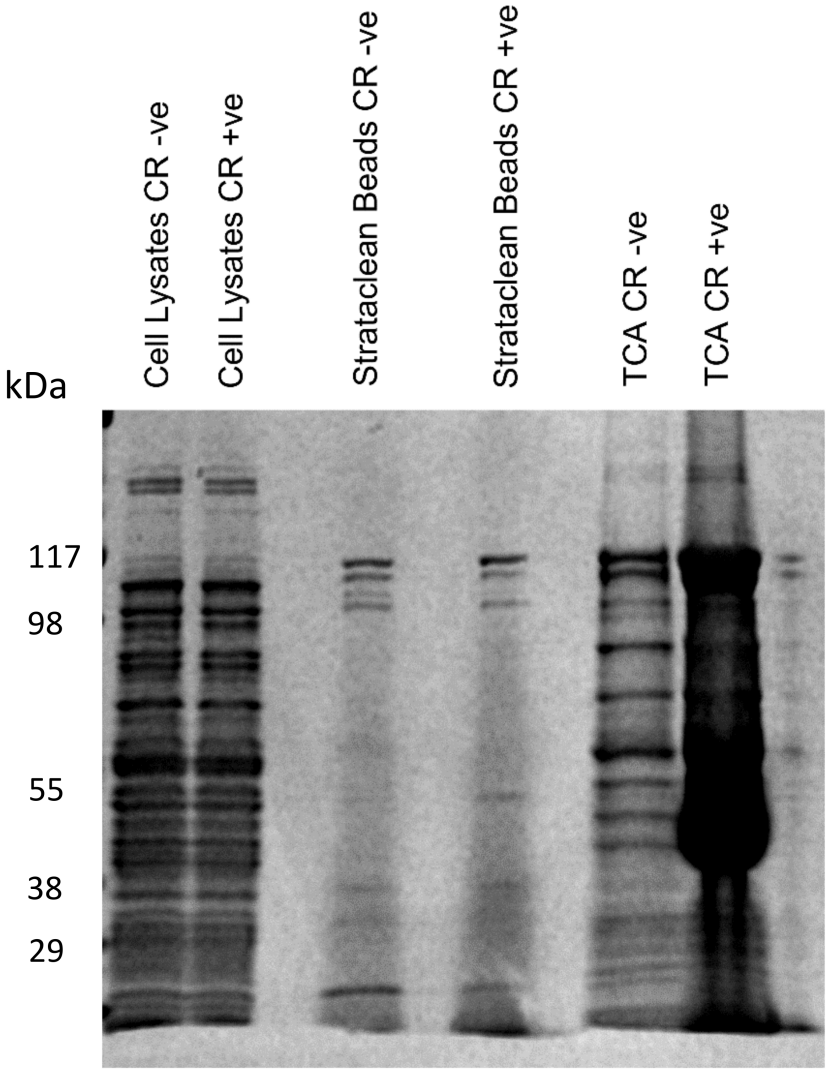


Figure 3.1: Comparison of the Use of Strataclean Beads and TCA for precipitating proteins from *S. flexneri* bacterial supernatants. Supernatants were collected from *S. flexneri* after 4 hours incubation at 37°C with (CR +ve) or without (CR -ve) the addition of 20 μM Congo Red. Proteins were precipitated with Strataclean beads or TCA. Half the total volume of precipitated proteins were separated by reducing SDS-PAGE and visualised by Coomassie Blue staining.

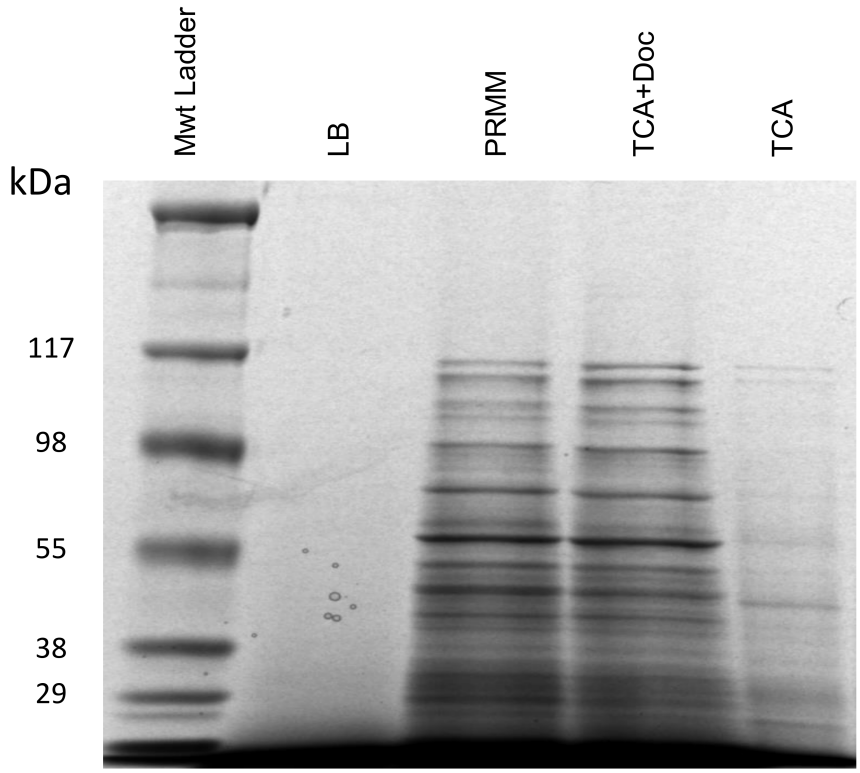


Figure 3.2: Comparison of PRMM, TCA and TCA with DOC for precipitating proteins from *S. flexneri* bacterial supernatants. Supernatants were collected from *S. flexneri* after 4 hours incubation at 37ºC with the addition of 20 μM Congo Red. Proteins were precipitated by PRMM, TCA+DOC or TCA methods as described in Chapter 2. Equal proportions of the precipitated proteins were separated by reducing SDS-PAGE and visualised by Coomassie Blue staining. Lane 2 is LB media precipitated with PRMM (LB).

as possible means to increase the output of the known effector protein BopE. As controls, the standard laboratory media LB and TSB were used. A single colony of *B. pseudomallei* 10276 and a *bsa* T3SS-null mutant, *bsaZ*::pDM4, were used to inoculate 10 ml of LB which was then incubated at 37°C overnight with shaking. The following day the bacteria were centrifuged and the supernatant was replaced with fresh LB to an OD_{600} of 1.0. Of the adjusted culture, 1 ml was used to inoculate 9 ml of each of the different media: LB, TSB, LB without NaCl, LB containing 320 mM NaCl, and LB containing 10 mM EGTA. Bacterial numbers were determined by plating dilutions and all samples had similar starting numbers of about 10^5 CFU/ml. The cultures were incubated at 37°C for 6 hours. The bacterial numbers after the incubation were determined by plating of samples and all cultures again had a similar number of CFUs at about 10^7/ml, except for *B. pseudomallei* grown in the presence of 10 mM EGTA which showed a 10 fold reduction in bacterial counts (10^6 CFU/ml). The supernatant was collected by centrifugation and filtered through a 0.2 μm low protein binding cellulose acetate syringe filter, and the proteins were precipitated using the PRMM method. Equal volumes of the precipitated proteins were analysed by SDS-PAGE and visualised by Coomassie staining and by Western blot using a rabbit α-BopE antibody (Stevens *et al.*, 2003). When visualised by Coomassie staining, it was apparent that *B. pseudomallei* secretes a complex set of proteins into the supernatant and it was not clear which proteins may be specifically Type 3 secreted when compared to the *bsaZ* mutant samples (Figure 3.3). Interestingly, there was not an increase in the amount of BopE in the supernatant of the WT *B. pseudomallei* under any of the conditions tested, when compared to the standard LB and TSB media by Western blot (Figure 3.3). Another interesting result is the presence of an unknown protein at about 50 kDa in the *bsaZ*::pDM4 supernatant. It is unlikely that this protein is a T3S protein, as the system is mutated in this strain, but may be a protein secreted in another manner, perhaps a metal ion acquisition protein, due to low abundance of calcium ions in the EGTA medium. It was determined that standard LB would be used for the bacterial secretion preparations for all other experiments as it is shows a similar profile to other media and had been used extensively in *B. pseudomallei* culture. The supernatants of the *B. pseudomallei* pDM4::*bsaZ* samples contained little or no BopE indicating that minimal cell lysis had occurred. The culture and precipitation methods yielded very consistent results over the course of this study with similar bacterial growth rates, protein yields, and Western blot patterns each time the method was performed.

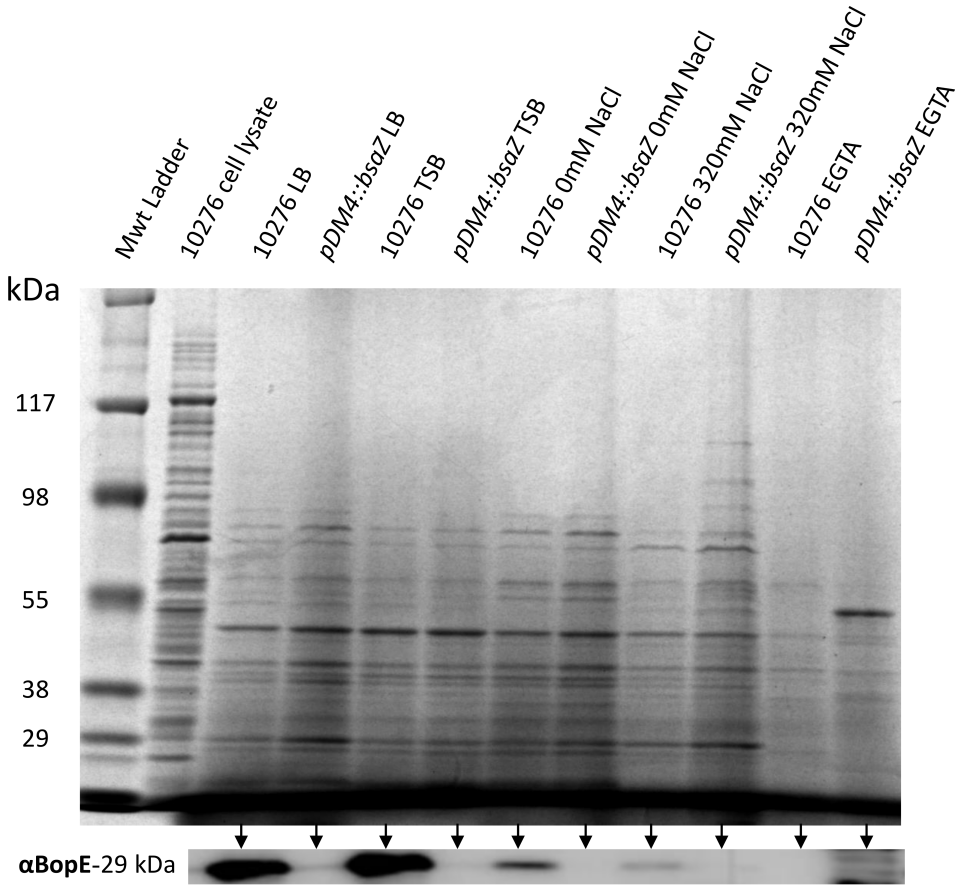


Figure 3.3: Attempts at chemical induction of the *B. pseudomallei* 10276 Bsa T3SS. Supernatants were collected from *B. pseudomallei* strains 10276 and 10276 *bsaZ*::pDM4 after culture for 6 hours at 37°C in LB, TSB, LB w/ 0 mM NaCl, LB w/ 320 mM NaCl or LB+10 mM EGTA. Equal volumes of protein were separated by reducing SDS-PAGE and visualised by Coomassie blue staining or transferred to a PVDF membrane for protein detection using polyclonal rabbit α-BopE (Stevens *et al.*, 2003).

3.2.4 Construction and Characterization of Hyper-secreting *Bsa* Mutants

As chemical induction failed to induce secretion of larger amounts of BopE into the supernatant when compared to standard growth conditions (LB), methods of genetic dysregulation of the Bsa T3SS were explored. It was hypothesized that BsaP may control the timing and magnitude of effector secretion based on homology to 'gatekeeper' proteins from the T3SSs of other Gram-negative bacterial pathogens. BLAST analysis of available genomes indicated that BsaP shares 33% identity over 92% coverage (E-value $1e^{-41}$) with the *Shigella* MxiC gatekeeper protein and 34% identity over 88% coverage (E-value $4e^{-32}$) with the *Salmonella* InvE gatekeeper protein (Figure 3.4). A non-polar *bsaP* deletion mutant was therefore constructed in *B. pseudomallei* strain 10276 by double homologous recombination (Logue *et al.*, 2009).

In order to make the deletion of *bsaP* (BPSS1544), a deletion allele containing 'start-stop' codons was created for eventual homologous recombination into the chromosome (Figure 3.5 A). Upstream and downstream fragments of DNA were chosen that were outside of the coding region of *bsaP* and unique within the *B. pseudomallei* K96243 chromosome to avoid recombination with non-target sequences. The upstream fragment was amplified by PCR using the primers bsaP1/bsaP2 to amplify a region of 540 bp of intergenic sequence while the downstream fragment was amplified by PCR using the primers bsaP3/bsaP4 to amplify a region of 575 bp of intergenic sequence. To form the start-stop deletion allele, PCR-ligation-PCR was used (Ali and Steinkasserer, 1995). The two PCR products were phosphorylated and then ligated together followed by PCR amplification using bsaP1/bsaP4 to yield a 1115 bp product. The deleted allele was then ligated into the p-GemT plasmid and propagated in *E. coli* XL1-Blue. The insert sequence was verified by sequencing before it was transferred into the suicide vector pDM4 in *E. coli* PIR1. pDM4 is a suicide vector containing the R6Kγ origin which requires the pi initiation protein, encoded by the *pir* gene to replicate. pDM4 can be maintained in *pir*+ hosts such as *E. coli* PIR1 and S17-1, but not in *B. pseudomallei* (Penfold and Pemberton, 1992). The pDM4-Δ*bsaP* plasmid was transformed into *E. coli* S17-1 from which it was introduced into *B. pseudomallei* by conjugation. *B. pseudomallei* cannot replicate the pDM4 plasmid, therefore selection for Cm resistance, selects for bacteria that have undergone a homologous recombination event, inserting the pDM4-Δ*bsaP* sequence into the chromosome (Figure 3.5 B). A second homologous recombination was selected by growth on me-

```
BsaP      MSSIIGGASAARRGFSIDGTGSAANRLDAEPSLDD---APQTG-------AAGAADVQAQ     50
InvE      ---MIPGST---SGISFSR---ILSRQTSHQDATQHTDAQQAEIQQAAEDSSPGAEVQKF     51
MxiC      ---MLDVKN---TGVFSSA---FIDRLNAMTNSDD-------GDETADAELDSGLANSKY     44
             ::   .    *.  .      .*  :  .  :                 .   .

BsaP      LAGVDEEAANAAAQFGR-FRASERKGRRSDELERILDTDADEKLDELAALLGG----RAD     105
InvE      VQSTDE-MSAALAQFRNRRDYEKKSSNLSNSFERVLEDEALPKAKQILKLISV---HGGA     107
MxiC      IDSSDE-MASALSSFINRRDLEKLKGTNSDSQERILDGEEDEINHKIFDLKRTLKDNLPL     103
          : . **  : * :.* .    .: ..  *:. **:*: :     .::  *

BsaP      LATLLRDARERFRDESDLLLALRELRRRRRLDGESVDALERAIDELLAGDGAKRIKAGIN     165
InvE      LEDFLRQARSLFPDPSDLVLVLRELLRRKDLEEIVRKKLESLLKHVEEQTDPKTLKAGIN     167
MxiC      DRDFIDRLKRYFKDPSDQVLALRELLNEKDLTAEQVELLTKIINEII-SGSEKSVNAGIN     162
             ::   :  * * ** :*.**** ..: *     . *   :..:      * ::****

BsaP      AALKAKVFGARMQLDARRLRELYRQFLEFDGSHLVIYEDWIEQFGASRRKRILDYVSAAL     225
InvE      CALKARLFGKTLSLKPGLLRASYRQFIQSESHEVEIYSDWIASYGYQRRLVVLDFIEGSL     227
MxiC      SAIQAKLFGNKMKLEPQLLRACYRGFIMGNISTTDQYIEWLGNFGFNHRHTIVNFVEQSL     222
          .*::*::**  :.*.   **  ** *:  :      * :*: .:* .:*  :::::. :*

BsaP      SYDMQSHDPSCGCAAEFGPLLGTLHRARMLASADEQFVGRLLDDALARDCGLTEARALAT     285
InvE      LTDIDANDASCS-RLEFGQLLRRLTQLKMLRSADLLFVSTLLSYSFTKAFNAEESSWLLL     286
MxiC      IVDMDSEKPSCN-AYEFGFVLSKLIAIKMIRTSDVIFMKKLESSSLLKDGSLSAEQLLLT     281
            *:::.. **    *** :*  *   :*: ::*  *:  * . :: :         *

BsaP      MLGGLQRPFSVADVLLGTLGDLLEPLAPARRSQLLQLALRAFAGVPIALYGDADARRAAL     345
InvE      MLSLLQQPHEVDSLLADIIGLNALLLSHKEHASFLQIFYQVCKAIPSSLFYEEYWQEELL     346
MxiC      LLYIFQYPSESEQILTSVIEVSRA--S-HEDSVVYQTYLSSVNESPHDIFKSESEREIAI     338
          :*  :* * .  .:*   :       :  . : . *         *  :: .   :.  :

BsaP      GALEELIGATYARERRQARPRAD---     368
InvE      MALRSMTDIAYKHEMAEQRRTIEKLS     372
MxiC      NILRELVTSAYKKELSR---------     355
            *..:   :* :*  .
```

Figure 3.4: Amino acid sequence alignment of *B. pseudomallei* K96243 BsaP with Salmonella InvE and Shigella MxiC 'gatekeeper' proteins. Amino acid sequences (BsaP, YP_111550.1; InvE, NP_461818.1; MxiC, NP_085309.1) were aligned using Clustal Omega software (Sievers *et al.*, 2011). BsaP shares 33% identity over 92% coverage (E-value $1e^{-41}$) with the *Shigella* MxiC gatekeeper protein and 34% identity over 88% coverage (E-value $4e^{-32}$) with the *Salmonella* InvE gatekeeper protein. Amino acid conservation is indicated as fully conserved (*), or having strongly similar (: , scoring >0.5 in the Gonnet PAM 250 matrix), or weakly similar properties (. , scoring ≤0.5 in the Gonnet PAM 250 matrix).

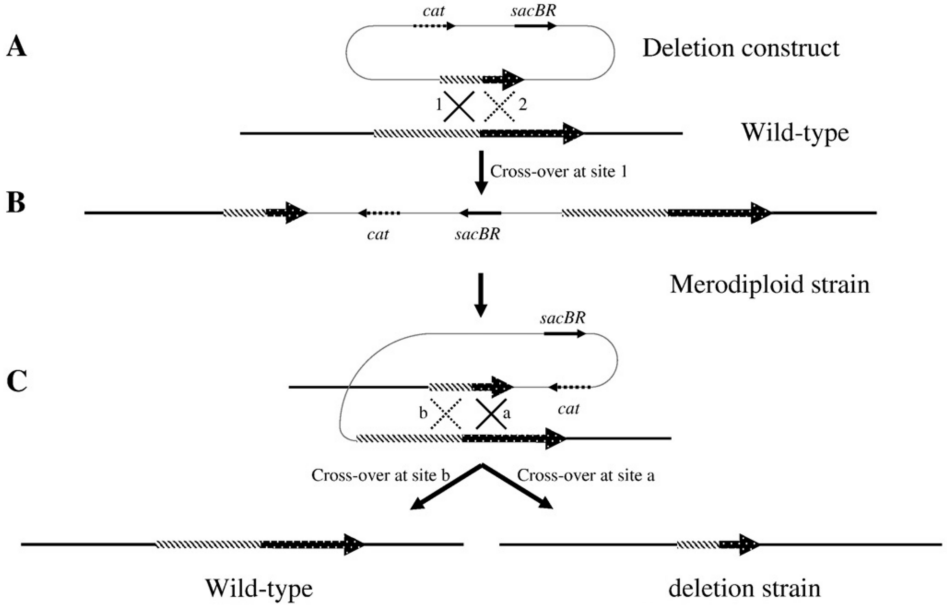


Figure 3.5: Mutagenesis of the bacterial chromosome by double homologous recombination using the suicide vector pDM4. (A) A PCR product with homologous sequence to upstream and downstream regions of the gene to be deleted is cloned into the vector pDM4. **(B)** pDM4 is introduced into *B. pseudomallei* by conjugation, and due to the inability of the bacteria to replicate the plasmid, homologous recombination into the chromosome at the sites flanking the gene of interest is selected using the antibiotic Cm. **(C)** The inserted plasmid is excised from the chromosome by negative selection with sucrose due to the presence of products of the plasmid encoded *sacBR* genes metabolising the sugar into toxic end products. Resulting colonies are screened for Cm sensitivity and sucrose resistance, followed by PCR and sequencing across the target region. Figure taken from Logue *et al.* (2009).

dia containing sucrose (Figure 3.5 C). The pDM4 vector contains the *sacB* gene which codes for the enzyme levansucrase which catalyses the synthesis of levans (Reviewed by Ried and Collmer (1987)). It is thought that the build-up of high molecular weight levans is fatal to the cell resulting in a sucrose-sensitive phenotype. Only bacteria that have lost the *sacB* gene by excision of the plasmid can survive, resulting in either WT or mutant strains. Rarely, a third outcome of escape due to inactivation of the *sacB* gene can occur, which can lead to false positive mutations by PCR (Hmelo *et al.*, 2015). These are detectable by screening for loss of Cm resistance and screening for protein production by Western blot. Of the resulting colonies, 15 were screened for the *bsaP* chromosomal deletion by amplifying across the *bsaP* adjoining regions by PCR, of which 2 colonies had mutations. As expected the resulting product was about 1100 bp smaller than that of the WT allele (Figure 3.6) and one colony was taken forward for all further assays.

Since *bsaP* is predicted to reside in the middle of an operon, with seven genes upstream and two downstream, the deletion of *bsaP* was complemented using a constitutive expression vector encoding *bsaP* to confirm any phenotypes were not caused by polar effects. *bsaP* was cloned into the vector pBHR1 under the control of the kanamycin resistance gene promoter. The 10276 *bipD*::pDM4 lacking the BipD needle tip protein that has been previously reported to secrete elevated levels of the effector protein BopE was analysed alongside the *bsaP* mutant (Stevens *et al.*, 2003).

Figure 3.7 is a diagram showing the location and function of each Bsa T3SS mutant used in this study. Bacteria-free culture supernatants were prepared by growing an overnight culture in LB at 37°C from a single colony of *B. pseudomallei* 10276, 10276 *bsaZ*::pDM4, 10276 *bipD*::pDM4, 10276 Δ*bsaP*, and 10276 Δ*bsaP*(p*bsaP*). The cultures were centrifuged and the media was replaced with fresh LB to an OD of 1.0, 1 ml was taken from the adjusted culture and added to 10 ml of fresh LB, and the cultures were incubated for 6 hours shaking at 37°C. Bacterial counts taken after the secretion preparations were comparable (10^7 CFU/ml) in all strains indicating there were no significant differences in growth rates. The supernatants were collected by centrifugation and were precipitated overnight using PRMM. The secreted proteins were analysed by SDS-PAGE followed by Coomassie Blue staining. The secreted protein profile of *B. pseudomallei* LB-culture supernatant is highly complex with few obvious differences between the strains (Figure 3.8). The bacterial supernatants and whole cell lysates were also analysed by Western blot using antibodies to de-

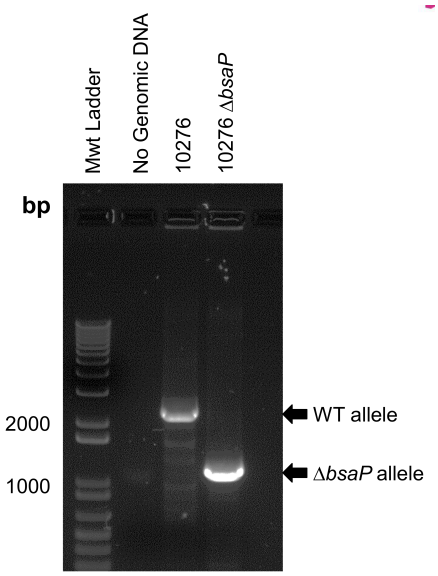


Figure 3.6: PCR confirmation of deletion of the *bsaP* gene in *B. pseudomallei* 10276Δ*bsaP* strain. The region flanking the *bsaP* gene in *B. pseudomallei* 10276 was amplified in the Δ*bsaP* deletion mutant using the primers bsaPSeqF/bsaPSeqR and was visualised on a 1% TAE gel. The WT allele produced a PCR product of about 2300 bp while the Δ*bsaP* deletion mutant produced a PCR product of around 1200 bp, which corresponds to the expected deleted allele of 1104 bp.

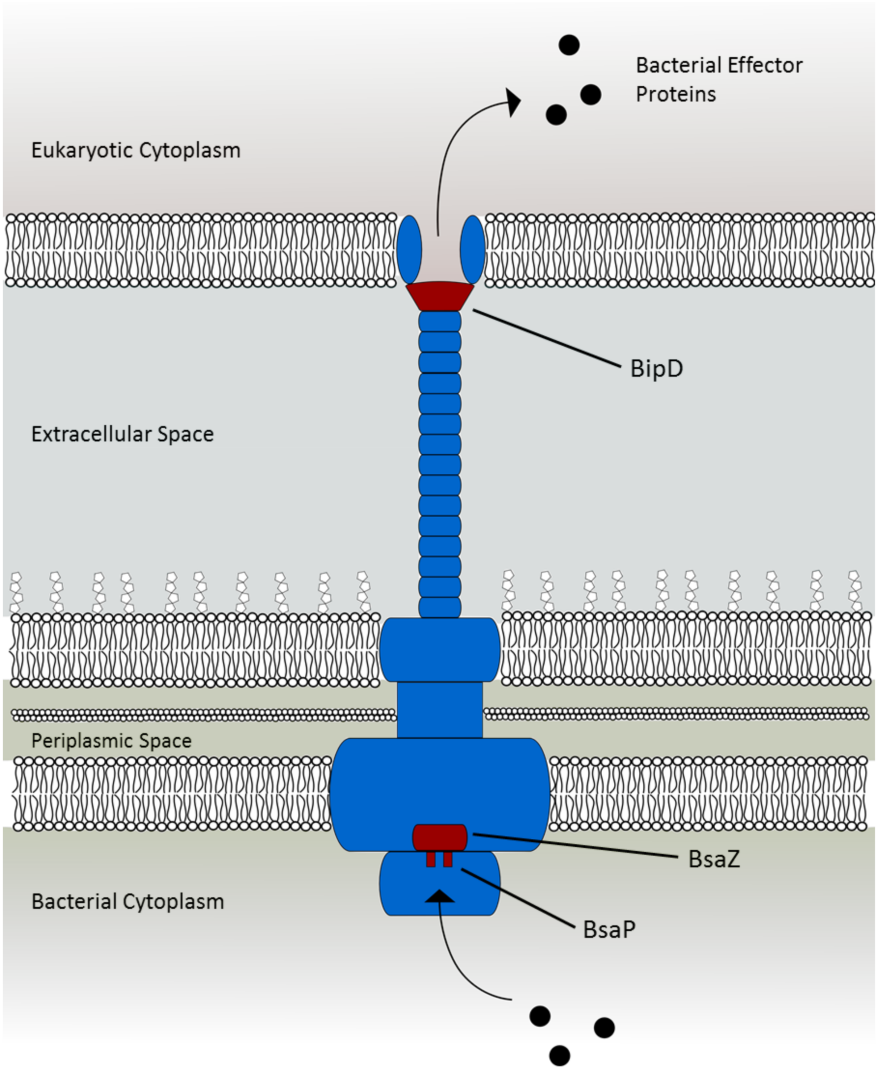


Figure 3.7: *B. pseudomallei* 10276 Bsa T3SS mutants used in this study. The *B. pseudomallei* Bsa T3SS facilitates secretion of effector proteins from the bacterial cytoplasm into the cytoplasm of a target eukaryotic cell. *B. pseudomallei* strain 10276 *bsaZ*::pDM4 is an insertion mutant where the gene encoding an integral structural component of the inner membrane (*bsaZ*) has been disrupted by integration of the pDM4 suicide vector. *B. pseudomallei* strain 10276 *bipD*::pDM4 is also an insertion mutant where the pDM4 suicide vector has integrated into the *bipD* gene, thereby abrogating expression of the needle tip protein. *B. pseudomallei* strain 10276Δ*bsaP* is a deletion mutant where the gene encoding BsaP, a predicted 'gatekeeper' family protein which plays a role in T3SS substrate specificity, has been removed.

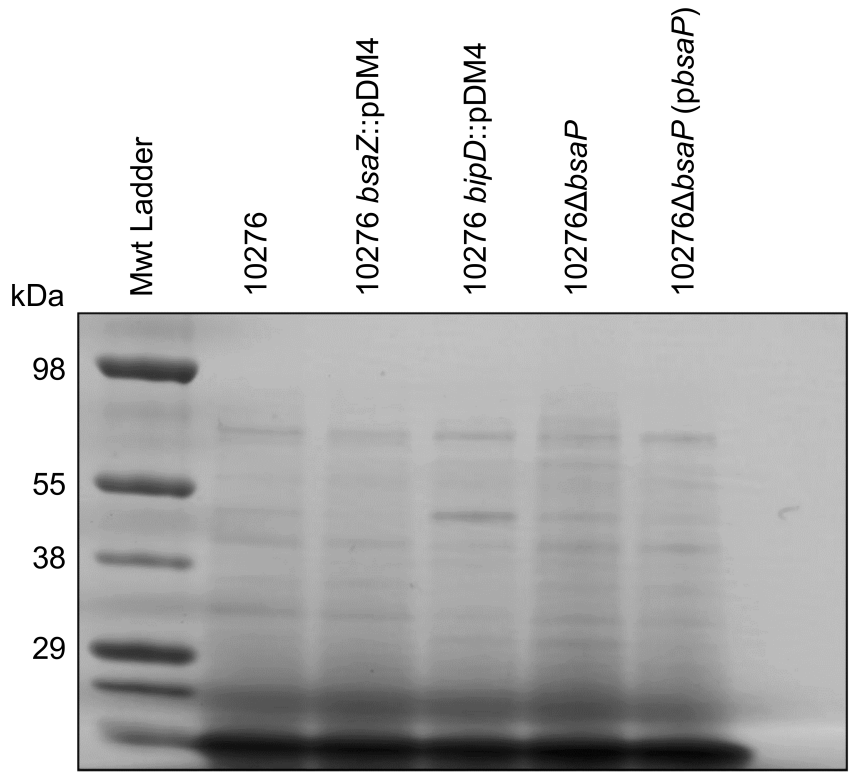


Figure 3.8: *B. pseudomallei* 10276 and mutant strain secreted protein profiles. Supernatants were collected from *B. pseudomallei* strains 10276, 10276 *bsaZ*::pDM4, 10276 *bipD*::pDM4, 10276Δ*bsaP* and 10276Δ*bsaP* (p*bsaP*) after culture for 6 hours at 37ºC. Equal amounts of protein were separated by reducing SDS-PAGE and visualised by Coomassie Blue staining.

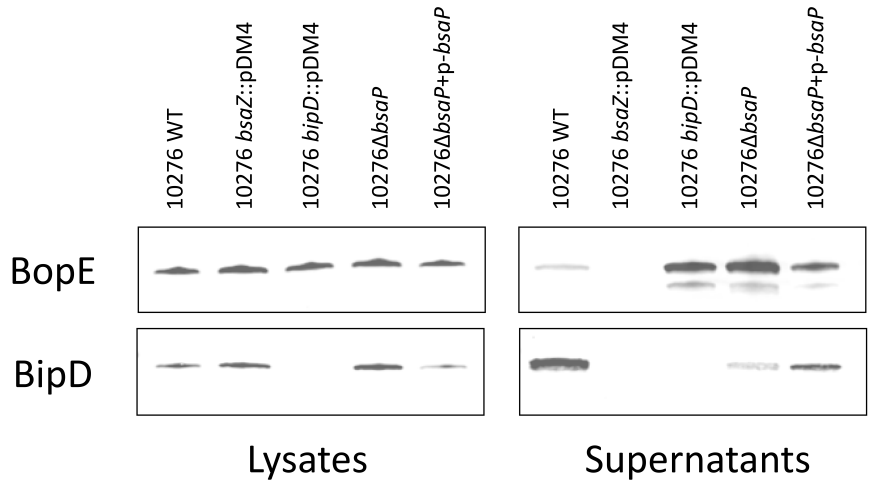


Figure 3.9: Western blot analysis of the expression and secretion of BopE and BipD proteins by *B. pseudomallei* 10276 and mutant strains. 10276, 10276 *bsaZ*::pDM4, 10276 *bipD*::pDM4, 10276Δ*bsaP*, and 10276Δ*bsaP* p-*bsaP* were cultured for 6 hours at 37°C. Equal quantities of protein from the whole cell lysates or cell-free supernatants were separated by denaturing SDS-PAGE and proteins transferred to a nitrocellulose membrane for protein detection using polyclonal rabbit α-BopE (Stevens *et al.*, 2003) or α-BipD (Stevens *et al.*, 2004).

tect the BopE effector protein and the BipD translocon protein (Stevens *et al.*, 2004) (Figure 3.9). The absence of both BopE and BipD in the supernatants of the 10276 *bsaZ::*pDM4 insertion mutant indicates that there was no detectable cell lysis at the time when the secretome was sampled. When compared with the WT strain, both 10276 *bipD::*pDM4 and 10276 Δ*bsaP* strains demonstrated increased secretion of BopE. Interestingly, the levels of BipD secreted into the supernatant was reduced in 10276 Δ*bsaP* compared with WT. This pattern of increased levels of the effector BopE and reduced secretion of the translocator BipD provides the first evidence of a role for BsaP as a "gatekeeper" protein, controlling a switch between the secretion of translocators and effectors. In the case of both BopE and BipD, the phenotype of 10276 Δ*bsaP* was partially restored by plasmid-mediated complementation, indicating the effects are unlikely to be caused by polar or secondary defects.

3.2.5 Characterization of the Core *B. pseudomallei* Secretome Under Standard Laboratory Conditions

Having identified two *bsa* mutant strains with dysregulated BopE secretion profiles in bacterial culture supernatants, the next step was to identify the total secreted protein profile from these two strains in comparison to the isogenic parent strain (10276) and a *bsa*-null mutant strain. To allow for relative quantitative comparisons of protein levels in the samples, iTRAQ was chosen as the proteomics method to use. iTRAQ offers a few advantages over SILAC in this case. iTRAQ has the ability to multiplex 4 differentially labelled samples simultaneously allowing WT, *bsaZ*::pDM4, *bipD*::pDM4, and Δ*bsaP B. pseudomallei* 10276 to be pooled and analysed in a single MS analysis. iTRAQ also does not require generation of amino acid synthesis mutants. The iTRAQ work flow used in this study consisted of generating 3 biological replicates of bacterial secreted proteins which were then pooled, digested, labelled with the iTRAQ reagent, and analysed by MS/MS in 3 technical replicates (Figure 3.10). Given the intrinsic variability introduced by the complexity of the process involved in LC-MS/MS analysis, it was decided that at least 3 technical replicates would need to be performed. While three independent biological replicates each with separate technical replicates would have been ideal, the cost of this experimental design was prohibitive, hence the decision to pool the biological replicates.

In three independent experiments, culture supernatants were prepared from the four test strains *B. pseudomallei* 10276, 10276 *bsaZ::*pDM4, 10276

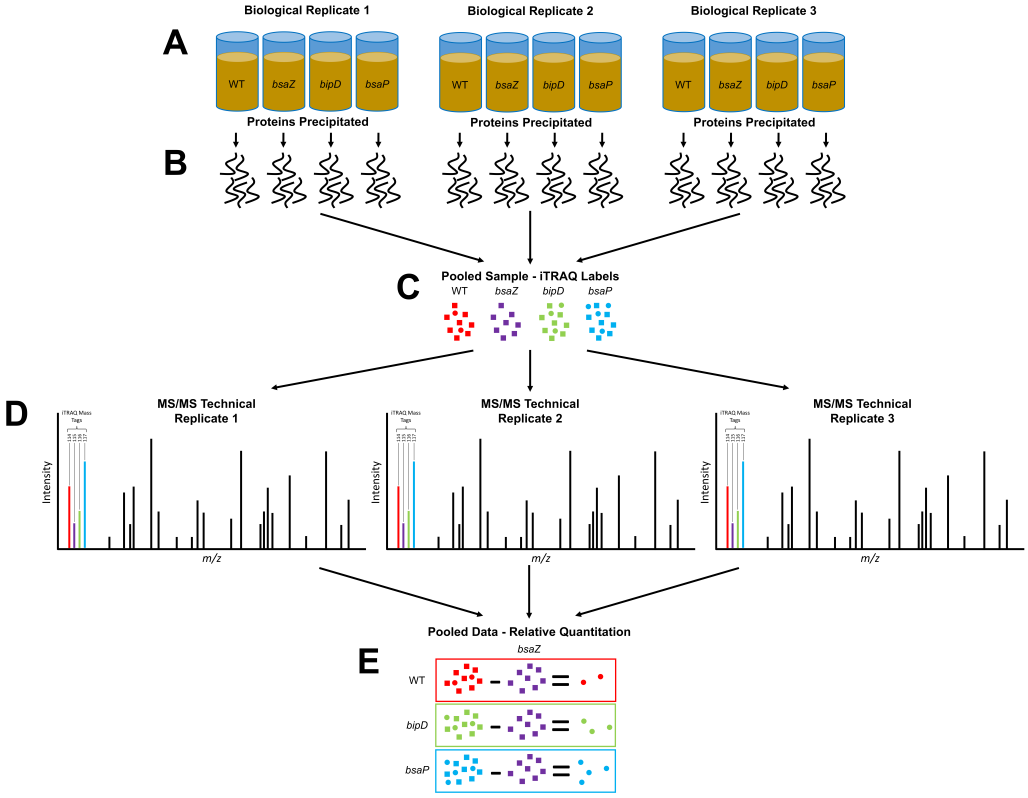


Figure 3.10: Work flow for analysis of *B. pseudomallei* secreted proteins by iTRAQ. A, Bacterial supernatants were generated in 3 independent biological replicates. **B**, Proteins were precipitated from the bacterial supernatants. Samples were checked for lysis and sample quality by immunoblotting for BopE (Figure 3.11). **C**, Equal volumes of protein from each sample were pooled, digested into peptides with trypsin and labelled with isobaric tags. **D**, The labelled peptides were pooled and submitted to 3 technical replicates of MS/MS. **E**, The data was combined, proteins were identified using MASCOT and quantitation was performed relative to the *B. pseudomallei* 10276::*bsaZ* sample.

*bipD::*pDM4, and 10276 Δ*bsaP*. Bacterial strains were cultured overnight shaking in LB at 37°C, washed in fresh LB, adjusted to an OD_{600} of 1.0, and 1 ml of the adjusted culture was used to inoculate 10 ml of fresh LB. The culture was incubated with shaking for 6 hours at 37°C after which the bacterial supernatants were collected by centrifugation and sterilised using a 0.2 μm low protein binding cellulose acetate syringe filter. Bacterial counts were assessed before and after the 6 hour incubation and all strains demonstrated similar bacterial numbers and growth rates (10^5 CFU/ml at 0 hours and 10^7 CFU/ml at 6 hours). Proteins were precipitated overnight using PRMM. Prior to pooling the biological replicates, the individual samples were all assessed individually for a lack of cell lysis and suitability by analysing equal amounts of protein by SDS-PAGE and immunoblotting for BopE. All 10276 *bsaZ::*pDM4 samples lacked BopE, indicating the samples were suitable for analysis (Figure 3.11 A). After mixing equimolar amounts of each of the three biological replicates, equal volumes of the mixed samples were visualised by SDS-PAGE and Coomassie Blue staining to ensure similar amounts of protein appeared in each lane and ensuring no extensive protein degradation had occurred during the stages of sample assessment and pooling (Figure 3.11 B). The protein profiles of each strain are similar due to the large amount of proteins secreted by *B. pseudomallei* and the relatively low abundance of T3S effectors when compared to other secreted proteins. As a final step, the pooled samples were checked for suitability by immunoblotting for BopE, which showed a similar profile to the samples before pooling had taken place (Figure 3.11 B).

The samples were subjected to iTRAQ labelling and three technical replicates of MS/MS analysis at Dundee Cell Products as described under "Experimental Procedures." iTRAQ allowed the simultaneous identification and relative quantification of peptide fragments in each of the four samples, resulting in the positive identification of a total of 475 proteins present in all samples. The data was expressed as ratios of relative protein abundance either in the 10276, 10276 *bipD::*pDM4, or 10276 Δ*bsaP* samples over the 10276 *bsaZ::*pDM4 sample as a denominator (*i.e.* 10276 WT/10276 *bsaZ::*pDM4, 10276 *bipD::*pDM4/10276 *bsaZ::*pDM4, and 10276 Δ*bsaP*/10276 *bsaZ::*pDM4). The ratios were normalized to the median for each strain and a density plot showed that the majority of protein ratios cluster around the median of one, indicating that the mutations made did not radically change the secretion profile of the bulk of proteins (Figure 3.12). This analysis identified a core set of 426 proteins which were secreted at similar levels in all strains (Figure 3.13), out of the pre-

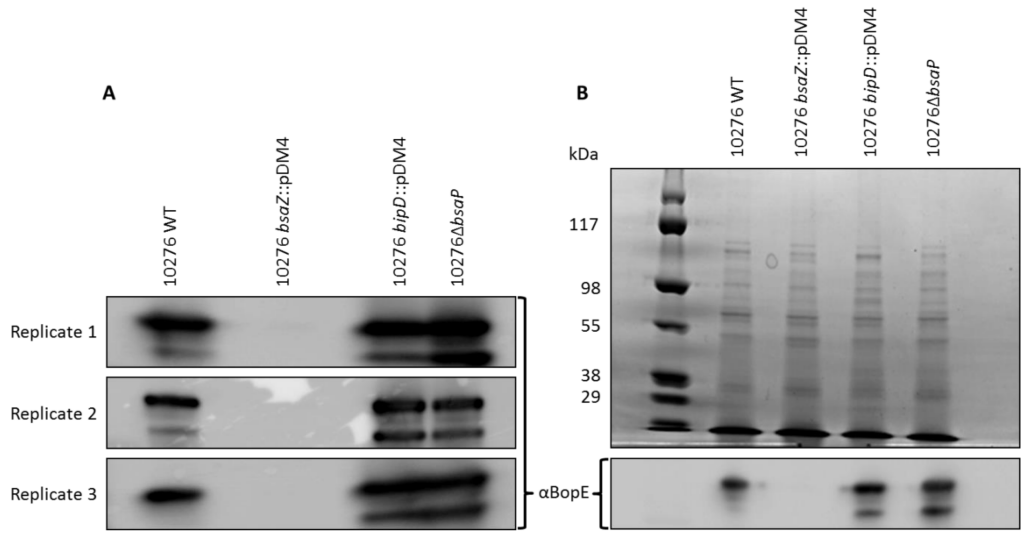


Figure 3.11: Western blots of 3 biological replicates before and after pooling for iTRAQ labelling. (A) In three independent experiments, supernatants were collected from *B. pseudomallei* 10276, 10276 *bsaZ*::pDM4, 10276 *bipD*::pDM4, and 10276Δ*bsaP* after culture for 6 hours at 37°C. Equal quantities of protein from the cell-free supernatants were separated by denaturing SDS-PAGE and transferred to a nitrocellulose membrane for protein detection using polyclonal rabbit α-BopE (Stevens *et al.*, 2003). (B) The supernatants from the three independent biological replicates where pooled in equimolar ratios. Equal quantities of protein were separated by denaturing SDS-PAGE and visualised by Coomassie Blue staining or transferred to a nitrocellulose membrane for protein detection using polyclonal rabbit α-BopE (Stevens *et al.*, 2003).

dicted total proteome of *B. pseudomallei* K96243 of about 5900 proteins (Holden *et al.*, 2004). Strikingly, the majority of these proteins (about 80%) are encoded by Chromosome 1.

Of the proteins identified in the core secretome, 54 are annotated with reference to the K96243 genome as hypothetical (uncharacterised) proteins, several more are annotated with metabolic functions . The core secretome also consisted of several elongation factors (Ts, G, P, Tu) and heat shock/chaperone proteins (GroES, GroEL), many of which have previously been reported to be present on the surface of *B. pseudomallei* or part of the outer membrane proteome and recognized by the sera of recovering melioidosis patients (Felgner *et al.*, 2009, Harding *et al.*, 2007, Su *et al.*, 2008, Schell *et al.*, 2011). In addition to the presence of a collagenase, chitobiase, bacterioferritin, and Sec secretory pathway constituents, the secretome also harboured several proteases and lipoproteins. Several phage components, Type I fimbriae and flagellar subunits were also present, although there was a notable lack of any of the predicted T6SS structural or effector proteins or the Type V family of autotransporters. This is in agreement with previous studies which found low expression of the *virAG* virulence regulator, as well as both the T6SS and the Type V auto transporter *bimA*, when *B. pseudomallei* was cultured in rich media (Chen *et al.*, 2011, Burtnick *et al.*, 2011, Burtnick and Brett, 2013).

3.2.6 Identification of the Potential Bsa Effector Repertoire

Putative T3SS effector proteins were identified in the data sets primarily on the calculated iTRAQ protein abundance ratios. The protein abundances obtained in each of the WT or mutant strain samples were each expressed as a ratio of the 10276 *bsaZ*::pDM4 sample and proteins with an iTRAQ ratio higher than the 1.5 x interquartile range (IQR), together with at least two unique peptides with a MASCOT peptide score $\geq$21, were taken to be T3SS effector protein candidates.

The 1.5 x IQR values were calculated using the R software and the cut-offs set at 1.56 for the 10276 WT/10276 *bsaZ*::pDM4 data set, 1.79 for the 10276 *bipD*::pDM4/10276 *bsaZ*::pDM4 data set and 1.46 for the 10276 Δ*bsaP*/ 10276 *bsaZ*::pDM4 data set, based on the criteria described above. When the data was plotted as a boxplot, the data showed a trend toward more proteins with larger ratios in the 10276 *bipD*::pDM4/10276 *bsaZ*::pDM4 and 10276 Δ*bsaP*/10276 *bsaZ*::pDM4 data sets when compared with the 10276 WT/10276 *bsaZ*::pDM4 data set (Figure 3.14*A*). A total of 26 proteins met the selection

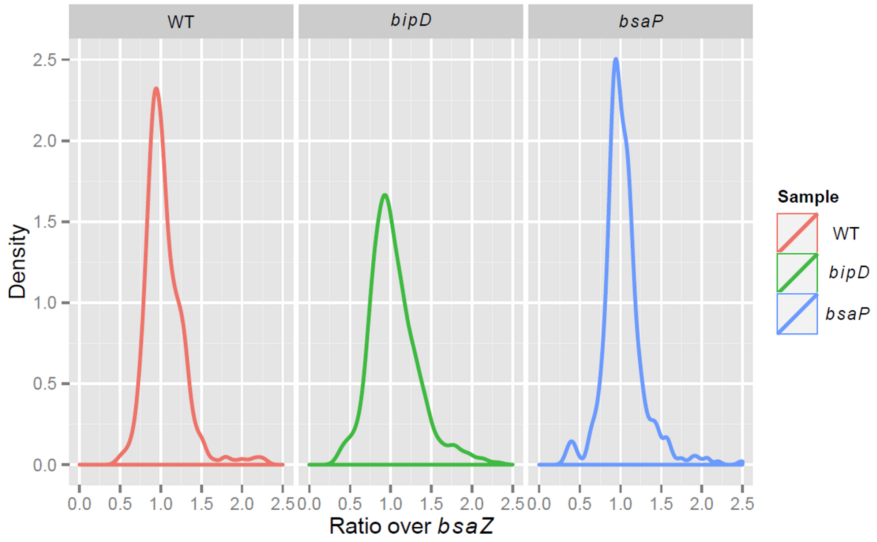


Figure 3.12: Density plot constructed with R software (R Core Team, 2015) illustrating the distribution of the median normalised iTRAQ ratios. This density plot displays proteins with a ratio between 0 and 2.5 in each of the three datasets, where protein ratios were expressed as either 10276 (WT), 10276 *bipD*::pDM4 (*bipD*) or 10276 Δ*bsaP* (*bsaP*) samples compared to the 10276 *bsaZ*::pDM4 (*bsaZ*) sample. Ratios close to 1 represent proteins that were present in similar quantities in the supernatants of a given strain when compared to the *bsa*-null mutant.

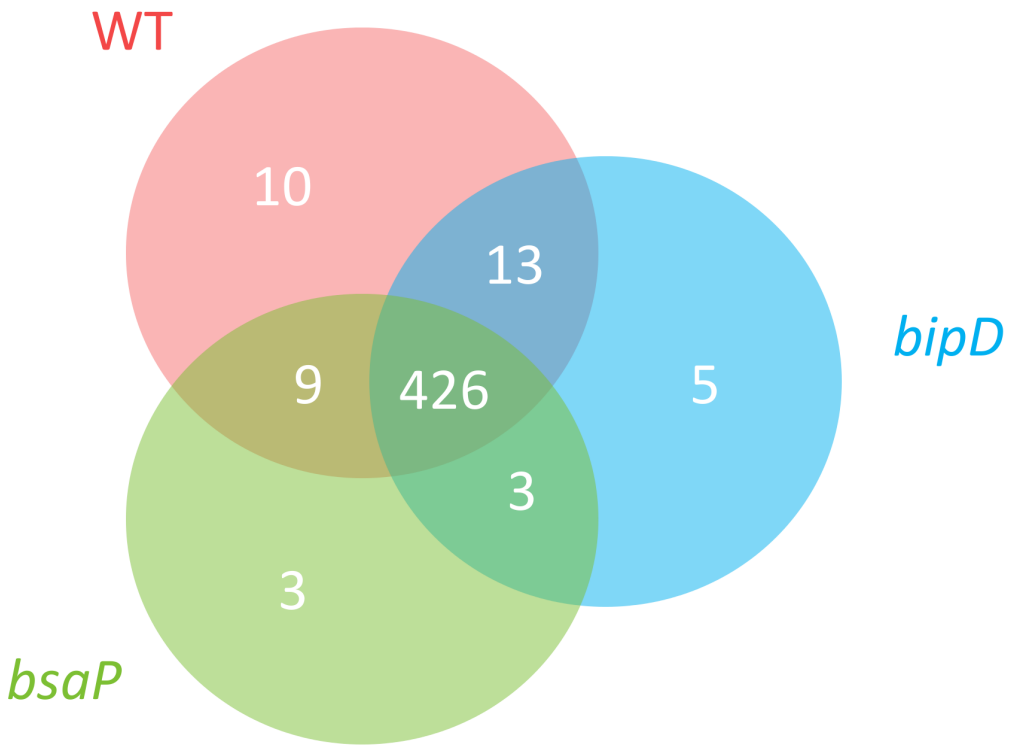


Figure 3.13: Venn diagram of the core secretome of *B. pseudomallei*. Proteins present in the secretome of 10276, 10276 *bipD*::pDM4 and 10276 Δ*bsaP* compared to the 10276 *bsaZ*::pDM4 sample under standard laboratory conditions were used to construct the Venn diagram. Each circle represents the set of proteins for each strain which had iTRAQ ratios within the cut off limit of 1.5 x IQR, indicating there was no change compared to the 10276 *bsaZ*::pDM4 sample. A total of 426 proteins had ratios within the cut off limit in all strains and can be considered part of the core secretome of *B. pseudomallei* 10276.

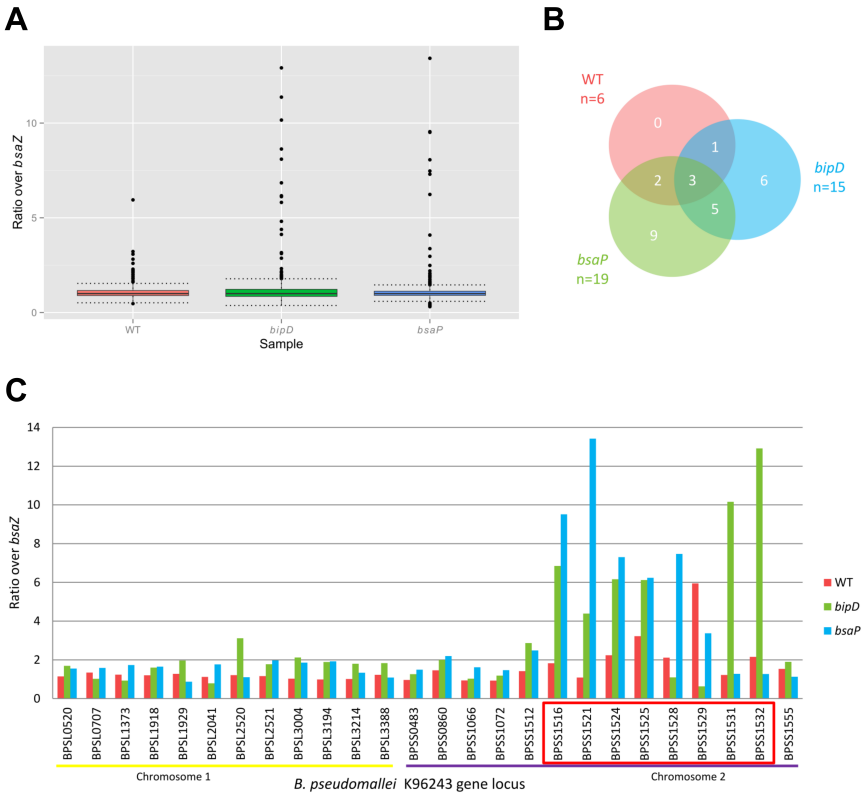


Figure 3.14: Proteins with high iTRAQ protein abundance ratios are enriched in hyper-secreting *B. pseudomallei* strains and encoded within the Bsa T3SS locus. **A**, Boxplot generated with R software (R Core Team, 2015) showing the distribution and median values of the ratios of the protein abundances in the 10276 (WT), 10276 *bipD*::pDM4 (*bipD*), or 10276 Δ*bsaP* (*bsaP*) samples compared with the 10276 *bsaZ*::pDM4 (*bsaZ*) sample. The cut-off values (calculated using R software) are shown by the dotted lines. Points shown above the cut-off value are candidate T3SS effectors. **B**, A Venn diagram depicting the number of strain-specific and shared candidate T3SS effector proteins identified in each of the strains 10276 (WT), 10276 *bipD*::pDM4 (*bipD*), and 10276 Δ*bsaP* (*bsaP*). **C**, Distribution of the candidate T3SS effector proteins plotted according to *B. pseudomallei* gene number across both chromosomes and their ratios. Gene numbers refer to the *B. pseudomallei* K96243 reference strain. The Bsa T3SS locus is indicated by the red box.

criteria and can be considered putative effectors (Table 3.1). Of the 26 proteins there were strain-specific subsets, with eight proteins with high ratios in two of the data sets and three proteins with high ratios in all three (Figure 3.14*B*). The three proteins that displayed high ratios in all three data sets, BopC, BopA, and BopE, are all known *B. pseudomallei* Type III secreted (T3S) effector proteins or predicted to be T3S proteins based on their T3SS-dependent secretion in a surrogate host system (Muangman *et al.*, 2011, Stevens *et al.*, 2003, Whitlock *et al.*, 2008) (Figure 3.14*B*). Of the 26 proteins, 20 were only found in the hyper-secreting mutant strain samples and would not have been identified had this study focused solely on the secreted proteins of the 10276 WT strain (Figure 3.14*B*). Plotting the iTRAQ ratios of the 26 putative effector proteins against their *B. pseudomallei* K96243 genetic locus number, it is clear that there is a concentration of eight proteins with especially high ratios encoded within the annotated *Bsa* T3SS locus on Chromosome 2 compared with that of the rest of the genome (Table 3.1, Figure 3.14*C*).

As expected, the Bsa T3SS-dependent hyper-secretion of BopE in the 10726 *bipD*::pDM4 and 10276Δ*bsaP* strains was observed, in full agreement with Western blot data (Figure 3.9). BopC and BopA, the latter of which has only been proven to be secreted in a T3SS-dependent manner in Enteropathogenic *E. coli* (EPEC), followed a similar pattern of secretion to BopE. Although both of the two putative translocator proteins, BipB and BipC, were secreted at higher levels in 10276 WT than 10276*bsaZ*::pDM4, only BipB was secreted at levels above the cut-off ratio of 1.56. Similar to the effect of *Shigella ipaD* mutation, the mutation of *bipD* in *B. pseudomallei* 10276 caused an increase in secretion of both BipB and BipC into the supernatant compared with WT. Where 10276 *bipD*::pDM4 had increased ratios of the translocators, 10276Δ*bsaP* showed a decrease in ratios below that of WT in agreement with Western blot data (Figure 3.9). This is further evidence that BsaP plays a similar role in *B. pseudomallei* to its homologue InvE in *Salmonella*as a gatekeeper protein. The only proven effector missing from this screen was CHBP, however this is not surprising as we have recently reported that the gene encoding CHBP, *bpss1385*, is absent from the genome of the *B. pseudomallei* 10276 strain used here (Pumirat *et al.*, 2014).

Besides the needle tip protein BipD, both putative translocators BipB and BipC, BopA, BopC, and BopE, there are also two hypothetical proteins encoded within the *bsa* T3SS locus identified by the screen that have high iTRAQ ratios. The first, BapA (BPSS1528), is a predicted 880 amino acid protein with

NCBI Accession number	*B. pseudomallei* Gene Number	Gene Name	Protein Abundance Ratio			Protein Score	Number of Unique Peptides	Percent Coverage
			WT/*bsaZ*	*bipD*/*bsaZ*	*bsaP*/*bsaZ*			
YP_107146.2	BPSL0520		1.147	1.688	1.553	568	4	19.12%
YP_107336.1	BPSL0707		1.342	1.022	1.585	2105.51	16	32.94%
YP_107998.1	BPSL1373		1.235	0.926	1.731	586.47	5	41.18%
YP_108518.1	BPSL1918	*infB*	1.201	1.600	1.653	115.12	2	2.87%
YP_108528.1	BPSL1929		1.274	1.966	0.869	78.78	2	15.22%
YP_108638.1	BPSL2041		1.118	0.789	1.762	138.41	2	2.11%
YP_109116.1	BPSL2520		1.208	3.113	1.100	39.3	2	8.59%
YP_109117.1	BPSL2521	*gyrA*	1.163	1.772	1.975	104.91	2	3.58%
YP_109599.1	BPSL3004	*rpmA*	1.027	2.120	1.858	345.09	2	32.18%
YP_109788.1	BPSL3194	*rplO*	0.986	1.889	1.922	350.21	5	36.81%
YP_109808.1	BPSL3214	*rpsJ*	1.009	1.799	1.339	87.34	3	18.45%
YP_109980.1	BPSL3388		1.226	1.831	1.083	69.47	2	5.54%
YP_110505.1	BPSS0483		0.959	1.258	1.495	122.93	2	6.25%
YP_110870.1	BPSS0860		1.462	1.995	2.198	10864.54	29	81.07%
YP_111077.1	BPSS1066		0.939	1.027	1.620	2043.11	2	37.99%
YP_111083.1	BPSS1072		0.932	1.186	1.471	773.27	11	33.33%
YP_111519.1	BPSS1512	*tssM*	1.416	2.868	2.486	6007.8	11	81.24%
YP_111522.1	BPSS1516	*bopC*	1.826	6.846	9.512	14429.09	38	47.62%
YP_111527.1	BPSS1521	*bprD*	1.088	4.387	13.419	1726.33	12	64.45%
YP_111530.1	BPSS1524	*bopA*	2.240	6.164	7.301	14932.39	43	77.39%
YP_111531.1	BPSS1525	*bopE*	3.219	6.118	6.233	8631.3	24	28.86%
YP_111534.1	BPSS1528	*bapA*	2.111	1.098	7.471	4147.77	21	35.81%
YP_111535.1	BPSS1529	*bipD*	5.946	0.635	3.373	1504.99	9	68.02%
YP_111537.1	BPSS1531	*bipC*	1.222	10.159	1.280	8921.42	23	69.19%
YP_111538.1	BPSS1532	*bipB*	2.156	12.914	1.267	13376.14	44	64.78%
YP_111561.1	BPSS1555		1.534	1.897	1.127	7757.19	27	83.80%

Table 3.1: Candidate Bsa T3SS effector proteins identified by iTRAQ. The table lists proteins in either the 10276, 10276 *bipD*::pDM4 or 10276 Δ*bsaP* culture supernatant samples that displayed protein abundance ratios (compared to the 10276 *bsaZ*::pDM4 mutant) higher than the calculated cut-off values for each comparison. The cut-off values were set at 1.56 for the 10276 WT/10276 *bsaZ*::pDM4 dataset, 1.79 for the 10276 *bipD*::pDM4/10276 *bsaZ*::pDM4 data set, and 1.46 for the 10276 Δ*bsaP*/10276 *bsaZ*::pDM4 data set, as described in "Experimental Procedures." Additional criteria for protein identification included the presence of at least two unique peptides with a MASCOT peptide score of ±21 corresponding to a 95% confidence level. The proteins are listed in order of gene number with genes from chromosome one listed first. Those proteins fulfilling the criteria for selection as candidate T3SS effector proteins are highlighted in the coloured boxes, each colour representing a different strain. Protein score refers to the adjusted sum of scores of the individual peptide scores as calculated by MASCOT. Number of unique peptides refers to the number of significant peptides specific to a protein.

no conserved domains and homologues only in the closely related species *B. mallei* and *B. thailandensis*. Unlike the known effector proteins in the iTRAQ screen, although secretion of BapA appears to be Bsa-dependent in 10276 WT and the ratio increases in the 10276 Δ*bsaP* data set, it does not appear to be secreted abundantly by the 10276*bipD*::pDM4 mutant. Interestingly, under the conditions used there was no detection of BapB or BapC, which are encoded downstream of BapA in the same operon and predicted to be substrates of the T3SS (Stevens *et al.*, 2002).

The other candidate effector protein encoded in the *bsa* T3SS locus is BprD (BPSS1521), which is annotated as a hypothetical regulator (Sun *et al.*, 2010). Predicted to be much smaller than BapA at 147aa, BprD is another protein with no known conserved domains and homologues that exist only within closely related*Burkholderia* species. The iTRAQ ratios suggest that it is not secreted at detectable levels by 10276 WT *B. pseudomallei*, but secreted by both 10276 *bipD*::pDM4 and 10276Δ*bsaP*, with the ratio of 13.4 in the 10276 Δ*bsaP*/10276 *bsaZ*::pDM4 data set being the highest of any protein described in this iTRAQ study.

Outside of the Bsa T3SS locus the remaining 18 proteins with high ratios are distributed across both *B. pseudomallei* chromosomes. One of the proteins encoded by a gene closely flanking the *bsa* locus is the virulence factor TssM (BPSS1512), which is known to be co-regulated with the Bsa T3SS as well as secreted in a Type II-dependent manner (Burtnick *et al.*, 2014).

3.2.7 Validation of iTRAQ Data by Analysis of the Secretion of Epitope-Tagged Candidate Effector Proteins

To confirm a number of targets are secreted in a Bsa-dependent manner, a number of candidates were selected to be expressed as in-frame C-terminal c-Myc tagged fusion proteins. The targets chosen were BprD, BapA, BPSS0860, BPSS1512, BopE, and BopA, as well as BPSS1916, a protein with a very high iTRAQ ratio in all strains that did not meet the initial selection criteria due to being identified with only a single unique peptide. Targets were chosen to represent proteins with both high and low protein scores, high and low numbers of peptides, and to be encoded inside and outside of the *bsa* T3SS locus. All of the proteins selected had high ratios in both the 10276 *bipD*::pDM4 and 10276 Δ*bsaP*/10276 strains. Proteins known to be ribosomal subunits were excluded from the selection. Initially the target effector proteins were cloned as in-frame

C-terminal c-Myc fusions in the shuttle vector pBHRT under a constitutive kanamycin resistance gene promoter. The plasmids were transformed into strains 10276, 10276*bsaZ*::pDM4, 10276 *bipD*::pDM4 and 10276Δ*bsaP*. Control strains containing pBHRT-*bopE* indicated that BopE-c-Myc was being secreted in a BsaZ-independent manner. This was surprising, as endogenous BopE is not secreted by the *bsaZ* mutant (Stevens *et al.*, 2003) (Figure 3.9). To ensure this was not due to the c-Myc antibody interacting non-specifically with other *B. pseudomallei* proteins, the samples were probed again using the α-BopE antibody. The western blots confirmed that BopE-c-Myc was secreted in a BsaZ-independent manner, possibly owing to the high level of expression (Figure 3.15). To investigate the possibility that the presence of BopE in the *bsaZ* supernatants was due to lysis of the bacterial cell, supernatants and bacterial cell lysates were probed using an α-GAPDH antibody. One would expect to only find GAPDH in the bacterial whole cell lysates, unless lysis of bacterial cells occurred, releasing GAPDH into the supernatants. GAPDH was found in the cell lysates of all samples, but none of the supernatant samples, suggesting BsaZ-independent secretion BopE-c-Myc was occurring in a cell lysis-independent manner, likely as a result of abnormal expression levels (Figure 3.16). In samples containing an empty pBHRT vector, BopE was secreted in a similar manner to the corresponding untransformed *B. pseudomallei* strains, ruling out cell lysis or dysregulation caused by the pBHRT vector itself. Upon overexpression it is possible that BopE secreted through one of the other T3SSs or the flagellar secretion system.

It was therefore elected to clone effector-c-Myc fusions under an IPTG-inducible *lacI* promoter in the plasmid pME6032 (Heeb *et al.*, 2002). The plasmids were transformed into strains 10276, 10276 *bsaZ*::pDM4, 10276 *bipD*::pDM4 and 10276Δ*bsaP*. Three concentrations of IPTG were tested (0 mM, 0.5 mM and 2.0 mM) and 0.5 mM was selected as the lowest level of inducer at which BsaZ-dependent BopE-c-Myc secretion was observed (Figure 3.17). BopA-c-Myc was absent in the supernatant of the 10276 *bsaZ*::pDM4 strain, but secreted by the parent strain and secreted at elevated levels by 10276Δ*bsaP* (Figure 3.18), confirming for the first time in *B. pseudomallei* that it is a substrate of the Bsa T3SS, not just the locus of enterocyte effacement-encoded T3SS in EPEC (Whitlock *et al.*, 2008). Furthermore, both of the putative effector proteins located within the *bsa* locus, BprD and BapA, were secreted in a BsaZ-dependent manner (Figure 3.18), confirming that these are novel effectors of the Bsa apparatus.

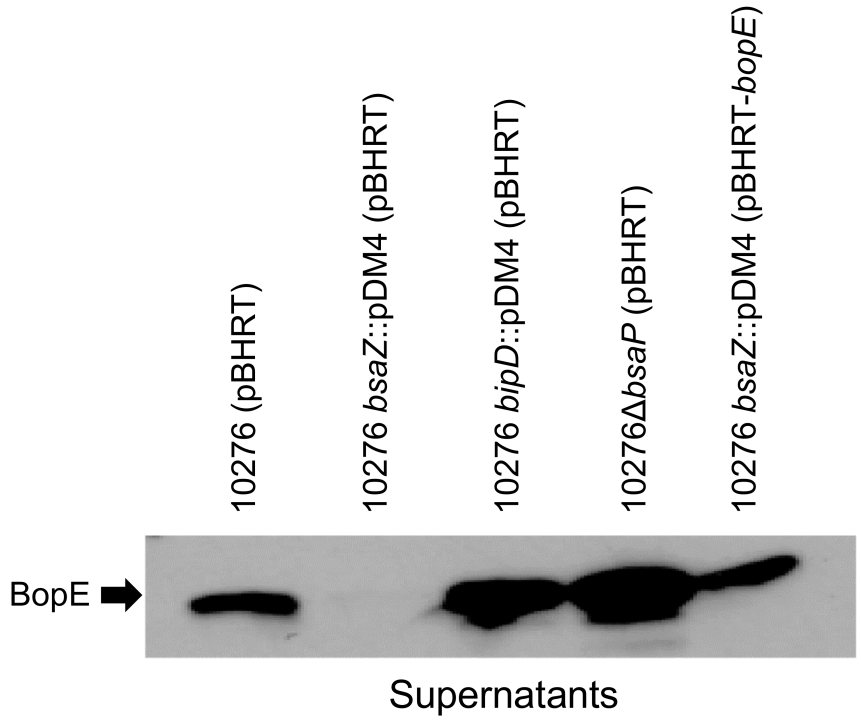


Figure 3.15: Constitutive expression of the effector protein BopE by the plasmid pBHRT causes T3SS-independent secretion of BopE in *B. pseudomallei* 10276. The coding region of *bopE* was expressed with a c-terminal c-Myc tag in the constitutive expression vector pBHRT in *B. pseudomallei* 10276 *bsaZ*::pDM4. The controls for BopE secretion were empty pBHRT in *B. pseudomallei* strains 10276, 10276 *bsaZ*::pDM4, 10276 *bipD*::pDM4 or 10276 Δ*bsaP*. Supernatant were collected after 6 hours of incubation at 37°C. Equal quantities of protein were separated by reducing SDS-PAGE, blotted onto PVDF membranes and probed using polyclonal rabbit α-BopE (Stevens *et al.*, 2003).

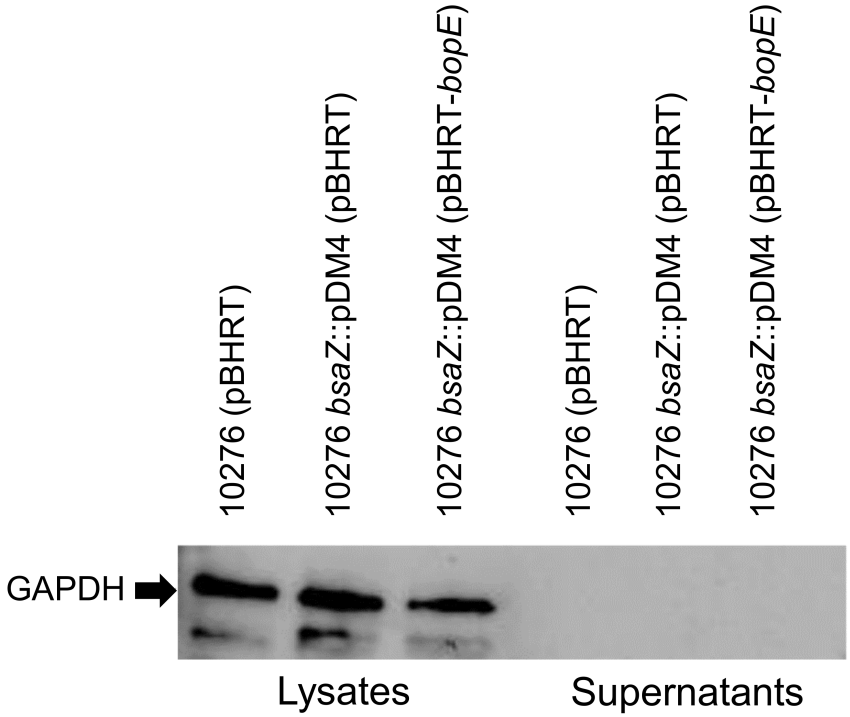


Figure 3.16: Leaky secretion of constitutively expressed BopE in *B. pseudomallei* 10276 *bsaZ*::pDM4 is not caused by bacterial cell lysis. BopE was expressed with a c-terminal c-Myc tag in the constitutive expression vector pBHRT in *B. pseudomallei* 10276 *bsaZ*::pDM4 and compared to empty pBHRT in *B. pseudomallei* strains 10276 and 10276 *bsaZ*::pDM4. Supernatant and whole cell fractions were collected after 6 hours of incubation at 37°C. Equal quantities of protein were separated by reducing SDS-PAGE, blotted onto PVDF membranes and probed using HRP linked polyclonal rabbit α-GAPDH antibody.

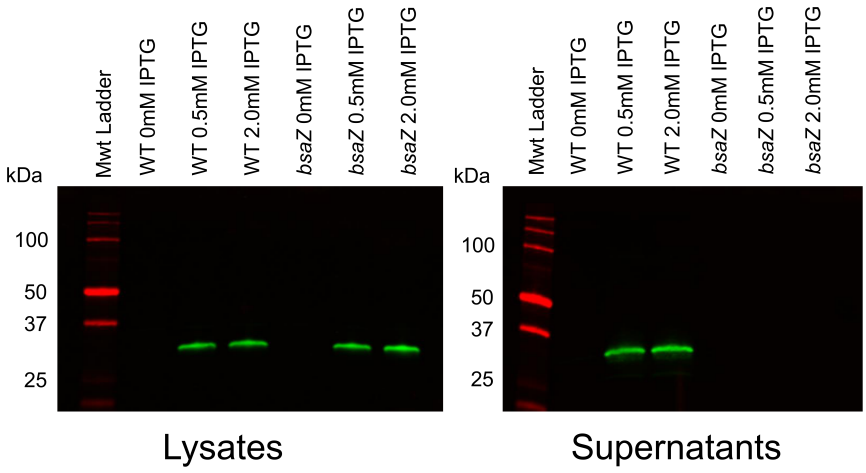


Figure 3.17: Western blot analysis of the effect of IPTG on expression and secretion of the known *B. pseudomallei* Bsa T3SS effector protein BopE expressed as c-Myc tagged fusion protein. BopE was expressed with a c-terminal c-Myc tag by the IPTG-inducible expression vector pME6032 in *B. pseudomallei* strains 10276 and 10276 *bsaZ*::pDM4. Supernatant and whole cell fractions were collected after 6 hours of incubation at 37°C in the presence of 0 mM, 0.5 mM or 2.0 mM IPTG. Equal volumes of protein were separated by reducing SDS-PAGE, blotted onto nitrocellulose membranes and probed using polyclonal rabbit α-c-Myc antibody.

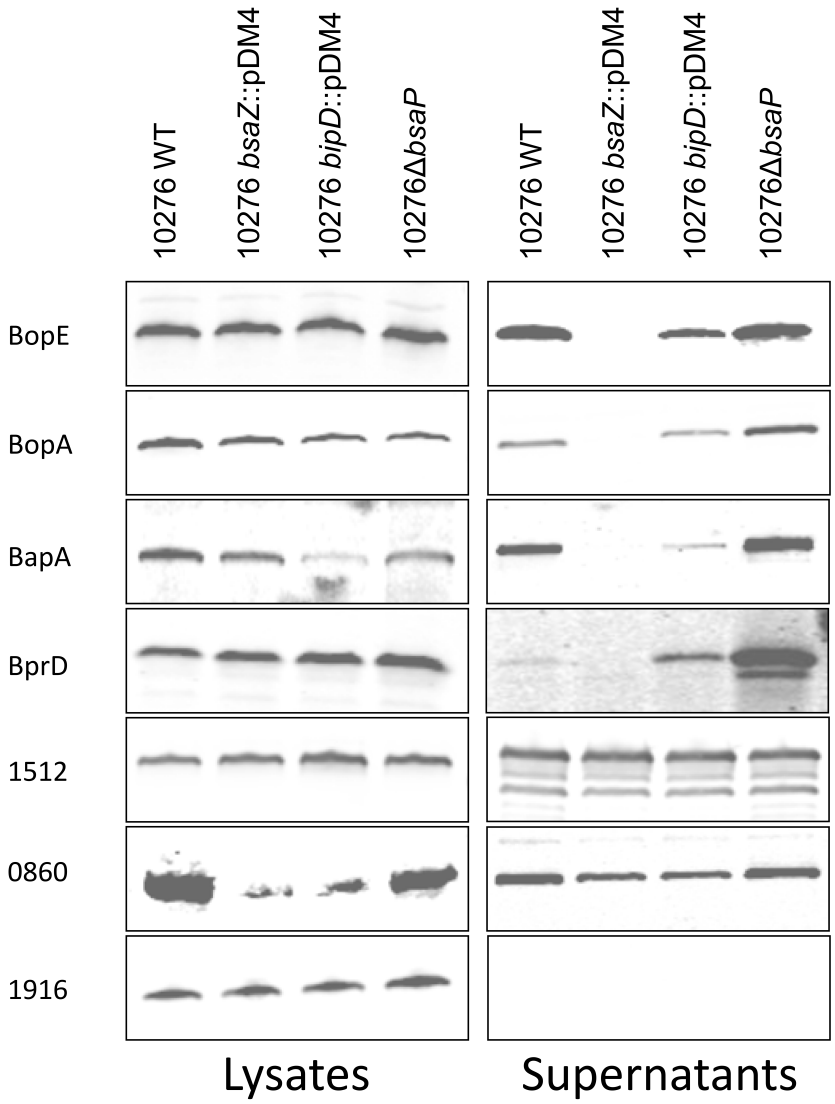


Figure 3.18: Western blot analysis of the expression and secretion of putative *B. pseudomallei* Bsa T3SS effector proteins expressed as c-Myc tagged fusion proteins. The coding region of *bopE*, *bopA*, BPSS0860, BPSS1512, BPSS1916, *bprD*, and *bapA* were expressed with a c-terminal c-Myc tag in the IPTG-inducible expression vector pME6032 in *B. pseudomallei* strains 10276, 10276 *bsaZ*::pDM4, 10276 *bipD*::pDM4 or 10276 Δ*bsaP*. Supernatant and whole cell fractions were collected after 6 hours of incubation at 37°C in the presence of 0.5 mM IPTG. Equal quantities of protein were separated by reducing SDS-PAGE, blotted onto nitrocellulose membranes and probed using polyclonal rabbit α-c-Myc antibody.

Interestingly, Bsa-dependent secretion of proteins encoded outside of the Bsa T3SS locus could not be validated. BPSS0860 and BPSS1512 appeared in the supernatants of all strains, including 10276 *bsaZ*::pDM4, indicating that although they are secreted, the Bsa system is not required for their secretion (Figure 3.18). Secretion of the protein BPSS1916 could not be detected in any of the strains tested (Figure 3.18). These examples highlight the need for validation of such data sets.

3.3 Discussion

One of the known virulence factors that is important for *B. pseudomallei* invasion, intracellular net replication and virulence in mice is the Bsa T3SS (Stevens *et al.*, 2002, 2004, Warawa and Woods, 2005, Burtnick *et al.*, 2008), but the repertoire of effector proteins secreted by the system has not yet been fully characterized. This study describes an effective way to reliably precipitate *B. pseudomallei* supernatants in small volumes using a protocol adapted from Caldwell and Lattemann (2004). To establish a better understanding of the Bsa T3SS, mutations were made in key structural components shown to dysregulate other T3SSs. It is demonstrated that these mutations lead to hyper-secretion of known effector proteins. Using these mutants, a quantitative proteomic analysis of the total secretome of the Bsa T3SS system was performed. This iTRAQ analysis identified all known effector proteins and translocators present in *B. pseudomallei* 10276, as well as identifying a number of novel putative effector proteins, two of which were independently validated. Also, examining the changes in the abundance of effectors and translocators secreted by the different mutants provides insight into the role the proteins likely play in the temporal regulation of the Bsa T3SS compared with other T3SSs of other Gram-negative bacteria.

The inability of previous proteomics studies to identify known Bsa T3SS effectors highlights the need for the use of more sensitive techniques such as iTRAQ in combination with genetic dysregulation. The *B. pseudomallei* secretome is very complex (Figure 3.8). This is not surprising when taking into account the large 7.2 Mb genome (Holden *et al.*, 2004), which encodes about 5900 proteins, of which over 55% are expressed in LB (Ooi *et al.*, 2013). This study produced one of the most comprehensive secretomes of *B. pseudomallei* to date, identifying a core secretome of 426 proteins secreted under standard laboratory conditions.

Although known effectors were absent from the secreted proteome of the *bsaZ* mutant by Western blotting (Figure 3.9) and largely undetectable by iTRAQ (Table 3.1) implying a lack of cell lysis, a number of ribosomal proteins that are enriched in the supernatant when compared with the supernatant harvested from the 10276 *bsaZ*::pDM4 strain were observed. This observation has been made in several other proteomic screens of T3SS effector repertoires (Deng *et al.*, 2012, Schumacher *et al.*, 2014, Kurushima *et al.*, 2012, Bergh *et al.*, 2013) and may be because of a combination of the high abundance of ribosomal proteins in the bacterial cell coupled with the sensitivity of iTRAQ.

Concurrent to this study, a proteome analysis investigating Type II secreted proteins of *B. pseudomallei* strain MSHR688 was published (Burtnick *et al.*, 2014). From our screen, 27 of the 38 proteins identified as being substrates of Type II secretion in LB by Burtnick *et al.* (2014) were also identified in our *B. pseudomallei* 10276 culture supernatants. Whether all 38 Type II secreted proteins identified in *B. pseudomallei* MSHR688 are encoded by *B. pseudomallei* 10276 is unknown because the genome sequence for *B. pseudomallei* 10726 is not yet available. Interestingly, three of the Type II secreted proteins were enriched in the supernatants of the hyper-secreting mutants (BPSL0707, BPSS1512, BPSS1555) and two of the proteins are encoded by regions flanking the Bsa T3SS locus, BPSS1512 and BPSS1555. The deubiquitinase BPSS1512 (TssM) has been shown to be secreted inside host cells where it suppresses the host innate immune response (Shanks *et al.*, 2009, Tan *et al.*, 2010). Although TssM is secreted independently of the Bsa T3SS, its expression appears to be co-regulated with the Bsa T3SS and T6SS-5 (Tan *et al.*, 2010, Burtnick *et al.*, 2011). This co-regulation may explain the increased levels of TssM in the supernatants of the hyper-secreting mutants in this study and again highlights the importance of validating candidate effector proteins.

The profile of secreted proteins encoded within the Bsa T3SS locus provides a comprehensive picture of the secreted levels of the three known effector proteins. The profiles of both BopE and BopC in the iTRAQ screen correspond with previous studies in which they were shown to be secreted in a Bsa-dependent manner (Muangman *et al.*, 2011, Stevens *et al.*, 2003). Although BopA from *B. mallei* has been shown to be Type 3 secreted in a surrogate host (Whitlock *et al.*, 2008), this study has confirmed its secretion to be dependent on the Bsa T3SS in *B. pseudomallei* and not one of the other T3SSs.

Two of the putative Bsa T3SS substrates encoded by the Bsa T3SS locus (BapA and BprD) were validated as Bsa-dependent by Western blotting to

detect C-terminal c-Myc tagged proteins expressed extra-chromosomally. Although the function of BapA is currently unknown, a *bapA* insertion mutation was not attenuated in a Syrian hamster model of acute melioidosis (Warawa and Woods, 2005). BprD was previously annotated as a transcriptional regulator (Sun *et al.*, 2010). In a previous study, when *bprD* was deleted along with *bprB* and *bprC*, there was no change in levels of transcription of other Bsa T3SS genes leaving the role of BprD as a regulator in doubt (Sun *et al.*, 2010). More recently, a *bprD* mutant of *B. pseudomallei* K96243 was shown to have increased expression of *bprC* (Chirakul *et al.*, 2014), a downstream gene in the same operon shown to be involved in regulation of the virulence-associated T6SS (Chen *et al.*, 2011). The *bprD* mutant also showed decreased time to death in intraperitoneally inoculated BALB/c mice demonstrating its importance *in vivo* and indicating its possible role as a negative regulator of virulence (Chirakul *et al.*, 2014). It is not without precedent that a regulator of the T3SS is also a substrate for secretion, for example, LcrQ of *Yersinia* (Cambronne *et al.*, 2000).

Another candidate protein identified in this study, BPSS0860, appears to be a *fliD* homologue. There is a second copy of *fliD* (BPSL3320) located within the flagellar locus on Chromosome 1, which had protein abundance ratios that were similar between all strains. Interestingly, the expression of BPSL3320 was up-regulated, whereas the expression of BPSS0860 was down-regulated in the organs of hamsters infected with *B. pseudomallei* when compared with bacteria cultured*in vitro* (Tuanyok *et al.*, 2006). Using a c-Myc expression system, Bsa-dependent secretion of BPSS0860 was not established; however, it is possible it may be co-regulated with the Bsa T3SS in a similar manner to BPSS1512. One recent study has shown an effector protein may be secreted by more than one secretion system, thereby masking its secretion by the T3SS (Neeld *et al.*, 2014). This could also be the case for BPSS0860. It is also possible these proteins may be false positive results. Because this study involved a set of pooled biological replicates, a higher resolution would be obtained by using three separate biological replicates which may help to narrow down the list of putative effector proteins, as well as identify any that may not have been detected.

At the time of writing, little is known about the post-translational control of the Bsa T3SS. Generally it is accepted that T3SSs are under tight temporal regulation to ensure substrates are secreted in the correct order (reviewed in Büttner (2012)). This starts with assembly of the membrane-associated structural components, assembly of the needle with needle tip, secretion of translocators to form a pore in the host cell membrane, followed by secretion of ef-

fector proteins. Changes in the patterns of secreted translocators and effector proteins in different mutant strains can inform us of the possible role these proteins play in the hierarchy of secretion.

Inactivation of the needle tip protein of *B. pseudomallei*, BipD, shows a large increase in levels of both translocators and effectors in the culture supernatant, in agreement with data published for the homologous *Shigella* protein IpaD (Parsot *et al.*, 1995, Picking *et al.*, 2005). IpaD is the needle cap protein, acting to block secretion of effector proteins until host cell contact has taken place (Roehrich *et al.*, 2013). Because of its high similarity in both sequence and structure (Erskine *et al.*, 2006) it is perhaps unsurprising that BipD would have a similar effect on the levels of substrates secreted by the Bsa T3SS. Interestingly there was a high ratio of BipB, but not BipC in the WT *B. pseudomallei* 10276 strain culture supernatant compared with 10276 *bsaZ*::pDM4 (Table 3.1). In *Shigella*, IpaB is present in the needle tip in complex with IpaD, whereas IpaC is secreted later, only upon host cell contact or activation (Epler *et al.*, 2009). With this in mind, it is possible that the stimuli required for BipC secretion in WT *B. pseudomallei* 10276 is lacking when cultured in LB.

Here, evidence is presented that BsaP functions as a gatekeeper protein for effectors in a manner similar to the homologous T3SS proteins InvE/ SepL/ MxiC/ YopN-TyeA (Kubori and Galán, 2002, Kresse *et al.*, 2000, Deng *et al.*, 2004, 2005, Botteaux *et al.*, 2009, Forsberg *et al.*, 1991, Iriarte *et al.*, 1998). Members of this family of proteins function differently from each other, but are all thought to be important in allowing effectors to be secreted by the mature T3SS. Here, it is shown that deletion of *bsaP* creates a phenotype in which effector proteins are hyper-secreted and levels of translocators decrease. To fully understand BsaP in the context of the other members of the gatekeeper family of proteins, more work would be required to determine the molecular interactions of BsaP with other components of the Bsa T3SS.

This study is another example of the power of a combination of classic targeted mutagenesis and a gel-free quantitative proteomics approach, such as iTRAQ, to study a complex secretion system, providing insights into the involvement of certain proteins on the regulation of the T3SS itself. Two new substrates of the Bsa T3SS were revealed by the study, confirming the effector repertoire is more complex than reported so far.

Note: Much of the data from this chapter has been published in Molecular and Cellular Proteomics in 2015. A copy of the publication is included as an appendix.

Chapter 4

Identification of Effector Protein Interacting Partners

4.1 Introduction

From the putative effector proteins identified during the iTRAQ screen (Chapter 3), three were chosen for further characterisation; BipC, BprD and BapA. BipC is homologous to SipC from *Salmonella* (Stevens *et al.*, 2002), a protein known to have a dual function as a translocator and an effector which can bind and polymerise host cell actin (Hayward and Koronakis, 1999). The molecular function of BipC has not been described thus far and its study may provide important insights as to whether it has a role beyond that of being a translocator protein. BapA and BprD, share no homology with any protein outside of the closely related *Burkholderia* species and contain no known conserved protein domains. This makes BapA and BprD exciting candidates for interesting and novel biology, but also makes determining the function of these proteins difficult, as homology is often used to inform potentially useful functional assays.

One method of discovering the function of an unknown protein is to identify any other proteins it may interact with. There are many methods for investigating protein-protein interactions which can be broadly split into two categories; low-throughput such as X-ray crystallography and nuclear magnetic resonance spectroscopy (NMR) for studying single known protein-protein interactions and high-throughput methods such as yeast two-hybrid (Y2H) and antibody or tag based methods for interrogating vast numbers of interactions simultaneously (Reviewed in Williamson and Sutcliffe (2010)). The most prevalent methods used to detect protein-protein interactions are Y2H and affinity purification (Reviewed in Brückner *et al.* (2009)). Each method has dis-

tinct advantages and disadvantages. Important differences between the two systems are that Y2H is *in vivo* and identifies binary (direct) protein-protein interactions while affinity purification is *in vitro* and identifies entire interacting complexes (Reviewed in Brückner *et al.* (2009)). Some other advantages of Y2H are that it is relatively less expensive than affinity purification and does not require access to advanced MS equipment (Reviewed in Brückner *et al.* (2009)).

Y2H was originally described by Fields and Song (1989) as a genetic system using the GAL4 protein in *Saccharomyces cerevisiae* to identify protein-protein interactions. GAL4 is a transcriptional activator required for the activation of genes responsible for galactose metabolism and has separate domains for DNA activation and DNA binding (Reviewed in Traven *et al.* (2006)). The Y2H system exploits modular characteristics of the *S. cerevisiae* GAL4 gene by separating the two domains and fusing them to proteins to be screened for interaction (Fields and Song, 1989). These are expressed in a reporter yeast strain where the specific DNA sequences that the GAL4 DNA binding domain recognises are placed upstream of the *GAL1* promoter sequence fused to the reporter gene *lacZ* (Fields and Song, 1989). If proteins interact, bringing the modular GAL4 DNA activation domain in close proximity to the DNA activation domain, *lacZ* transcription occurs resulting in β-galactosidase production, which can be measured enzymatically (Figure 4.1) (Fields and Song, 1989). Later, greater specificity was added to the system by adding a larger number of reporter genes, notably genes required for *S. cerevisiae* growth on media lacking adenine and histidine and the creation of library systems to screen large numbers of proteins simultaneously (James *et al.*, 1996). While a very effective method for the discovery of protein-protein interactions, Y2H screening has some limitations. The classical Y2H system can only detect interactions that take place inside the nucleus of *S. cerevisiae* and proteins toxic to the yeast can not be studied, hydrophobic membrane proteins function poorly in the screen and post-translational modifications required for interactions may not take place (Reviewed in Koegl and Uetz (2007)). The screen also suffers from false-negative and false-positive results, the latter of which is addressed by confirming interactions detected by Y2H using independent methods (Reviewed in Koegl and Uetz (2007)).

Y2H has been used successfully in the past to identify the interacting partners and characterise T3SS effector proteins in other Gram negative bacteria such as: *E. coli* EspF (Viswanathan *et al.*, 2004), NleA (Lee *et al.*, 2008), NleH

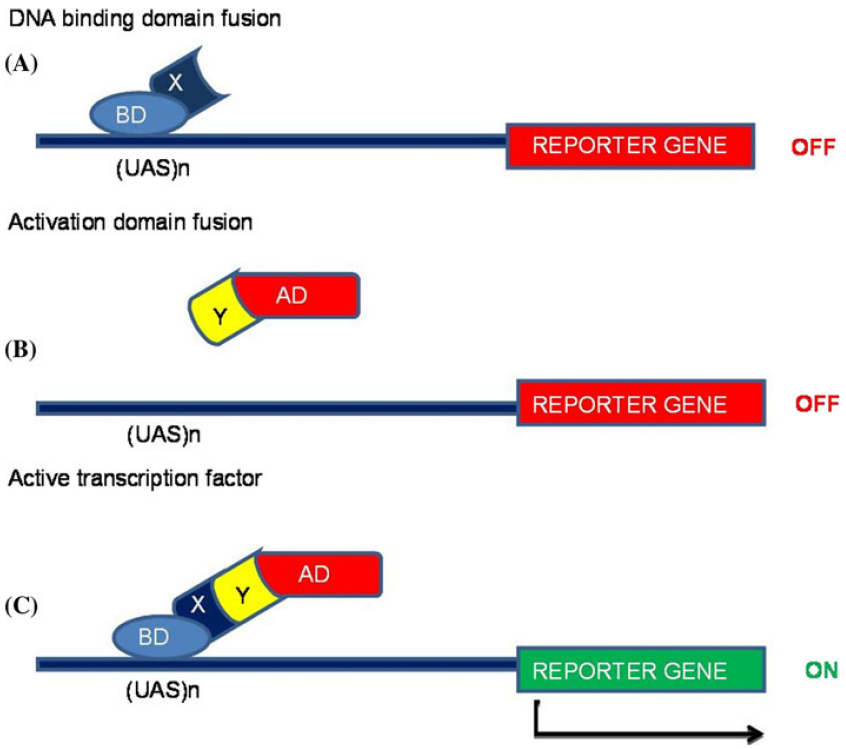


Figure 4.1: The yeast two-hybrid system for identifying protein-protein interactions. In the yeast two-hybrid system, the modular GAL4 DNA activating and binding domains are fused to bait (X) and prey (Y) proteins. **(A)** The GAL4 DNA binding domain (BD) fused to protein X binds the upstream activating sequence (UAS), but can not activate the reporter gene alone. **(B)** The GAL4 activating domain (AD) fused to protein Y in the absence of the GAL4 BD can not bind to UAS so the reporter gene is not activated. **(C)** When proteins X and Y interact, they bring the GAL4 BD and AD into close proximity leading to activation of the reporter gene. Figure taken from Ferro and Trabalzini (2013).

(Hemrajani *et al.*, 2010); *Shigella flexneri* IpaH4.5 (Wang *et al.*, 2013); and *Pseudomonas aeruginosa* ExoS (Okuda *et al.*, 2014). In this study, three Bsa T3SS effector proteins, BprD (BPSS1521), BapA (BPSS1528), and BipC (BPSS1531), were selected for a Y2H screen using a universal library of human proteins. From the screen, two human proteins were identified as interacting partners for BapA and 14 human proteins were identified as interacting partners for BipC. Interestingly, no interacting partners were identified for BprD. One protein shown to interact with both BipC and BapA, Complement component 1 Q subcomponent-binding protein (C1QBP), was confirmed using protein pull-downs. This allows informed design for future studies to determine a possible role for both BipC and BapA in *B. pseudomallei* pathogenesis.

4.2 Results

4.2.1 Investigation of BipC-Protein Interactions Using Pull-Downs and Mass Spectrometry

To explore the possible function of the Bsa T3SS effectors of interest, a decision was made to investigate possible protein-protein interactions with eukaryotic host cell proteins. Under my supervision, an honours student in the lab, Stefanie Küchler, performed pull-downs using cell lysates followed by MS analysis using glutathione S-transferase (GST)-BipC fusion proteins. A GST fusion of another *B. pseudomallei* effector protein, BopE, was prepared as a control. GST was chosen as an affinity tag because it produces high yields of fusion protein when expressed in *E. coli* and requires mild elution conditions and cell lysates were used because they allow for a high concentration of host cell protein (Reviewed in Waugh (2005)). BopE has been shown be a guanine nucleotide exchange factor for Cdc42 and Rac1 (Stevens *et al.*, 2003). This provides known targets to assess the quality of the pull-down and MS analysis. The full length proteins were expressed in *E. coli* Rosetta BL21 (Novagen) using the vector pGEX-4T-1 which adds an in-frame N-terminal GST to the protein of interest. Protein expression was induced in culture using IPTG, bacteria were collected, lysed with bugbuster, and the bacterial cell lysates were incubated for 1 hour at room temperature with GSH linked sepharose beads. The beads were washed and then incubated for 1 hour at room temperature with A549 cell lysates. A549 cells were selected as they are a well studied in vitro model of *B. pseudomallei* infection (Reviewed in Allwood *et al.* (2011)). The

beads were washed and proteins were visualised by SDS-PAGE followed by silver staining.

Pull-downs using A549 cells resulted in protein levels that were too low for downstream MS analysis when visualised by silver staining (Figure 4.2). It was hypothesised that premature elution of proteins from the GSH-linked sepharose beads or low protein concentration in the A549 cell lysates may have caused the lack of protein in the final sample. The presence of the GST protein at 23 kDa in the BopE sample was also seen, possibly due to early termination of transcription or translation of the fusion protein. To address this, GST-BopE was produced again using the conditions above and the GST-fusion proteins were eluted from the sepharose beads and covalently linked to the UltraLink Biosupport beads, which prevents loss of the fusion proteins. The GST proteins bound to UltraLink beads were then incubated for 1 hour at room temperature with murine splenic lysates (MSL), which had a higher protein concentration than the A549 cell lysates (MSL = 6.357 mg/ml; A549 = 0.48 mg/ml). The beads were washed and proteins were visualised by SDS-PAGE followed by silver staining or Western blotting with rabbit α-Cdc42 or rabbit α-Rac1 antibodies. Rabbit α-actin antibodies were also used as it was hypothesised that due to its homology (Stevens *et al.*, 2002) to the actin binding protein SipC (*Salmonella*) (Hayward and Koronakis, 1999), BipC may also bind actin.

The UltraLink beads and MSLs yielded more protein than GSH-linked sepharose beads and A549 cell lysates, with different banding patterns being seen between the GST and GST-BipC lanes by silver staining (Figure 4.3). The GST-BopE lane had less protein than the other two lanes. When immunoblotting with an α-actin antibody was performed, actin could be seen in all lanes including the GST only control lane, though at lower levels than the GST BipC lane (Figure 4.4). As GST should not bind actin (Stevens *et al.*, 2005), this may have been due to the high concentration of protein in the MSL or improper washing. Yet, Cdc42 and Rac1 were not seen in the GST-BopE samples by Western blot (data not shown). To better understand what proteins may be bound to the different fusion proteins, 14 bands were excised from the silverstained gel and submitted to MS analysis using the in-house proteomics facility at the Roslin Institute (Figure 4.3). Proteins appearing in the GST only sample were removed as background proteins and the web-based database CRAPome (http//www.crapome.org/) was used to remove a set of proteins commonly found as false-positives in pull-down experiments.

The resulting list of interacting proteins for GST-BipC contained 27 unique

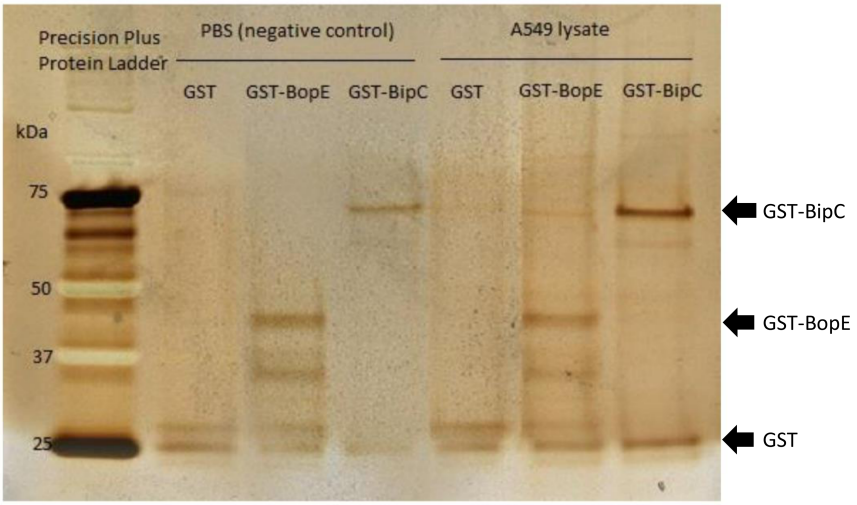


Figure 4.2: Pull-downs using A549 cell lysates and GST-fusion proteins bound to GSH-linked sepharose beads visualised by silver staining. GST, GST-BopE and GST-BipC bound to GSH-linked sepharose beads were incubated with A549 cell lysates or PBS for 1 hour. Proteins remaining bound to the beads following washing were analysed by SDS-PAGE followed by silver staining.

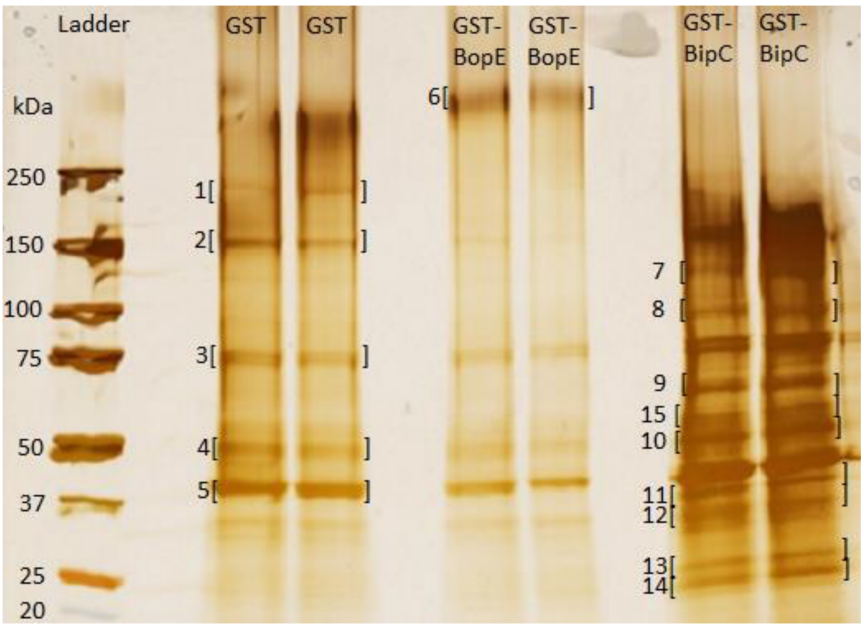


Figure 4.3: Pull-downs using murine splenic lysates and GST-fusion proteins bound to UltraLink Biosupport beads visualised by silver staining. GST, GST-BopE and GST-BipC covalently bound to UltraLink Biosupport beads were incubated with murine splenic lysates for 1 hour. Proteins remaining bound to the beads following washing were analysed by SDS-PAGE followed by silver staining.

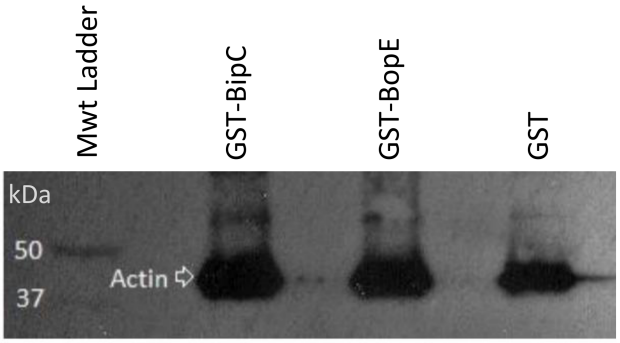


Figure 4.4: α-actin immunoblot of proteins pulled-down from murine splenic lysates by GST-BipC and GST-BopE. GST, GST-BopE and GST-BipC covalently bound to UltraLink Biosupport beads were incubated with murine splenic lysates for 1 hour. Proteins remaining bound to the beads following washing were analysed by SDS-PAGE followed by Western blotting using a rabbit α-actin antibody.

identifications which were investigated using the Uniprot database, while there were no proteins identified in the BopE sample (Table 4.1). Neither Cdc42 or Rac1 was present in the GST-BopE sample. One hypothesis is that the interaction of BopE with these proteins is transient or that the pull-down conditions were not appropriate for the interaction. The list of proteins present in the GST-BipC sample included proteins involved in multiple metabolic processes, apoptosis, cell proliferation, endocytosis as well as cytoskeletal components, making it difficult to infer a specific pathway that BipC may be interacting with.

Table 4.1: Proteins identified as possible BipC-interacting partners using pull-downs and mass spectrometry analysis. The table contains the Protein name and the cellular location of identified proteins as found in the Uniprot database.

Protein Name	Location in Cell
α-Actin	cytoskeleton
β-Actin	cytoskeleton
γ-Actin	cytoskeleton
Actin-related protein 2	Arp2/3 complex, actin cap, cytoskeleton, cell cortex, cell projection
Fructose-bisphosphate aldolase B	centriolar satellites, microtubule organising centre, cytoskeleton
Asialoglycoprotein receptor 1	plasma membrane, extracellular
Formin-like protein 1	cytoplasm, phagocytic vesicles, plasma membrane
Formimidoyltransferase-cyclodeaminase	golgi apparatus, cytoskeleton
Glutamine synthetase	cell body, cytoplasm
Prolow-density lipoprotein receptor-related protein 1	cytoplasm, clathrin coated vesicles, endosome, plasma membrane, lysosomal membrane, neuronal cell body, nucleus, receptor complex
Acetyl-CoA acetyltransferase	cytoplasm, nucleus, mitochondria
Alcohol dehydrogenase 1	cytoplasm, plasma membrane
Alcohol dehydrogenase [NADP(+)]	cytoplasm
Estradiol 17 beta-dehydrogenase 5	cytoplasm, nucleus
Delta-aminolevulinic acid dehydratase	cytoplasm, extracellular space
Cytosolic 10-formyltetrahydrofolate dehydrogenase	cytoplasm, mitochondria
Argininosuccinate synthase	cell body fibre, cytoplasm, ER, lysosome, mitochondria, nucleus
Carbonic anhydrase 3	cytoplasm
L-xylulose reductase	brush border, plasma membrane
Fructose-1,6-bisphosphatase 1	cytoplasm
Galactokinase	cytoplasm
Aspartate aminotransferase	cytoplasm
Glycylpeptide N-tetradecanoyltransferase 2	golgi apparatus, plasma membrane, cytoplasm
Ornithine carbamoyltransferase	cytoplasm, mitochondria
Selenium-binding protein 2	cytoplasm, nucleus
Sepiapterin reductase	cytoplasm, mitochondria, nucleus
14-3-3 protein theta	cytoplasm

4.2.2 Generation of Strains and Validation of the Yeast Two-Hybrid System

Because of the presence of actin in the negative control lane in Figure 4.4 and the lack of Cdc42 and Rac1 in the BopE control by Western blot as well as a lack of detection of BopE interacting partners by MS, it was decided that direct protein-protein interactions would be explored using a Y2H approach. The Clontech Matchmaker GAL4 Two-Hybrid System 3, which reports protein-protein interactions by activating transcription of the reporter genes *ADE2*, *HIS3*, *lacZ* as well as *MEL1* was utilised. Activation of the reporter genes allow growth on media lacking adenine and histidine. Reporter gene activation can also be measured by the production of β-galactosidase and α-galactosidase, facilitating blue/white screening.

The Y2H system uses two plasmids; the bait plasmid pGBKT7 which encodes the GAL4 DNA binding domain and the prey plasmid pGADT7 which encodes the GAL4 DNA activating domain. The three effector proteins of interest selected for this analysis were BipC, BapA, and BprD. The full length coding sequences of BipC, BprD, and BapA from *B. pseudomallei* strain 10276 were cloned into the vector pGBKT7, which encodes an in-frame N-terminal fusion of the first 147 amino acids of the *GAL4* DNA binding domain and an N-terminal c-Myc tag. The plasmid also contains the gene *TRP1*, allowing the *S. cerevisiae* strains to replicate in the absence of tryptophan. The plasmids were confirmed to contain the correct in-frame sequence by sequencing using the T7 Forward and DNA-BD primers (Figures 4.5, 4.6, 4.7, 4.8). Because the sequence of *B. pseudomallei* 10276 is not available, the amino acid sequences of the proteins were compared to that of *B. pseudomallei* K96243, and differences in the amino acid sequence were checked against other *B. pseudomallei* strains to confirm they are natural and not due to mutations introduced during cloning.

The BipC sequence contained one difference at amino acid A63G that was present in other *B. pseudomallei* strains (Figure 4.5). Due to its length, the BapA sequence was sequenced in four sections which were combined. There are 14 amino acids that are not present in pGBKT7-BapA that are present in the *B. pseudomallei* K96243 reference sequence (Figure 4.6). However, the *B. pseudomallei* 10276 strain is not sequenced so it is not known whether this amino acid deletion is naturally occurring. To address this issue, the cloned pGBKT7-BapA was searched against all sequenced WT strains of *B. pseudomallei* to identify whether it represented a natural variant of the BapA protein. The same 14 amino acid deletion is present in the sequenced strain MSHR511, indicating

```
pGBKT7-bipC     MSIGVQSSGINISHAELSRLVDAGKSEQGDKAVRDDGRALARADAALAAVVGERVAARRD      60
K96243          MSIGVQSSGINISHAELSRLVDAGKSEQGDKAVRDDGRALARADAALAAVVGERVAARRD      60
Pakistan9       MSIGVQSSGINISHAELSRLVDAGKSEQGDKAVRDDGRALARADAALAAVVGERVAARRD      60
                ************************************************************

pGBKT7-bipC     AVGGSGAQRVELARPKPDAQTRATDRRTVSGLEREHKRLAASQTPRVTGMHDALVQRHVS      120
K96243          AVAGSGAQRVELARPKPDAQTRATDRRTVSGLEREHKRLAASQTPRVTGMHDALVQRHVS      120
Pakistan9       AVGGSGAQRVELARPKPDAQTRATDRRTVSGLEREHKRLAASQTPRVTGMHDALVQRHVS      120
                **.********************************************************

pGBKT7-bipC     LDGAKAAHGEGVKRAAGDAPRAAADAPQRFAFADDKAFDAMLALGAAMQKNVQSDLAMQG      180
K96243          LDGAKAAHGEGVKRAAGDAPRAAADAPQRFAFADDKAFDAMLALGAAMQKNVQSDLAMQG      180
Pakistan9       LDGAKAAHGEGVKRAAGDAPRAAADAPQRFAFADDKAFDAMLALGAAMQKNVQSDLAMQG      180
                ************************************************************

pGBKT7-bipC     KLTMLAHDAMMSAAAQDRSIGAAQMTAAIAGGALQATTSLGGAMQQMKSLSTKSMSIEKE      240
K96243          KLTMLAHDAMMSAAAQDRSIGAAQMTAAIAGGALQATTSLGGAMQQMKSLSTKSMSIEKE      240
Pakistan9       KLTMLAHDAMMSAAAQDRSIGAAQMTAAIAGGALQATTSLGGAMQQMKSLSTKSMSIEKE      240
                ************************************************************

pGBKT7-bipC     LKPQAELKQFHAEQALELRGINKPVLSNDEVSHVKIKRDTGETVRHEIDHGGERMSDEHA      300
K96243          LKPQAELKQFHAEQALELRGINKPVLSNDEVSHVKIKRDTGETVRHEIDHGGERMSDEHA      300
Pakistan9       LKPQAELKQFHAEQALELRGINKPVLSNDEVSHVKIKRDTGETVRHEIDHGGERMSDEHA      300
                ************************************************************

pGBKT7-bipC     SVLAQEAPARQHRIDMHGMRHEENLVKAGRQQMKGDLLQSGGQIGKNQIDGASAQQQGAD      360
K96243          SVLAQEAPARQHRIDMHGMRHEENLVKAGRQQMKGDLLQSGGQIGKNQIDGASAQQQGAD      360
Pakistan9       SVLAQEAPARQHRIDMHGMRHEENLVKAGRQQMKGDLLQSGGQIGKNQIDGASAQQQGAD      360
                ************************************************************

pGBKT7-bipC     RAEQKEDENAQQTAMAAASTRDEAAHRSREAAQKAIDAAKSQVANDNAVAAQVAGNLRT       419
K96243          RAEQKEDENAQQTAMAAASTRDEAAHRSREAAQKAIDAAKSQVANDNAVAAQVAGNLRT       419
Pakistan9       RAEQKEDENAQQTAMAAASTRDEAAHRSREAAQKAIDAAKSQVANDNAVAAQVAGNLRT       419
                ***********************************************************
```

Figure 4.5: Comparison of the amino acid sequence of BipC expressed by pGBKT7. The entire coding sequence of the *bipC* gene (BPSS1531) from *B. pseudomallei* 10276 was cloned into the Y2H vector pGBKT7. The insert was sequenced and Clustal Omega (Sievers *et al.,* 2011) was used to compare the translated pGBKT7-*bipC* DNA sequence with the amino acid sequence of BipC from *B. pseudomallei* K96243 (YP_111537.1) and *B. pseudomallei* Pakistan 9 (EEH27955.1).

```
pGBKT7-BapA     MPPSIHRTSSINSTPAVTAAGARRASGPGGVLSADVAHVASARRHTMPEIGARRGVDGDR      60
K96243          MPPSIHRTSSINSTPAVTAAGARRASGPGGVLSADVARVASARRHTMPEIGARRGVDGDR      60
MSHR511         MPPSIHRTSSINSTPAVTAAGARRASGPGGVLSADVARVASARRHTMPEIGARRSVDGDR      60
                **********************************:***************.*****

pGBKT7-BapA     AAPAPRESFRRRLETVSSRAPTPPPEADSRAANARTTGAADGAGATGAAAGPSHGATSLD      120
K96243          AAPAPRESFRRRLETVSSRAPTPPPEADSRAANARTTGAADGAGATGAAAGPSHGATSLD      120
MSHR511         AAPAPRESFRRRLETVSSRAPTPPPEADSRAANARTTDAADGAGATGAAAGPSHGATSLD      120
                ********************************** **********************

pGBKT7-BapA     AARAYLAELAGDRGGALTTLVAQLNGHDRRALDHLALTVHALHLSVDDASHAKTFAGIGD      180
K96243          AARAYLAELAGDRGGALTTLVAQLNGHDRRALDHLALTVHALHLSVDDASHAKTFAGIGD      180
MSHR511         AARAYLAELAGDRGGALTTLVAQLNGHDRRALDHLALTVHALHLSVDDASHAKTFAGIGD      180
                ************************************************************

pGBKT7-BapA     ALASFLAAAARANAKPGSTPRDLCVEGNKGYRKLCECVGALLRSDGIANALFGRARERGD      240
K96243          ALASFLAAAARANAKPGSTPRDLCVEGNKGYRKLCECVGALLRSDGIANALFGRARERGD      240
MSHR511         ALASFLATAARANAKPGSTPRDLCVEGNKGYRKLCECVGALLRSDGIANALFGRARERGD      240
                *******:****************************************************

pGBKT7-BapA     AAADTLVSERLGGRMDGHVRTNGMVNRHGGDAQRRMADAAQRFALGARHATNLVDMVGTA      300
K96243          AAADTLVSERLGGRMDGHVRTNGMVNRHGGDAQRRMADAAQRFALGARHATNLVDMVGTA      300
MSHR511         AAADTLVSERLGGRMDGHVRTNGMVNRHGGDAQRRMADAAQRFALGARHATNLVDMVGTA      300
                ************************************************************

pGBKT7-BapA     LELLGRTDQLLNDVSLKRPAAEPGGPRAPGGGP--------------AAPVVVNNHNENN      346
K96243          LELLGRTDQLLNDVSLKRPAAEPGGPRAPGGGRAAPAGPASGAAQQPAAPVVVNNHNENN      360
MSHR511         LELLGRTDQLLNDVSLKRPAAEPGGPRAPGGGPAAPAGPASGAAQQPAAPVVVNNHNENN      360
                ********************************              *************

pGBKT7-BapA     VNVNLDGLERLVGDLGKMMGALLERMGAYDPSHTRPAAPDANGPAPVRTGGHTTVVKSPV      406
K96243          VNVNLDGLERLVGDLGKMMGALLERMGAYDPSHTRPAAPDANGPAPVRTGGHTTVVKSPV      420
MSHR511         VNVNLDGLERLVGDLGKMMGALLERMGAYDPSHTRPAAPDANGPAPVRTGGHTTVVKSPV      420
                ************************************************************

pGBKT7-BapA     SVARTSNNGAPGSPAADGTRGDAPMPPALSATPTTPTTPAMSPAGGPSMDERTPATNTLE      466
K96243          SVARTSNNGAPGSPAADGTRGDAPMPPTTPALPATPATPTTPPAGGPSMDERTPATNTLE      480
MSHR511         SVARTSNNGAPGSPAADGTRGEAPMPPALSATPTTPTTPAMSPAGGPSMDERTPATNTLE      480
                **********************:*****:  * *:**:**:  ******************

pGBKT7-BapA     RGAGNGGASPTGAWRRGDDGGWRMARGNPVVRTTEGATRIDPFSRVGARAASGVGAARAW      526
K96243          RGAGNGGASPTGAWRRGDDGGWRMARGNPVVRTTEGATRIDPFSRVGARAASGAGAARAW      540
MSHR511         RGAGNGGASPTGAWRRGDDGGWRMARGNPVVRTTEGATRIDPFSRVGARAASGAGAARAW      540
                ****************************************************.******

pGBKT7-BapA     RDAAADATQRSLASGTSGGAADAIAPRAGAGAAAGGDAARVARRMPDVRAGGPERDAPGE      586
K96243          RDAAADATQRSLASGTSGGAADAIAPRAGAGAAAGGDAARVARRMPDVRAGGLERDAPGE      600
MSHR511         RDAAADATQRSLASGTSGGAADAIAPRAGAGAAAGGDAARVARRMPDVRAGGPERDAPGE      600
                ************************************************ *******

pGBKT7-BapA     RAAGPNGSNGSAVGQPIAGHAPAGGPDAADFSDASGTGGTGARAPGMPPATGSWSRDPAS      646
K96243          RAAGPNGSNGSAVGQPIAGHAPAGGPDAADFSDASGTGGTGARAPGIPPATGSWSRDPAS      660
MSHR511         RAAGPNGSNGSAVGQPIAGHAPAGGPDAVDFSDASGTGGTGARAPGMPPATGSWSRDPAS      660
                ****************************.****************:**************

pGBKT7-BapA     GRWLRAGGGVPLRSTEGFGRIDPFAGAQRNASATGASAVSSPSFASASMSVGSTGALPAG      706
K96243          GRWLRAGGGVPLRSTEGFGRIDPFAGVQRNASATGASAVSSPSFASASMSVGSTGALPAG      720
MSHR511         GRWLRAGGGVPLRSTEGFGRIDPFAGAQRNASATGASAVSSPSFASASMSVGSTGALPAG      720
                *************************.**********************************

pGBKT7-BapA     SSIASPDTSGIAPAVASGGALDVASNVASGVTSNVTSNVASGVTSGVTSGVTSGVTSGVA      766
K96243          SSIASPDTSGIAPAVASGGALDVASNVASNVTSNVTSNVASG--------VTSGVTSGVA      772
MSHR511         SSIASPDTSGIAPAVASGGALDVASNVASNVASNVTSNVASGVTSGVTSGVTSGVA      780
                **************************** *:***:***:*         **********

pGBKT7-BapA     PDGTAWTRPSALAPRNIDPRRMNRAQLERAGLYPLVDDALPPSSQSAPADAGDAGDAAAR      826
K96243          PDGTAWTRPSALAPRNIDPRRMNRAQLERAGLYPLVDDALPPSSQSAPADAGDAGDAAAR      832
MSHR511         PDGTAWTRPSALAPRNIDPRRMNRAQLERAGLYPLVDDALPPSSQSAPADAGDAGDAAAR      840
                ************************************************************

pGBKT7-BapA     RASRPDTGAPQPGAAKTFPSVAPAHRIVTTEGAARVGWNDSIANGTKR                  874
K96243          RASRPDTGAPQPGAAKTFPSVAPAHRIVTTEGAARVGWNDSIANGTKR                  880
MSHR511         RASRPDTGAPQPGAAKTFPSVAPAHRIVTTEGAARVGWNDSIANGTKR                  888
                ************************************************
```

Figure 4.6: Comparison of the amino acid sequence of BapA expressed by pGBKT7. The entire coding sequence of the *bapA* gene (BPSS1528) from *B. pseudomallei* 10276 was cloned into the Y2H vector pGBKT7. The insert was sequenced and Clustal Omega (Sievers *et al.*, 2011) was used to compare the translated pGBKT7-*bapA* DNA sequence with the amino acid sequence of BapA from *B. pseudomallei* K96243 (YP_111534.1) and *B. pseudomallei* MSHR511 (AHG37918.1).

```
pGBKT7-bapA     MPDVRAGGPERDAPGERAAGPNGSNGSAVGQPIAGHAPAGGPDAADFSDASGTGGTGARA   60
K96243          MPDVRAGGLERDAPGERAAGPNGSNGSAVGQPIAGHAPAGGPDAADFSDASGTGGTGARA   60
MSHR2451        MPDVRAGGPERDAPGERAAGPNGSNGSAVGQPIAGHAPAGGPDAADFSDASGTGGTGARA   60
NTCT13179       MPDVRAGGPERDAPGERAAGPNGSNGSAVGQPIAGHAPAGGPDAADFSDASGTGGTGARA   60
576             MPDVRAGGLERDAPGERAAGPNGSNGSAVGQPIAGHAPAGGPDAADFSDASGTGGTGARA   60
                ******** **************************************************

pGBKT7-bapA     PGMPPATGSWSRDPASGRWLRAGGGVPLRSTEGFGRIDPFAGAQRNASATGASAVSSPSF   120
K96243          PGIPPATGSWSRDPASGRWLRAGGGVPLRSTEGFGRIDPFAGVQRNASATGASAVSSPSF   120
MSHR2451        PGMPPATGSWSRDPASGRWLRAGGGVPLRSTEGFGRIDPFAGAQRNASATGASAVSSPSF   120
NTCT13179       PGMPPATGSWSRDPASGRWLRAGGGVPLRSTEGFGRIDPFAGAQRNASATGASAVSSPSF   120
576             PGIPPATGSWSRDPASGRWLRAGGGVPLRSTEGFGRIDPFAGVQRNASATGASAVSSPSF   120
                **:*************************************.*****************

pGBKT7-bapA     ASASMSVGSTGALPAGSSIASPDTSGIAPAVASGGALDVASNVASGVTSNVTSNVASGVT   180
K96243          ASASMSVGSTGALPAGSSIASPDTSGIAPAVASGGALDVASNVASNVTSNVTSN------   174
MSHR2451        ASASMSVGSTGALPAGSSIASPDTSGIAPAVASGGALDVASNAASNVTSNVTSNVASGVT   180
NTCT13179       ASASMSVGSTGALPAGSSIASPDTSGIAPAVASGGALDVASNVASNVASNVTSNVTSNVA   180
576             ASASMSVGSTGALPAGSSIASPDTSGIAPAVASGGALDVASNVASNVTSNVTSNVTSNVA   180
                ****************************************.** *:******

pGBKT7-bapA     SGVTSGVTSGVTSGVAPDGTAWTRPSALAPRNIDPRRMNRAQLERAGLYPLVDDALPPSS   240
K96243          --VASGVTSGVTSGVAPDGTAWTRPSALAPRNIDPRRMNRAQLERAGLYPLVDDALPPSS   232
MSHR2451        SGVTSGVTSGVTSGVAPDGTAWTRPSALAPRNIDPRRMNRAQLERAGLYPLVDDALPPSS   240
NTCT13179       SGVTSGVTSGVTSGVAPDGTAWTRPSALAPRNIDPRRMNRAQLERAGLYPLVDDALPPSS   240
576             SGVTSGVTSGVTSGVAPDGTAWTRPSALAPRNIDPRRMNRAQLERAGLYPLVDDALPPSS   240
                  *:*****************************************************

pGBKT7-bapA     QSAPADAGD------------AGDAAARRASRPDTGAPQPGAAKTFPSVAPAHRIVTTEG   288
K96243          QSAPADAGD------------AGDAAARRASRPDTGAPQPGAAKTFPSVAPAHRIVTTEG   280
MSHR2451        QSAPADAGDAG---------DAGDAAARRASRPDTGAPQPGAAKTFPSVAPAHRIVTTEG   291
NTCT13179       QSAPADAGD------------AGDAAARRASRPDTGAPQPGAAKTFPSVAPAHRIVTTEG   288
576             QSAPADAGDAGDAGDAGDAGDAGDAAARRASRPDTGAPQPGAAKTFPSVAPAHRIVTTEG   300
                *********            ************************************

pGBKT7-bapA     AARVGWNDSIANGTKR    304
K96243          AARVGWNDSIANGTKR    296
MSHR2451        AARVGWNDSIANGTKR    307
NTCT13179       AARIGWNDSIANGTKR    304
576             AARVGWNDSIANGTKR    316
                ***:************
```

Figure 4.7: Comparison of the amino acid sequence of the C-terminus of BapA expressed by pGBKT7. Clustal Omega (Sievers *et al.*, 2011) was used to compare the C-terminal 304 amino acids of the translated pGBKT7-*bapA* DNA sequence with the amino acid sequence of BapA from *B. pseudomallei* strains K96243 (YP_111534.1), MSHR_2451 (KGW34630.1), NTCT_13179 (AGZ32639.1), and 576 (EEC31748.1).

```
pGBKT7-bprD     MKLNGMTAAQAQHRHGAIERHAPGKDDGRRTAGVADEREGRTMKGEIKAIRMDVLKEIRF      60
K96243          MKLNGMTAAQAQHRHGAIERHAPGKDDGRRTAGVADEREGRTMKGEIKAIRMDVLKEIRF      60
                ************************************************************

pGBKT7-bprD     NSAVSTPVLLAKRNRIAANIREVSEKIDRKGLFGKMFEAVKCVAQRGLYYDRRALRKLDA      120
K96243          NSAVSTPVLLAKRNRIAANIREVSEKIDRKGLFGKMFEAVKCVAQRGLYYDRRALRKLDA      120
                ************************************************************

pGBKT7-bprD     FVVRHIGDRPEDRKFKVLPTRAQRPAP  147
K96243          FVVRHIGDRPEDRKFKVLPTRAQRPAP  147
                ***************************
```

Figure 4.8: Comparison of the amino acid sequence of BprD expressed by pGBKT7. The entire coding sequence of the *bprD* gene (BPSS1521) from *B. pseudomallei* 10276 was cloned into the Y2H vector pGBKT7. The insert was sequenced and Clustal Omega (Sievers *et al.,* 2011) was used to compare the translated pGBKT7-*bprD* DNA sequence with the amino acid sequence of BprD from *B. pseudomallei* K96243 (YP_111527.1).

it is present in WT *B. pseudomallei*. The BapA protein does appear to show variability in sequence, especially towards the C-terminus, and all differences identified between the cloned C-terminal BapA sequence and the *B. pseudomallei* K96243 reference sequence were also identified as naturally occurring in other *B. pseudomallei* strains (Figure 4.7). Interestingly, one difference identified in the pGBKT7-BapA construct, as well as other *B. pseudomallei* strains, is a variation in four amino acid repeats, spanning amino acids 735–770 with reference to the *B. pseudomallei* K96243 BapA protein. The repeats consist of the amino acids V[A/T]S[N/G]. Another difference is in the number of D-A-G repeats spanning amino acids 238–243 with reference to the *B. pseudomallei* K96243 BapA protein. The BprD sequence contained no amino acid differences when compared to the *B. pseudomallei* K96243 reference strain (Figure 4.8).

The sequenced pGBKT7-BipC, pGBKT7-BprD and pGBKT7-BapA plasmids were transformed into *S. cerevisiae* strain AH109. In order to confirm proper expression of the fusion proteins, two colonies from each of the *S. cerevisiae* strains were cultured at 30°C overnight with agitation in SD/-Trp broth. Cells were collected by centrifugation and lysed using Yeast Buster. Cell lysates were visualised by SDS-PAGE followed by Western blotting using a rabbit α-c-Myc antibody to detect the myc-tagged proteins. c-Myc-reactive proteins were detected at the expected size for the effector proteins: GAL4 DNA binding domain fusions in *S. cerevisiae* containing pGBKT7-BipC ($\sim$45 kDa) or pGBKT7-BapA ($\sim$130 kDa), (Figure 4.9). As the high molecular weight band seen in the BapA samples was not present in the other samples, it was hypothesised that this was indeed due to the production of BapA by the yeast. The BprD expressing yeast strain showed a c-Myc-reactive band of $\sim$60 kDa, which is four times the expected molecular weight ($\sim$15 kDa). At the present time it is not clear why this occurs, but could be due to the formation of multimers by BprD.

Two of the known issues that can affect Y2H screening are toxicity of the expressed bait protein and auto-activation of the reporter genes by the bait protein in the absence of the GAL4 activation domain. The strains were checked for toxicity by assessing growth rate and colony size when grown at 30°C for 3 days on SD/-Trp plates. When compared to WT *S. cerevisiae*, the strains expressing the proteins of interest did not show any notable growth defect, showing formation of colonies of about 3 mM after 3 days growth, indicating they were suitable for Y2H screening. To test for auto-activation, the *S. cerevisiae* strains expressing the proteins of interest were streaked onto both SD/-Trp

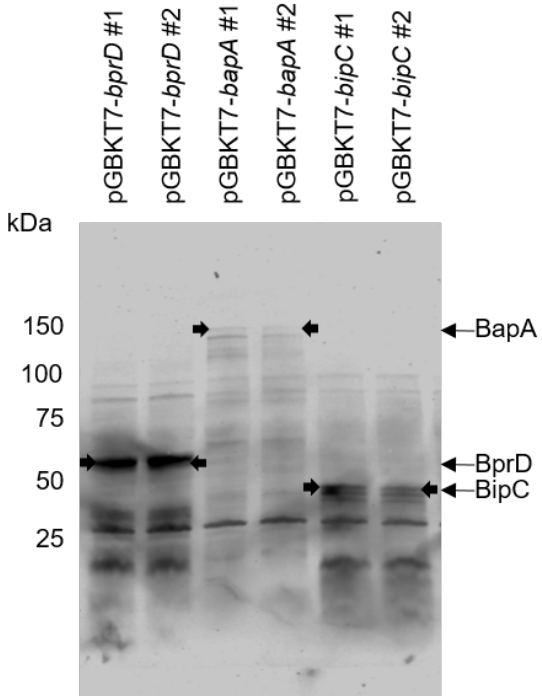


Figure 4.9: Western blot showing expression of BapA, BprD and BipC fusion proteins in *S. cerevisiae* AH109. Two colonies from each of the *S. cerevisiae* AH109 strains containing pGBKT7-BipC, pGBKT7-BprD or pGBKT7-BapA were cultured overnight at 30°C with agitation. The yeast was collected by centrifugation, lysed with Yeast Buster, and of the resulting lysates, equal amounts were visualised by SDS-PAGE and probed by Western blot using a rabbit α-c-Myc antibody. Arrows indicate the c-Myc-reactive fusion proteins.

plates, to select for the pGBKT7 plasmid, and SD/-Trp/-Ade/-His, to test for activation of the *Ade2* and *His3* reporter genes. The plates were incubated at 30°C for 5 days. While all three strains showed growth on the control media (SD/-Trp), none of the strains grew on the SD/-Trp/-Ade/-His plates, indicating the strains were suitable for further testing (Figures 4.10 and 4.11).

In Y2H testing, it is important to test the stringency of the media, as growth of *S. cerevisiae* on selective media in the absence of protein-protein interactions would produce false-positive results. Positive (*S. cerevisiae* AH109 pGBKT7-53 pGADT7-T) and negative (*S. cerevisiae* AH109- pGBKT7-LAM pGADT7-T) control strains were produced by performing a double transformation using plasmids supplied by the manufacturer. The plasmids in the positive control strain encode the proteins murine p53 and simian vacuolating virus 40 (SV40) large T-antigen which are known to interact in the Y2H system. The plasmids in the negative control strain encode the proteins human lamin C and SV40 large T-antigen which do not interact in the Y2H system. The plasmid pGADT7 contains the gene *LEU2* allowing *S. cerevisiae* strains to grow on media lacking leucine. The strains were plated onto SD/-Trp/-Leu and SD/-Trp/-Leu/-Ade/-His plates to ensure selectivity of the media. In a working Y2H system both the positive and negative strains would grow on the SD/-Trp/-Leu media, but only the positive control strain in which the GAL4 DNA binding and activating domains are brought into close proximity through a bait-prey protein-protein interaction should grow on the SD/-Trp/-Leu/-Ade/-His media. The media proved to be very stringent, as 5 days of growth at 30°C yielded no colonies on the SD/-Trp/-Leu/-Ade/-His plates for the negative control strain, while the positive control formed colonies on all plates (Figure 4.12).

4.2.3 Yeast Two-Hybrid Screen of BipC, BprD and BapA

To perform the Y2H screen, the *S. cerevisiae* AH109 strains containing pGBKT7-BipC, pGBKT7-BprD and pGBKT7-BapA were mated with *S. cerevisiae* Y187 containing a universal human cDNA library that had been normalised to reduce high abundance transcripts. The library genes were cloned into the plasmid pGADT7. Quality control data pertaining to the library include: titer: $\pm 5 \times 10^7$ CFU/ml, number of independent clones: 1.84×10^7, average cDNA size: 1.43 kb, cDNA size range: 0.5–2.9 kb. The total number of cells in each 1 ml aliquot of library was estimated to be between 0.7–2.25×10^9 cells/ml using a cell counter. Overnight cultures of *S. cerevisiae* AH109 strains containing

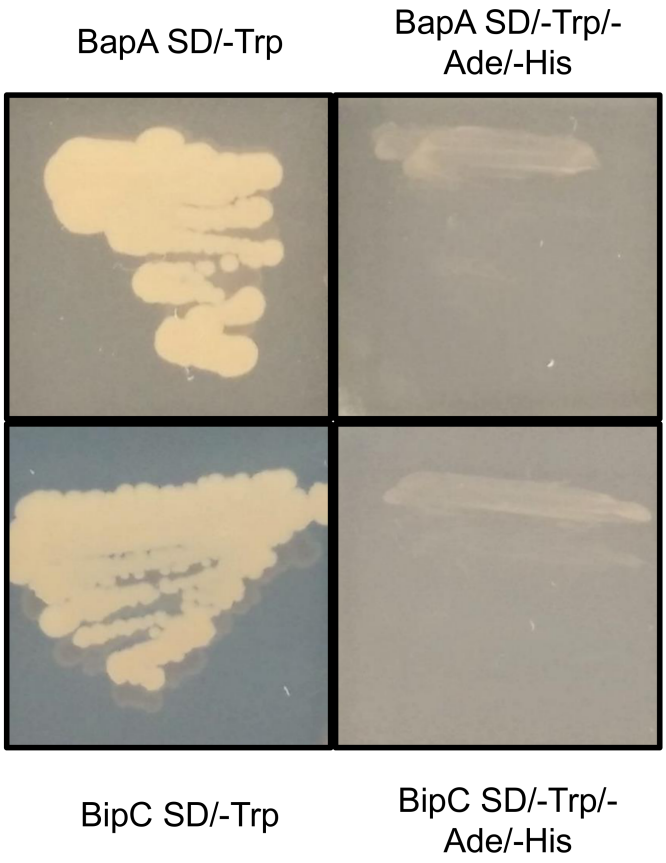


Figure 4.10: Auto-activation of *S. cerevisiae* containing pGBKT7-BapA or pGBKT7-BipC. *S. cerevisiae* AH109 containing pGBKT7-BapA or pGBKT7-BipC were streaked onto SD/-Trp and SD/-Trp/-Ade/-His plates followed by incubation at 30ºC for 3 days. Growth on SD/-Trp/-Ade/-His plates indicates auto-activation of the *Ade2* and *His3* reporter genes.

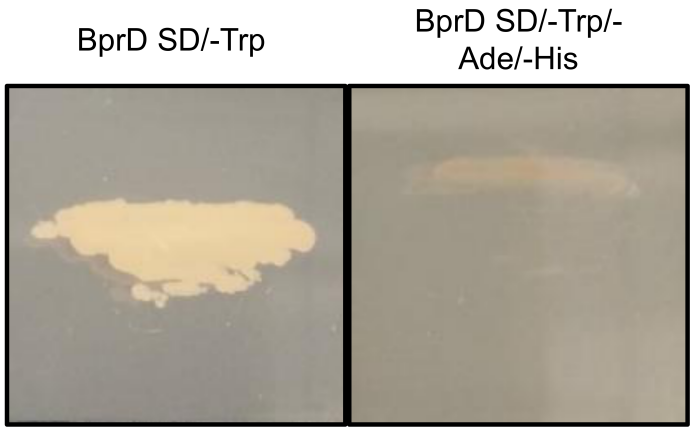


Figure 4.11: Auto-activation of *S. cerevisiae* containing pGBKT7-BprD. *S. cerevisiae* AH109 containing pGBKT7-BprD was streaked onto SD/-Trp and SD/-Trp/-Ade/-His plates followed by incubation at 30°C for 3 days. Growth on SD/-Trp/-Ade/-His plates indicates auto-activation of the *Ade2* and *His3* reporter genes.

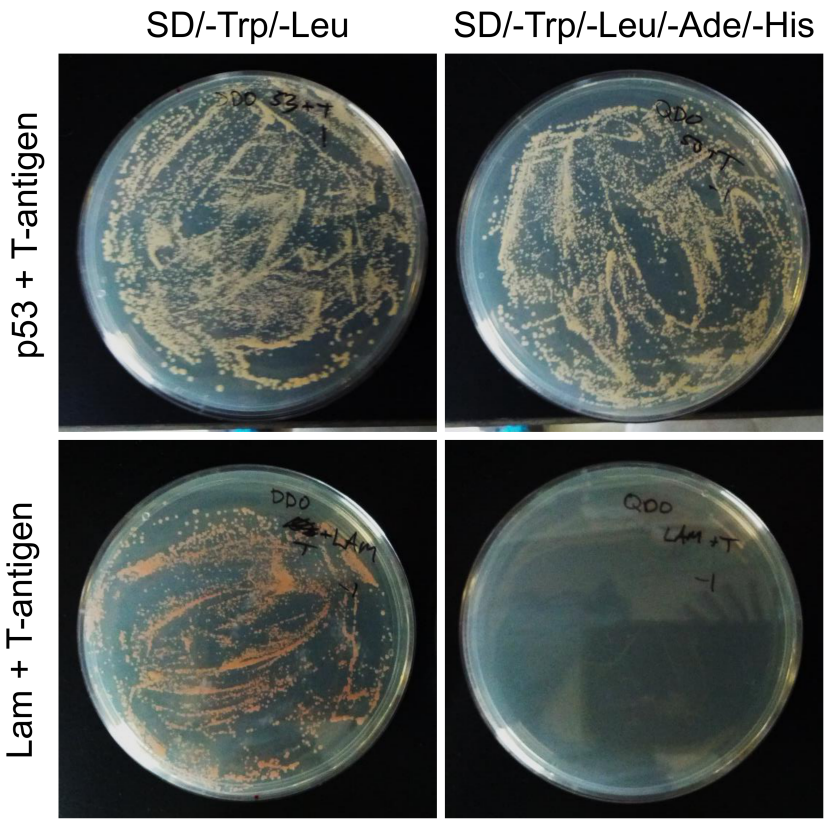


Figure 4.12: Validation of Y2H media stringency. Positive (*S. cerevisiae* AH109 pGBKT7-53 pGADT7-T) and negative (*S. cerevisiae* pGBKT7-LAM pGADT7-T) control strains were plated onto SD/-Trp/-Leu and SD/-Trp/-Leu/-Ade/-His plates followed by incubation at 30°C for 5 days. Stringent media will allow for growth of the positive control, but not the negative control on SD/-Trp/-Leu/-Ade/-His plates.

pGBKT7-BipC, pGBKT7-BprD or pGBKT7-BapA were mixed with individual aliquots of *S. cerevisiae* Y187 containing the universal human cDNA library according to the manufacturers protocol. Yeast mating was allowed to proceed for 24 hours in 50 ml of 2xYPDA media at 30°C, shaking at 45 RPM, to ensure the cells did not sediment. Before plating onto selective media, the culture was examined using a light microscope at 40X magnification for the formation of zygotes in order to confirm mating had taken place. Figure 4.13 shows representative images showing the lobed appearance of the zygotes of *S. cerevisiae*, indicating that the yeast had undergone mating. The culture was washed and suspended in 10 ml of de-ionised water. From the culture, 100 μl was removed and dilutions were plated onto SD/-Trp/Leu media to determine the number of colonies screened. The remainder of the mated culture was plated onto SD/-Trp/-Leu/-Ade/-His plates to select for activation of the reporter genes. The plates were incubated at 30°C for 10 days. Resulting colonies were re-streaked onto SD/-Trp/-Leu/-Ade/-His plates and incubated a further 3 days at 30°C. The number of independent clones screened for each Y2H experiment were: BipC 42 million, BprD 4.2 million, and BapA 17 million; all above the recommended minimum of 1 million independent clones suggested by the manufacturer for a Y2H experiment using a normalised library. The colonies showing growth on the SD/-Trp/-Leu/-Ade/-His plates were counted. From the *S. cerevisiae* pGBKT7-BapA library mating, 11 colonies were obtained (Figure 4.14) and from the *S. cerevisiae* pGBKT7-BipC library mating, 212 colonies were obtained (Figure 4.15). The *S. cerevisiae* pGBKT7-BprD library mating yielded no colonies, possibly due to a problem with BprD production within the yeast as was seen by Western blot (Figure 4.9).

As yeast has the ability to maintain multiple plasmids conferring the same resistance, colonies were streaked multiple times onto SD/-Trp/-Leu/-Ade/-His plates and grown at 30°C for 3 days to segregate any plasmids. As there were only 11 colonies for BapA, plasmids were extracted from all 11 *S. cerevisiae* colonies and then transformed into *E. coli*, selecting for the library plasmid pGADT7 using Amp. The plasmids were propagated in the bacteria, purified, and sequenced using the primers T7 Forward and DNA-AD. For BipC, instead of purifying the plasmids from the yeast, colony PCR was performed on the 212 yeast colonies using the primers T7 Forward and DNA-AD after which the product was run on an agarose gel to visualize the PCR product size differences (Figure 4.16) (Supplemental figure 7.2). From the colony PCR, 65 colonies ($\sim$30%) were selected for sequencing representing a range of band sizes. PCRs

were performed on the 65 selected colonies and the PCR product was purified and sent for sequencing using the primers T7 Forward and DNA-AD. The sequencing results were searched against the UniProtKB/Swiss-Prot database of human proteins using Blastx, resulting in 10 identifications for BapA and 52 identifications for BipC. Several colonies (BipC: 13, BapA: 1) yielded PCR products or plasmids which returned poor quality sequences, even after repeated attempts to re-isolate DNA from these colonies. Reasons for this are unknown.

The names of the human proteins identified as well as the number of independent identifications made for each of the proteins are listed in Table 4.2. Of the 10 identified proteins from the *S. cerevisiae* pGBKT7-BapA library mating, 2 unique proteins were identified. Five colonies contained a plasmid encoding PRKC apoptosis WT1 regulator protein (PAWR) and five colonies contained a plasmid encoding Complement component 1 Q subcomponent-binding protein (C1QBP). Of the 52 identified proteins from *S. cerevisiae* containing pGBKT7-BipC, a total of 14 unique proteins were identified. The most frequent identifications were C1QBP, Staufen homologue 2 (STAU2), and PAWR (Table 4.2).

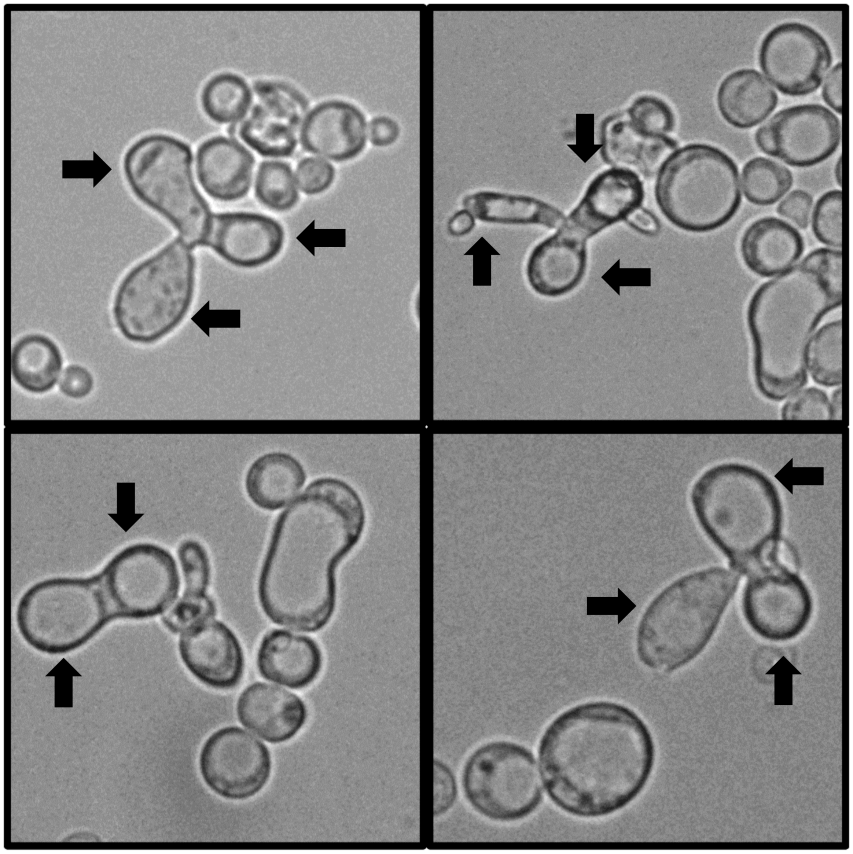


Figure 4.13: Microscope images of *S. cerevisiae* AH109 zygotes. Examples of microscope images taken 24 hours after *S. cerevisiae* AH109 cultures containing either pGBKT7-BipC or pGBKT7-BapA were mixed with *S. cerevisiae* Y187 containing a universal human cDNA library to allow mating to occur. The mixed culture was incubated at 30°C with shaking at 45 RPM after which a 10 μl sample was imaged using a light microscope at 40X magnification. The lobed structure indicates the formation of *S. cerevisiae* zygotes and successful mating of the yeast strains.

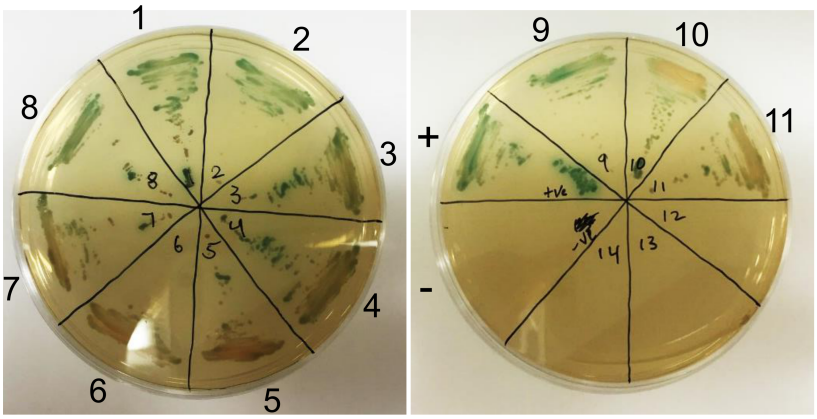


Figure 4.14: Positive *S. cerevisiae* colonies resulting from the BapA Y2H screen. After mating of *S. cerevisiae* AH109 containing pGBKT7-BapA with the universal human library, the culture was plated onto SD/-Trp/-Leu/-Ade/-His media to select for protein-protein interactions. The 11 resulting colonies were re-streaked onto SD/-Trp/-Leu/-Ade/-His/X-α-Gal plates. The blue colour indicates the activation of the α-galactosidase gene.

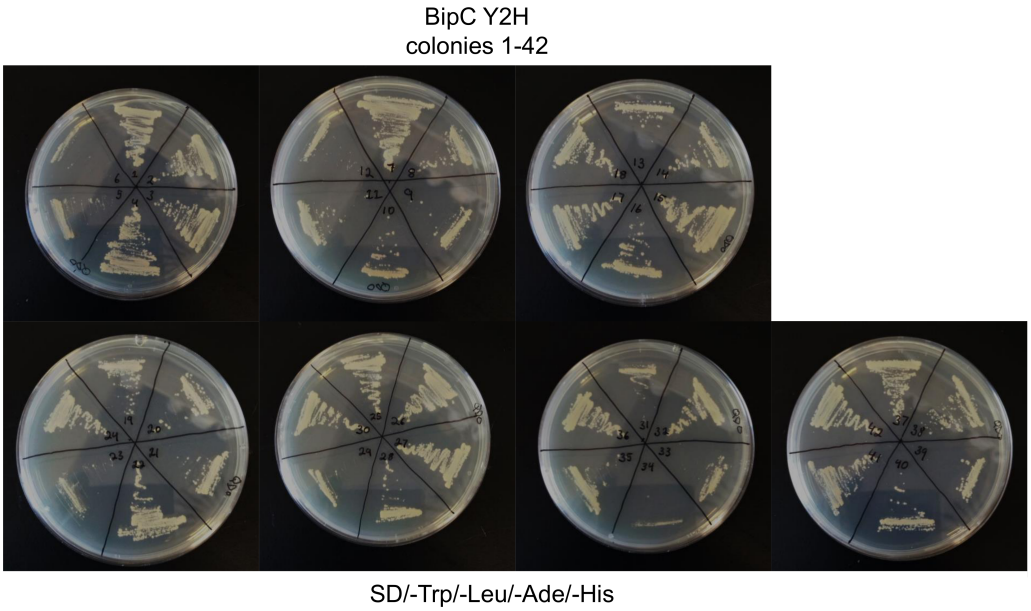


Figure 4.15: Positive *S. cerevisiae* colonies resulting from the BipC Y2H screen. After mating of *S. cerevisiae* AH109 containing pGBKT7-BipC with the universal human library, the culture was plated onto SD/-Trp/-Leu/-Ade/-His media to select for protein-protein interactions. The 212 resulting colonies were re-streaked onto SD/-Trp/-Leu/-Ade/-His plates. This image shows the first 42 colonies from the BipC Y2H screen.

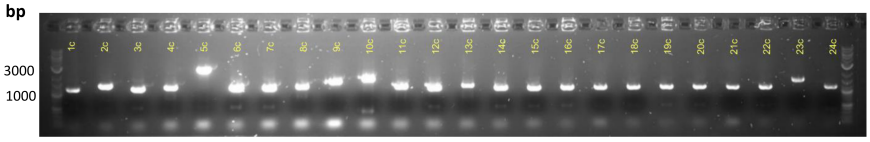


Figure 4.16: Example of a PCR screen from *S. cerevisiae* colonies containing pGBKT7-BipC after mating. *S. cerevisiae* pGBKT7-BipC was mated with *S. cerevisiae* containing a library of human genes cloned into the plasmid pGADT7. PCR was performed to amplify the human DNA insert in the bait plasmid from resulting colonies and shows the range of insert sizes obtained. Pictured is gel #6.

Table 4.2: Human proteins identified as interacting parters for BapA and BipC by Y2H screening. The table contains the Uniprot gene name of each protein identified from a universal human library as an interacting partner with BapA or BipC in a Y2H screen as well as the Entrez gene identifier and the number of independent identifications made for each protein.

Name of Interacting Protein (Entrez Identifier)	Number of Identifications With BipC	Number of Identifications With BapA
C1QBP (708)	25	5
PAWR (5074)	4	5
STAU2 (27067)	5	—
PNISR (25957)	3	—
SLC7A13 (157724)	3	—
TMED7 (51014)	3	—
SCEL (8796)	2	—
COMMD1 (150684)	1	—
DMRTA (63951)	1	—
FAIM1 (55179)	1	—
CMPK1 (51727)	1	—
MARCH7 (64844)	1	—
MMAD (27249)	1	—
RNF2 (6045)	1	—

4.2.4 Confirmation of Yeast-Two Hybrid Results

The Y2H screens of both BipC and BapA resulted in the identification of C1QBP and PAWR as potential interacting partners. These two proteins were therefore chosen for further confirmation and validation. It is important to address the possibility of the prey proteins causing auto-activation of the reporter genes, independent of interactions with the bait protein. To confirm C1QBP and PAWR did not appear in the screen due to auto-activation of the reporter genes, the pGADT7 plasmids encoding C1QBP and PAWR were transformed into *S. cerevisiae* AH109 with a clean background and plated onto SD/-Leu and SD/-Leu/-Ade/-His plates. The plates were incubated at 30ºC for 5 days. *S. cerevisiae* AH109 containing either pGADT7-C1QBP or pGADT7-PAWR formed colonies on SD/-Leu plates, but neither of the strains formed colonies on SD/-Leu/-Ade/-His plates indicating that the prey proteins were not auto-activating the reporters *His* and *Ade* (Figure 4.17). Because it is possible for yeast to contain multiple plasmids with the same selectable marker, pGADT7-PAWR and pGADT7-C1QBP were transformed into a clean background of *S. cerevisiae* AH109 containing either pGBKT7-BapA or pGBKT7-BipC. Colonies were streaked onto SD/-Trp/-Leu and SD/-Trp/-Leu/-Ade/-His plates and incubated at 30ºC for 5 days. The yeast expressing GAL4-DNA BD-BapA or -BipC grew on both SD/-Trp/-Leu and SD/-Trp/-Leu/-Ade/-His plates when GAL4-DNA AD-C1QBP or -PAWR were also expressed, indicating a activation of the reporter genes was not caused by a contaminating plasmid (Figures 4.18, 4.19).

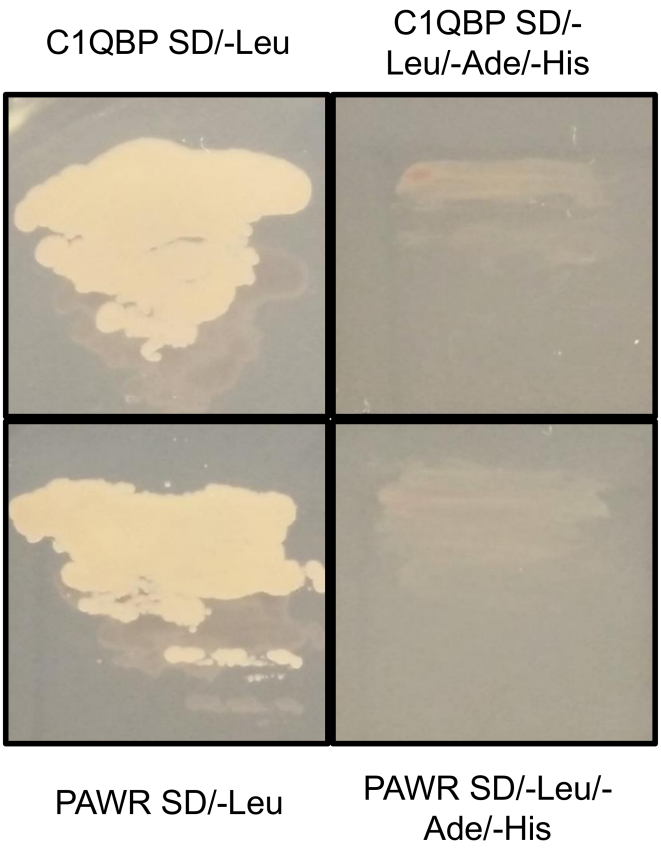


Figure 4.17: Testing the bait proteins PAWR and C1QBP for auto-activation. pGADT7-PAWR or pGADT7-C1QBP were transformed into *S. cerevisiae* AH109 with a clean background and plated onto SD/-Leu and SD/-Leu/-Ade/-His plates followed by incubation at 30°C for 5 days. Growth on SD/-Leu/-Ade/-His plates indicates auto-activation of the reporter genes.

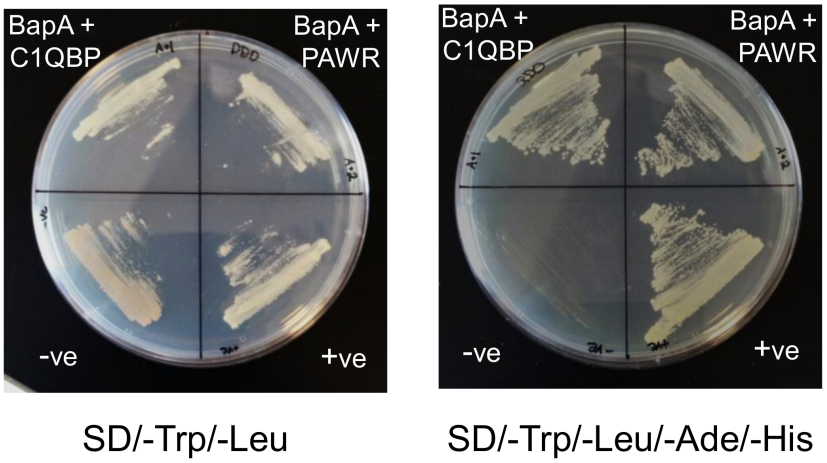


Figure 4.18: Testing BapA interaction with PAWR and C1QBP in a clean *S. cerevisiae* AH109 background. pGBKT7-BapA and pGADT7-PAWR or pGADT7-C1QBP were transformed into *S. cerevisiae* AH109 with a clean background and streaked onto SD/-Trp/-Leu and SD/-Trp/-Leu/-Ade/-His plates followed by incubation at 37°C for 5 days. This was performed to confirm that interactions between the proteins were not due to other plasmids that may be in the mated strains. *S. cerevisiae* AH109 containing both pGBKT7-53 and pGADT7-T was used as a positive control and *S. cerevisiae* AH109 containing both pGBKT7-Lam and pGADT7-T was used as a negative control for growth on SD/-Trp/-Leu/-Ade/-His plates.

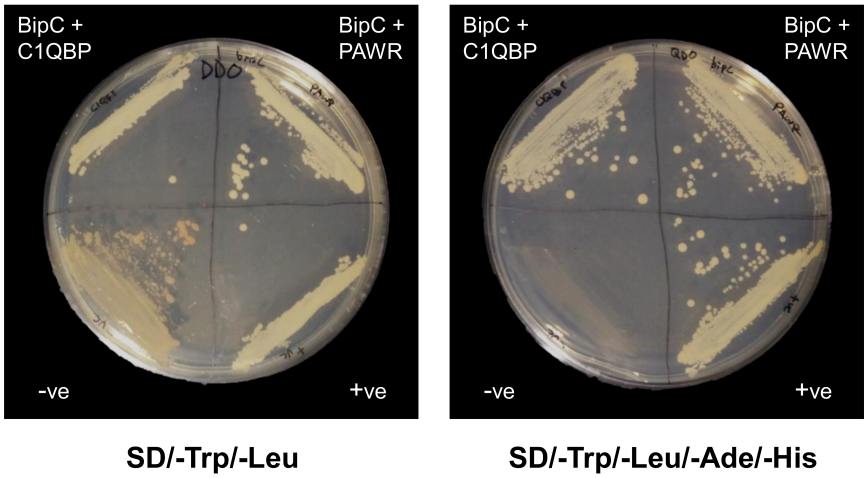


Figure 4.19: Testing BipC interaction with PAWR and C1QBP in a clean *S. cerevisiae* AH109 background. pGBKT7-BipC and pGADT7-PAWR or pGADT7-C1QBP were transformed into *S. cerevisiae* AH109 with a clean background and streaked onto SD/-Trp/-Leu and SD/-Trp/-Leu/-Ade/-His plates followed by incubation at 37ºC for 5 days. This was performed to confirm that interactions between the proteins were not due to other plasmids that may be in the mated strains. *S. cerevisiae* AH109 containing both pGBKT7-53 and pGADT7-T was used as a positive control and *S. cerevisiae* AH109 containing both pGBKT7-Lam and pGADT7-T was used as a negative control for growth on SD/-Trp/-Leu/-Ade/-His plates.

4.2.5 Independent Validation of Protein Interactions

With screens such as Y2H, that potentially generate some false-positives, it is important to validate the results using an independent method (Reviewed in (Brückner *et al.*, 2009)). The method chosen to validate the interactions of BipC and BapA with PAWR and C1QBP, was protein pull-downs. BipC and BapA were expressed in *E. coli* Rosetta BL21 as N-terminal GST-fusion proteins in the plasmid pGEX-4T-1. Protein expression was induced in culture using IPTG, bacteria were collected, lysed with Bugbuster, and the bacterial cell lysates were incubated on ice for 1 hour with GSH-linked sepharose beads. The coated sepharose beads were washed thoroughly with PBS. At the same time HeLa cell lysates were prepared by lysing 10^7 cells in 1 ml of NP-40 lysis buffer containing protease inhibitors and 2 mM EDTA. The GST proteins bound to the GSH-linked sepharose beads were incubated overnight at 4°C with the HeLa cell lysates, washed thoroughly, and then visualised by SDS-PAGE and Western blot with rabbit α-C1QBP and rabbit α-PAWR antibodies. Figure 4.20 shows the GST-fusion protein input into the pull-down assay analysed by SDS-PAGE and Coomassie staining, demonstrating the presence of full length fusion proteins at the expected sizes (GST: 26 kDa, GST-BipC: 70 kDa, GST-BapA: 150 kDa) and in similar quantities. The Western blots confirmed the interaction of C1QBP with both GST-BipC (Figure 4.21) and GST-BapA (Figure 4.23), but no interaction was detected between PAWR and the two effector proteins (Figures 4.22 and 4.24). Also, it would be advantageous in the future to use GST fused to a scrambled protein as a further control for non-specific binding.

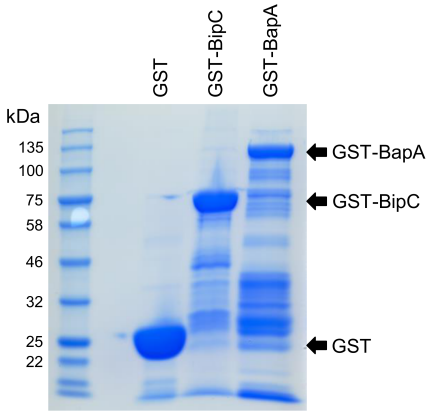


Figure 4.20: Coomassie stained gel of BipC-GST and BapA-GST fusion proteins used in pull-down assays. BipC and BapA were expressed as in-frame N-terminal GST-tagged fusion proteins. The proteins were bound to GSH-linked sepharose beads and were analysed by SDS-PAGE and Coomassie staining.

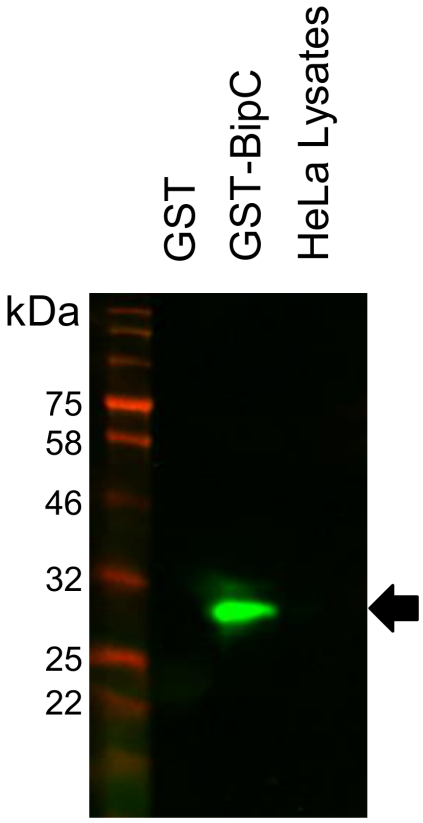


Figure 4.21: Validation of BipC-C1QBP interaction using protein pull-downs. GST and GST-BipC sepharose beads were incubated with HeLa cell lysates overnight at 4°C. The beads were washed and visualised by SDS-PAGE followed by Western blotting using rabbit α-C1QBP antibodies.

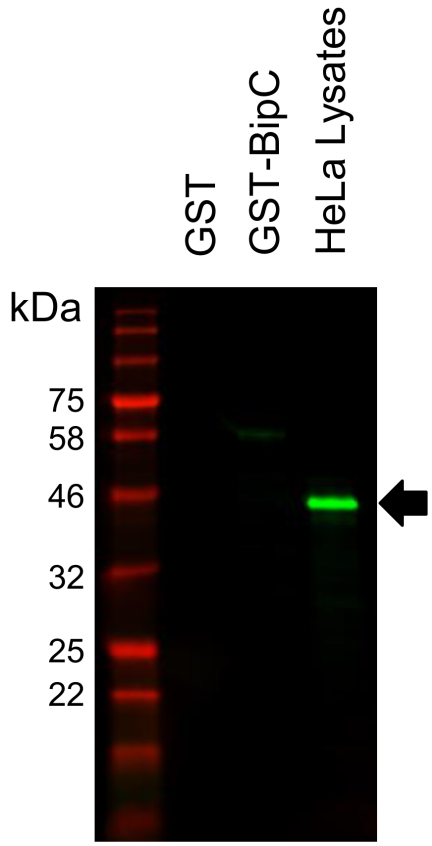


Figure 4.22: Validation of BipC-PAWR interaction using protein pull-downs. GST and GST-BipC sepharose beads were incubated with HeLa cell lysates overnight at 4°C. The beads were washed and visualised by SDS-PAGE followed by Western blotting using rabbit α-PAWR antibodies.

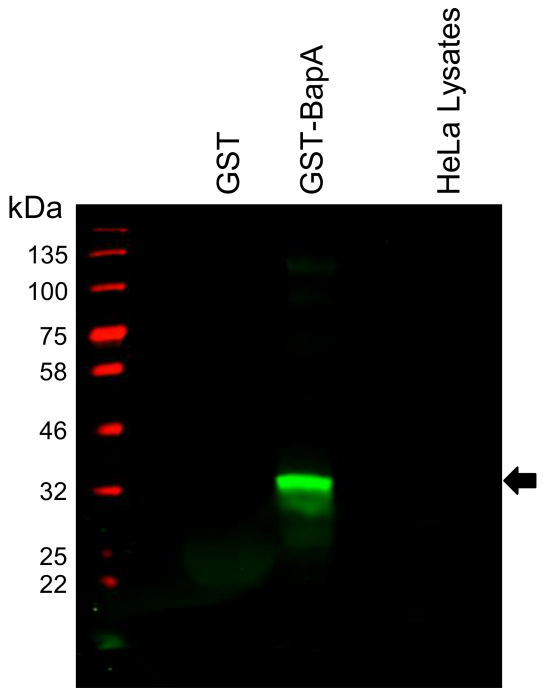


Figure 4.23: Validation of BapA-C1QBP interaction using protein pull-downs. GST and GST-BapA sepharose beads were incubated with HeLa cell lysates overnight at 4ºC. The beads were washed and visualised by SDS-PAGE followed by Western blotting using rabbit α-C1QBP antibodies.

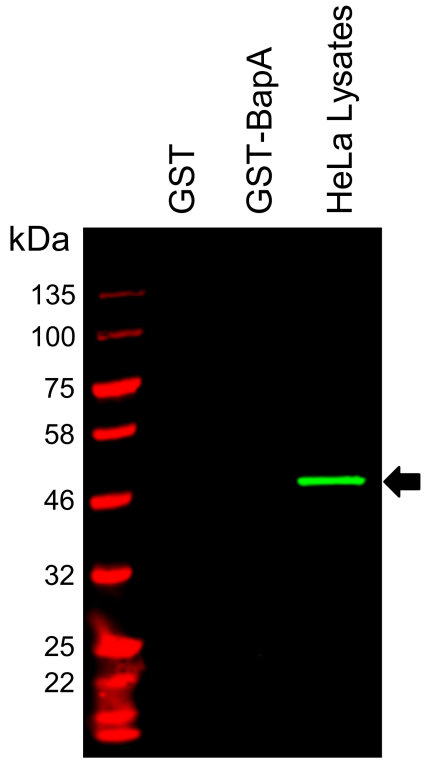


Figure 4.24: Validation of BapA-PAWR interaction using protein pull-downs. GST and GST-BapA sepharose beads were incubated with HeLa cell lysates overnight at 4ºC. The beads were washed and visualised by SDS-PAGE followed by Western blotting using rabbit α-PAWR antibodies.

4.3 Discussion

In the previous chapter (Chapter 3), the effector repertoire of the *B. pseudomallei* Bsa T3SS was described, including the identification of two novel effector proteins, BprD and BapA. Yet, the functions of many of the effector proteins in the T3SS locus are poorly understood. One method commonly used to inform the investigation of protein function is to identify protein-protein interactions. Initial work was performed using GST-fusion protein pull-downs followed by MS analysis. GST-BipC bound to GSH-linked sepharose beads were incubated with murine splenic lysates. When visualised by Western blotting using a rabbit α-actin antibody, actin was present in a GST-alone sample. This may be due to the high concentrations of protein in the murine splenic lysates. It is also known that buffer conditions can have a large impact on the outcome of pull-down experiments (Vikis and Guan, 2004). Bands were excised and analysed by MS analysis yielding a large numbers of proteins that were members of broad cellular pathways. A feature of pull-downs is the ability to identify protein complexes, which explains the large number of proteins identified by MS. Yet, for the purpose of identifying protein function, knowing which proteins BipC directly interacts with may be more helpful in forming a hypothesis. For this reason, it was decided a Y2H system would be used to detect direct protein-protein interactions. BprD (BPSS1521), BapA (BPSS1528), and BipC (BPSS1531) were analysed in a Y2H screen against a universal human library. The system resulted in the identification of 2 human proteins which interact with BapA, and 14 human proteins which interact with BipC. Interestingly, the two human proteins C1QBP and PAWR interacted with both BapA and BipC.

One of the important considerations in Y2H screening is missing true interactions (false-negatives), and incorrectly identifying interactions (false-positives). False-negatives may be caused by a number of factors including a lack of post-translational modifications, steric hindrance caused by fusion of the GAL4 domains, or missing co-factors in the yeast nuclear environment (Reviewed in (Brückner *et al.*, 2009)). Another class of interactions that are often not identified are membrane proteins (Reviewed in Brückner *et al.* (2009)). This may be hinder detection of protein interactions with T3SS effectors, as the system is often involved in bacterial entry through the host cell membrane (Stevens *et al.*, 2003), as well as escape from the endosome (Stevens *et al.*, 2002). Both of these processes are likely to involve membrane proteins. False-positives are arguably more important than false-negatives in this setting due to the potential for misinforming future research efforts. In an investigation of

false-positives in the Y2H system, Serebriiskii *et al.* (2000) state that with appropriate bait proteins, the Y2H system reports around 70% true interactions. Yet, this still means at least some of the identified proteins are likely to be false-positives. Classes of commonly found false-positives include heat-shock proteins, ribosomal proteins and mitochondrial proteins (Serebriiskii *et al.*, 2000). A list of common protein types that yield false-positives in Y2H screens can be found at http://www.fccc.edu/research/labs/golemis/InteractionTrapInWork.html. Because of the possibility of false-positives, the interactions identified by Y2H screens should always be validated by independent methods such as coimmunoprecipitation or pull-downs (Reviewed in (Brückner *et al.*, 2009)).

Though Y2H has not been performed on *B. pseudomallei* Bsa T3SS effector proteins, a previous study has screened T3SS effector protein interactions in the closely related species *B. mallei*. Memišević *et al.* (2013) screened a list of *B. mallei* ATCC 23344 proteins predicted to be involved in pathogenesis against whole human and whole murine libraries in a Y2H system. Among the proteins they screened were the homologues of the *B. pseudomallei* K96243 proteins BopA, BopE, BipB, BipC and BipD (Memišević *et al.*, 2013). BapA and BprD were not tested in the *B. mallei* screen. The only interaction identified when *B. mallei* BipC was screened against the human library was C1QBP, agreeing with this study and lending confidence to the identification, although this does not eliminate the need to independently validate this data. Protein pull-downs performed with GST-BipC incubated with HeLa cell lysates successfully identified C1QBP as a binding partner of BipC. BapA was also confirmed to bind C1QBP by protein pull-down.

The possible importance of the interaction between BipC/BapA and C1QBP is difficult to predict. C1QBP (also known as gC1q-R, HABP1, p32, and p33) is a protein involved in inflammation, immunity and autophagy (Reviewed inGhebrehiwet and Peerschke (2004)). There are conflicting reports as to the sub-cellular localisation of C1QBP, with it being reported as primarily mitochondrial (MengJie *et al.*, 2013), but also being reported as being localised at the cell surface (Peerschke *et al.*, 2003). C1QBP is a receptor for the first component of complement C1q involved in the Bradykinin proinflammatory pathway (Ghebrehiwet *et al.*, 2014). C1QBP is also required for the morphology and function of mitochondria and the endoplasmic reticulum (MengJie *et al.*, 2013) and has also been shown to be involved in TLR4-induced production of IL-12 through the PI 3-kinase pathway (Waggoner *et al.*, 2005). C1QBP has been reported as an important target for viruses and bacteria in the human

cell. In HIV-1 the viral protein gp41 has been shown to interact with C1QBP, causing production of reactive oxygen species and expression of the natural cytotoxicity receptor NKp44L on the surface of infected $CD4^+$ T cells, targeting them for lysis by NK cells (Fausther-Bovendo *et al.*, 2010). The *Coxiella burnetii* type IV secretion system effector protein AnkG has been shown to interact with C1QBP (Lührmann *et al.*, 2010). When injected into host cells by *Legionella pneumophila*, AnkG prevents cellular apoptosis allowing intracellular replication of the *L. pneumophila* (Lührmann *et al.*, 2010). The *Listeria monocytogenes* protein InlB interacts with C1QBP on the cell surface, causing the recruitment and activation of PI 3-kinase and mediating bacterial entry into the cell (Braun *et al.*, 2000). Hepatitis C virus core proteins bind to C1QBP, inhibiting T cell proliferation through cell cycle arrest (Yao *et al.*, 2003) as well as inhibiting gamma interferon production (Yao *et al.*, 2005). C1QBP has also shown to be important in gamma herpes virus infections for down-regulation of host immunity (Liang *et al.*, 2004) and nuclear egress (Wang *et al.*, 2014). C1QBP has also been shown to inhibit RIG-I and MDA-5 antiviral signalling through MAVS (Xu *et al.*, 2009). Such a precedent for pathogens interacting with C1QBP to exploit host cell function is encouraging. It is possible that by interacting with C1QBP, BipC and BapA may interfere with the cells ability to recognise intracellular double stranded DNA through MAVS increasing bacterial survival. This could be tested using C1QBP knockout cell lines along with bacterial BipC and BapA to investigate the importance of this interaction in *in vitro* infection. Ideally, it would also be useful to express fragments of both C1QBP and BipC/BapA to map what portions of the proteins are involved in the interaction.

The other protein identified as an interacting partner for both BipC and BapA by the Y2H screen was PAWR. PAWR (also known as par-4) is a proapoptotic protein which traffics Fas/FasL to the cellular membrane and has also been shown to inhibit the transcription of NF-κB (Reviewed in Hebbar *et al.* (2012)). Unlike C1QBP, independent validation of the interaction of PAWR with BipC and BapA did not occur, possibly due to inappropriate pull-down conditions, the interaction being transient, or a false-positive interaction. This highlights the need for independent validation, and while it does not rule out BipC/BapA and PAWR interacting, more work would need to be done to explore this hypothesis. It is possible that under different, more physiological conditions, such as inside cellular cytoplasm BipC/BapA and PAWR may interact.

A number of other putative BipC interacting partners were identified by Y2H that were not taken forward for validation. When considering proteins with 3 or more independent identifications, the most interesting of these hits is Transmembrane Emp24 Protein Transport Domain Containing 7 (TMED7). TMED7 is thought to be involved in trafficking of TLR4, though two recent reports are conflicting as to whether TMED7 inhibits or enhances the activity of TLR4 (Doyle *et al.*, 2012, Liaunardy-Jopeace *et al.*, 2014). Another of the proteins identified, Staufen Double-Stranded RNA Binding Protein 2 (STAU2) is a double stranded RNA binding protein involved in Staufen-mediated mRNA decay (Park and Maquat, 2013). PNN-interacting serine/arginine-rich protein (PNISR or SFRS18) is a poorly characterised mRNA splicing factor that has been identified in another Y2H screen as an interacting partner of a Vesicular Stomatitis Virus protein, but this interaction was not validated (Moerdyk-Schauwecker *et al.*, 2011). Solute carrier family 7 member 13 (SLC7A13 or S7A13) is an amino acid transporter only characterised by its homology to other transporters of the same family (Blondeau, 2002).

This study provides the first evidence that the Bsa T3SS effector proteins BapA and BipC interact with human proteins. One protein shown to interact with BipC and BapA, C1QBP, was confirmed using protein pull-downs. Due to C1QBP's role in innate immunity as well as the numerous examples of other pathogens exploiting the protein for their benefit, the effect of the interaction between BipC/BapA and C1QBP on the host cell is an interesting area for further investigation.

Chapter 5

Functional Characterisation of the Bsa T3SS Translocon Protein BipC

5.1 Introduction

Burkholderia pseudomallei is a facultative intracellular pathogen capable of invasion of both phagocytic and non-phagocytic cells (Reviewed in Wiersinga *et al.* (2006)). The mechanisms behind *B. pseudomallei* cellular invasion are not well characterised. One common theme in bacterial entry into host cells is the exploitation of host cell actin to assist invasion (Reviewed in Pizarro-Cerda and Cossart (2006)). This can be accomplished by different mechanisms such as direct manipulation of the host cell protein actin or transmission of a signal to host cell machinery disrupting the actin cytoskeleton (Reviewed in Pizarro-Cerda and Cossart (2006)). Within important pathogenic Gram negative bacteria, such as *Yersinia*, *Salmonella* and *Shigella*, the Type 3 secretion system (T3SS) delivers bacterial effector proteins which subvert host actin (Reviewed in Büttner (2012)). The T3SS functions similarly to a molecular syringe, allowing delivery of proteins from the bacterial cytosol directly into the cytosol of a target host cell (Reviewed in Wagner *et al.* (2010)). Figure 5.1 shows two major intracellular pathogens, *Shigella* and *Salmonella*, and the use of their T3SSs to subvert host cell actin and induce uptake (Reviewed in Pizarro-Cerda and Cossart (2006)). *Salmonella* injects SipC and SipA causing actin polymerisation and bundling, while SopE and SopB activate Rho GTPases causing further host cell actin polymerisation leading to membrane ruffling and bacterial uptake. SptP has an inverse effect, inactivating the Rho GTPases to restore the cellular surface after *Salmonella* entry. *Shigella* injects IpaC which polymerises actin, VirA which activates Rho GTPases, and IpgD which disrupts the actin

host cytoskeleton inducing membrane ruffle formation. Similarly to SptP, IpaA causes actin depolymerisation leading to recovery of the actin cytoskeleton at the site of bacterial entry.

The *B. pseudomallei* Bsa T3SS is homologous to the Inv-Spa (*Salmonella* pathogenicity island (SPI)-1) and Mxi-Spa T3SSs of *Salmonella* spp. and *Shigella flexneri*, respectively (Stevens *et al.*, 2002) and has also been shown to be involved in bacterial invasion of non-phagocytic host cells by injecting the effector protein BopE, a guanine nucleotide exchange factor homologous to SopE (*Salmonella*) (Stevens *et al.*, 2003). Yet, compared to *Salmonella* and *Shigella*, the invasion process of *B. pseudomallei* is poorly characterised. The *B. pseudomallei* effector protein BopE, activates the Rho GTPases Cdc42 and Rac1 inducing host actin cytoskeleton rearrangements (Stevens *et al.*, 2003). The less characterised proteins BopC and BipC are also required for full invasion efficiency(Muangman *et al.*, 2011, Kang *et al.*, 2015). Of particular interest is BipC, a homologue of the translocators SipC from *Salmonella* and IpaC from *Shigella* (Stevens *et al.*, 2002). T3SS translocator proteins are responsible for forming a pore in the eukaryotic cell membrane allowing the injection of effector proteins into the cytoplasm (Reviewed in Diepold and Wagner (2014)). Though SipC and IpaC are both bacterial translocators, they also have effector functions with the ability to directly bind and polymerise host cell actin (Hayward and Koronakis, 1999, Terry *et al.*, 2008).

SipC was first shown to directly interact with actin by Hayward and Koronakis (1999). It was demonstrated that SipC has the ability to polymerise actin as well as bundle F-actin in the absence of host cell proteins (Hayward and Koronakis, 1999, McGhie *et al.*, 2001). The ability of SipC to polymerise and bundle F-actin, as well as form the translocation pore, are all dependant on the C-terminal 209 amino acids of the 409 amino acid protein (Hayward and Koronakis, 1999, Chang *et al.*, 2005, Myeni and Zhou, 2010). Yet, the ability to polymerise actin is distinct from the translocation function and important for invasion. *Salmonella* containing a mutated form of *sipC* that is unable to bundle actin, but still able to act as a translocon, was less invasive than WT *Salmonella* (Myeni and Zhou, 2010). In order to efficiently polymerise actin SipC forms either dimers or multimers (Chang *et al.*, 2007), and another actin binding protein, SipA, stabilises actin filaments enhancing the polymerisation function of SipC (McGhie *et al.*, 2001). SipC also interacts with host Syntaxin 6 and thereby recruit LAMP1 to the Salmonella-containing vacuole (SCV), helping to stabilise its membrane (Madan *et al.*, 2012). It is clear that SipC is a multi-functional pro-

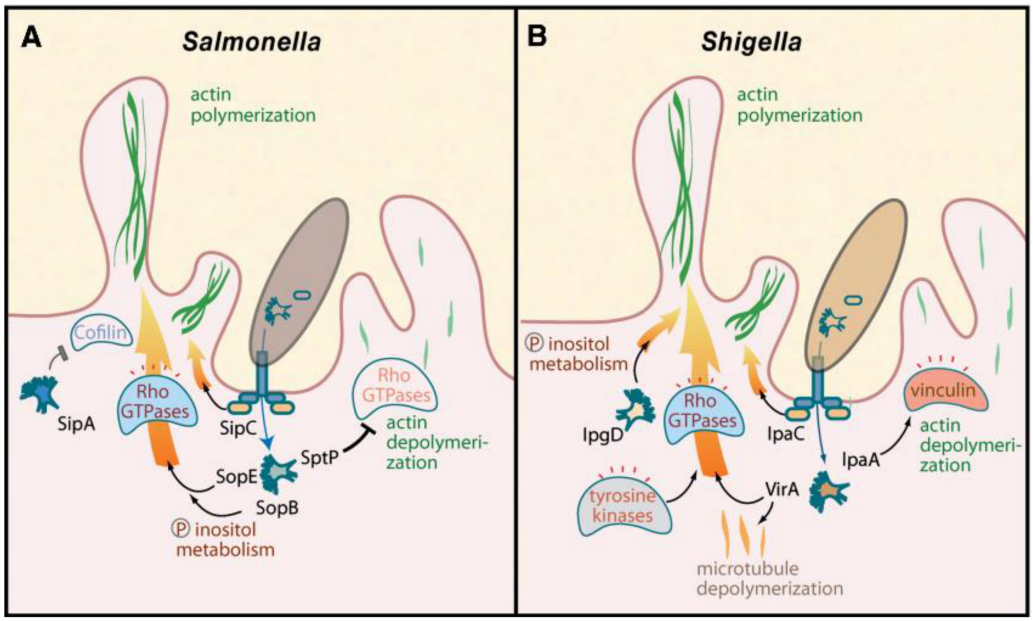


Figure 5.1: Entry of host cells by *Salmonella* and *Shigella* via T3SS induced actin rearrangement. Upon host cell contact, effector proteins are injected into the host cell by the Inv-Spa (*Salmonella* spp.) and Mxi-Spa T3SS (*Shigella flexneri*) where they alter host actin networks to induce uptake. **(A)** *Salmonella* injects SipC and SipA causing actin polymerisation and bundling, while SopE and SopB activate Rho GTPases causing further host cell actin polymerisation leading to membrane ruffling and bacterial uptake. SptP has an inverse effect, inactivating the Rho GTPases helping to restore the cellular surface after *Salmonella* entry. **(B)** *Shigella* injects IpaC which polymerises actin, VirA which activates Rho GTPases, and IpgD which disrupts the actin host cytoskeleton inducing membrane ruffle formation. Similar to SptP, IpaA causes actin depolymerisation leading to recovery of the actin cytoskeleton at the site of bacterial entry. Figure adapted from Pizarro-Cerda and Cossart (2006).

tein leading to the hypothesis that BipC may also have roles beyond that of a translocator protein.

Another homologue of BipC is IpaC from *Shigella* (Osiecki *et al.*, 2001). IpaC also causes actin polymerisation when expressed or microinjected into cells (Van Nhieu *et al.*, 1999) and the C-terminus of the protein nucleates actin (Terry *et al.*, 2008). IpaC can recruit Src kinase which causes actin polymerisation followed by membrane ruffling which is thought to facilitate bacterial entry (Mounier *et al.*, 2009). While IpaC and SipC are similar, they also have their differences. Interestingly, when expressed on a plasmid, SipC and IpaC are able to complement a *Salmonella sipC* mutant, but only IpaC can complement a *Shigella ipaC* mutant (Osiecki *et al.*, 2001). This indicates that the proteins have some differences in their biochemical function. The authors suggest the different functions may be due to the different intracellular lifestyles of the pathogens, with *Salmonella* residing in the vacuole and *Shigella* escaping into the cytosol (Osiecki *et al.*, 2001). It is therefore possible BipC may also have distinct functions compared to the other homologues.

Research focused on BipC has been limited. A *B. pseudomallei* K96243 *bipC* insertion mutant showed reduced cell adhesion and invasion of A549 cells when compared to the WT strain (Kang *et al.*, 2015). This BipC mutant also showed a delay in escape from the phagosome leading to a delay in formation of actin tails and intracellular growth (Kang *et al.*, 2015). The mutant was also attenuated in BALB/c mice infected intraperitoneally when compared to WT (Kang *et al.*, 2015). While this shows a clear role of the importance of BipC in virulence both *in vivo* and *in vitro*, it does not separate BipC's role as a translocator necessary for a functional T3SS from roles it may have as an effector protein. Particularly, there has been no evidence that BipC is capable of polymerising actin.

In this study, the first evidence of an interaction between BipC and actin is reported. It is shown that this interaction does not require the presence of other host cell proteins and that BipC has the ability to polymerise actin *in vitro*. BipC preferentially binds F-actin, but does not stabilize F-actin under depolymerising conditions. HeLa cells expressing N-terminal Myc-tagged BipC show disruption of the actin cytoskeleton and pseudopodia formation suggesting involvement in actin dynamics *in vivo*. A surrogate host system in EPEC was established for the downstream study of BipC translocation into cells. This study furthers the understanding of the role BipC may play beyond its role as a translocator.

5.2 Results

5.2.1 BipC Directly Binds Actin

Due the similarity of BipC to SipC (*Salmonella*, 58% coverage, 24% identity) and IpaC (*Shigella*, 58% coverage, 22% identity), we hypothesised that BipC would be an actin-binding protein and may possess the ability to bundle F-actin. Figure 5.2 shows an amino acid alignment of BipC with SipC and IpaC. To investigate the ability of BipC to bind actin, a pull-down experiment was performed using N-terminal GST fusion proteins and murine splenic lysates under actin-polymerising conditions. BipC was expressed in *E. coli* Rosetta BL21 as an N-terminal GST-fusion protein using the plasmid pGEX-4T-1-BipC. GST-SipC *Salmonella* and GST-BimA, the known *B. pseudomallei* actin-binding and polymerising protein (Stevens *et al.*, 2005), were used as positive controls. As a negative control GST alone was prepared. Protein expression was induced in culture using IPTG, bacteria were collected, lysed with bugbuster, and the bacterial cell lysates were incubated at room temperature for 1 hour with GSH-linked sepharose beads. The GST-fusion proteins bound to the sepharose beads were analysed by SDS-PAGE and visualised by Coomassie staining demonstrating that each protein was expressed at the expected molecular weight and there was relatively similar amounts of protein present in all pull-down samples (Figure 5.3). The coated sepharose beads were washed thoroughly with PBS and incubated for 30 minutes at room temperature with murine splenic lysates (MSL) suspended in polymerisation buffer supplemented with 100 μM $CaCl_2$. The beads were washed thoroughly with PBS and then visualised by SDS-PAGE and by Western blot with a rabbit α-actin antibody. When probed with the α-actin antibody, actin is present in all three test lanes of GST-BimA, GST-SipC, and GST-BipC (Figure 5.3). The negative control lacks actin, indicating the interaction is not due to the N-terminal GST fusion or due to non-specific binding of actin to the sepharose beads (Figure 5.3).

Because pull-downs may identify interactions that are indirect through large protein complexes (Reviewed in Brückner *et al.* (2009)), it must be determined if BipC has the ability to bind actin directly, or if the binding is indirect and requires other proteins for the binding of the actin molecules. To test this, GSH-linked sepharose beads were coated with GST, GST-BimA, GST-SipC, or GST-BipC. Polymerisation buffer containing 1 μM rhodamine-labelled actin was added to the beads on a microscope slide. The beads were immediately

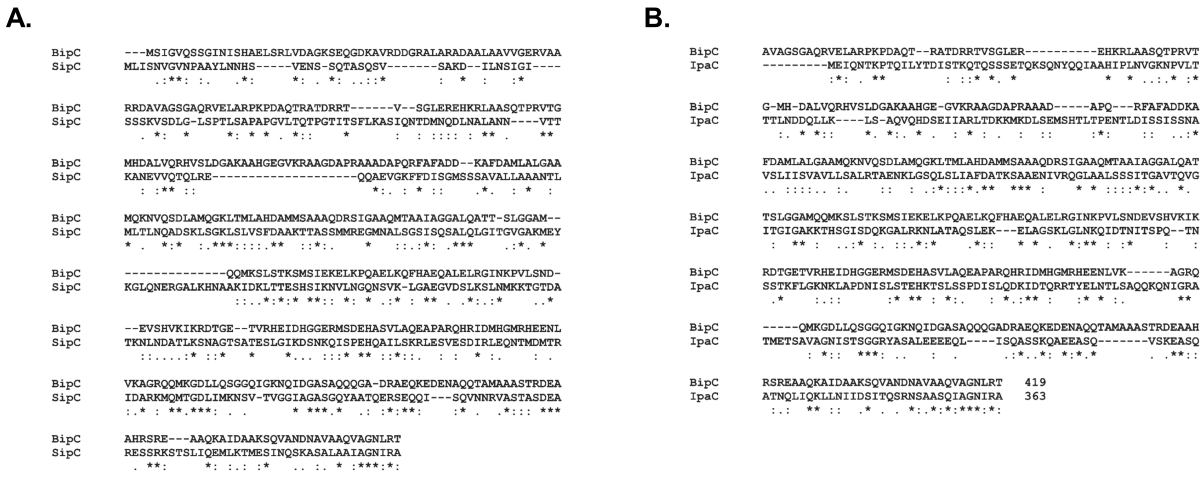


Figure 5.2: Amino acid alignment of BipC (*B. pseudomallei*) with SipC (*Salmonella*) and IpaC (*Shigella*). The alignment was performed using Clustal Omega (Sievers *et al.*, 2011). In the alignment, a (*) indicates conserved residues, a (:) indicates highly similar amino acids, and a (.) indicates weakly similar amino acids. Accession numbers for the proteins are; BipC (YP_111537.1), SipC (EHY68440.1) and IpaC (EGK31204.1)

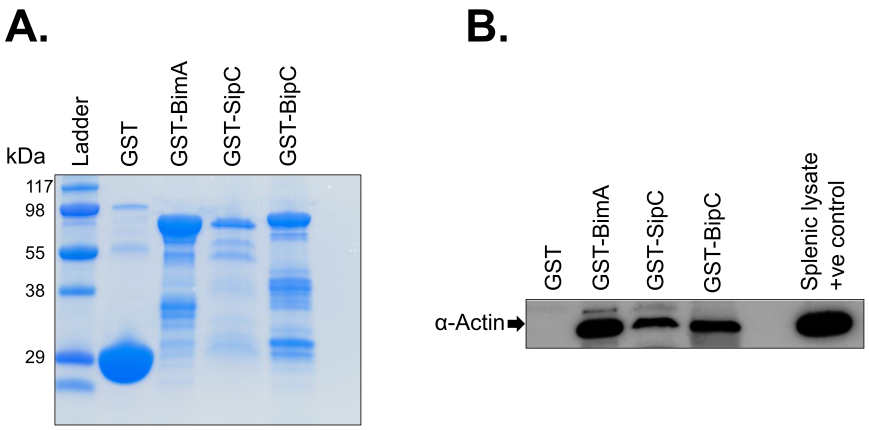


Figure 5.3: Pull-down assay using GST-BipC and murine splenic lysates. GST, GST-BimA, GST-SipC and GST-BimA bound to GSH-linked sepharose beads were incubated with murine splenic lysates (MSL) in polymerisation buffer for 30 minutes at room temperature. The beads were washed and analysed by SDS-PAGE. **A.** The Coomassie stained gel shows the proteins input into the pull-down assay demonstrating each protein was present in relatively similar amounts. **B.** The α-actin Western blot indicates actin binding to the fusion proteins.

visualised using a confocal microscope. If a protein is able to bind actin, it creates a high concentration of the rhodamine-labelled actin at the surface of the sepharose bead, which appears as a red 'halo' around the clear bead in microscope images. The results show a red halo around both the GST-BimA and GST-BipC coated beads (Figure 5.4). The beads coated with GST alone show no ring, while surprisingly the GST-SipC beads show only a faint red halo (Figure 5.4). This may be due to a relatively low concentration of GST-SipC on the beads. The results demonstrate that BipC is able to bind actin directly, in the absence of other proteins. This is the first evidence that BipC is an actin-binding protein.

With evidence that BipC has the ability to bind actin directly, it was surprising that actin was not identified as an interacting partner for BipC in the Y2H screen (Chapter 4). Because this could have been missed in the screen as a false-negative result, this interaction was tested independently in a clean *S. cerevisiae* AH109 background. pGBKT7-BipC and pGADT7 containing the coding sequence of β actin (pGADT7-Actin) were transformed into *S. cerevisiae* AH109 and cultured on SD/-Trp/-Leu and SD/-Trp/-Leu/-Ade/-His plates for 5 days at 30^{o}C to test for activation of the reporter genes. *S. cerevisiae* containing pGBKT7-BipC and pGADT7-Actin did not form colonies on the SD/-Trp/-Leu/-Ade/-His media, but did form colonies on the control media containing SD/-Trp/-Leu, confirming that BipC and Actin do not interact in the Y2H system (Figure 5.5). This may be due to the yeast nucleus not supporting actin polymerising conditions which may be required for interactions with BipC.

It was hypothesised that one reason actin was not identified in the Y2H screen may be due to BipC binding filamentous actin (F-actin) preferentially. To investigate this, an actin co-sedimentation assay was performed, similar to that of Stevens *et al.* (2005). Purified GST, GST-BipC, GST-SipC, and GST-BimA (1 μM) were incubated with 10 μg of pre-polymerised actin in G-Mg buffer for 30 minutes at room temperature. The mixtures were then separated by ultra-centrifugation, which results in the co-sedimentation of F-actin and any protein bound to the F-actin. Monomeric G-actin and proteins bound to G-actin, or proteins that are unbound, remain in the supernatant. The supernatants and pellets were then analysed by SDS-PAGE and visualised by silver staining. The GST protein is only present in the supernatant since it does not bind F-actin (Figure 5.6). GST-BimA is present in both the pellet and supernatant, but in higher amounts in the supernatants indicating it preferentially

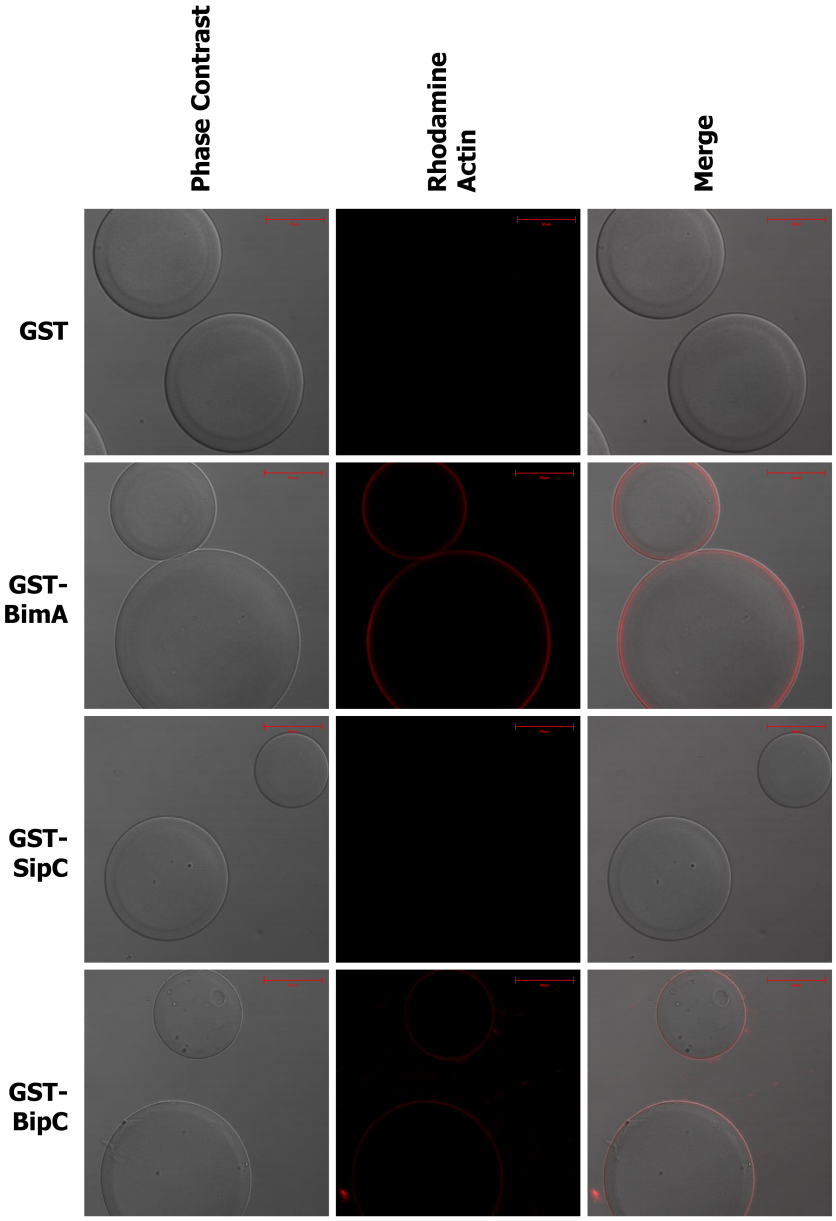


Figure 5.4: Direct binding of rhodamine-labelled actin by GST-BipC. Sepharose beads coated with either GST, GST-BimA, GST-SipC or GST-BipC were mixed with rhodamine-labelled actin and immediately imaged using a confocal microscope. The formation of a red ”halo” around the bead indicates binding and a high concentration of the labelled actin at the bead surface. Scale bar = 50 μm.

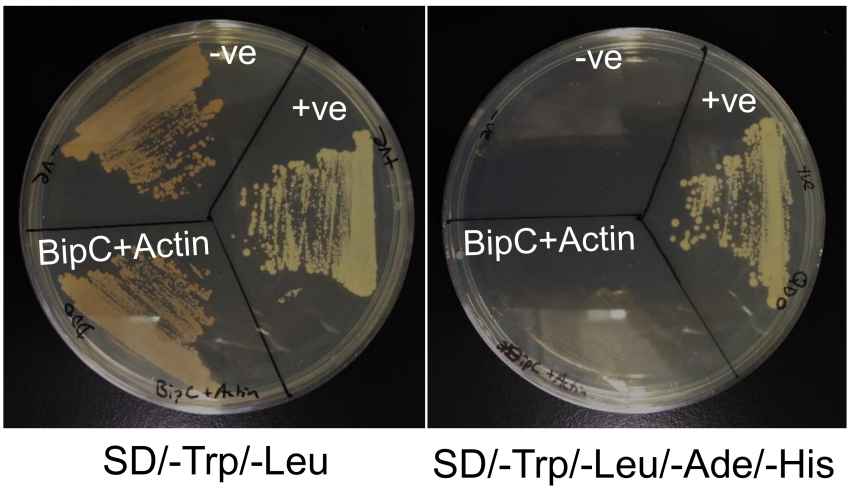


Figure 5.5: Testing BipC interaction with Actin in a clean *S. cerevisiae* AH109 background. pGBKT7-BipC and pGADT7-Actin were transformed into *S. cerevisiae* AH109 with a clean background and streaked onto SD/-Trp/-Leu and SD/-Trp/-Leu/-Ade/-His plates followed by incubation at 37°C for 5 days. *S. cerevisiae* AH109 containing pGBKT7-53 and pGADT7-T was used as a positive control and *S. cerevisiae* AH109 containing pGBKT7-Lam and pGADT7-T was used as a negative control for growth on SD/-Trp/-Leu/-Ade/-His plates.

binds G-actin (Figure 5.6), as previously demonstrated (Stevens *et al.*, 2005). GST-SipC shows larger amounts of protein present in the pellet demonstrating its preferential binding to F-actin in agreement with Hayward and Koronakis (1999) (Figure 5.6). Interestingly, GST-BipC is almost exclusively found in the pellet indicating that it preferentially binds F-actin under the conditions used in the sedimentation assay (Figure 5.6).

To further test the hypothesis that BipC preferentially binds to actin polymers, a pull-down assay was performed, but instead of polymerisation buffer, NP-40 lysis buffer was used. GST-BipC bound to GSH-linked sepharose beads was incubated with HeLa cell lysates prepared in NP-40 lysis buffer containing protease inhibitors and EDTA. The sepharose beads were incubated overnight at 4^{o}C with the HeLa cell lysates, washed thoroughly, and then visualised by SDS-PAGE and Western blot with rabbit α-actin antibodies. A band at the size corresponding to actin (about 43 kDa) was present in the HeLa cell lysate control, but not in the GST or GST-BipC samples (Figure 5.7). This is in contrast to the earlier pull-down in which polymerisation buffer was used (Figure 5.3). This suggests that BipC may only interact with actin under conditions in which actin polymerisation is feasible.

5.2.2 BipC Polymerises Actin and Co-localises With the Actin Cytoskeleton in HeLa Cells

SipC has the ability to bind and bundle F-actin, but also to polymerise actin (Hayward and Koronakis, 1999). To determine if BipC is also able to polymerise actin, a polymerisation assay was performed with pyrene-labelled actin which emits fluorescence as it polymerises (Stevens *et al.*, 2005). An increase in the fluorescence intensity indicates an increase in actin polymerisation. GST, GST-BimA, GST-SipC, and GST-BipC (1 μM) were incubated with 2.3 μM of pyrene actin in polymerisation buffer and compared in their ability to polymerise actin over a 1 hour period. SipC showed a statistically significant increased rate of polymerisation (average rate of increase in fluorescence intensity = 14.656$\pm$5.01 U/s) when compared to the GST control (average rate of increase in fluorescence intensity = 7.453$\pm$3.65 U/s) which mimics the rate of intrinsic actin polymerisation in the absence of a polymerising factor (Figure 5.8). BipC also showed a statistically significant increase in the rate of actin polymerisation (average rate of increase in fluorescence intensity = 9.876$\pm$3.87 U/s) when compared to the GST control indicating an intrinsic actin poly-

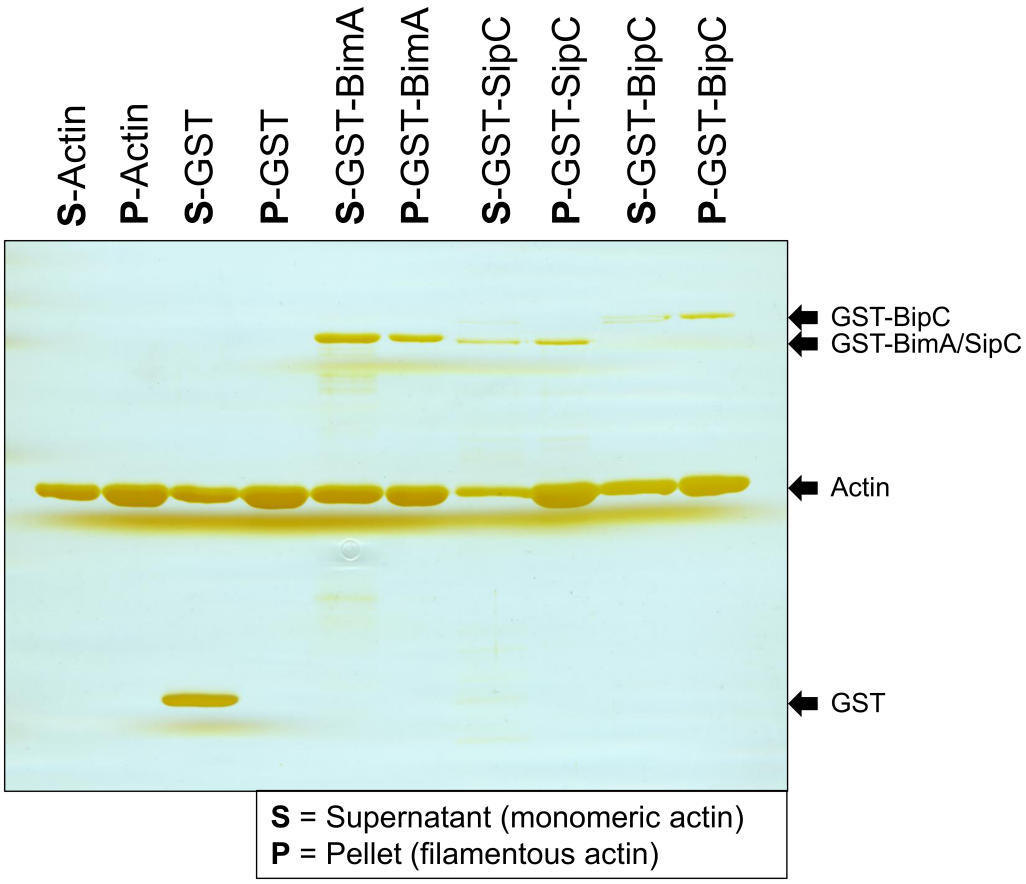


Figure 5.6: Co-sedimentation assay of GST-BipC with actin. Mg-actin was allowed to polymerise at room temperature for 2 hours before being mixed with GST, GST-BimA, GST-SipC or GST-BipC followed by a 30 minute incubation. The mixtures were submitted to a high speed centrifugation at 100,000 RCF for 1 hour to separate the monomeric actin (Supernatant) and the filamentous actin (pellet). The supernatant and pellet were carefully separated and suspended and denatured in Laemelli buffer. The samples were separated by SDS-PAGE and visualised using silver staining.

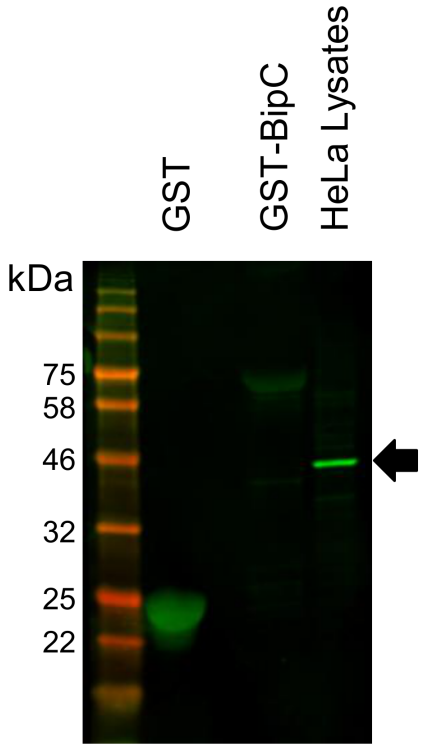


Figure 5.7: Investigation of BipC-Actin interaction using protein pull-downs. GST and GST-BipC sepharose beads were incubated with HeLa cell lysates overnight at 4ºC. The beads were washed and visualised by SDS-PAGE followed by Western blotting using rabbit α-Actin antibodies.

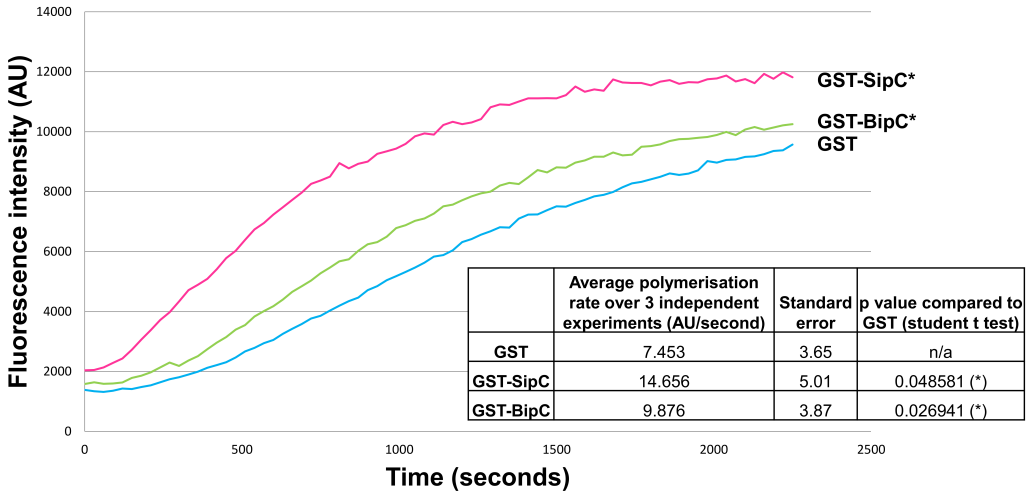
merising activity (Figure 5.8).

In *Salmonella*, the ability of SipC to polymerise and bundle F-actin is enhanced by another T3SS effector protein SipA (McGhie *et al.*, 2001). Due to their F-actin bundling ability, SipC and SipA inhibit the depolymerisation of F-actin. However, there is no homologue of SipA in *B. pseudomallei*. To investigate whether BipC may have the ability to stabilise F-actin on its own, a depolymerisation assay was performed. The inverse of the polymerisation assay, the depolymerisation assay measures a reduction in fluorescence indicating conversion of actin filaments (F-actin) to actin monomers (G-actin) over time. GST, GST-BimA, GST-SipC, or GST-BipC (1 μM) were incubated with 2.3 μM of pre-polymerised pyrene-actin for 1 hour in G-Mg buffer (depolymerising conditions). Both GST and BipC showed similar levels of depolymerisation to that of the actin only control and did not appear to stabilise F-actin (Figure 5.9). F-actin incubated with SipC was stabilised and showed slower rates of depolymerisation. Surprisingly, actin filaments incubated with GST-BimA underwent rapid depolymerisation.

With the establishment of BipC's ability to bind and polymerise actin *in vitro*, it is important to investigate whether BipC retains this ability *in vivo*. The full length BipC gene into the eukaryotic expression vector pRK5-Myc, which adds an in-frame N-terminal Myc tag to a protein of interest. HeLa cells were transfected with pRK5-Myc-BipC, or pEGFP as a control, using lipofectamine 2000. After 48 hours the HeLa cells were fixed in paraformaldehyde and probed using phalloidin to label F-actin and rabbit α-Myc antibodies to label BipC. Cells were imaged using a confocal microscope. Figure 5.10 is a representative image where the actin cytoskeleton (red) of the cells transfected with pRK5-Myc-BipC (green) appears irregular when compared to untransfected HeLa cells and HeLa cells transfected with pEGFP. BipC-expressing cells clearly demonstrate an altered morphology and evidence of perturbation of actin dynamics, especially at the plasma membrane. The Myc tagged BipC appeared to localise to the cellular membrane at membrane protrusions.

5.2.3 BipC is Secreted Independently of the Bsa T3SS

While BipC has been assumed to be secreted by the Bsa T3SS due to its position within the *bsa* T3SS locus and its close homology to SipC from *Salmonella*, this has not been formally shown. To demonstrate BipC is secreted in a manner dependant on the Bsa T3SS, the *bipC* gene was cloned into the inducible



	Average polymerisation rate over 3 independent experiments (AU/second)	Standard error	p value compared to GST (student t test)
GST	7.453	3.65	n/a
GST-SipC	14.656	5.01	0.048581 (*)
GST-BipC	9.876	3.87	0.026941 (*)

Figure 5.8: Polymerisation of pyrene-actin by *B. pseudomallei* GST-BipC. GST, GST-SipC and GST-BipC were mixed with monomeric pyrene-actin in actin polymerisation buffer. The polymerisation assay was monitored every 30 seconds for 40 minutes using a plate reader with an excitation wavelength of 365 nm and an emission wavelength of 407 nm. Both GST-SipC and GST-BipC show statistically faster rates of increase in fluorescence intensity than the GST control. The graph represents the average of 3 independent replicates each containing 3 technical replicates.

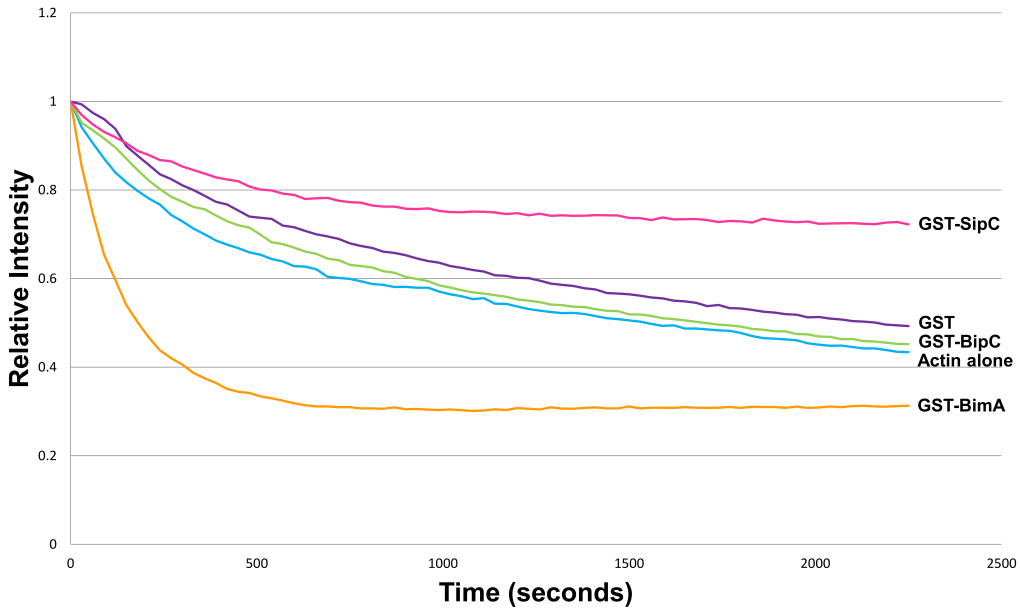


Figure 5.9: F-actin depolymerisation in the presence of GST-BipC. GST, GST-BipC, GST-SipC and GST-BimA were added to pyrene labelled F-actin. Fluorescence (excitation wavelength 365 nm; emission wavelength 407 nm) was measured for 40 minutes in 30 second intervals. The graph represents the average of 3 independent replicates each containing 3 technical replicates.

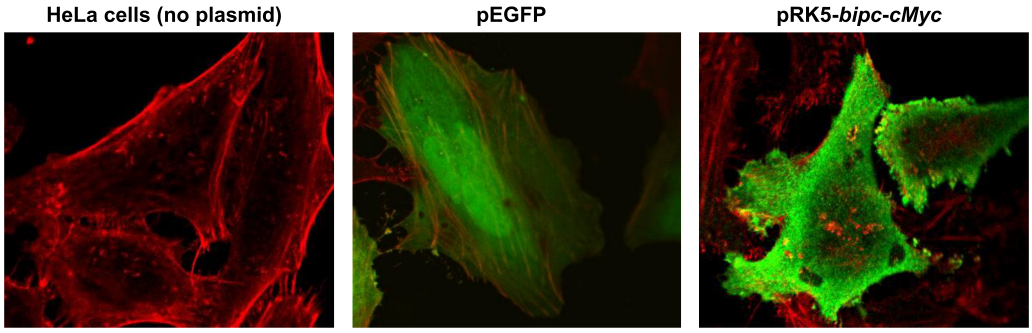


Figure 5.10: Confocal microscope images of HeLa cells eptopically expressing Myc tagged BipC. HeLa cells were transfected with pRK5-Myc-BipC using lipofectamine 2000. The HeLa cells were fixed in paraformaldehyde 48 hours post-transfection, probed using phalloidin and rabbit α-Myc antibodies, then imaged using a confocal microscope. Untransfected HeLa cells or HeLa cells transfected with pEGFP were also imaged. In the representative images, the actin cytoskeleton stained with (phalloidin) appears red and Myc-BipC or pEGFP appear green.

expression vector pME6032 (Heeb *et al.*, 2002) and expressed as an in-frame C-terminal c-Myc tagged fusion protein. pME6032-*bipC* was transformed into *B. pseudomallei* 10276 WT, 10276*bsaZ*::pDM4, 10276 *bipD*::pDM4 and 10276Δ*bsaP*. The strains were cultured overnight shaking at 37ºC in LB. The following day the overnight cultured was centrifuged and the supernatant was replaced with fresh LB containing 0.5 mM IPTG to an OD_{600} of 1.0. Of the adjusted culture 1 ml was added to 10 ml of LB containing 0.5 mM IPTG which was then incubated for 6 hours shaking at 37ºC. WT *B. pseudomallei* grown in the absence of IPTG was used as a control. Bacterial counts were assessed before and after the 6 hour incubation period, with all strains showing similar bacterial numbers. The bacterial supernatants were collected and the proteins were precipitated using PRMM. Equal volumes of protein were analysed by SDS-PAGE and assessed by Western blot for the presence of the myc-tagged BipC. c-Myc tagged BipC (molecular weight approximately 45 kDa) was detected in all of the bacterial cell lysates that had been induced with 0.5 mM IPTG (Figure 5.11). There was also a small non-specific band detected in the lysates of all strains, but it did not interfere with detection of myc-tagged BipC. Surprisingly, BipC-c-Myc was also present in equivalent levels in all supernatant samples induced by 0.5 mM IPTG, including the 10276*bsaZ*::pDM4 strain which is unable to secrete the known Bsa T3SS effector, BopE.

It was hypothesised that the Bsa T3SS-independent secretion of the tagged BipC proteins may be due to the presence of multiple T3SSs as well as a flagellar system in *B. pseudomallei* (Reviewed in Wiersinga *et al.* (2006)). It was also of interest to formally show that BipC is translocated into host cells. As *B. pseudomallei* is an intracellular pathogen, it is difficult to separate protein that may be translocated by the T3SS from protein that may be exported by other means once the bacterium is in the cytosol. Two possible solutions to this problem are to prevent the *B. pseudomallei* from invading the cell, or to use a surrogate host containing a functional T3SS that remains extracellular. Enteropathogenic *E. coli* (EPEC) is a major cause of foodborne illness which, upon making contact with host cells, forms a pedestal on the surface of the host cell using its T3SS where it can then continue to inject a series of T3S effector proteins (Reviewed in Wong *et al.* (2011)). EPEC encodes only one non-flagellar T3SS (Reviewed in Dean and Kenny (2009)). This feature makes EPEC an ideal surrogate host for studying T3SS translocation and it has been used with success in previous studies of the *B. pseudomallei* effector protein BopC (Muangman *et al.*, 2011) and the *B. mallei* effector protein BapA (Whitlock *et al.*, 2008).

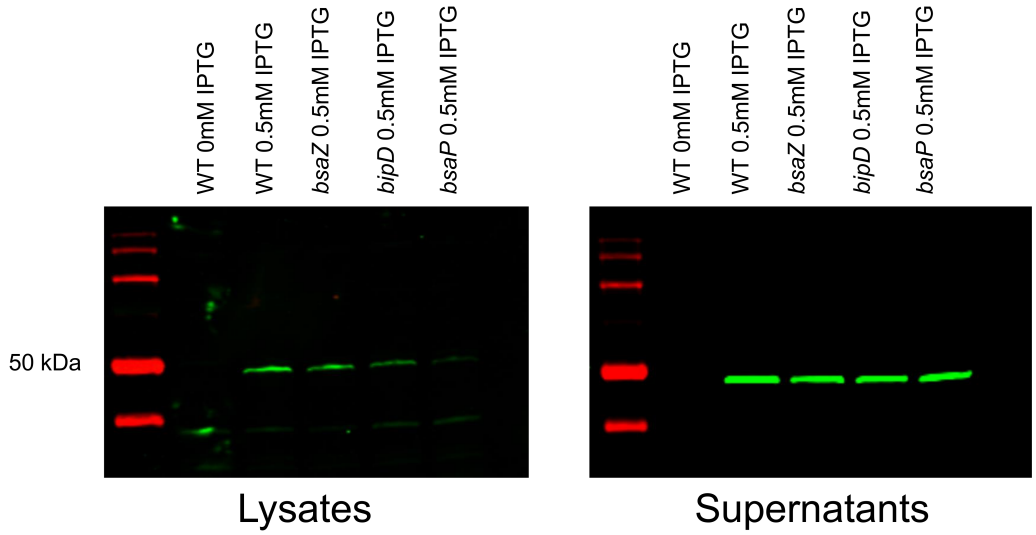


Figure 5.11: Western blot analysis of the *B. pseudomallei* Bsa T3SS effector/translocator protein BipC expressed as a c-Myc tagged fusion protein. The coding region of *bipC* was expressed with a C-terminal c-Myc tag in the IPTG-inducible expression vector pME6032 in *B. pseudomallei* strains 10276 WT, 10276 *bsaZ*::pDM4, 10276 *bipD*::pDM4 or 10276 Δ*bsaP*. Supernatant and whole cell fractions were collected after 6 hours of incubation at 37ºC in the presence of 0.5 mM IPTG. Equal quantities of protein were separated by reducing SDS-PAGE, blotted onto nitrocellulose membranes and probed using polyclonal rabbit α-c-Myc antibody.

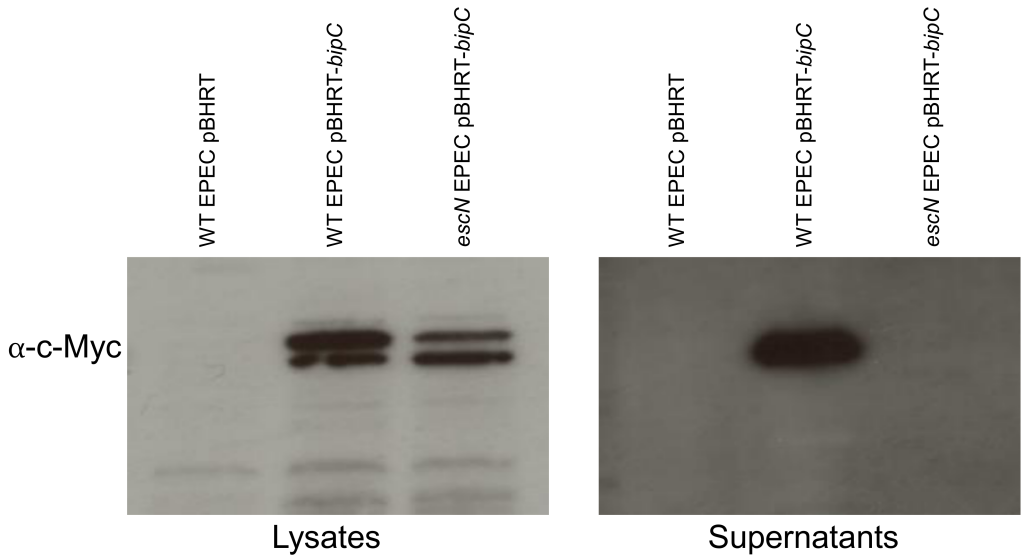


Figure 5.12: Western blot of BipC secretion using EPEC as a surrogate host. The full length coding region of *bipC* was expressed with a C-terminal c-Myc tag in the constitutive expression vector pBHRT. EPEC strain E2348/69 WT and Δ*escN* containing pBHRT-BipC were cultured for 4 hours in DMEM containing 25 mM HEPES shaking at 37°C. WT EPEC E2348/69 containing empty pBHRT was used as a control. The bacterial supernatants were collected and the proteins were precipitated using PRMM. Equal volumes of protein were separated by SDS-PAGE and assessed by Western blot using a c-Myc tag-specific polyclonal antibody.

BipC was cloned as a c-Myc fusion in the shuttle vector pBHRT under a constitutive kanamycin resistance gene promoter. The plasmid was transformed into EPEC O127:H6 strain E2348/69 WT and an isogenic Δ*escN* mutant (Marchés *et al.*, 2005), which is unable to secrete proteins via the T3SS. WT EPEC E2348/69 containing empty pBHRT was used as a negative control. The strains were cultured overnight shaking at 37°C in LB. The following day the overnight cultured was centrifuged and the supernatant was replaced with DMEM containing 25 mM HEPES to an OD_{600} of 1.0. Of the adjusted culture 1 ml was added to 10 ml of DMEM containing 25 mM HEPES which was then incubated for 4 hours shaking at 37°C. The bacterial supernatants were collected and the proteins were precipitated using PRMM. Equal volumes of protein were analysed by SDS-PAGE and assessed by Western blot for the presence of the tagged BipC using a c-Myc tag-specific polyclonal antibody. The bacterial cell lysates of EPEC WT and Δ*escN* express BipC-c-Myc (45 kDa) indicating the tagged protein was being produced in the strains (Figure 5.12). In the bacterial supernatants, BipC-c-Myc was secreted in a T3SS-dependant manner and was only found in the WT sample. This is evidence that EPEC can be used as a surrogate host for the study of translocation of *B. pseudomallei* BipC. Interestingly, BipC was seen as a doublet in the bacterial lysates, possible due to degradation by cytoplasmic proteases. It would be useful in the future to run the lysates next tot he supernatant on a SDS-PAGE gel to determine which of the doublet bands correspond to the secreted form of BipC in EPEC.

5.3 Discussion

The *B. pseudomallei* translocon protein BipC is homologous to the T3SS proteins SipC from *Salmonella* and IpaC from *Shigella* (Stevens *et al.*, 2002). Both SipC and IpaC bind and nucleate actin (Hayward and Koronakis, 1999, Terry *et al.*, 2008), facilitating bacterial invasion of host cells (Mounier *et al.*, 2009, Myeni and Zhou, 2010), a function that has not previously been demonstrated for BipC. In order to investigate this, pull-down experiments were performed using a GST-BipC fusion protein and murine splenic lysates in polymerisation buffer which resulted in the first evidence that BipC is an actin-binding protein. It was also demonstrated that GST-BipC has the ability to bind to actin directly, in the absence of other proteins.

The interaction between BipC and actin was further characterised using a co-sedimentation assay in which GST-BipC primarily co-sedimented with F-

actin. This suggests that BipC preferentially binds F-actin. This is similar to SipC, which has been shown to co-sediment primarily with F-actin (Myeni and Zhou, 2010). Further, actin was not found in GST-BipC samples when protein pull-downs were performed under non-polymerising conditions. Beyond its ability to directly bind actin, it was further demonstrated that BipC has the ability to polymerise actin *in vitro*. The activity appears to be lower than that of the SipC control. It has been shown that the activity of SipC is increased by another *Salmonella* T3SS effector protein SipA (McGhie *et al.*, 2001). It is possible that other *B. pseudomallei* T3SS effector proteins may work synergistically to polymerise actin with BipC. BipC did not appear to stabilize F-actin, suggesting that its role in actin dynamics may differ from that of SipC.

These findings may explain why actin was not identified as a binding partner for BipC in the Y2H screen described in Chapter 4. In agreement, the study by Memišević *et al.* (2013) did not identify actin as an interacting partner for *B. mallei* BipC. Another study using a Y2H system to investigate SipC protein-protein interactions resulted in the identification of cytokeratins as interacting partners, but actin identified by the screen (Carlson *et al.*, 2002). Due to the possibility of the interaction being missed in a high-throughput library screen, the ability of BipC and actin to interact was tested in a clean *S. cerevisiae* background using the plasmids pGBKT7-BipC and pGADT7-actin, which again resulted in no activation of the Y2H reporter genes and lack of growth on selective media. It is possible that the environment of the yeast nucleus is not conducive of BipC-F-actin binding. When expressed as an N-terminal Myc tagged protein in HeLa cells, BipC appears to cause the formation of pseudopodia and membrane protrusions at the cell membrane. The Myc-tagged BipC localised to the cell membrane with F-actin and the pseudopodia. These areas of actin disruption on the cell periphery are similar to what has been described as "membrane ruffles", seen in an *ipaC*-dependant manner when Swiss 3T3 cells were permeabilised in the presence of *Shigella* supernatants (Van Nhieu *et al.*, 1999). Further work will need to be done to explore the mechanisms by which BipC binds and nucleates actin, as well the role this may play in *B. pseudomallei* pathogenesis.

It is tempting to speculate that the ability of BipC to polymerise actin is involved in the invasion of host cells. Though it was previously demonstrated that a *bipC* mutant is deficient in its ability to invade A549 cells, this function was not separated from BipC's role as a translocator(Kang *et al.*, 2015). A mutation in another *B. pseudomallei* Bsa T3SS translocator *bipB* also showed an

invasion defect in HeLa cells (Suparak *et al.*, 2005). Because the insertion of the translocon into the host cell membrane is necessary for the subsequent injection of effector proteins (Reviewed in Büttner (2012)), studies of secondary functions of translocator proteins must be carefully controlled in order to draw conclusions.

Interestingly, BipC expressed as a C-terminal c-Myc tagged protein by an inducible expression vector was secreted independently of the Bsa T3SS under the conditions used in this study. There are a number of possible explanations for this. One possibility is that the bacterial cell may have been overwhelmed with levels of BipC-c-Myc, similar to what was hypothesized when BopE-c-Myc was expressed constitutively (Chapter 2, Figure 3.15). However, in the case of BipC, an inducible expression vector was used with levels of inducer that were appropriate for other effector proteins to be secreted in a Bsa-dependent manner. Another possibility is that BipC is being promiscuously secreted by one of the other two plant-like T3SSs or the flagellar T3SS of *B. pseudomallei*. This phenomenon is not without precedent. The Hrp Plant T3SS of *Xanthomonas* can secrete the effector protein YopE of *Yersinia* (Rossier *et al.*, 1999). Removal of the ability of SopE in *Salmonella* to bind it's chaperone InvB, caused secretion through both the flagellar and SPI-1 virulence associated T3SS (Lee and Galán, 2004, Ehrbar *et al.*, 2006). Virulence associated T3SS effectors can be secreted by the bacterial flagellar T3SS in *Yersinia* (Young and Young, 2002, Warren and Young, 2005). Full length BipC-c-Myc was also secreted by EPEC, which only contains one T3SS (Reviewed in Dean and Kenny (2009)), in a T3SS-dependant manner. This suggests BipC may be more promiscuous in which T3SSs it can be secreted from. More work needs to be performed, such as expression of BipC without the N-terminal T3SS signal, to determine whether BipC-c-Myc secretion is dependant on any T3SS or may be through an independent mechanism. As an added benefit, this study established EPEC as an acceptable host for study of translocation of BipC-c-Myc, which may be useful in downstream studies.

Chapter 6

General Discussion

6.1 Impact of This Study

The primary aim of this study was to identify the repertoire of effector proteins secreted by the *B. pseudomallei* Bsa T3SS. It was hypothesised that under standard laboratory conditions this system was under tight regulation and would need to be dysregulated. To this end *bsaP*, which is predicted to encode a structural component of the T3SS, was deleted from the chromosome. It was shown that BsaP functions similarly to T3SS gatekeeper proteins in other Gram-negative bacteria that are involved in controlling a switch from secretion of translocator proteins to effector proteins (Reviewed in Büttner (2012)). The identification of proteins with homologous function within the T3SS may allow for the informed design or use of previously existing T3SS inhibitors as a method of treatment. For example, a small molecule ATPase inhibitor effective in *Yersinia pestis* prevented the secretion of BopE in *B. pseudomallei* and treatment of infected RAW 264.7 cells with the inhibitor reduced bacterial survival (Gong *et al.*, 2015). There are a range of other small molecule inhibitors of the T3SS effective in other Gram negative bacteria not yet tested in *B. pseudomallei* (Reviewed in Gu *et al.* (2015)).

Another possible outcome of dysregulating the Bsa T3SS is the potential for use as a live attenuated vaccines. A *B. pseudomallei bsaZ* mutant lacking a functional Bsa T3SS is highly attenuated in a murine melioidosis model, although still lethal to the mice over time (Stevens *et al.*, 2004). It is possible that a dysregulated T3SS (*bsaP* mutant) may be similarly attenuated due to a lack of translocator proteins, but create a stronger immune response due to the presence of high levels of bacterial effector proteins.

In this thesis bacterial supernatants were generated from WT, a Bsa T3SS

null mutant (*bsaZ*) and two structural mutants that hyper-secrete the known effector BopE (*bipD* and *bsaP*). Proteins precipitated from the supernatants were digested, labelled with mass tags and analysed by mass spectrometry using a method known as iTRAQ. The resulting data set is the most complete set of *B. pseudomallei* secreted proteins so far produced and is published in Molecular and Cellular Proteomics (Vander Broek *et al.*, 2015). This data set will prove important to the wider community as a reference for selecting secreted proteins for further study. The list contains some proteins that were annotated as hypothetical which are know known to be translated. The community could use the resource to produce a list of possible vaccine candidates by looking for extracellular proteins which may be readily visible to the host immune system. It also allows for scanning of different factors that may be shared with other bacteria useful in informing antigen choice for vaccines that protect against multiple pathogenic bacterial species. One study has shown CD4 T cells that recognise *B. pseudomallei* FliC epitopes cross-react with FliC from *B. cenocepacia* and *B. multivorans*, species often involved in infection in cystic fibrosis patients (Musson *et al.*, 2014).

Beyond the core secretome of *B. pseudomallei*, BapA and BprD were identified as novel Bsa T3SS effector proteins and BipC and BapA were shown to be secreted in a Bsa T3SS-dependent manner for the first time. The first steps towards understanding the role of BipC and BapA were taken in the form of yeast two-hybrid screening. The human protein C1QBP was identified and confirmed as an interacting partner for both BipC and BapA. As well as helping to understand the disease process, the subtle effects of T3SS effector proteins have on host cell processes can provide important tools to help interrogate host cell biology (Reviewed by Lee *et al.* (2013)). C1QBP plays a role in cancers and is involved in innate immunity, pathogen binding and major inflammation pathways (Reviewed in Peerschke and Ghebrehiwet (2014) and Peerschke and Ghebrehiwet (2007)). This makes C1QBP an attractive target for further study and potential therapies.

In this study it was shown that BipC, similar to the homologous proteins SipC (*Salmonella*) and IpaC (*Shigella*), is able to directly bind and polymerise actin (Hayward and Koronakis, 1999, Terry *et al.*, 2008). The actin polymerisation function of SipC has been shown to be involved in the entry of *Salmonella* into host cells (Myeni and Zhou, 2010) and it is tempting to hypothesis BipC may function similarly in *B. pseudomallei*. Blocking the entry into host cells may be an effective way to treat *B. pseudomallei* infection.

6.2 Future Work

6.2.1 iTRAQ Analysis of the Bsa T3SS Secretome

The work presented in this thesis forms the basis of several potential future studies. In particular, the iTRAQ screen resulted in a large dataset that warrants further investigation. While the most obvious candidates from the iTRAQ screen were validated, it would be interesting to validate other targets that were close to the selected cut-offs. It is possible that that some of theses "borderline" proteins may indeed be effector proteins, and simply are secreted at low levels under the culture conditions used in this study. As the effector protein CHBP was only secreted in infected cells Pumirat *et al.* (2014), it would be interesting to analyse Bsa T3SS-dependent proteins secreted into infected cells using iTRAQ. Due to the drastically different environment within a host cell it is certainly possible that a different set of proteins may be present in a BsaZ dependant manner than were present in LB media. This would not only give further insight into the full Bsa T3SS effector repertoire, but would also inform global changes in the general *B. pseudomallei* secretome during infection.

One interesting aspect of T3SS effector proteins is different repertoires can exist between different bacterial strains of the same species, often due to horizontal gene transfer (Rohmer *et al.*, 2004). This is highlighted in *B. pseudomallei* by the known Bsa T3SS effector protein CHBP which was present in 76.7% of *B. pseudomallei* strains surveyed by Pumirat *et al.* (2014). This effector protein was absent from the strain used in this study, 10276. Also, *B. pseudomallei* is known to have large genomic variability. A recent study of 37 *B. pseudomallei* isolates found that on average, there were 152 strain-specific genes per isolate (Spring-Pearson *et al.*, 2015). This suggests there is the possibility of other effector proteins in other *B. pseudomallei* strains. It would be interesting to use comparative proteomics to compare the repertoire of proteins secreted in a Bsa T3SS-dependent manner between different isolates of *B. pseudomallei* such as those from Australia, Thailand, Africa and the Americas, or from strains with defined differences in virulence.

In this study BrpD and BapA were identified as novel effector proteins secreted in a Bsa T3SS-dependent manner, but it has not yet been demonstrated that the proteins are translocated into host cells by the T3SS. This is more difficult to investigate in *B. pseudomallei* because it is an intracellular pathogen. It is necessary to separate proteins injected into a host cell from the outside of the

cell by the T3SS from proteins that are secreted for example through the vacuolar membrane into the cytoplasm. One solution is to ensure the *B. pseudomallei* can not enter the host cell following treatment with cytochalasin D. Cytochalasin D inhibits actin polymerisation, stopping microfilament function and preventing actin mediated bacterial entry into the host cell (Reviewed by Rosenshine *et al.* (1994)). By preventing bacterial entry into the host cell, proteins injected into the host cell can be evaluated by selectively lysing the eukaryotic cells and testing for the presence of eptopically expressed myc-tagged effector proteins using SDS-PAGE and Western blot. As demonstrated in Chapter 5, the use of an extracellular surrogate host, such as EPEC, is another effective way to study the function of an effector protein such as BipC, without the actin disrupting effects of cytochalasin D. The EPEC host system could be used to investigate other effector proteins in the future.

With the creation of the *bsaP* mutant as a tool to study the Bsa T3SS, it would also be possible to test the outcome of this mutation in infection models. During this study, the *Galleria mellonella* (Wax moth) infection model (Wand *et al.*, 2011) was adapted for screening of the *B. pseudomallei* T3SS (Figure 7.1, more information included in the appendix). This system could be used to compare the attenuation of the *bsaP* mutant to other structural mutations in the Bsa T3SS in order to justify later experiments in more complex models, such as the murine model of melioidosis.

6.2.2 Yeast-Two Hybrid Screen of BapA, BipC and BprD

It was surprising that no human proteins were found to interact with BprD. Previous studies state that BprD is a bacterial regulator which may explain why it does not interact with human proteins (Chirakul *et al.*, 2014). The number of independent library clones screened in the Y2H analysis of BprD was 10 fold and 4 fold lower than that of BipC and BapA respectively. There may be value in repeating the screen to survey a larger number of independent clones. Also, a lower stringency could be used to attempt to detect lower affinity interactions.

One of the studies that interests me the most is to explore which domains or regions of BapA and BipC bind to specific regions of C1QBP. Both effector proteins binding the same human protein raise the question as to whether BapA and BipC may share sequence homology that allows binding of C1QBP at a specific site. It is also possible that the two proteins bind C1QBP at different sites and may have distinct effects on C1QBP. It is not unheard of that two ef-

fector proteins bind to similar targets causing different outcomes. This is highlighted by *Salmonella* SopE and SptP which activate and deactivate Cdc42 and Rac1 respectively, modulating host cell actin, but maintaining balance within the cell (Kubori and Galán, 2003).

Though two proteins may interact in an artificial environment, *in vivo* the proteins may never come into proximity with each other and the interaction may not be relevant to infection. To investigate this, confocal microscopy could be used to analyse co-localisation of either BapA or BipC with C1QBP. In addition, cells in which C1QBP is knocked down by either siRNA or the CRISPR/Cas9 system could be used to determine the importance of C1QBP on the intracellular life of *B. pseudomallei*. Unfortunately, C1QBP knockout mice are embryonic lethal prohibiting investigation of the role of C1QBP in a murine model of melioidosis (Yagi *et al.*, 2012).

6.2.3 Investigation of the Interaction Between BipC and Actin

One important study to complete is to identify which BipC domain is responsible for binding/polymerisation of actin. *B. pseudomallei bipC* mutants could be complemented with *bipC* retaining translocator function, but lacking the ability to polymerise actin. This would allow the study of the role BipC plays in bacterial entry to be separated from its function as a translocator.

One very interesting observation made during this study was the Bsa T3SS-independent secretion of BipC. This is in contrast to the other proteins within the Bsa T3SS locus. One hypothesis is that BipC may be promiscuously secreted by another T3SS or the flagellar system. One way this could be confirmed is by creating a series of structural mutations in each secretion system and determining its effect on BipC secretion by SDS-PAGE and Western blot.

6.2.4 Closing Statement

Burkholderia pseudomallei has attracted much attention in the UK and the USA following its classification as a Bioterrorism agent with high mortality rates, no available vaccine and resistance to many antibiotics (Reviewed in Gilad *et al.* (2007)). Yet despite this growing body of research, in endemic Thailand, *B. pseudomallei* is the leading cause of community-acquired bacteraemia and the third most common cause of death from infectious disease, after HIV and tuberculosis (Limmathurotsakul *et al.*, 2010). *B. pseudomallei* is an emerging disease and with improved surveillance the bacteria is now found outside of

the endemic region in sub-tropical soils in Africa, the Americas and the Indian Sub-continent (Reviewed in Currie *et al.* (2008)). For these reasons, the continued investigation of both basic biology and clinical aspects of this neglected tropical pathogen are vital in order to improve control and treatment in the future.

Bibliography

Abe, A., M. De Grado, R. A. Pfuetzner, C. Sánchez-SanMartín, R. DeVinney, J. L. Puente, N. C. Strynadka, and B. B. Finlay (1999). Enteropathogenic *Escherichia coli* translocated intimin receptor, Tir, requires a specific chaperone for stable secretion. *Molecular microbiology*, 33(6):1162–1175.

Akeda, Y. and J. E. Galán (2005). Chaperone release and unfolding of substrates in type III secretion. *Nature*, 437(7060):911–915.

Ali, S. A. and A. Steinkasserer (1995). PCR-ligation-PCR mutagenesis: a protocol for creating gene fusions and mutations. *Biotechniques*, 18(5):746–50.

Allwood, E. M., R. J. Devenish, M. Prescott, B. Adler, and J. D. Boyce (2011). Strategies for intracellular survival of *Burkholderia pseudomallei*. *Frontiers in microbiology*, 2(170).

Anderson, D. M. and O. Schneewind (1997). A mRNA signal for the type III secretion of Yop proteins by *Yersinia enterocolitica*. *Science*, 278(5340):1140–1143.

Arnold, R., S. Brandmaier, F. Kleine, P. Tischler, E. Heinz, S. Behrens, A. Niinikoski, H.-W. Mewes, M. Horn, and T. Rattei (2009). Sequence-based prediction of type III secreted proteins. *PLoS pathogens*, 5(4):e1000376.

Barrett, B. S., W. L. Picking, W. D. Picking, and C. R. Middaugh (2008). The response of type three secretion system needle proteins MxiHΔ5, BsaLΔ5, and PrgIΔ5 to temperature and pH. *Proteins: structure, function, and bioinformatics*, 73(3):632–643.

Bast, A., K. Krause, I. H. Schmidt, M. Pudla, S. Brakopp, V. Hopf, K. Breitbach, and I. Steinmetz (2014). Caspase-1-dependent and -independent cell death pathways in *Burkholderia pseudomallei* infection of macrophages. *PLoS pathogens*, 10:e1003986.

Bensadoun, A. and D. Weinstein (1976). Assay of proteins in the presence of interfering materials. *Analytical biochemistry*, 70(1):241–250.

Bergh, P. V., M. Heller, S. Braga-Lagache, and J. Frey (2013). The *Aeromonas salmonicida subsp. salmonicida* exoproteome: determination of the complete repertoire of Type-Three Secretion System effectors and identification of other virulence factors. *Proteome science*, 11(1):1–20.

Bingle, L. E., C. M. Bailey, and M. J. Pallen (2008). Type VI secretion: a beginner's guide. *Current opinion in microbiology*, 11(1):3–8.

Birnie, E., W. J. Wiersinga, D. Limmathurotsakul, and M. P. Grobusch (2015). Melioidosis in Africa: should we be looking more closely? *Future microbiology*, 10(2):273–281.

Birtalan, S. and P. Ghosh (2001). Structure of the *Yersinia* type III secretory system chaperone SycE. *Nature structural & molecular biology*, 8(11):974–978.

Blocker, A., P. Gounon, E. Larquet, K. Niebuhr, V. Cabiaux, C. Parsot, and P. Sansonetti (1999). The tripartite type III secreton of *Shigella flexneri* inserts IpaB and IpaC into host membranes. *The Journal of cell biology*, 147(3):683–693.

Blocker, A., N. Jouihri, E. Larquet, P. Gounon, F. Ebel, C. Parsot, P. Sansonetti, and A. Allaoui (2001). Structure and composition of the *Shigella flexneri* 'needle complex', a part of its type III secreton. *Molecular microbiology*, 39(3):652–663.

Blondeau, J.-P. (2002). Homologues of amino acid permeases: cloning and tissue expression of XAT1 and XAT2. *Gene*, 286(2):241–248.

Boddey, J. A., C. J. Day, C. P. Flegg, R. L. Ulrich, S. R. Stephens, I. R. Beacham, N. A. Morrison, and I. R. Peak (2007). The bacterial gene *lfpA* influences the potent induction of calcitonin receptor and osteoclast-related genes in *Burkholderia pseudomallei*-induced TRAP-positive multinucleated giant cells. *Cellular microbiology*, 9(2):514–531.

Boisvert, F.-M., Y. W. Lam, D. Lamont, and A. I. Lamond (2010). A quantitative proteomics analysis of subcellular proteome localization and changes induced by DNA damage. *Molecular & cellular proteomics*, 9(3):457–470.

Botteaux, A., M. P. Sory, L. Biskri, C. Parsot, and A. Allaoui (2009). MxiC is secreted by and controls the substrate specificity of the *Shigella flexneri* type III secretion apparatus. *Molecular microbiology*, 71(2):449–460.

Braun, L., B. Ghebrehiwet, and P. Cossart (2000). gC1q-R/p32, a C1q-binding protein, is a receptor for the InlB invasion protein of *Listeria monocytogenes*. *The EMBO journal*, 19(7):1458–1466.

Brett, P., D. Deshazer, and D. Woods (1997). Characterization of *Burkholderia pseudomallei* and *Burkholderia pseudomallei*-like strains. *Epidemiology and infection*, 118(02):137–148.

Brett, P. J., D. DeShazer, and D. E. Woods (1998). Note *Burkholderia thailandensis* sp. nov., a *Burkholderia pseudomallei*-like species. *International journal of systematic bacteriology*, 48(1):317–320.

Brodbeck, W. G. and J. M. Anderson (2009). Giant cell formation and function. *Current opinion in hematology*, 16(1):53.

Brook, M., B. Currie, and P. Desmarchelier (1997). Isolation and identification of *Burkholderia pseudomallei* from soil using selective culture techniques and the polymerase chain reaction. *Journal of applied microbiology*, 82(5):589–596.

Brückner, A., C. Polge, N. Lentze, D. Auerbach, and U. Schlattner (2009). Yeast two-hybrid, a powerful tool for systems biology. *International journal of molecular sciences*, 10(6):2763–2788.

Burtnick, M. N. and P. J. Brett (2013). *Burkholderia mallei* and *Burkholderia pseudomallei* cluster 1 type VI secretion system gene expression is negatively regulated by iron and zinc. *PloS one*, 8(10):e76767.

Burtnick, M. N., P. J. Brett, and D. DeShazer (2014). Proteomic analysis of the *Burkholderia pseudomallei* type II secretome reveals hydrolytic enzymes, novel proteins, and the deubiquitinase TssM. *Infection and immunity*, 82(8):3214–3226.

Burtnick, M. N., P. J. Brett, S. V. Harding, S. A. Ngugi, W. J. Ribot, N. Chantratita, A. Scorpio, T. S. Milne, R. E. Dean, D. L. Fritz, *et al.* (2011). The cluster 1 type VI secretion system is a major virulence determinant in *Burkholderia pseudomallei*. *Infection and immunity*, 79(4):1512–1525.

Burtnick, M. N., P. J. Brett, V. Nair, J. M. Warawa, D. E. Woods, and F. C. Gherardini (2008). *Burkholderia pseudomallei* type III secretion system mutants exhibit delayed vacuolar escape phenotypes in RAW 264.7 murine macrophages. *Infection and immunity*, 76(7):2991–3000.

Büttner, D. (2012). Protein export according to schedule: architecture, assembly, and regulation of type III secretion systems from plant-and animal-pathogenic bacteria. *Microbiology and molecular biology reviews*, 76(2):262–310.

Caldwell, R. B. and C. T. Lattemann (2004). Simple and reliable method to precipitate proteins from bacterial culture supernatant. *Applied and environmental microbiology*, 70(1):610–612.

Cambronne, E. D., L. W. Cheng, and O. Schneewind (2000). LcrQ/YscM1, regulators of the *Yersinia yop* virulon, are injected into host cells by a chaperone-dependent mechanism. *Molecular microbiology*, 37(2):263–273.

Campbell-Valois, F.-X., M. Sachse, P. J. Sansonetti, and C. Parsot (2015). Escape of Actively Secreting *Shigella flexneri* from ATG8/LC3-Positive Vacuoles Formed during Cell-To-Cell Spread Is Facilitated by IcsB and VirA. *mBio*, 6(3):e02567–14.

Carlson, S. A., M. B. Omary, and B. D. Jones (2002). Identification of cytokeratins as accessory mediators of *Salmonella* entry into eukaryotic cells. *Life sciences*, 70(12):1415–1426.

Chang, J., J. Chen, and D. Zhou (2005). Delineation and characterization of the actin nucleation and effector translocation activities of *Salmonella* SipC. *Molecular microbiology*, 55(5):1379–1389.

Chang, J., S. K. Myeni, T. L. Lin, C. C. Wu, C. J. Staiger, and D. Zhou (2007). SipC multimerization promotes actin nucleation and contributes to *Salmonella*-induced inflammation. *Molecular microbiology*, 66(6):1548–1556.

Chen, Y., I. Schröder, C. T. French, A. Jaroszewicz, X. J. Yee, B.-E. Teh, I. J. Toesca, J. F. Miller, and Y.-H. Gan (2014). Characterization and analysis of the *Burkholderia pseudomallei* BsaN virulence regulon. *BMC microbiology*, 14(1):206.

Chen, Y., J. Wong, G. W. Sun, Y. Liu, G.-Y. G. Tan, and Y.-H. Gan (2011). Regulation of type VI secretion system during *Burkholderia pseudomallei* infection. *Infection and immunity*, 79(8):3064–3073.

Cheng, A. C. and B. J. Currie (2005). Melioidosis: epidemiology, pathophysiology, and management. *Clinical microbiology reviews*, 18(2):383–416.

Chirakul, S., T. Bartpho, T. Wongsurawat, S. Taweechaisupapong, N. Karoonutaisiri, A. M. Talaat, S. Wongratanacheewin, R. K. Ernst, and R. W. Sermswan (2014). Characterization of BPSS1521 (*bprD*), a regulator of *Burkholderia pseudomallei* virulence gene expression in the mouse model. *PLoS one*, P. e104313.

Choi, K.-H., A. Kumar, and H. P. Schweizer (2006). A 10-min method for preparation of highly electrocompetent *Pseudomonas aeruginosa* cells: application for DNA fragment transfer between chromosomes and plasmid transformation. *Journal of microbiological methods*, 64(3):391–397.

Coenye, T. and P. Vandamme (2003). Diversity and significance of *Burkholderia* species occupying diverse ecological niches. *Environmental microbiology*, 5(9):719–729.

Compant, S., J. Nowak, T. Coenye, C. Clément, and E. A. Barka (2008). Diversity and occurrence of *Burkholderia* spp. in the natural environment. *FEMS microbiology reviews*, 32(4):607–626.

Costa, T. R., C. Felisberto-Rodrigues, A. Meir, M. S. Prevost, A. Redzej, M. Trokter, and G. Waksman (2015). Secretion systems in Gram-negative bacteria: structural and mechanistic insights. *Nature reviews microbiology*, 13(6):343–359.

Cui, J., Q. Yao, S. Li, X. Ding, Q. Lu, H. Mao, L. Liu, N. Zheng, S. Chen, and F. Shao (2010). Glutamine deamidation and dysfunction of ubiquitin/NEDD8 induced by a bacterial effector family. *Science*, 329(5996):1215–1218.

Cullinane, M., L. Gong, X. Li, N.-L. Adler, T. Tra, E. Wolvetang, M. Prescott, J. D. Boyce, R. J. Devenish, and B. Adler (2008). Stimulation of autophagy suppresses the intracellular survival of *Burkholderia pseudomallei* in mammalian cell lines. *Autophagy*, 4(6):744–753.

Currie, B. J., D. A. Dance, and A. C. Cheng (2008). The global distribution of *Burkholderia pseudomallei* and melioidosis: an update. *Transactions of the royal society of tropical medicine and hygiene*, 102(Supplement 1):S1–S4.

Currie, B. J. and S. P. Jacups (2003). Intensity of rainfall and severity of melioidosis, Australia. *Emerging infectious diseases*, 9(12):1538.

Currie, B. J., L. Ward, and A. C. Cheng (2010). The epidemiology and clinical spectrum of melioidosis: 540 cases from the 20 year Darwin prospective study. *PLoS neglected tropical diseases*, 4(11):e900.

Dance, D., V. Wuthiekanun, P. Naigowit, and N. White (1989). Identification of *Pseudomonas pseudomallei* in clinical practice: use of simple screening tests and API 20NE. *Journal of clinical pathology*, 42(6):645–648.

D'Cruze, T., L. Gong, P. Treerat, G. Ramm, J. D. Boyce, M. Prescott, B. Adler, and R. J. Devenish (2011a). Role for the *Burkholderia pseudomallei* type three secretion system cluster 1 *bpscN* gene in virulence. *Infection and immunity*, 79(9):3659–3664.

D'Cruze, T., L. Gong, P. Treerat, G. Ramm, J. D. Boyce, M. Prescott, B. Adler, and R. J. Devenish (2011b). Role for the *Burkholderia pseudomallei* type three secretion system cluster 1 *bpscN* gene in virulence. *Infection and immunity*, 79(9):3659–3664.

Dean, P. and B. Kenny (2009). The effector repertoire of enteropathogenic *E. coli*: ganging up on the host cell. *Current opinion in microbiology*, 12(1):101–109.

Deng, W., C. L. de Hoog, B. Y. Hong, Y. Li, M. A. Croxen, N. A. Thomas, J. L. Puente, L. J. Foster, and B. B. Finlay (2010). A comprehensive proteomic analysis of the type III secretome of *Citrobacter rodentium*. *Journal of biological chemistry*, 285(9):6790–6800.

Deng, W., B. Y. Hong, C. L. de Hoog, N. Stoynov, Y. Li, L. J. Foster, and B. B. Finlay (2012). Quantitative proteomic analysis of type III secretome of enteropathogenic *Escherichia coli* reveals an expanded effector repertoire for attaching/effacing bacterial pathogens. *Molecular & cellular proteomics*, 11(9):692–709.

Deng, W., Y. Li, P. R. Hardwidge, E. A. Frey, R. A. Pfuetzner, S. Lee, S. Gruenheid, N. C. Strynakda, J. L. Puente, and B. B. Finlay (2005). Regulation of type III secretion hierarchy of translocators and effectors in attaching and effacing bacterial pathogens. *Infection and immunity*, 73(4):2135–2146.

Deng, W., J. L. Puente, S. Gruenheid, Y. Li, B. A. Vallance, A. Vázquez, J. Barba, J. A. Ibarra, P. O'Donnell, P. Metalnikov, *et al.* (2004). Dissecting virulence: systematic and functional analyses of a pathogenicity island. *Proceedings of the national academy of sciences*, 101(10):3597–3602.

DeShazer, D., P. J. Brett, and D. E. Woods (1998). The type II O-antigenic polysaccharide moiety of *Burkholderia pseudomallei* lipopolysaccharide is required for serum resistance and virulence. *Molecular microbiology*, 30(5):1081–1100.

Diepold, A., M. Amstutz, S. Abel, I. Sorg, U. Jenal, and G. R. Cornelis (2010). Deciphering the assembly of the *Yersinia* type III secretion injectisome. *The EMBO journal*, 29(11):1928–1940.

Diepold, A. and S. Wagner (2014). Assembly of the bacterial type III secretion machinery. *FEMS microbiology reviews*, 38(4):802–822.

Diepold, A., U. Wiesand, and G. R. Cornelis (2011). The assembly of the export apparatus (YscR, S, T, U, V) of the *Yersinia* type III secretion apparatus occurs independently of other structural components and involves the formation of an YscV oligomer. *Molecular microbiology*, 82(2):502–514.

Douglas, M. W., G. Lum, J. Roy, D. A. Fisher, N. M. Anstey, and B. J. Currie (2004). Epidemiology of community-acquired and nosocomial bloodstream infections in tropical Australia: a 12-month prospective study. *Tropical medicine & international health*, 9(7):795–804.

Doyle, S. L., H. Husebye, D. J. Connolly, T. Espevik, L. A. O'Neill, and A. F. McGettrick (2012). The GOLD domain-containing protein TMED7 inhibits TLR4 signalling from the endosome upon LPS stimulation. *Nature communications*, 3:707.

Draper, A., M. Mayo, G. Harrington, D. Karp, D. Yinfoo, L. Ward, A. Haslem, B. Currie, and M. Kaestli (2010). Association of the melioidosis agent *Burkholderia pseudomallei* with water parameters in rural water supplies in Northern Australia. *Applied and environmental microbiology*, 76(15):5305–5307.

Drevinek, P. and E. Mahenthiralingam (2010). *Burkholderia cenocepacia* in cystic fibrosis: epidemiology and molecular mechanisms of virulence. *Clinical microbiology and infection*, 16(7):821–830.

Druar, C., F. Yu, J. L. Barnes, R. T. Okinaka, N. Chantratita, S. Beg, C. W. Stratilo, A. J. Olive, G. Soltes, M. L. Russell, *et al.* (2008). Evaluating *Burkholderia pseudomallei* Bip proteins as vaccines and Bip antibodies as detection agents. *FEMS immunology & medical microbiology*, 52(1):78–87.

Ehrbar, K., A. Friebel, S. I. Miller, and W.-D. Hardt (2003). Role of the *Salmonella* pathogenicity island 1 (SPI-1) protein InvB in type III secretion of SopE and SopE2, two *Salmonella* effector proteins encoded outside of SPI-1. *Journal of bacteriology*, 185(23):6950–6967.

Ehrbar, K., B. Winnen, and W.-D. Hardt (2006). The chaperone binding domain of SopE inhibits transport via flagellar and SPI-1 TTSS in the absence of InvB. *Molecular microbiology*, 59(1):248–264.

Elliott, M. H., D. S. Smith, C. E. Parker, and C. Borchers (2009). Current trends in quantitative proteomics. *Journal of mass spectrometry*, 44(12):1637–1660.

Epler, C. R., N. E. Dickenson, A. J. Olive, W. L. Picking, and W. D. Picking (2009). Liposomes recruit IpaC to the *Shigella flexneri* type III secretion apparatus needle as a final step in secretion induction. *Infection and immunity*, 77(7):2754–2761.

Erhardt, M., M. E. Mertens, F. D. Fabiani, and K. T. Hughes (2014). ATPase-independent type-III protein secretion in *Salmonella enterica*. *PLoS genetics*, 10:e1004800.

Erskine, P., M. Knight, A. Ruaux, H. Mikolajek, N. W. F. Sang, J. Withers, R. Gill, S. Wood, M. Wood, G. Fox, *et al.* (2006). High resolution structure of BipD: an invasion protein associated with the type III secretion system of *Burkholderia pseudomallei*. *Journal of molecular biology*, 363(1):125–136.

Espina, M., S. F. Ausar, C. R. Middaugh, M. A. Baxter, W. D. Picking, and W. L. Picking (2007). Conformational stability and differential structural analysis of LcrV, PcrV, BipD, and SipD from type III secretion systems. *Protein science*, 16(4):704–714.

Espina, M., A. J. Olive, R. Kenjale, D. S. Moore, S. F. Ausar, R. W. Kaminski, E. V. Oaks, C. R. Middaugh, W. D. Picking, and W. L. Picking (2006). IpaD localizes to the tip of the type III secretion system needle of *Shigella flexneri*. *Infection and immunity*, 74(8):4391–4400.

Fausther-Bovendo, H., V. Vieillard, S. Sagan, G. Bismuth, and P. Debre (2010). HIV gp41 engages gC1qR on CD4+ T cells to induce the expression of an NK ligand through the PIP3/H2O2 pathway. *PLoS pathogens*, 6(7):e1000975.

Felgner, P. L., M. A. Kayala, A. Vigil, C. Burk, R. Nakajima-Sasaki, J. Pablo, D. M. Molina, S. Hirst, J. S. Chew, D. Wang, *et al.* (2009). A *Burkholderia pseudomallei* protein microarray reveals serodiagnostic and cross-reactive antigens. *Proceedings of the national academy of sciences*, 106(32):13499–13504.

Ferro, E. and L. Trabalzini (2013). The yeast two-hybrid and related methods as powerful tools to study plant cell signalling. *Plant molecular biology*, 83(4-5):287–301.

Fields, S. and O.-k. Song (1989). A novel genetic system to detect protein-protein interactions. *Nature*, 340:245–246.

Forsberg, Å., A.-M. Viitanen, M. Skurnik, and H. Wolf-Watz (1991). The surface-located YopN protein is involved in calcium signal transduction in *Yersinia pseudotuberculosis*. *Molecular microbiology*, 5(4):977–986.

Forsberg, A. and H. Wolf-Watz (1988). The virulence protein Yop5 of *Yersinia pseudotuberculosis* is regulated at transcriptional level by plasmid-plB1-encoded trans-acting elements controlled by temperature and calcium. *Molecular microbiology*, 2(1):121–133.

French, C. T., I. J. Toesca, T.-H. Wu, T. Teslaa, S. M. Beaty, W. Wong, M. Liu, I. Schröder, P.-Y. Chiou, M. A. Teitell, *et al.* (2011). Dissection of the *Burkholderia* intracellular life cycle using a photothermal nanoblade. *Proceedings of the national academy of sciences*, 108(29):12095–12100.

Frithz-Lindsten, E., R. Rosqvist, L. Johansson, and Å. Forsberg (1995). The chaperone-like protein YerA of *Yersinia pseudotuberculosis* stabilizes YopE in the cytoplasm but is dispensable for targeting to the secretion loci. *Molecular microbiology*, 16(4):635–647.

Galan, J. E. and R. Curtiss (1989). Cloning and molecular characterization of genes whose products allow *Salmonella* Typhimurium to penetrate tissue culture cells. *Proceedings of the national academy of sciences*, 86(16):6383–6387.

Galán, J. E., M. Lara-Tejero, T. C. Marlovits, and S. Wagner (2014). Bacterial type III secretion systems: specialized nanomachines for protein delivery into target cells. *Annual review of microbiology*, 68:415.

Galyov, E. E., P. J. Brett, and D. DeShazer (2010). Molecular insights into *Burkholderia pseudomallei* and *Burkholderia mallei* pathogenesis. *Annual review of microbiology*, 64:495–517.

Gee, J. E., C. J. Allender, A. Tuanyok, M. G. Elrod, and A. R. Hoffmaster (2014). *Burkholderia pseudomallei* type G in Western Hemisphere. *Emerging infectious diseases*, 20(4):682.

Gee, J. E., M. B. Glass, R. T. Novak, D. Gal, M. J. Mayo, A. G. Steigerwalt, P. P. Wilkins, and B. J. Currie (2008). Recovery of a *Burkholderia thailandensis*-like isolate from an Australian water source. *BMC microbiology*, 8(1):54.

Gemski, P., J. Lazere, T. Casey, and J. Wohlhieter (1980). Presence of a virulence-associated plasmid in *Yersinia pseudotuberculosis*. *Infection and immunity*, 28(3):1044–1047.

Ghebrehiwet, B., Y. Ji, A. Valentino, L. Pednekar, M. Ramadass, D. Habiel, R. R. Kew, K. H. Hosszu, D. K. Galanakis, U. Kishore, *et al.* (2014). Soluble gC1qR is an autocrine signal that induces B1R expression on endothelial cells. *The Journal of immunology*, 192(1):377–384.

Ghebrehiwet, B. and E. I. Peerschke (2004). cC1q-R (calreticulin) and gC1q-R/p33: ubiquitously expressed multi-ligand binding cellular proteins involved in inflammation and infection. *Molecular immunology*, 41(2):173–183.

Gietz, R. D. and R. A. Woods (2002). Transformation of yeast by lithium acetate/single-stranded carrier DNA/polyethylene glycol method. *Methods in enzymology*, 350:87–96.

Gilad, J., D. Schwartz, and Y. Amsalem (2007). Clinical features and laboratory diagnosis of infection with the potential bioterrorism agents *Burkholderia mallei* and *Burkholderia pseudomallei*. *International journal of biomedical science*, 3(3):144.

Glass, M. B., J. E. Gee, A. G. Steigerwalt, D. Cavuoti, T. Barton, R. D. Hardy, D. Godoy, B. G. Spratt, T. A. Clark, and P. P. Wilkins (2006a). Pneumonia and septicemia caused by *Burkholderia thailandensis* in the United States. *Journal of clinical microbiology*, 44(12):4601–4604.

Glass, M. B., A. G. Steigerwalt, J. G. Jordan, P. P. Wilkins, and J. E. Gee (2006b). *Burkholderia oklahomensis* sp. nov., a *Burkholderia pseudomallei*-like species formerly known as the Oklahoma strain of *Pseudomonas pseudomallei*. *International journal of systematic and evolutionary microbiology*, 56(9):2171–2176.

Gong, L., M. Cullinane, P. Treerat, G. Ramm, M. Prescott, B. Adler, J. D. Boyce, and R. J. Devenish (2011). The *Burkholderia pseudomallei* type III secretion

system and BopA are required for evasion of LC3-associated phagocytosis. *PLoS one*, 6(3):e17852.

Gong, L., S.-C. Lai, P. Treerat, M. Prescott, B. Adler, J. D. Boyce, and R. J. Devenish (2015). *Burkholderia pseudomallei* Type III Secretion System Cluster 3 ATPase BsaS, a Chemotherapeutic Target for Small-Molecule ATPase Inhibitors. *Infection and immunity*, 83(4):1276–1285.

Goodyear, A., H. Bielefeldt-Ohmann, H. Schweizer, and S. Dow (2012). Persistent gastric colonization with *Burkholderia pseudomallei* and dissemination from the gastrointestinal tract following mucosal inoculation of mice. *PLoS one*, 7(5):e37324.

Gophna, U., E. Z. Ron, and D. Graur (2003). Bacterial type III secretion systems are ancient and evolved by multiple horizontal-transfer events. *Gene*, 312:151–163.

Gu, L., S. Zhou, L. Zhu, C. Liang, and X. Chen (2015). Small-Molecule Inhibitors of the Type III Secretion System. *Molecules*, 20(9):17659–17674.

Gutierrez, M. G., T. L. Pfeffer, and J. M. Warawa (2015). Type 3 Secretion System cluster 3 is a critical virulence determinant for lung-specific melioidosis. *PLoS neglected tropical diseases*, 9(1):e3441.

Haque, A., K. Chu, A. Easton, M. P. Stevens, E. E. Galyov, T. Atkins, R. Titball, and G. J. Bancroft (2006). A Live Experimental Vaccine against *Burkholderia pseudomallei* Elicits CD4+ T Cell–Mediated Immunity, Priming T Cells Specific for 2 Type III Secretion System Proteins. *Journal of infectious diseases*, 194(9):1241–1248.

Haraga, A., T. E. West, M. J. Brittnacher, S. J. Skerrett, and S. I. Miller (2008). *Burkholderia thailandensis* as a model system for the study of the virulence-associated type III secretion system of *Burkholderia pseudomallei*. *Infection and immunity*, 76(11):5402–5411.

Harding, S. V., M. Sarkar-Tyson, S. J. Smither, T. P. Atkins, P. C. Oyston, K. A. Brown, Y. Liu, R. Wait, and R. W. Titball (2007). The identification of surface proteins of *Burkholderia pseudomallei*. *Vaccine*, 25(14):2664–2672.

Hardt, W.-D., L.-M. Chen, K. E. Schuebel, X. R. Bustelo, and J. E. Galán (1998). *S.* Typhimurium encodes an activator of Rho GTPases that induces membrane ruffling and nuclear responses in host cells. *Cell*, 93(5):815–826.

Hayward, R. D., R. J. Cain, E. J. McGhie, N. Phillips, M. J. Garner, and V. Koronakis (2005). Cholesterol binding by the bacterial type III translocon is essential for virulence effector delivery into mammalian cells. *Molecular microbiology*, 56(3):590–603.

Hayward, R. D. and V. Koronakis (1999). Direct nucleation and bundling of actin by the SipC protein of invasive *Salmonella*. *The EMBO journal*, 18(18):4926–4934.

Hebbar, N., C. Wang, and V. M. Rangnekar (2012). Mechanisms of apoptosis by the tumor suppressor Par-4. *Journal of cellular physiology*, 227(12):3715–3721.

Heeb, S., C. Blumer, and D. Haas (2002). Regulatory RNA as mediator in GacA/RsmA-dependent global control of exoproduct formation in *Pseudomonas fluorescens* CHA0. *Journal of bacteriology*, 184(4):1046–1056.

Heine, S. J., J. Diaz-McNair, F. J. Martinez-Becerra, S. P. Choudhari, J. D. Clements, W. L. Picking, and M. F. Pasetti (2013). Evaluation of immunogenicity and protective efficacy of orally delivered *Shigella* type III secretion system proteins IpaB and IpaD. *Vaccine*, 31(28):2919–2929.

Hemrajani, C., C. N. Berger, K. S. Robinson, O. Marchès, A. Mousnier, and G. Frankel (2010). NleH effectors interact with Bax inhibitor-1 to block apoptosis during enteropathogenic *Escherichia coli* infection. *Proceedings of the national academy of sciences*, 107(7):3129–3134.

Hmelo, L. R., B. R. Borlee, H. Almblad, M. E. Love, T. E. Randall, B. S. Tseng, C. Lin, Y. Irie, K. M. Storek, J. J. Yang, *et al.* (2015). Precision-engineering the *Pseudomonas aeruginosa* genome with two-step allelic exchange. *Nature protocols*, 10(11):1820–1841.

Holden, M. T., R. W. Titball, S. J. Peacock, A. M. Cerdeño-Tárraga, T. Atkins, L. C. Crossman, T. Pitt, C. Churcher, K. Mungall, S. D. Bentley, *et al.* (2004). Genomic plasticity of the causative agent of melioidosis, *Burkholderia pseudomallei*. *Proceedings of the national academy of sciences*, 101(39):14240–14245.

Hovis, K. M., S. Mojica, J. E. McDermott, L. Pedersen, C. Simhi, R. G. Rank, G. S. Myers, J. Ravel, R.-c. Hsia, and P. M. Bavoil (2013). Genus-optimized strategy for the identification of *Chlamydial* type III secretion substrates. *Pathogens and disease*, 69(3):213–222.

Iriarte, M., M.-P. Sory, A. Boland, A. P. Boyd, S. D. Mills, I. Lambermont, and G. R. Cornelis (1998). TyeA, a protein involved in control of Yop release and in translocation of *Yersinia* Yop effectors. *The EMBO journal*, 17(7):1907–1918.

James, P., J. Halladay, and E. A. Craig (1996). Genomic libraries and a host strain designed for highly efficient two-hybrid selection in yeast. *Genetics*, 144(4):1425–1436.

Jamison, W. P. and T. Hackstadt (2008). Induction of type III secretion by cell-free *Chlamydia trachomatis* elementary bodies. *Microbial pathogenesis*, 45(5):435–440.

Jarvis, K. G., J. A. Giron, A. E. Jerse, T. K. McDaniel, M. S. Donnenberg, and J. B. Kaper (1995). Enteropathogenic *Escherichia coli* contains a putative type III secretion system necessary for the export of proteins involved in attaching and effacing lesion formation. *Proceedings of the national academy of sciences*, 92(17):7996–8000.

Jitprasutwit, S., W. Thaewpia, V. Muangsombut, A. Lulitanond, C. Leelayuwat, G. Lertmemongkolchai, and S. Korbsrisate (2010). Effect of acidic pH on the invasion efficiency and the type III secretion system of *Burkholderia thailandensis*. *Journal of microbiology*, 48(4):526–532.

Johnson, S., P. Roversi, M. Espina, A. Olive, J. E. Deane, S. Birket, T. Field, W. D. Picking, A. J. Blocker, E. E. Galyov, *et al.* (2007). Self-chaperoning of the type III secretion system needle tip proteins IpaD and BipD. *Journal of biological chemistry*, 282(6):4035–4044.

Jones, A. L., T. J. Beveridge, and D. E. Woods (1996). Intracellular survival of *Burkholderia pseudomallei*. *Infection and immunity*, 64(3):782–790.

Jones, S., J. Ellis, P. Russell, K. Griffin, and P. Oyston (2002). Passive protection against *Burkholderia pseudomallei* infection in mice by monoclonal antibodies against capsular polysaccharide, lipopolysaccharide or proteins. *Journal of medical microbiology*, 51(12):1055–1062.

Kang, W.-T., K. M. Vellasamy, E.-G. Chua, and J. Vadivelu (2015). Functional characterizations of effector protein BipC, a type III secretion system protein, in *Burkholderia pseudomallei* pathogenesis. *Journal of infectious diseases*, 211(5):827–834.

Kayath, C. A., S. Hussey, K. Nagra, D. Philpott, A. Allaoui, *et al.* (2010). Escape of intracellular *Shigella* from autophagy requires binding to cholesterol through the type III effector, IcsB. *Microbes and infection*, 12(12):956–966.

Kespichayawattana, W., S. Rattanachetkul, T. Wanun, P. Utaisincharoen, and S. Sirisinha (2000). *Burkholderia pseudomallei* induces cell fusion and actin-associated membrane protrusion: a possible mechanism for cell-to-cell spreading. *Infection and immunity*, 68(9):5377–5384.

Khan, I., L. Wieler, F. Melzer, M. Elschner, G. Muhammad, S. Ali, L. Sprague, H. Neubauer, and M. Saqib (2013). Glanders in animals: a review on epidemiology, clinical presentation, diagnosis and countermeasures. *Transboundary and emerging diseases*, 60(3):204–221.

Kim, J. S., J. S. Eom, J. Im Jang, H. G. Kim, D. W. Seo, I.-S. Bang, S. H. Bang, I. S. Lee, and Y. K. Park (2011). Role of *Salmonella* pathogenicity island 1 protein IacP in *Salmonella enterica* serovar Typhimurium pathogenesis. *Infection and immunity*, 79(4):1440–1450.

Knight, M., A. Ruaux, H. Mikolajek, P. Erskine, R. Gill, S. Wood, M. Wood, and J. Cooper (2006). Crystallization and preliminary X-ray diffraction analysis of BipD, a virulence factor from *Burkholderia pseudomallei*. *Acta crystallographica section F: structural biology and crystallization communications*, 62(8):761–764.

Koegl, M. and P. Uetz (2007). Improving yeast two-hybrid screening systems. *Briefings in functional genomics & proteomics*, 6(4):302–312.

Kresse, A. U., F. Beltrametti, A. Müller, F. Ebel, and C. A. Guzmán (2000). Characterization of SepL of enterohemorrhagic *Escherichia coli*. *Journal of bacteriology*, 182(22):6490–6498.

Kubori, T. and J. E. Galán (2002). *Salmonella* type III secretion-associated protein InvE controls translocation of effector proteins into host cells. *Journal of bacteriology*, 184(17):4699–4708.

Kubori, T. and J. E. Galán (2003). Temporal regulation of *Salmonella* virulence effector function by proteasome-dependent protein degradation. *Cell*, 115(3):333–342.

Kubori, T., Y. Matsushima, D. Nakamura, J. Uralil, M. Lara-Tejero, A. Sukhan, J. E. Galán, and S.-I. Aizawa (1998). Supramolecular structure of

the *Salmonella* Typhimurium type III protein secretion system. *Science*, 280(5363):602–605.

Kubori, T., A. Sukhan, S.-I. Aizawa, and J. E. Galán (2000). Molecular characterization and assembly of the needle complex of the *Salmonella* Typhimurium type III protein secretion system. *Proceedings of the national academy of sciences*, 97(18):10225–10230.

Kurushima, J., A. Kuwae, and A. Abe (2012). The type III secreted protein BspR regulates the virulence genes in *Bordetella bronchiseptica*. *PloS one*, 7(6).

Lafont, F., G. T. Van Nhieu, K. Hanada, P. Sansonetti, and F. G. van der Goot (2002). Initial steps of *Shigella* infection depend on the cholesterol/sphingolipid raft-mediated CD44–IpaB interaction. *The EMBO journal*, 21(17):4449–4457.

Leakey, A. K., G. C. Ulett, and R. G. Hirst (1998). BALB/c and C57Bl/6 mice infected with virulent *Burkholderia pseudomallei* provide contrasting animal models for the acute and chronic forms of human melioidosis. *Microbial pathogenesis*, 24(5):269–275.

Lee, A. H.-Y., M. A. Middleton, D. S. Guttman, and D. Desveaux (2013). Phytopathogen type III effectors as probes of biological systems. *Microbial biotechnology*, 6(3):230–240.

Lee, S. F., M. Kelly, A. McAlister, S. N. Luck, E. L. Garcia, R. A. Hall, R. M. Robins-Browne, G. Frankel, and E. L. Hartland (2008). AC-terminal class I PDZ binding motif of EspI/NleA modulates the virulence of attaching and effacing *Escherichia coli* and *Citrobacter rodentium*. *Cellular microbiology*, 10(2):499–513.

Lee, S. H. and J. E. Galán (2003). InvB is a type III secretion-associated chaperone for the *Salmonella enterica* effector protein SopE. *Journal of bacteriology*, 185(24):7279–7284.

Lee, S. H. and J. E. Galán (2004). *Salmonella* type III secretion-associated chaperones confer secretion-pathway specificity. *Molecular microbiology*, 51(2):483–495.

Lee, V. T., S. K. Mazmanian, and O. Schneewind (2001). A program of *Yersinia enterocolitica* type III secretion reactions is activated by specific signals. *Journal of bacteriology*, 183(17):4970–4978.

Lee, Y. H., Y. Chen, X. Ouyang, and Y.-H. Gan (2010). Identification of tomato plant as a novel host model for *Burkholderia pseudomallei*. *BMC microbiology*, 10(1):28.

Lertpatanasuwan, N., K. Sermsri, A. Petkaseam, S. Trakulsomboon, V. Thamlikitkul, and Y. Suputtamongkol (1999). Arabinose-positive *Burkholderia pseudomallei* infection in humans: case report. *Clinical infectious diseases*, 28(4):927–928.

Liang, X., Y. C. Shin, R. E. Means, and J. U. Jung (2004). Inhibition of interferon-mediated antiviral activity by murine gammaherpesvirus 68 latency-associated M2 protein. *Journal of virology*, 78(22):12416–12427.

Liaunardy-Jopeace, A., C. E. Bryant, and N. J. Gay (2014). The COP II adaptor protein TMED7 is required to initiate and mediate the delivery of TLR4 to the plasma membrane. *Science signaling*, 7(336):ra70–ra70.

Limmathurotsakul, D., S. Wongratanacheewin, N. Teerawattanasook, G. Wongsuvan, S. Chaisuksant, P. Chetchotisakd, W. Chaowagul, N. P. Day, and S. J. Peacock (2010). Increasing incidence of human melioidosis in Northeast Thailand. *The American journal of tropical medicine and hygiene*, 82(6):1113–1117.

Logue, C.-A., I. R. Peak, and I. R. Beacham (2009). Facile construction of unmarked deletion mutants in *Burkholderia pseudomallei* using *sacB* counter-selection in sucrose-resistant and sucrose-sensitive isolates. *Journal of microbiological methods*, 76(3):320–323.

Lower, M. and G. Schneider (2009). Prediction of type III secretion signals in genomes of gram-negative bacteria. *PloS one*, 4(6):e5917.

Lührmann, A., C. V. Nogueira, K. L. Carey, and C. R. Roy (2010). Inhibition of pathogen-induced apoptosis by a *Coxiella burnetii* type IV effector protein. *Proceedings of the national academy of sciences*, 107(44):18997–19001.

Madan, R., R. Rastogi, S. Parashuraman, and A. Mukhopadhyay (2012). *Salmonella* acquires lysosome-associated membrane protein 1 (LAMP1) on phagosomes from Golgi via SipC protein-mediated recruitment of host Syntaxin6. *Journal of biological chemistry*, 287(8):5574–5587.

Madden, T. (2013). The BLAST Sequence Analysis Tool. In *The NCBI Handbook*, J. McEntyre and J. Ostell, eds., volume Aug 13, 2003, chapter 16. Bethesda (MD): National Center for Biotechnology Information (US): National Center for Biotechnology Information (US). Available from: http://www.ncbi.nlm.nih.gov/books/NBK21097/.

Maegraith, B. and C. Leithead (1964). Melioidosis: a case-report. *The Lancet*, 283(7338):862–863.

Maharjan, B., N. Chantratita, M. Vesaratchavest, A. Cheng, V. Wuthiekanun, W. Chierakul, W. Chaowagul, N. P. Day, and S. J. Peacock (2005). Recurrent melioidosis in patients in northeast Thailand is frequently due to reinfection rather than relapse. *Journal of clinical microbiology*, 43(12):6032–6034.

Marchés, O., S. Wiles, F. Dziva, R. M. La Ragione, S. Schüller, A. Best, A. D. Phillips, E. L. Hartland, M. J. Woodward, M. P. Stevens, *et al.* (2005). Characterization of two non-locus of enterocyte effacement-encoded type III-translocated effectors, NleC and NleD, in attaching and effacing pathogens. *Infection and immunity*, 73(12):8411–8417.

Markham, A. P., S. E. Birket, W. D. Picking, W. L. Picking, and C. R. Middaugh (2008). pH sensitivity of type III secretion system tip proteins. *Proteins: structure, function, and bioinformatics*, 71(4):1830–1842.

Marlovits, T. C., T. Kubori, A. Sukhan, D. R. Thomas, J. E. Galán, and V. M. Unger (2004). Structural insights into the assembly of the type III secretion needle complex. *Science*, 306(5698):1040–1042.

Martinez-Becerra, F. J., X. Chen, N. E. Dickenson, S. P. Choudhari, K. Harrison, J. D. Clements, W. D. Picking, L. L. Van De Verg, R. I. Walker, and W. L. Picking (2013). Characterization of a novel fusion protein from IpaB and IpaD of *Shigella* spp. and its potential as a pan-*Shigella* vaccine. *Infection and immunity*, 81(12):4470–4477.

Martinez-Becerra, F. J., J. M. Kissmann, J. Diaz-McNair, S. P. Choudhari, A. M. Quick, G. Mellado-Sanchez, J. D. Clements, M. F. Pasetti, and W. L. Picking (2012). Broadly protective *Shigella* vaccine based on type III secretion apparatus proteins. *Infection and immunity*, 80(3):1222–1231.

Maurelli, A., B. Baudry, H. d'Hauteville, T. Hale, and P. Sansonetti (1985). Cloning of plasmid DNA sequences involved in invasion of HeLa cells by *Shigella flexneri*. *Infection and immunity*, 49(1):164–171.

McCormick, J. B., R. E. Weaver, P. S. Hayes, J. M. Boyce, and R. A. Feldman (1977). Wound infection by an indigenous *Pseudomonas pseudomallei*-like organism isolated from the soil: case report and epidemiologic study. *Journal of infectious diseases*, 135(1):103–107.

McDermott, J. E., A. Corrigan, E. Peterson, C. Oehmen, G. Niemann, E. D. Cambronne, D. Sharp, J. N. Adkins, R. Samudrala, and F. Heffron (2011). Computational prediction of type III and IV secreted effectors in gram-negative bacteria. *Infection and immunity*, 79(1):23–32.

McGhie, E. J., R. D. Hayward, and V. Koronakis (2001). Cooperation between actin-binding proteins of invasive *Salmonella*: SipA potentiates SipC nucleation and bundling of actin. *The EMBO journal*, 20(9):2131–2139.

Memišević, V., N. Zavaljevski, R. Pieper, S. V. Rajagopala, K. Kwon, K. Townsend, C. Yu, X. Yu, D. DeShazer, J. Reifman, *et al.* (2013). Novel *Burkholderia mallei* virulence factors linked to specific host-pathogen protein interactions. *Molecular & cellular proteomics*, 12(11):3036–3051.

MengJie, H., A. C. Simon, C. H. Darren, H. Ivan, J. Esther, X. Yuekang, A. F. Mark, A. J. David, and A. B. Marie (2013). p32 protein levels are integral to mitochondrial and endoplasmic reticulum morphology, cell metabolism and survival. *Biochemical journal*, 453(3):381–391.

Miao, E. A., D. P. Mao, N. Yudkovsky, R. Bonneau, C. G. Lorang, S. E. Warren, I. A. Leaf, and A. Aderem (2010). Innate immune detection of the type III secretion apparatus through the NLRC4 inflammasome. *Proceedings of the national academy of sciences*, 107(7):3076–3080.

Michiels, T. and G. R. Cornelis (1991). Secretion of hybrid proteins by the *Yersinia* Yop export system. *Journal of bacteriology*, 173(5):1677–1685.

Milton, D. L., R. O'Toole, P. Horstedt, and H. Wolf-Watz (1996). Flagellin A is essential for the virulence of *Vibrio anguillarum*. *Journal of bacteriology*, 178(5):1310–1319.

Moerdyk-Schauwecker, M., D. DeStephanis, E. Hastie, and V. Z. Grdzelishvili (2011). Detecting protein–protein interactions in vesicular stomatitis virus using a cytoplasmic yeast two hybrid system. *Journal of virological methods*, 173(2):203–212.

Moore, R. A., S. Reckseidler-Zenteno, H. Kim, W. Nierman, Y. Yu, A. Tuanyok, J. Warawa, D. DeShazer, and D. E. Woods (2004). Contribution of gene loss to the pathogenic evolution of *Burkholderia pseudomallei* and *Burkholderia mallei*. *Infection and immunity*, 72(7):4172–4187.

Mounier, J., M. R. Popoff, J. Enninga, M. C. Frame, P. J. Sansonetti, and G. T. Van Nhieu (2009). The IpaC carboxyterminal effector domain mediates Src-dependent actin polymerization during *Shigella* invasion of epithelial cells. *PLoS pathogens*, 5(1):e1000271–e1000271.

Muangman, S., S. Korbsrisate, V. Muangsombut, V. Srinon, N. L. Adler, G. N. Schroeder, G. Frankel, and E. E. Galyov (2011). BopC is a type III secreted effector protein of *Burkholderia pseudomallei*. *FEMS microbiology letters*, 323(1):75–82.

Muangsombut, V., S. Suparak, P. Pumirat, S. Damnin, P. Vattanaviboon, V. Thongboonkerd, and S. Korbsrisate (2008). Inactivation of *Burkholderia pseudomallei bsaQ* results in decreased invasion efficiency and delayed escape of bacteria from endocytic vesicles. *Archives of microbiology*, 190(6):623–631.

Musson, J. A., C. J. Reynolds, D. Rinchai, A. Nithichanon, P. Khaenam, E. Favry, N. Spink, K. K. Chu, A. De Soyza, G. J. Bancroft, *et al.* (2014). CD4+ T cell epitopes of FliC conserved between strains of *Burkholderia*: implications for vaccines against melioidosis and cepacia complex in cystic fibrosis. *The Journal of immunology*, 193(12):6041–6049.

Myeni, S. K., L. Wang, and D. Zhou (2013). SipB-SipC complex is essential for translocon formation. *PloS one*, 8(3).

Myeni, S. K. and D. Zhou (2010). The C terminus of SipC binds and bundles F-actin to promote *Salmonella* invasion. *Journal of biological chemistry*, 285(18):13357–13363.

Neeld, D., Y. Jin, C. Bichsel, J. Jia, J. Guo, F. Bai, W. Wu, U.-H. Ha, N. Terada, and S. Jin (2014). *Pseudomonas aeruginosa* injects NDK into host cells through a type III secretion system. *Microbiology*, 160(Pt 7):1417–1426.

Ngauy, V., Y. Lemeshev, L. Sadkowski, and G. Crawford (2005). Cutaneous melioidosis in a man who was taken as a prisoner of war by the Japanese during World War II. *Journal of clinical microbiology*, 43(2):970–972.

Nougayrède, J.-P., M. Boury, C. Tasca, O. Marchès, A. Milon, E. Oswald, and J. De Rycke (2001). Type III Secretion-Dependent Cell Cycle Block Caused in HeLa Cells by Enteropathogenic *Escherichia coli* O103. *Infection and immunity*, 69(11):6785–6795.

Nussbaum, J. J., D. S. Hull, and M. J. Carter (1980). *Pseudomonas pseudomallei* in an Anophthalmic Orbit. *Archives of ophthalmology*, 98(7):1224–1225.

Okuda, J., A. Hanabusa, and N. Gotoh (2014). ExoS of *Pseudomonas aeruginosa* binds to a human KIF7 to induce cytotoxicity in cultured human bronchial epithelial cells. *Journal of infection and chemotherapy*, 20(2):121–127.

Olive, A. J., R. Kenjale, M. Espina, D. S. Moore, W. L. Picking, and W. D. Picking (2007). Bile salts stimulate recruitment of IpaB to the *Shigella flexneri* surface, where it colocalizes with IpaD at the tip of the type III secretion needle. *Infection and immunity*, 75(5):2626–2629.

Olsen, J. V., L. M. de Godoy, G. Li, B. Macek, P. Mortensen, R. Pesch, A. Makarov, O. Lange, S. Horning, and M. Mann (2005). Parts per million mass accuracy on an Orbitrap mass spectrometer via lock mass injection into a C-trap. *Molecular & cellular proteomics*, 4(12):2010–2021.

Ong, S.-E., B. Blagoev, I. Kratchmarova, D. B. Kristensen, H. Steen, A. Pandey, and M. Mann (2002). Stable isotope labeling by amino acids in cell culture, SILAC, as a simple and accurate approach to expression proteomics. *Molecular & cellular proteomics*, 1(5):376–386.

Ooi, W. F., C. Ong, T. Nandi, J. F. Kreisberg, H. H. Chua, G. Sun, Y. Chen, C. Mueller, L. Conejero, M. Eshaghi, *et al.* (2013). The condition-dependent transcriptional landscape of *Burkholderia pseudomallei*. *PLoS genetics*, 9(9):e1003795.

Osiecki, J. C., J. Barker, W. L. Picking, A. B. Serfis, E. Berring, S. Shah, A. Harrington, and W. D. Picking (2001). IpaC from Shigella and SipC from *Salmonella* possess similar biochemical properties but are functionally distinct. *Molecular microbiology*, 42(2):469–481.

Pal, M., P. Erskine, R. Gill, S. Wood, and J. Cooper (2010). Near-atomic resolution analysis of BipD, a component of the type III secretion system of *Burkholderia pseudomallei*. *Acta crystallographica section F: structural biology and crystallization communications*, 66(9):990–993.

Park, E. and L. E. Maquat (2013). Staufen-mediated mRNA decay. *Wiley interdisciplinary reviews: RNA*, 4(4):423–435.

Parsot, C. (2009). *Shigella* type III secretion effectors: how, where, when, for what purposes? *Current opinion in microbiology*, 12(1):110–116.

Parsot, C., R. Ménard, P. Gounon, and P. J. Sansonetti (1995). Enhanced secretion through the *Shigella flexneri* Mxi-Spa translocon leads to assembly of extracellular proteins into macromolecular structures. *Molecular microbiology*, 16(2):291–300.

Paul, K., M. Erhardt, T. Hirano, D. F. Blair, and K. T. Hughes (2008). Energy source of flagellar type III secretion. *Nature*, 451(7177):489–492.

Peacock, S. J. (2006). Melioidosis. *Current opinion in infectious diseases*, 19(5):421–428.

Pearson, T., P. Giffard, S. Beckstrom-Sternberg, R. Auerbach, H. Hornstra, A. Tuanyok, E. P. Price, M. B. Glass, B. Leadem, J. S. Beckstrom-Sternberg, *et al.* (2009). Phylogeographic reconstruction of a bacterial species with high levels of lateral gene transfer. *BMC biology*, 7(1):78.

Peerschke, E. I. and B. Ghebrehiwet (2007). The contribution of gC1qR/p33 in infection and inflammation. *Immunobiology*, 212(4):333–342.

Peerschke, E. I. and B. Ghebrehiwet (2014). cC1qR/CR and gC1qR/p33: Observations in cancer. *Molecular immunology*, 61(2):100–109.

Peerschke, E. I., T. K. Murphy, B. Ghebrehiwet, *et al.* (2003). Activation-dependent surface expression of gC1qR/p33 on human blood platelets. *Thrombosis haemostasis*, 89(2):331–339.

Pei, J. and N. V. Grishin (2009). The Rho GTPase inactivation domain in *Vibrio cholerae* MARTX toxin has a circularly permuted papain-like thiol protease fold. *Proteins: structure, function, and bioinformatics*, 77(2):413–419.

Penfold, R. J. and J. M. Pemberton (1992). An improved suicide vector for construction of chromosomal insertion mutations in bacteria. *Gene*, 118(1):145–146.

Persson, C., N. Carballeira, H. Wolf-Watz, and M. Fällman (1997). The PTPase YopH inhibits uptake of *Yersinia*, tyrosine phosphorylation of p130Cas and

FAK, and the associated accumulation of these proteins in peripheral focal adhesions. *The EMBO journal*, 16(9):2307–2318.

Picking, W. L., H. Nishioka, P. D. Hearn, M. A. Baxter, A. T. Harrington, A. Blocker, and W. D. Picking (2005). IpaD of *Shigella flexneri* is independently required for regulation of Ipa protein secretion and efficient insertion of IpaB and IpaC into host membranes. *Infection and immunity*, 73(3):1432–1440.

Pilatz, S., K. Breitbach, N. Hein, B. Fehlhaber, J. Schulze, B. Brenneke, L. Eberl, and I. Steinmetz (2006). Identification of *Burkholderia pseudomallei* genes required for the intracellular life cycle and *in vivo* virulence. *Infection and immunity*, 74(6):3576–3586.

Pitt, T. L., S. Trakulsomboon, and D. A. Dance (2007). Recurrent melioidosis: possible role of infection with multiple strains of *Burkholderia pseudomallei*. *Journal of clinical microbiology*, 45(2):680–681.

Pizarro-Cerda, J. and P. Cossart (2006). Bacterial adhesion and entry into host cells. *Cell*, 124(4):715–727.

Price, E. P., D. S. Sarovich, M. Mayo, A. Tuanyok, K. P. Drees, M. Kaestli, S. M. Beckstrom-Sternberg, J. S. Babic-Sternberg, T. J. Kidd, S. C. Bell, *et al.* (2013). Within-host evolution of *Burkholderia pseudomallei* over a twelve-year chronic carriage infection. *mBio*, 4(4):e00388–13.

Pruksachartvuthi, S., N. Aswapokee, and K. Thankerngpol (1990). Survival of *Pseudomonas pseudomallei* in human phagocytes. *Journal of medical microbiology*, 31(2):109–114.

Pumirat, P., J. Cuccui, R. A. Stabler, J. M. Stevens, V. Muangsombut, E. Singsuksawat, M. P. Stevens, B. W. Wren, and S. Korbsrisate (2010). Global transcriptional profiling of *Burkholderia pseudomallei* under salt stress reveals differential effects on the Bsa type III secretion system. *BMC microbiology*, 10(1):171.

Pumirat, P., P. Saetun, S. Sinchaikul, S.-T. Chen, S. Korbsrisate, and V. Thongboonkerd (2009). Altered secretome of *Burkholderia pseudomallei* induced by salt stress. *Biochimica et biophysica acta - proteins and proteomics*, 1794(6):898–904.

Pumirat, P., C. Vander Broek, N. Juntawieng, V. Muangsombut, P. Kiratisin, K. Pattanapanyasat, J. M. Stevens, M. P. Stevens, and S. Korbsrisate (2014).

Analysis of the prevalence, secretion and function of a cell cycle-inhibiting factor in the melioidosis pathogen *Burkholderia pseudomallei*. *PLoS ONE*, 9:e96298.

R Core Team (2015). *R: A Language and Environment for Statistical Computing*. R Foundation for Statistical Computing, Vienna, Austria.

Rabilloud, T. and C. Lelong (2011). Two-dimensional gel electrophoresis in proteomics: a tutorial. *Journal of proteomics*, 74(10):1829–1841.

Radics, J., L. Königsmaier, and T. C. Marlovits (2014). Structure of a pathogenic type 3 secretion system in action. *Nature structural & molecular biology*, 21(1):82–87.

Rainbow, L., C. A. Hart, and C. Winstanley (2002). Distribution of type III secretion gene clusters in *Burkholderia pseudomallei*, *B. thailandensis* and *B. mallei*. *Journal of medical microbiology*, 51(5):374–384.

Reckseidler, S. L., D. DeShazer, P. A. Sokol, and D. E. Woods (2001). Detection of bacterial virulence genes by subtractive hybridization: identification of capsular polysaccharide of *Burkholderia pseudomallei* as a major virulence determinant. *Infection and immunity*, 69(1):34–44.

Reckseidler-Zenteno, S. L., R. DeVinney, and D. E. Woods (2005). The capsular polysaccharide of *Burkholderia pseudomallei* contributes to survival in serum by reducing complement factor C3b deposition. *Infection and immunity*, 73(2):1106–1115.

Ried, J. L. and A. Collmer (1987). An *nptI-sacB-sacR* cartridge for constructing directed, unmarked mutations in gram-negative bacteria by marker exchange-eviction mutagenesis. *Gene*, 57(2):239–246.

Roehrich, A. D., E. Guillossou, A. J. Blocker, and I. Martinez-Argudo (2013). *Shigella* IpaD has a dual role: signal transduction from the type III secretion system needle tip and intracellular secretion regulation. *Molecular microbiology*, 87(3):690–706.

Rohmer, L., D. S. Guttman, and J. L. Dangl (2004). Diverse evolutionary mechanisms shape the type III effector virulence factor repertoire in the plant pathogen *Pseudomonas syringae*. *Genetics*, 167(3):1341–1360.

Rolim, D. B., D. C. F. L. Vilar, A. Q. Sousa, I. S. Miralles, D. C. A. de Oliveira, G. Harnett, L. O'Reilly, K. Howard, I. Sampson, and T. J. Inglis (2005). Melioidosis, northeastern Brazil. *Emerging infectious diseases*, 11(9).

Rosenshine, I., S. Ruschkowski, and B. B. Finlay (1994). Inhibitors of cytoskeletal function and signal transduction to study bacterial invasion. *Methods in enzymology*, 236:467.

Rossier, O., K. Wengelnik, K. Hahn, and U. Bonas (1999). The *Xanthomonas* Hrp type III system secretes proteins from plant and mammalian bacterial pathogens. *Proceedings of the national academy of sciences*, 96(16):9368–9373.

Rotz, L. D., A. S. Khan, S. R. Lillibridge, S. M. Ostroff, and J. M. Hughes (2002). Public health assessment of potential biological terrorism agents. *Emerging infectious diseases*, 8(2):225–230.

Roversi, P., S. Johnson, T. Field, J. E. Deane, E. E. Galyov, and S. M. Lea (2006). Expression, purification, crystallization and preliminary crystallographic analysis of BipD, a component of the *Burkholderia pseudomallei* type III secretion system. *Acta crystallographica section F: structural biology and crystallization communications*, 62(9):861–864.

Samudrala, R., F. Heffron, and J. E. McDermott (2009). Accurate prediction of secreted substrates and identification of a conserved putative secretion signal for type III secretion systems. *PLoS pathogens*, 5(4):e1000375.

Sarkar-Tyson, M., J. Thwaite, S. Harding, S. Smither, P. Oyston, T. Atkins, and R. Titball (2007). Polysaccharides and virulence of *Burkholderia pseudomallei*. *Journal of medical microbiology*, 56(8):1005–1010.

Sato, H., D. W. Frank, C. J. Hillard, J. B. Feix, R. R. Pankhaniya, K. Moriyama, V. Finck-Barbançon, A. Buchaklian, M. Lei, R. M. Long, *et al.* (2003). The mechanism of action of the *Pseudomonas aeruginosa*-encoded type III cytotoxin, ExoU. *The EMBO journal*, 22(12):2959–2969.

Schell, M. A., P. Zhao, and L. Wells (2011). Outer membrane proteome of *Burkholderia pseudomallei* and *Burkholderia mallei* from diverse growth conditions. *Journal of proteome research*, 10(5):2417–2424.

Schesser, K., E. Frithz-Lindsten, and H. Wolf-Watz (1996). Delineation and mutational analysis of the *Yersinia pseudotuberculosis* YopE domains which

mediate translocation across bacterial and eukaryotic cellular membranes. *Journal of bacteriology*, 178(24):7227–7233.

Schraidt, O. and T. C. Marlovits (2011). Three-dimensional model of *Salmonella's* needle complex at subnanometer resolution. *Science*, 331(6021):1192–1195.

Schumacher, J., C. J. Waite, M. H. Bennett, M. F. Perez, K. Shethi, and M. Buck (2014). Differential secretome analysis of *Pseudomonas syringae pv tomato* using gel-free MS proteomics. *Frontiers in plant science*, 5.

Schwarz, S., P. Singh, J. D. Robertson, M. LeRoux, S. J. Skerrett, D. R. Goodlett, T. E. West, and J. D. Mougous (2014). VgrG-5 is a *Burkholderia* type VI secretion system-exported protein required for multinucleated giant cell formation and virulence. *Infection and immunity*, 82(4):1445–1452.

Serebriiskii, I., J. Estojak, M. Berman, and E. A. Golemis (2000). Approaches to detecting false positives in yeast two-hybrid systems. *Biotechniques*, 28(2):328–337.

Shanks, J., M. N. Burtnick, P. J. Brett, D. M. Waag, K. B. Spurgers, W. J. Ribot, M. A. Schell, R. G. Panchal, F. C. Gherardini, K. D. Wilkinson, *et al.* (2009). *Burkholderia mallei tssM* encodes a putative deubiquitinase that is secreted and expressed inside infected RAW 264.7 murine macrophages. *Infection and immunity*, 77(4):1636–1648.

Sievers, F., A. Wilm, D. Dineen, T. J. Gibson, K. Karplus, W. Li, R. Lopez, H. McWilliam, M. Remmert, J. Söding, *et al.* (2011). Fast, scalable generation of high-quality protein multiple sequence alignments using Clustal Omega. *Molecular systems biology*, 7(1):539.

Sikora, A. E., R. A. Zielke, D. A. Lawrence, P. C. Andrews, and M. Sandkvist (2011). Proteomic analysis of the *Vibrio cholerae* type II secretome reveals new proteins, including three related serine proteases. *Journal of biological chemistry*, 286(19):16555–16566.

Sim, S. H., Y. Yu, C. H. Lin, R. Karuturi, V. Wuthiekanun, A. Tuanyok, H. H. Chua, C. Ong, S. S. Paramalingam, G. Tan, *et al.* (2008). The core and accessory genomes of *Burkholderia pseudomallei*: implications for human melioidosis. *PLoS pathogens*, 4(10):e1000178.

Smith, M., B. Angus, V. Wuthiekanun, and N. White (1997). Arabinose assimilation defines a nonvirulent biotype of *Burkholderia pseudomallei*. *Infection and immunity*, 65(10):4319–4321.

Sory, M.-P., A. Boland, I. Lambermont, and G. R. Cornelis (1995). Identification of the YopE and YopH domains required for secretion and internalization into the cytosol of macrophages, using the *cyaA* gene fusion approach. *Proceedings of the national academy of sciences*, 92(26):11998–12002.

Spring-Pearson, S. M., J. K. Stone, A. Doyle, C. J. Allender, R. T. Okinaka, M. Mayo, S. M. Broomall, J. M. Hill, M. A. Karavis, K. S. Hubbard, *et al.* (2015). Pangenome Analysis of *Burkholderia pseudomallei*: Genome Evolution Preserves Gene Order despite High Recombination Rates. *PloS one*, 10(10):e0140274.

Srinivasan, A., C. N. Kraus, D. DeShazer, P. M. Becker, J. D. Dick, L. Spacek, J. G. Bartlett, W. R. Byrne, and D. L. Thomas (2001). Glanders in a military research microbiologist. *New England journal of medicine*, 345(4):256–258.

Srinon, V., S. Muangman, N. Imyaem, V. Muangsombut, N. R. Lazar Adler, E. E. Galyov, and S. Korbsrisate (2013). Comparative assessment of the intracellular survival of the *Burkholderia pseudomallei bopC* mutant. *Journal of microbiology*, 51:522–526.

Stebbins, C. E. and J. E. Galán (2001). Maintenance of an unfolded polypeptide by a cognate chaperone in bacterial type III secretion. *Nature*, 414(6859):77–81.

Stensrud, K. F., P. R. Adam, C. D. La Mar, A. J. Olive, G. H. Lushington, R. Sudharsan, N. L. Shelton, R. S. Givens, W. L. Picking, and W. D. Picking (2008). Deoxycholate interacts with IpaD of *Shigella flexneri* in inducing the recruitment of IpaB to the type III secretion apparatus needle tip. *Journal of biological chemistry*, 283(27):18646–18654.

Stevens, M. P., A. Friebel, L. A. Taylor, M. W. Wood, P. J. Brown, W.-D. Hardt, and E. E. Galyov (2003). A *Burkholderia pseudomallei* type III secreted protein, BopE, facilitates bacterial invasion of epithelial cells and exhibits guanine nucleotide exchange factor activity. *Journal of bacteriology*, 185(16):4992–4996.

Stevens, M. P., A. Haque, T. Atkins, J. Hill, M. W. Wood, A. Easton, M. Nelson, C. Underwood-Fowler, R. W. Titball, G. J. Bancroft, *et al.* (2004). Attenuated

virulence and protective efficacy of a *Burkholderia pseudomallei bsa* type III secretion mutant in murine models of melioidosis. *Microbiology*, 150(8):2669–2676.

Stevens, M. P., J. M. Stevens, R. L. Jeng, L. A. Taylor, M. W. Wood, P. Hawes, P. Monaghan, M. D. Welch, and E. E. Galyov (2005). Identification of a bacterial factor required for actin-based motility of *Burkholderia pseudomallei*. *Molecular microbiology*, 56(1):40–53.

Stevens, M. P., M. W. Wood, L. A. Taylor, P. Monaghan, P. Hawes, P. W. Jones, T. S. Wallis, and E. E. Galyov (2002). An Inv/Mxi-Spa-like type III protein secretion system in *Burkholderia pseudomallei* modulates intracellular behaviour of the pathogen. *Molecular microbiology*, 46(3):649–659.

Su, Y.-C., K.-L. Wan, R. Mohamed, and S. Nathan (2008). A genome level survey of *Burkholderia pseudomallei* immunome expressed during human infection. *Microbes and infection*, 10(12):1335–1345.

Sun, G. W., Y. Chen, Y. Liu, G.-Y. G. Tan, C. Ong, P. Tan, and Y.-H. Gan (2010). Identification of a regulatory cascade controlling Type III Secretion System 3 gene expression in *Burkholderia pseudomallei*. *Molecular microbiology*, 76(3):677–689.

Sun, G. W. and Y.-H. Gan (2010). Unravelling type III secretion systems in the highly versatile *Burkholderia pseudomallei*. *Trends in microbiology*, 18(12):561–568.

Sun, G. W., J. Lu, S. Pervaiz, W. P. Cao, and Y.-H. Gan (2005). Caspase-1 dependent macrophage death induced by *Burkholderia pseudomallei*. *Cellular microbiology*, 7(10):1447–1458.

Suparak, S., W. Kespichayawattana, A. Haque, A. Easton, S. Damnin, G. Lertmemongkolchai, G. J. Bancroft, and S. Korbsrisate (2005). Multinucleated giant cell formation and apoptosis in infected host cells is mediated by *Burkholderia pseudomallei* type III secretion protein BipB. *Journal of bacteriology*, 187(18):6556–6560.

Tan, K. S., Y. Chen, Y.-C. Lim, G.-Y. G. Tan, Y. Liu, Y.-T. Lim, P. MacAry, and Y.-H. Gan (2010). Suppression of host innate immune response by *Burkholderia pseudomallei* through the virulence factor TssM. *The Journal of immunology*, 184(9):5160–5171.

Teh, B. E., C. T. French, Y. Chen, I. G. J. Chen, T.-H. Wu, E. Sagullo, P.-Y. Chiou, M. A. Teitell, J. F. Miller, and Y.-H. Gan (2014). Type three secretion system-mediated escape of *Burkholderia pseudomallei* into the host cytosol is critical for the activation of NFκB. *BMC microbiology*, 14(1):115.

Terry, C. M., W. L. Picking, S. E. Birket, K. Flentie, B. M. Hoffman, J. R. Barker, and W. D. Picking (2008). The C-terminus of IpaC is required for effector activities related to *Shigella* invasion of host cells. *Microbial pathogenesis*, 45(4):282–289.

Tippayawat, P., M. Pinsiri, D. Rinchai, D. Riyapa, A. Romphruk, Y.-H. Gan, R. L. Houghton, P. L. Felgner, R. W. Titball, M. P. Stevens, *et al.* (2011). *Burkholderia pseudomallei* proteins presented by monocyte-derived dendritic cells stimulate human memory T cells *in vitro*. *Infection and immunity*, 79(1):305–313.

Titball, R. W., P. Russell, J. Cuccui, A. Easton, A. Haque, T. Atkins, M. Sarkar-Tyson, V. Harley, B. Wren, and G. J. Bancroft (2008). *Burkholderia pseudomallei*: animal models of infection. *Transactions of the royal society of tropical medicine and hygiene*, 102:S111–S116.

Toesca, I. J., C. T. French, and J. F. Miller (2014). The Type VI secretion system spike protein VgrG5 mediates membrane fusion during intercellular spread by *pseudomallei* group *Burkholderia* species. *Infection and immunity*, 82(4):1436–1444.

Traven, A., B. Jelicic, and M. Sopta (2006). Yeast Gal4: a transcriptional paradigm revisited. *EMBO reports*, 7(5):496–499.

Tuanyok, A., B. R. Leadem, R. K. Auerbach, S. M. Beckstrom-Sternberg, J. S. Beckstrom-Sternberg, M. Mayo, V. Wuthiekanun, T. S. Brettin, W. C. Nierman, S. J. Peacock, *et al.* (2008). Genomic islands from five strains of *Burkholderia pseudomallei*. *BMC genomics*, 9(1):566.

Tuanyok, A., M. Tom, J. Dunbar, and D. E. Woods (2006). Genome-wide expression analysis of *Burkholderia pseudomallei* infection in a hamster model of acute melioidosis. *Infection and immunity*, 74(10):5465–5476.

Upadhyay, A., H. Wu, C. Williams, T. Field, E. Galyov, J. van den Elsen, and S. Bagby (2008). The guanine-nucleotide-exchange factor BopE from *Burkholderia pseudomallei* adopts a compact version of the *Salmonella*

SopE/SopE2 fold and undergoes a closed-to-open conformational change upon interaction with Cdc42. *Biochemical journal*, 411:485–493.

Utaisincharoen, P., S. Arjcharoen, K. Limposuwan, S. Tungpradabkul, and S. Sirisinha (2006). *Burkholderia pseudomallei* RpoS regulates multinucleated giant cell formation and inducible nitric oxide synthase expression in mouse macrophage cell line (RAW 264.7). *Microbial pathogenesis*, 40(4):184–189.

Van Nhieu, G. T., E. Caron, A. Hall, and P. J. Sansonetti (1999). IpaC induces actin polymerization and filopodia formation during *Shigella* entry into epithelial cells. *The EMBO journal*, 18(12):3249–3262.

Van Zandt, K. E., M. T. Greer, and H. C. Gelhaus (2013). Glanders: an overview of infection in humans. *Orphanet journal of rare diseases*, 8:131.

Vander Broek, C. W., K. J. Chalmers, M. P. Stevens, and J. M. Stevens (2015). Quantitative Proteomic Analysis of *Burkholderia pseudomallei* Bsa Type III Secretion System Effectors Using Hypersecreting Mutants. *Molecular & cellular proteomics*, 14(4):905–916.

Vesaratchavest, M., S. Tumapa, N. P. Day, V. Wuthiekanun, W. Chierakul, M. T. Holden, N. J. White, B. J. Currie, B. G. Spratt, E. J. Feil, *et al.* (2006). Nonrandom distribution of *Burkholderia pseudomallei* clones in relation to geographical location and virulence. *Journal of clinical microbiology*, 44(7):2553–2557.

Vidyalakshmi, K., B. Shrikala, B. Bharathi, U. Suchitra, *et al.* (2007). Melioidosis: An under-diagnosed entity in western coastal India: A clinicomicrobiological analysis. *Indian journal of medical microbiology*, 25(3):245.

Vikis, H. G. and K.-L. Guan (2004). Glutathione-S-transferase-fusion based assays for studying protein-protein interactions. In *Protein-protein interactions*, Pp. 175–186. Springer.

Viswanathan, V., S. Lukic, A. Koutsouris, R. Miao, M. M. Muza, and G. Hecht (2004). Cytokeratin 18 interacts with the enteropathogenic *Escherichia coli* secreted protein F (EspF) and is redistributed after infection. *Cellular microbiology*, 6(10):987–997.

Waggoner, S. N., M. W. Cruise, R. Kassel, and Y. S. Hahn (2005). gC1q receptor ligation selectively down-regulates human IL-12 production through activation of the phosphoinositide 3-kinase pathway. *The Journal of immunology*, 175(7):4706–4714.

Wagner, S., L. Königsmaier, M. Lara-Tejero, M. Lefebre, T. C. Marlovits, and J. E. Galán (2010). Organization and coordinated assembly of the type III secretion export apparatus. *Proceedings of the national academy of sciences*, 107(41):17745–17750.

Wand, M. E., C. M. Müller, R. W. Titball, and S. L. Michell (2011). Macrophage and *Galleria mellonella* infection models reflect the virulence of naturally occurring isolates of *B. pseudomallei*, *B. thailandensis* and *B. oklahomensis*. *BMC microbiology*, 11(1):11.

Wang, F., Z. Jiang, Y. Li, X. He, J. Zhao, X. Yang, L. Zhu, Z. Yin, X. Li, X. Wang, *et al.* (2013). *Shigella flexneri* T3SS effector IpaH4. 5 modulates the host inflammatory response via interaction with NF-κB p65 protein. *Cellular microbiology*, 15(3):474–485.

Wang, Y., A. N. Ouellette, C. W. Egan, T. Rathinavelan, W. Im, and R. N. De Guzman (2007). Differences in the electrostatic surfaces of the type III secretion needle proteins PrgI, BsaL, and MxiH. *Journal of molecular biology*, 371(5):1304–1314.

Wang, Y., Y. Yang, S. Wu, S. Pan, C. Zhou, Y. Ma, Y. Ru, S. Dong, B. He, C. Zhang, *et al.* (2014). p32 Is a Novel Target for Viral Protein ICP34. 5 of Herpes Simplex Virus Type 1 and Facilitates Viral Nuclear Egress. *Journal of biological chemistry*, 289(52):35795–35805.

Wang, Y., Q. Zhang, M.-a. Sun, and D. Guo (2011). High-accuracy prediction of bacterial type III secreted effectors based on position-specific amino acid composition profiles. *Bioinformatics*, 27(6):777–784.

Warawa, J. and D. E. Woods (2005). Type III secretion system cluster 3 is required for maximal virulence of *Burkholderia pseudomallei* in a hamster infection model. *FEMS microbiology letters*, 242(1):101–108.

Warawa, J. M. (2010). Evaluation of surrogate animal models of melioidosis. *Frontiers in microbiology*, 1:141.

Warren, S. M. and G. M. Young (2005). An amino-terminal secretion signal is required for YplA export by the Ysa, Ysc, and flagellar type III secretion systems of *Yersinia enterocolitica* biovar 1B. *Journal of bacteriology*, 187(17):6075–6083.

Wasinger, V. C., M. Zeng, and Y. Yau (2013). Current status and advances in quantitative proteomic mass spectrometry. *International journal of proteomics*, 2013.

Waugh, D. S. (2005). Making the most of affinity tags. *Trends in biotechnology*, 23(6):316–320.

Whitlock, G. C., A. Deeraksa, O. Qazi, B. M. Judy, K. Taylor, K. L. Propst, A. J. Duffy, K. Johnson, G. B. Kitto, K. A. Brown, *et al.* (2010). Protective response to subunit vaccination against intranasal *Burkholderia mallei* and *B. pseudomallei* challenge. *Procedia in vaccinology*, 2(1):73–77.

Whitlock, G. C., D. M. Estes, G. M. Young, B. Young, and A. G. Torres (2008). Construction of a reporter system to study *Burkholderia mallei* type III secretion and identification of the BopA effector protein function in intracellular survival. *Transactions of the royal society of tropical medicine and hygiene*, 102(Supplement 1):S127–S133.

Whitlock, G. C., G. A. Valbuena, V. L. Popov, B. M. Judy, D. M. Estes, and A. G. Torres (2009). *Burkholderia mallei* cellular interactions in a respiratory cell model. *Journal of medical microbiology*, 58(5):554–562.

Whitmore, A. (1913). An account of a glanders-like disease occurring in Rangoon. *Journal of hygiene*, 13(01):1–34.

Wiersinga, W. J., B. J. Currie, and S. J. Peacock (2012). Melioidosis. *New England journal of medicine*, 367(11):1035–1044.

Wiersinga, W. J., T. Van der Poll, N. J. White, N. P. Day, and S. J. Peacock (2006). Melioidosis: insights into the pathogenicity of *Burkholderia pseudomallei*. *Nature reviews microbiology*, 4(4):272–282.

Wiese, S., K. A. Reidegeld, H. E. Meyer, and B. Warscheid (2007). Protein labeling by iTRAQ: a new tool for quantitative mass spectrometry in proteome research. *Proteomics*, 7(3):340–350.

Wilharm, G., V. Lehmann, K. Krauss, B. Lehnert, S. Richter, K. Ruckdeschel, J. Heesemann, and K. Trülzsch (2004). *Yersinia enterocolitica* type III secretion depends on the proton motive force but not on the flagellar motor components MotA and MotB. *Infection and immunity*, 72(7):4004–4009.

Williamson, E. (2009). Plague. *Vaccine*, 27:D56–D60.

Williamson, M. P. and M. J. Sutcliffe (2010). Experimental Approaches to Protein–Protein Interactions. *Biochemical society transactions*, 38(part 4):875–878.

Winstanley, C., B. Hales, and C. Hart (1999). Evidence for the presence in *Burkholderia pseudomallei* of a type III secretion system-associated gene cluster. *Journal of medical microbiology*, 48(7):649–656.

Wong, A. R., J. S. Pearson, M. D. Bright, D. Munera, K. S. Robinson, S. F. Lee, G. Frankel, and E. L. Hartland (2011). Enteropathogenic and enterohaemorrhagic *Escherichia coli*: even more subversive elements. *Molecular microbiology*, 80(6):1420–1438.

Wong, K., S. Puthucheary, and J. Vadivelu (1995). The histopathology of human melioidosis. *Histopathology*, 26(1):51–55.

Wuthiekanun, V., M. Smith, D. Dance, A. L. Walsh, T. Pitt, and N. White (1996). Biochemical characteristics of clinical and environmental isolates of *Burkholderia pseudomallei*. *Journal of medical microbiology*, 45(6):408–412.

Xu, L., N. Xiao, F. Liu, H. Ren, and J. Gu (2009). Inhibition of RIG-I and MDA5-dependent antiviral response by gC1qR at mitochondria. *Proceedings of the national academy of sciences*, 106(5):1530–1535.

Yabuuchi, E., Y. Kosako, H. Oyaizu, I. Yano, H. Hotta, Y. Hashimoto, T. Ezaki, and M. Arakawa (1992). Proposal of *Burkholderia* gen. nov. and transfer of seven species of the genus *Pseudomonas* homology group II to the new genus, with the type species *Burkholderia cepacia* (Palleroni and Holmes 1981) comb. nov. *Microbiology and immunology*, 36(12):1251–1275.

Yagi, M., T. Uchiumi, S. Takazaki, B. Okuno, M. Nomura, S.-i. Yoshida, T. Kanki, and D. Kang (2012). p32/gC1qR is indispensable for fetal development and mitochondrial translation: importance of its RNA-binding ability. *Nucleic acids research*, 40(19):9717–9737.

Yang, Y., J. Zhao, R. L. Morgan, W. Ma, and T. Jiang (2010). Computational prediction of type III secreted proteins from gram-negative bacteria. *BMC bioinformatics*, 11(Suppl 1):S47.

Yao, Z. Q., A. Eisen-Vandervelde, S. Ray, and Y. S. Hahn (2003). HCV core/gC1qR interaction arrests T cell cycle progression through stabilization of the cell cycle inhibitor p27 kip1. *Virology*, 314(1):271–282.

Yao, Z. Q., S. N. Waggoner, M. W. Cruise, C. Hall, X. Xie, D. W. Oldach, and Y. S. Hahn (2005). SOCS1 and SOCS3 are targeted by hepatitis C virus core/gC1qR ligation to inhibit T-cell function. *Journal of virology*, 79(24):15417–15429.

Yingst, S. L., P. Facemire, L. Chuvala, D. Norwood, M. Wolcott, and D. A. Alves (2014). Pathological findings and diagnostic implications of a rhesus macaque (Macaca mulatta) model of aerosol-exposure melioidosis (*Burkholderia pseudomallei*). *Journal of medical microbiology*, 63(1):118–128.

Young, B. M. and G. M. Young (2002). YplA is exported by the Ysc, Ysa, and flagellar type III secretion systems of *Yersinia enterocolitica*. *Journal of bacteriology*, 184(5):1324–1334.

Young, G. M., D. H. Schmiel, and V. L. Miller (1999). A new pathway for the secretion of virulence factors by bacteria: the flagellar export apparatus functions as a protein-secretion system. *Proceedings of the national academy of sciences*, 96(11):6456–6461.

Yu, Y., H. S. Kim, H. H. Chua, C. H. Lin, S. H. Sim, D. Lin, A. Derr, R. Engels, D. DeShazer, B. Birren, *et al.* (2006). Genomic patterns of pathogen evolution revealed by comparison of *Burkholderia pseudomallei*, the causative agent of melioidosis, to avirulent *Burkholderia thailandensis*. *BMC microbiology*, 6(1):46.

Zahrl, D., M. Wagner, K. Bischof, M. Bayer, B. Zavecz, A. Beranek, C. Ruckenstuhl, G. E. Zarfel, and G. Koraimann (2005). Peptidoglycan degradation by specialized lytic transglycosylases associated with type III and type IV secretion systems. *Microbiology*, 151(11):3455–3467.

Zarivach, R., W. Deng, M. Vuckovic, H. B. Felise, H. V. Nguyen, S. I. Miller, B. B. Finlay, and N. C. Strynadka (2008). Structural analysis of the essential self-cleaving type III secretion proteins EscU and SpaS. *Nature*, 453(7191):124–127.

Zhang, L., Y. Wang, W. L. Picking, W. D. Picking, and R. N. De Guzman (2006). Solution structure of monomeric BsaL, the type III secretion needle protein of *Burkholderia pseudomallei*. *Journal of molecular biology*, 359(2):322–330.

Zhao, Y., J. Yang, J. Shi, Y.-N. Gong, Q. Lu, H. Xu, L. Liu, and F. Shao (2011). The NLRC4 inflammasome receptors for bacterial flagellin and type III secretion apparatus. *Nature*, 477(7366):596–600.

Chapter 7

Supplemental

7.1 *Galleria mellonella* Infections

The *Galleria mellonella* (Wax moth) larvae infection model was investigated for its ability to detect differences in virulence between WT *B. pseudomallei* and *bsa* T3SS mutants. *G. mellonella* larvae were sourced fresh from the supplier (Live-food UK Ltd., Somerset, UK) and were stored at 15°C for no more than 1 week before use. *B. pseudomallei* 10276, 10276 *bsaZ::*pDM4, 10276 *bipD::*pDM4 and 10276 *bopE::*pDM4 were grown overnight in 10 ml of LB containing the appropriate antibiotics at 37°C with agitation. The cultures were then centrifuged at 4,000 RPM for 10 minutes and the supernatant was removed, replaced with PBS and the OD_{600} was adjusted to 0.5. Groups of 10 *G. mellonella* larvae were injected with 10 μl of either PBS or $2x10^2$ CFU *B. pseudomallei*. The larvae were incubated at 37°C for 50 hours and checked periodically for death. GraphPad Prism software was used to graph and analyse the data using a Log-rank (Mantel-Cox) test.

All *bsa* T3SS mutants show a significantly delayed time to death when compared to WT *B. pseudomallei* (Figure 7.1). Surprisingly, the *bipD* mutant shows a larger attenuation in virulence than the *bsaZ* structural mutant. This study indicates the *G. mellonella* larvae infection model is sensitive enough to assess other *bsa* T3SS mutants in the future, though with only two repeats, more work will need to be done to confirm this in the future.

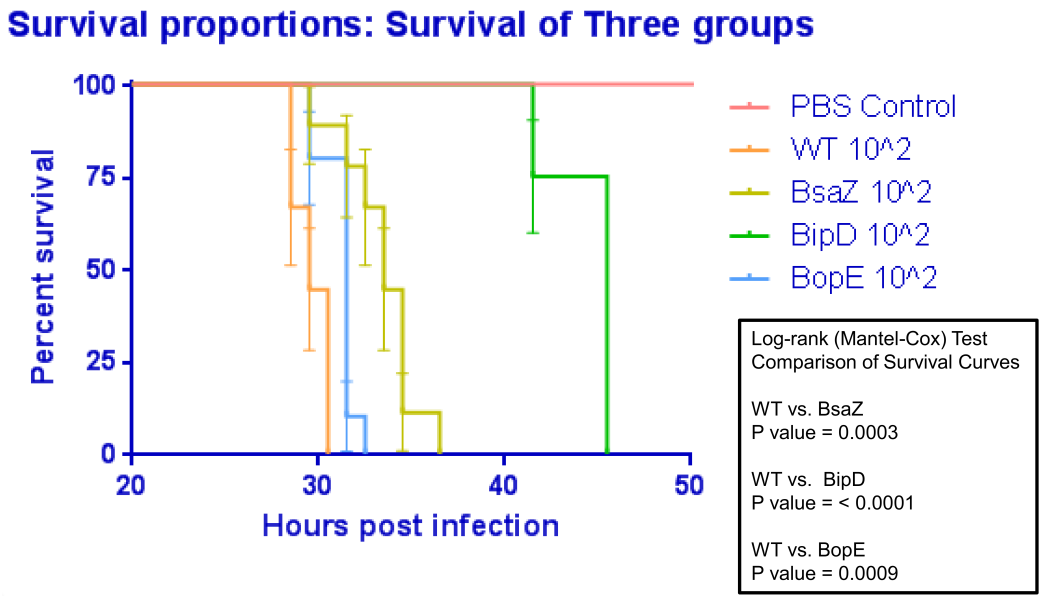


Figure 7.1: Infection of *Galleria mellonella* larvae using *B. pseudomallei* and *bsa* T3SS mutants. *B. pseudomallei* 10276, 10276 *bsaZ*::pDM4, 10276 *bipD*::pDM4 and 10276 *bopE*::pDM4 were injected into *G. mellonella* larvae with a dose of $2x10^2$ CFU. The larvae were incubated at 37°C for 50 hours and checked periodically for death. GraphPad Prism software was used to graph and analyse the data using a Log-rank (Mantel-Cox) test.

7.2 Y2H Colony PCRs

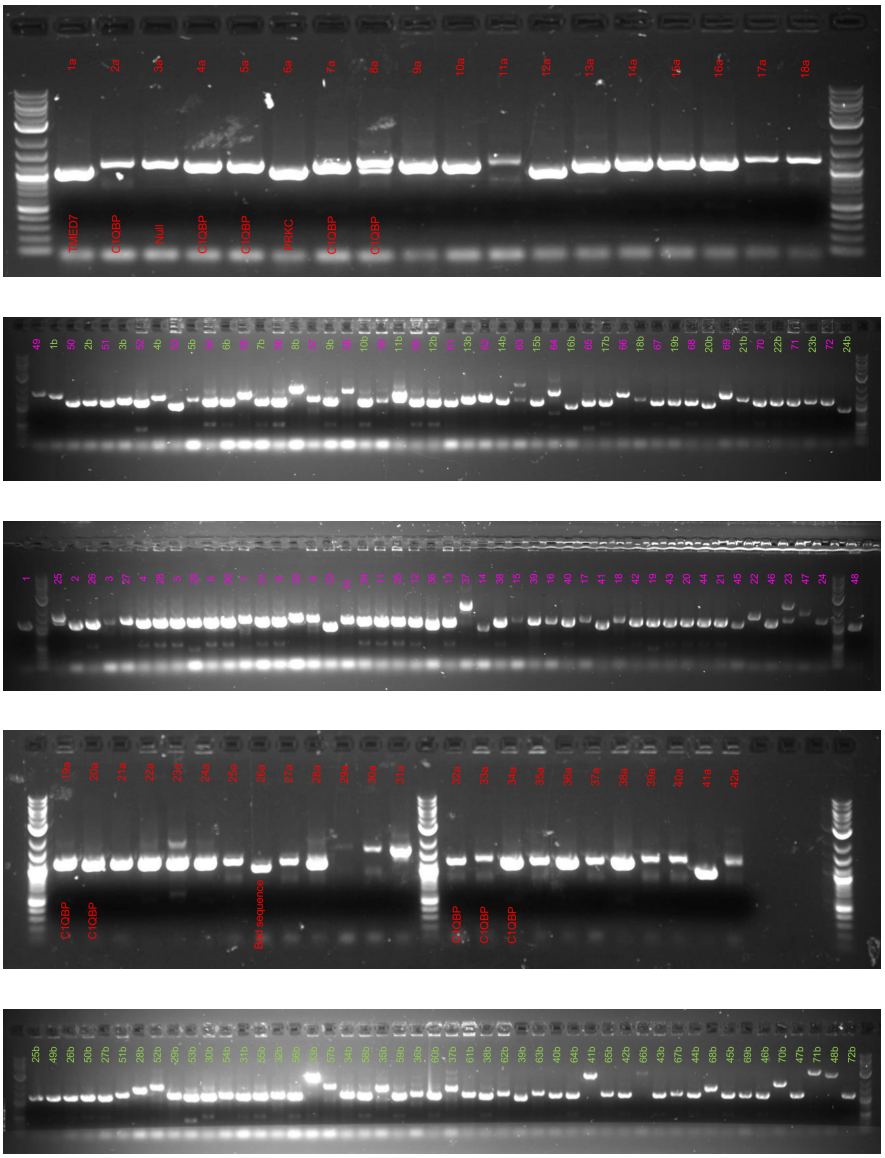


Figure 7.2: Colony PCR screen of *S. cerevisiae* containing pGBKT7-BipC after mating (gels 1-5).

7.3 Strains, Plasmids, Primers and Antibodies

Table 7.1: Strains and plasmids used in this study.

Strain or Plasmid	Characteristics	Source
***E. coli* Strains**		
XL1-Blue	Tet^r	Agilent
JM109		Life Technologies
One Shot TOP10		Life Technologies
One Shot TOP10 PIR1	Pir^+	Life Technologies
S17-1 λpir	Pir^+	Life Technologies
Rosetta BL21	Cm^r	Novagen
***B. pseudomallei* Strains**		
10276 WT	Isolated from a clinical infection. Cm^s, Kan^r	(Maegraith and Leithead, 1964)
10276 *bsaZ*::pDM4	10276 with an insertion in *bsaZ*, Cm^r, Kan^r	(Stevens *et al.*, 2002)
10276 *bipD*::pDM4	10276 with an insertion in *bipD*, Cm^r, Kan^r	(Stevens *et al.*, 2002)
10276 *bopE*::pDM4	10276 with an insertion in *bopE*, Cm^r, Kan^r	(Stevens *et al.*, 2002)

Continued on Next Page

Continuation of Table 7.1

Strain or Plasmid	Characteristics	Source
10276Δ*bsaP*	10276 with a 1,098-bp deletion in *bsaP*, Cm^s, Kan^r	This Study
***Salmonella* and Pathogenic *E. coli* Strains**		
Shigella flexneri 1016167	*S. flexneri* strain containing a functional Mxi-Spa T3SS	Mark Stevens
Enteropathogenic *E. coli* (EPEC) O127:H6 E2348/69	Prototype EPEC strain containing the locus of enterocyte effacement (LEE) encoded T3SS	(Marchés *et al.*, 2005)
EPEC O127:H6 E2348/69 Δ*escN*	(EPEC) O127:H6 strain E2348/69 containing a deletion in the ATPase of the LEE encoded T3SS	(Marchés *et al.*, 2005)
***S. cerevisiae* Strains**		
AH109	*MATa*, Ade^-, His^-, Leu^-, Trp^-	Clontech
Y187	*MAT*α, Ade^-, His^-, Leu^-, Trp^-	Clontech
Plasmids		
pGEM-T	Cloning vector, Amp^r	Promega
pGEM-T-Δ*bsaP*	pGEM-T containing a 1,115-bp fragment generated by joining *bsaP*-del-1/*bsaP*-del-2 and *bsaP*-del-3/*bsaP*-del-4 with PCR-ligation-PCR	This Study
pBHR1	Mobilisable expression vector, Cm^r, Kan^r	MoBiTec

Continued on Next Page

Continuation of Table 7.1

Strain or Plasmid	Characteristics	Source
pBHR1-bsaP	pBHR1 containing the full coding region of *bsaP*	This Study
pBHRT	pBHR1derivative where Cm^r has been replaced with Tet^r	This Study
pBHRT-bopE-myc	pBHRT containing the full coding region of *bopE* with an in-frame C-terminal c-Myc tag	This Study
pDM4	Suicide vector, R6Kγ origin, *sacBR*, Cm^r	(Milton *et al.*, 1996)
pDM4-Δ*bsaP*	pDM4 containing a 1,115-bp fragment generated by joining *bsaP1*/*bsaP2* and *bsaP3*/*bsaP4* with PCR-ligation-PCR	This Study
pME6032	IPTG inducible expression vector, Tet^r	(Heeb *et al.*, 2002)
pME6032-bopE-myc	pME6032 containing the full coding region of *bopE* with an in-frame C-terminal c-Myc tag	This Study
pME6032-BPSS0860-myc	pME6032 containing the full coding region of BPSS0860 with an in-frame C-terminal c-Myc tag	This Study
pME6032-bapA-myc	pME6032 containing the full coding region of *bapA* with an in-frame C-terminal c-Myc tag	This Study
pME6032-BPSS1512-myc	pME6032 containing the full coding region of BPSS1512 with an in-frame C-terminal c-Myc tag	This Study

Continued on Next Page

Continuation of Table 7.1

Strain or Plasmid	**Characteristics**	**Source**
pME6032-bopA-myc	pME6032 containing the full coding region of *bopA* with an in-frame C-terminal c-Myc tag	This Study
pME6032-bprD-myc	pME6032 containing the full coding region of *bprD* with an in-frame C-terminal c-Myc tag	This Study
pME6032-BPSS1916-myc	pME6032 containing the full coding region of BPSS1916 with an in-frame C-terminal c-Myc tag	This Study
pGEX-4T-1	In-frame N-terminal GST tag, Amp^r	GE Healthcare
pGEX-4T-1-$bimA_{48-384}$	pGEX-4T-1 containing *bimA* amino acids 48-384 (lacking the N-terminal secretion signal and the C-terminal membrane anchor) with an in-frame N-terminal GST tag	(Stevens *et al.*, 2005)
pGEX-4T-1-sipC	pGEX-4T-1 containing the full coding region of *sipC* with an in-frame N-terminal GST tag	This Study
pGEX-4T-1-bipC	pGEX-4T-1 containing the full coding region of *bipC* with an in-frame N-terminal GST tag	This Study, Junsoo Kim
pGEX-4T-1-bopA	pGEX-4T-1 containing the full coding region of *bopA* with an in-frame N-terminal GST tag	This Study, Stefanie Küchler
pGEX-4T-1-$bopE_{78-261}$	pGEX-4T-1 containing *bopE* amino acids 78-261 (lacking the N-terminal secretion signal) with an in-frame N-terminal GST tag, Amp^r	(Stevens *et al.*, 2003)

Continued on Next Page

Continuation of Table 7.1

Strain or Plasmid	Characteristics	Source
pEGFP-1	Mammalian expression vector encoding enhanced green fluorescence protein (EGFP)	Clontech
pRK5-myc	Mammalian expression vector encoding an in-frame N-terminal Myc tag	Clontech
pRK5-myc-bipC	pRK5-myc containing the full coding region of *bipC* with an in-frame N-terminal myc tag	This Study, Junsoo Kim
pGBKT7	*S. cerevisiae* expression vector encoding an in frame N-terminal GAL4 DNA binding domain and myc tag, Trp^+, Kan^r	Clontech
pGADT7	*S. cerevisiae* expression vector encoding an in frame N-terminal GAL4 DNA activating domain and HA tag, Leu^+, Amp^r	Clontech
pGBKT7-53	pGBKT7 control vector encoding murine p53 with an in frame N-terminal GAL4 DNA binding domain and myc tag, Trp^+, Kan^r	Clontech
pGBKT7-Lam	pGBKT7 control vector encoding human lamin C with an in frame N-terminal GAL4 DNA binding domain and myc tag, Trp^+, Kan^r	Clontech
pGADT7-T	pGADT7 control vector encoding simian vacuolating virus 40 (SV40) large T-antigen with an in frame N-terminal GAL4 DNA activating domain and HA tag, Leu^+, Amp^r	Clontech

Continued on Next Page

Continuation of Table 7.1

Strain or Plasmid	**Characteristics**	**Source**
pGBKT7-bipC	pGBKT7 containing the full coding region of *bipC* with an in frame N-terminal GAL4 DNA binding domain and myc tag, Trp^+, Kan^r	This Study
pGBKT7-bapA	pGBKT7 containing the full coding region of *bapA* with an in frame N-terminal GAL4 DNA binding domain and myc tag, Trp^+, Kan^r	This Study
pGBKT7-bprD	pGBKT7 containing the full coding region of *bprD* with an in frame N-terminal GAL4 DNA binding domain and myc tag, Trp^+, Kan^r	This Study
pGADT7-actin	pGADT7 containing the full coding region of actin with an in frame N-terminal GAL4 DNA activating domain and HA tag, Leu^+, Amp^r	This Study
pGADT7-RecAB-C1QBP	pGADT7-RecAB containing C1QBP with an in frame N-terminal GAL4 DNA activating domain and HA tag, isolated from library mating, Leu^+, Amp^r	This Study
pGADT7-RecAB-PAWR	pGADT7-RecAB containing PAWR with an in frame N-terminal GAL4 DNA activating domain and HA tag, isolated from library mating, Leu^+, Amp^r	This Study

End of Table

Table 7.2: Primers used in this study.

Primer Name	**Sequence** (restriction sites underlined)	**Purpose**
T7 Forward	TAATACGACTCACTATAGGGC	Sequencing
DNA-BD	ATCATAAATCATAAGAAATTCGCC	Sequencing of pGBKT7
DNA-AD	AGATGGTGCACGATGCACAG	Sequencing of pGADT7
bprD-Y2H-F	ATATATATCATATGATGAAGCTCAATGGAATGACCGCCGC	Cloning of *bprD* into pGBKT7
bprD-Y2H-R	ATATATATGGATCCCGGCGCCGGGCGCTGCGCCCGCGTAG	Cloning of *bprD* into pGBKT7
bapA-Y2H-F	ATATATATCATATGATGCCGCCGTCCATTCACCGAACTTC	Cloning of *bapA* into pGBKT7
bapA-Y2H-R	ATATATATGGATCCTCGCTTCGTGCCGTTGGCGATCGAAT	Cloning of *bapA* into pGBKT7
bipC-Y2H-F	ATATATATCATATGATGTCAATCGGTGTGCAAAGCAGCGG	Cloning of *bipC* into pGBKT7
bipC-Y2H-R	ATATATATGGATCCGGTCCGCAGATTGCCGGCCACCTGCG	Cloning of *bipC* into pGBKT7
bopC-Y2H-F	ATATATATCATATGATGACCGTCACGCGGACTACTTCGCA	Cloning of *bopC* into pGBKT7
bopC-Y2H-R	ATATATATGGATCCTGCGAGTGGGGTGTCCTGTTCCCGGA	Cloning of *bopC* into pGBKT7
bprD-pGEX-F	ATATATGGATCCATGAAGCTCAATGGAATGACCGCC	Cloning of *bprD* into pGEX-4T-1
bprD-pGEX-R	ATATATCTCGAGTCACGGCGCCGGGCGCTGCGCCCGC	Cloning of *bprD* into pGEX-4T-1

Continued on Next Page

Continuation of Table 7.2

Primer Name	**Sequence** (restriction sites underlined)	**Purpose**
bapA-pGEX-F	ATATATGGATCCATGCCGCCGTCCATTCACCGAACT	Cloning of *bapA* into pGEX-4T-1
bapA-pGEX-R	ATATATGAATTCTCATCGCTTCGTGCCGTTGGCGATC	Cloning of *bapA* into pGEX-4T-1
bsaP-del-1	ATATATACTAGTGACGTTCGACAGCAACCAGACGTTC	Deletion of *bsaP*
bsaP-del-2	GCTCATGACTTGTCGTCCATGTAGG	Deletion of *bsaP*
bsaP-del-3	TGACGCGCGGCGCCTTTCATTCAATC	Deletion of *bsaP*
bsaP-del-4	ATATATAGATCTTTCACGCTCGAGCGCCGAGCGGCGC	Deletion of *bsaP*
bsaP-chk-1	GATCGTGCTCACGCAGGAGAACGTG	Confirmation of *bsaP* deletion
bsaP-chk-2	CATCGCCCTTGATGAACTTCATC	Confirmation of *bsaP* deletion
bsaP-exp-F	ATATATATCGATAGGAGGTTGCCATCATGAGCTCGATCATCGGCGG	Complementation of *bsaP*
bsaP-exp-R	ATATATAAGCTTTCAGTCGGCGCGCGGGCGCGCCT	Complementation of *bsaP*
bapA-F	ATATATATGCATAGGAGGTTGCCATCATGCCGCCGTCCATTCACCGAACTTC	Expression of c-Myc tagged BapA
bapA-myc-R	ATATAGATCTTCACAGGTCCTCCTCGGAGATCAGCTTCTGCTCTCGCTTCGTGCCGTTGGCGATCG	Expression of c-Myc tagged BapA

Continued on Next Page

Continuation of Table 7.2

Primer Name	**Sequence** (restriction sites underlined)	**Purpose**
bopE-F	ATATATAGATCTAGGAGGTTGCCATCATGTCGCTTCATAGAATGAAATCGGT	Expression of c-Myc tagged BopE
bopE-myc-R	ATATCTCGAGTCACAGGTCCTCCTCGGAGATCAGCTTCTGCTCAGCCGGAGAACCCCGAGA	Expression of c-Myc tagged BopE
bprD-F	ATATATCCATGGAGGAGGTTGCCATCATGAAGCTCAATGGAATGACCGCCGC	Expression of c-Myc tagged BprD
bprD-myc-R	ATATAGATCTTCACAGGTCCTCCTCGGAGATCAGCTTCTGCTCCGGCGCCGGGCGCTGCGCCCGCGTA	Expression of c-Myc tagged BprD
BPSS0860-F	ATATATATCGATAGGAGGTTGCCATCATGGCGATCACCCAGACGGGGACCACCTCGCAAAG	Expression of c-Myc tagged BPSS0860
BPSS0860-myc-R	ATATCTCGAGTCACAGGTCCTCCTCGGAGATCAGCTTCTGCTCCTTGTTGTTCGCGAGCGCGCCCGAGC	Expression of c-Myc tagged BPSS0860
bopA-F	ATATATCCATGGAGGAGGTTGCCATCATGATCAATGTCGATGCATTCGT	Expression of c-Myc tagged BopA
bopA-myc-R	ATATAGATCTTCACAGGTCCTCCTCGGAGATCAGCTTCTGCTCGGCGGCGATCGCAGCCGCCATGA	Expression of c-Myc tagged BopA
BPSS1916-F	ATATATCCATGGAGGAGGTTGCCATCATGCAAGCAAAACGCGTGGCATT	Expression of c-Myc tagged BPSS1916

Continued on Next Page

Continuation of Table 7.2

Primer Name	**Sequence** (restriction sites underlined)	**Purpose**
BPSS1916-myc-R	ATATAGATCTTCACAGGTCCTCCTCGGAGATCAGCTTCTGCTCGGACATGTGCATCCCGCCGTTGA	Expression of c-Myc tagged BPSS1916
BPSS1512-F	ATATATCCATGGAGGAGGTTGCCATCATGAACGCTCGACGTCCGGCGTTCG	Expression of c-Myc tagged BPSS1512
BPSS1512-myc-R	ATATCTCGAGTCACAGGTCCTCCTCGGAGATCAGCTTCTGCTCTCGATAGATCGCGATTTCGATCGACA	Expression of c-Myc tagged BPSS1512

End of Table

Antibody (species)	**Specificity**	**Application (dilution/concentration used)**	**Reference/Source (catalogue number)**
α-BopE (rabbit polyclonal)	*B. pseudomallei*	WB (0.5 μg/ml)	(Stevens *et al.*, 2003)
α-BipD (rabbit polyclonal)	*B. pseudomallei*	WB (0.5 μg/ml)	(Stevens *et al.*, 2003)
α-c-Myc (rabbit polyclonal)	Human, Monkey	WB (1.0 μg/ml), IF (1:500)	Santa Cruz Biotechnology (sc-789)
α-Actin (rabbit polyclonal)	Human, Mouse, Rat	WB (1.0 μg/ml)	Santa Cruz Biotechnology (sc-1615)
α-PAWR (rabbit monoclonal)	Human, Mouse	WB (1:10,000)	Origene (TA307434)
α-C1QBP (rabbit monoclonal)	Human, Mouse, Rat	WB (1:10,000)	Abcam (ab134926)
α-CDC42 (rabbit polyclonal)	Human, Mouse, Rat	WB (1.0 μg/ml)	Santa Cruz Biotechnology (sc-87)
α-Rac1 (rabbit polyclonal)	Human, Mouse, Rat	WB (1.0 μg/ml)	Santa Cruz Biotechnology (sc-217)
α-GAPDH HRP (rabbit polyclonal)	Human, Mouse, Rat, *E. coli*	WB (1:5000)	Abcam (ab85760)
α-rabbit HRP (goat)	Rabbit IgG	WB (1:15,000)	Life Technologies (G-21234)
α-rabbit DyLight 800 (goat)	Rabbit IgG	WB (1:10,000)	Cell Signalling (5257)
α-rabbit 488 (goat)	Rabbit IgG	IF (1:200)	Molecular Probes (A-11008)

Table 7.3: Antibodies used in this study. Abbreviations in table include: Western blot (WB) and immunofluorescence (IF).

7.4 Publications

***Vander Broek, C. W.**, Chalmers, K. J., Stevens, M. P., & Stevens, J. M. (2015). Quantitative Proteomic Analysis of *Burkholderia pseudomallei* Bsa Type III Secretion System Effectors Using Hypersecreting Mutants. *Molecular & Cellular Proteomics*, 14(4), 905-916.

Pumirat, P., **Vander Broek, C.**, Juntawieng, N., Muangsombut, V., Kiratisin, P., Pattanapanyasat, K., ... & Korbsrisate, S. (2014). Analysis of the prevalence, secretion and function of a cell cycle-inhibiting factor in the melioidosis pathogen *Burkholderia pseudomallei*. *PLoS One*, 9(5), e96298.

McAdam, P. R., **Vander Broek, C. W.**, Lindsay, D. S., Ward, M. J., Hanson, M. F., Gillies, M., ... & Fitzgerald, J. R. (2014). Gene flow in environmental *Legionella pneumophila* leads to genetic and pathogenic heterogeneity within a Legionnaires' disease outbreak. *Genome Biol*, 15, 504.

* Publication attached below.

⌘ Author's Choice

© 2015 by The American Society for Biochemistry and Molecular Biology, Inc.
This paper is available on line at http://www.mcponline.org

Quantitative Proteomic Analysis of *Burkholderia pseudomallei* Bsa Type III Secretion System Effectors Using Hypersecreting Mutants

Charles W. Vander Broek‡, Kevin J. Chalmers§, Mark P. Stevens‡, and Joanne M. Stevens‡¶

Burkholderia pseudomallei **is an intracellular pathogen and the causative agent of melioidosis, a severe disease of humans and animals. One of the virulence factors critical for early stages of infection is the *Burkholderia* secretion apparatus (Bsa) Type 3 Secretion System (T3SS), a molecular syringe that injects bacterial proteins, called effectors, into eukaryotic cells where they subvert cellular functions to the benefit of the bacteria. Although the Bsa T3SS itself is known to be important for invasion, intracellular replication, and virulence, only a few genuine effector proteins have been identified and the complete repertoire of proteins secreted by the system has not yet been fully characterized. We constructed a mutant lacking *bsaP*, a homolog of the T3SS "gatekeeper" family of proteins that exert control over the timing and magnitude of effector protein secretion. Mutants lacking BsaP, or the T3SS translocon protein BipD, were observed to hypersecrete the known Bsa effector protein BopE, providing evidence of their role in post-translational control of the Bsa T3SS and representing key reagents for the identification of its secreted substrates. Isobaric Tags for Relative and Absolute Quantification (iTRAQ), a gel-free quantitative proteomics technique, was used to compare the secreted protein profiles of the Bsa T3SS hypersecreting mutants of *B. pseudomallei* with the isogenic parent strain and a *bsaZ* mutant incapable of effector protein secretion. Our study provides one of the most comprehensive core secretomes of *B. pseudomallei* described to date and identified 26 putative Bsa-dependent secreted proteins that may be considered candidate effectors. Two of these proteins, BprD and BapA, were validated as novel effector proteins secreted by the Bsa T3SS of *B. pseudomallei*. *Molecular & Cellular Proteomics 14: 10.1074/mcp.M114.044875, 905–916, 2015.***

From the ‡The Roslin Institute and Royal (Dick) School of Veterinary Studies, University of Edinburgh, Easter Bush, Midlothian, EH25 9RG, Scotland, UK.; §Dundee Cell Products, James Lindsay Place, Dundee Technopole, Dundee, DD1 5JJ, Scotland, UK

⌘ *Author's Choice*—Final version full access.

Received, September 25, 2014 and in revised form, January 7, 2015

Published, MCP Papers in Press, January 29, 2015, DOI 10.1074/mcp.M114.044875

Author contributions: C.W.V., K.J.C., M.P.S., and J.M.S. designed research; C.W.V. performed research; C.W.V., K.J.C., and J.M.S. analyzed data; C.W.V. and J.M.S. wrote the paper.

Burkholderia pseudomallei is a Gram-negative environmental saprophyte found in free-standing water and soil (1). The causative agent of melioidosis, *B. pseudomallei* causes severe disease in humans and animals with a range of clinical manifestations including severe pneumonia and septic shock, acute or chronic suppurative infections, genitourinary disease, and asymptomatic carriage (2). An emerging infectious disease, melioidosis is found primarily in South East Asia and Northern Australia, yet there is a growing body of evidence of a more widespread distribution in subtropical regions of Asia, the Americas, and Africa (3). Melioidosis is an important cause of community-acquired septicaemia in North-East Thailand, where it can cause mortality rates of up to 40% (4). Because of the lack of an effective vaccine, intrinsic antibiotic resistance, and the high mortality rates, there is a need to better understand the molecular mechanisms of pathogenesis to inform the design of treatments and vaccines (5).

B. pseudomallei is a facultative intracellular pathogen capable of invading both phagocytic and nonphagocytic cells (6). Once inside the cell, the bacteria can rapidly escape the endosome and polymerize host cell actin at one pole causing actin-based motility, a process dependent on the bacterial BimA protein (7). *B. pseudomallei* also causes host cell fusion creating multinucleated giant cells (MNGCs) that facilitates cell to cell spread while evading immune detection (8). The formation of MNGCs by *B. pseudomallei* is dependent on secretion of the protein VgrG5 by the virulence-associated type VI secretion system-5 (9–12).

One important virulence factor of *B. pseudomallei* that has also been shown to be important for infection in many other Gram-negative bacteria including pathogenic *Escherichia coli, Salmonella, Shigella,* and *Yersinia*, is the Type III Secretion System (T3SS)[1] (13–16). T3SSs act as a molecular syringe

[1] The abbreviations used are: T3SS, Type III secretion system; *B. pseudomallei*, *Burkholderia pseudomallei*; Bsa, *Burkholderia* secretion apparatus; iTRAQ, Isobaric tags for relative and absolute quantification; WT, wild-type; CHBP, Cif homolog of *Burkholderia pseudomallei*; IQR, interquartile range; Cm, chloramphenicol; Amp, ampicillin; Kan, kanamycin; Tet, tetracycline; EPEC, enteropathogenic *Escherichia coli*; MNGC, multinucleated giant cell.

ASBMB MOLECULAR & CELLULAR PROTEOMICS MCP

projecting outwards from the surface of the bacteria allowing for the transport of bacterial proteins into target eukaryotic cells (17). These bacterial proteins, termed effectors, subvert host cell processes to the advantage of the bacteria and rely on a second class of T3SS-secreted proteins (translocators) for delivery (18). *B. pseudomallei* contains three T3SSs, of which T3SS-1 and T3SS-2 share homology with T3SSs found in plant pathogens (19, 20). T3SS-3, also known as the Burkholderia Secretion Apparatus (Bsa) T3SS, is similar to the Inv-Spa (*Salmonella* pathogenicity island (SPI)-1) and Mxi-Spa T3SSs of the animal pathogens *Salmonella* spp. and *Shigella flexneri* respectively (21). The Bsa T3SS has been shown to be important in invasion, endosome escape and net intracellular replication in cultured cells and in virulence in murine and Syrian hamster models of melioidosis (21–24).

As the Bsa system influences pathogenesis, one may infer that its effectors also influence the outcome of infection. However, only three effectors, BopE, BopC, and CHBP, have so far been proven to be secreted by *B. pseudomallei* in a Bsa T3SS-dependent manner (25–27). BopE is a guanine nucleotide exchange factor that is involved in invasion of nonphagocytic cells (26). BopC has been shown to be important for invasion of A549 epithelial cells and endosome escape, and intracellular survival in J774A.1 macrophage-like cells (25, 28). CHBP is a homolog of *E. coli* Cif, a cyclomodulin that disrupts the eukaryotic cell cycle (29), for which evidence of Bsa-dependent translocation into host cells was recently presented (27). A fourth candidate effector, BopA, prevents LC3-associated host autophagy of intracellular bacteria and has been shown to be secreted in a T3SS-dependent manner in a surrogate enteropathogenic *E. coli* (EPEC) host (30, 31). Compared with the large number of effectors secreted by T3SSs in other Gram-negative pathogens, it is likely that there are other effectors of the Bsa T3SS yet to be characterized (32). Bsa-secreted proteins are known to be potent B- and T-cell antigens in humans (33–36) and subunit vaccines based on needle components or effectors are protective against other pathogens that deploy T3SSs (*e.g. Shigella* IpaB and IpaD, *Yersinia* V antigen, *Salmonella* SseI) (37–41).

One of the problems facing T3SS effector protein discovery is the tight regulation of the T3SS under laboratory conditions with different T3SSs responding to very different environmental cues (42–47). Although some genes involved in transcriptional control of the Bsa T3SS were recently identified (48), little is known about the post-translational regulation of the system and what environmental signals may activate it. Indeed, a recent proteomics study of *B. pseudomallei* failed to identify any of the known Bsa T3SS effectors in bacterial culture supernatants (49). To override the tight control of the T3SS, one solution employed in the study of other Gram-negative bacteria (for example EPEC and *Citrobacter rodentium*) was to generate mutations of T3SS components that dysregulate the system, thereby creating a hypersecretion phenotype. The bacterial supernatants were then analyzed using gel-free quantitative proteomics techniques to identify a range of novel effector proteins (50, 51).

In *Shigella*, deletion of IpaD, the needle tip protein, creates a "leaky" phenotype, in which higher levels of both translocators and effectors are seen in the supernatant (46, 52). The homolog of IpaD in *B. pseudomallei* is BipD (53) (supplemental Fig. S1). In a previous study, we have shown a 10276 *bipD*::pDM4 mutant secreted higher levels of the effector protein BopE into the bacterial culture supernatant by Western blot analysis, but it is unknown what effect *bipD* disruption may have on the secretion of other effectors and translocators (26).

Another group of T3SS proteins that have been shown in many systems to be involved in the control of effector and translocator secretion are the so called "gatekeeper" family of proteins, InvE/MxiC/SepL/YopN-TyeA of *Salmonella*/*Shigella*/*E. coli*/Yersinia, respectively (17). Investigation of these proteins has given insight into the temporal regulation of their respective T3SSs. Although deletion of all of these proteins causes an increase in levels of secreted effectors there are also differences between them. Deletion of InvE and SepL cause a reduction in secreted levels of translocators, deletion of MxiC has no effect on their levels, and deletion of YopN increases levels of secreted translocators (54–60). The closest homolog to this family of proteins in *B. pseudomallei* is the uncharacterized protein BsaP (BPSS1544) (supplemental Fig. S1).

Here, a 10276 Δ*bsaP* deletion mutant was generated and its effect on secreted levels of the known effector BopE was assessed. To define the total and Bsa-dependent repertoire of secreted proteins, Isobaric Tags for Relative and Absolute Quantification (iTRAQ), a gel-free quantitative proteomics technique, was used to quantify protein levels in the bacterial culture supernatants of *B. pseudomallei* mutant strains 10276 *bipD*::pDM4 and 10276 Δ*bsaP*. In order to identify candidate Bsa effector proteins, the secreted protein profiles from these hypersecreting mutants were then compared with the isogenic parent strain (10276 WT) and a T3SS structural-null mutant (10276 *bsaZ*::pDM4), which has been shown to be unable to secrete BipD and BopE (21). BsaZ is a homolog of YscU in *Yersinia*, which forms a key component of the inner membrane ring and is required for a functional T3SS (61) (supplemental Fig. S1). From this analysis we provide the first evidence of the involvement of both BipD and BsaP in control of known effector/translocator secretion in the Bsa T3SS. We also present a comprehensive general secretome for *B. pseudomallei*. Furthermore, we have identified 26 candidate effector proteins, including all known Bsa-secreted effectors, of which we show two proteins are novel substrates for secretion by the Bsa T3SS.

EXPERIMENTAL PROCEDURES

Strains, Media, Plasmids, and Oligonucleotides—Bacterial strains and plasmids are listed in supplemental Table S1. The insertion

ASBMB MOLECULAR & CELLULAR PROTEOMICS MCP

mutants 10276 *bipD*::pDM4 and 10276 *bsaZ*::pDM4 were produced by integration of the pDM4 suicide vector into the coding sequence of the target gene (21). Primers, purchased from Sigma Aldrich (Gillingham, UK), are listed in supplemental Table S2. Bacteria were routinely cultured at 37 °C on LB agar (Miller) or LB broth (Lennox). Antibiotic selection was performed at the following concentrations unless otherwise stated: ampicillin (Amp) 100 μg/ml, kanamycin (Kan) 50 μg/ml, chloramphenicol (Cm) 34 μg/ml, and tetracycline (Tet) 15 μg/ml. IPTG was used at a final concentration of 0.5 mM where appropriate. Unless otherwise stated all chemicals were purchased from Sigma Aldrich (Gillingham, UK).

B. pseudomallei Mutagenesis—The 10276 Δ*bsaP* in-frame deletion mutant was made using allelic exchange and the *sacB* containing positive-selection suicide vector pDM4 essentially as previously described (62). DNA fragments upstream and downstream of *bsaP* (BPSS1544) were amplified by PCR from *B. pseudomallei* 10276 genomic DNA using primer pair's *bsaP-del-1*/*bsaP-del-2* and *bsaP-del-3*/*bsaP-del-4*. The resulting DNA fragments were combined using PCR-ligation-PCR (63). A-tailing was performed to add an adenosine to the blunt-ended PCR product, which was then ligated into pGEM-T resulting in the plasmid pGEM-T-Δ*bsaP.* The insert was sequenced and a SpeI and BglII fragment containing the 10276 Δ*bsaP* fragment ligated into similarly digested pDM4 resulting in pDM4-Δ*bsaP*. To propagate pDM4-Δ*bsaP,* the plasmid was transformed into TOP 10 PIR1 cells (Life Technologies, Paisley, UK) before transfer into *E. coli* S17–1 λpir conjugal donor with selection for Cm resistance.

pDM4-Δ*bsaP* was introduced into *B. pseudomallei* strain 10276 by conjugation with *E. coli* S1–17 λpir and plated onto LA plates containing Cm (50 μg/ml) and Kan (50 μg/ml) to select for *B. pseudomallei* with pDM4-Δ*bsaP* integrated into the chromosome by homologous recombination (21). Colonies were patched onto LA plates containing Cm (50 μg/ml) and Kan (50 μg/ml) to confirm resistance. Overnight cultures of the Cm^r colonies were cultured without selection to allow for a second round of homologous recombination to take place either restoring the full length *bsaP* gene or resulting in *bsaP* deletion. To select for double recombinants lacking pDM4-Δ*bsaP* the overnight cultures were plated onto 15% sucrose plates lacking NaCl and cultured at 30 °C for 3 days. Chromosomal deletion of *bsaP* was confirmed in sucrose resistant/Cm^s colonies by colony PCR and the resulting strain designated 10276 Δ*bsaP,* where the *bsaP* gene has been replaced by an in-frame start-stop (atg-taa) cassette.

Complementation of the Δbsa P Mutant—For complementation of the Δ*bsaP* mutant the 10276 *bsaP* sequence was amplified by PCR using the forward primer *bsaP-exp-F* containing a ClaI restriction site and a ribosome-binding site and the reverse primer *bsaP-exp-R* containing a HindIII restriction site. The PCR fragment was cloned into pBHR1 (MoBiTec, 2B Scientific Ltd., Oxford, UK) to create pBHR1-*bsaP*. The plasmid was purified and transformed into *B. pseudomallei* 10276 Δ*bsaP* using the fast sucrose method of electroporation (64), creating strain 10276 Δ*bsaP*-p*bsaP*.

Cloning of Candidate Effectors to Express c-Myc Epitope-Tagged Fusion Proteins—The coding region for candidate effectors based on the *B. pseudomallei* K96243 genome sequence were amplified from *B. pseudomallei* 10276 genomic DNA by PCR with a 5′ forward primer containing a ribosome-binding site and a 3′ reverse primer encoding an in-frame c-Myc tag followed by a stop codon. Each primer also contained a restriction site suitable for directional insertion into the vector pME6032. Plasmids were transformed into *E. coli* and the inserts sequenced. Purified plasmids were then transformed into *B. pseudomallei* 10276 (WT), 10276 *bsaZ*::pDM4, 10276 *bipD*::pDM4, and 10276 Δ*bsaP.*

Preparation of Bacterial Culture Supernatants—Preparation of *B. pseudomallei* supernatants was performed by first centrifuging overnight cultures at 3220 RCF for 10 min at 4 °C followed by disposal of the supernatant and resuspension of the bacteria in fresh LB to an OD_{600} of 1.0. Of the bacterial suspension, 1 ml was then added to 10 ml of LB containing the appropriate antibiotics and IPTG if needed. The culture was incubated for 6 h shaking at 200 RPM at 37 °C. To determine the initial and final bacterial counts, a sample was removed from the culture before and after the 6 h incubation for serial dilution and plating on LA plates. After 6 h, the sample was centrifuged at 3220 RCF for 10 min at 4 °C. The culture supernatant was collected and centrifuged a second time to ensure no intact bacteria remained. The supernatant was then passed through a 0.2 μm low protein binding cellulose acetate membrane filter (Millipore, Watford, UK) and sterility tested.

Protein Precipitation—Proteins were precipitated using a Pyrogallol red-molybdate methanol (PRMM) solution (0.5 mM pyrogallol red (Alfa Aesar, Heysham, UK), 0.16 mM sodium molybdate, 1.0 mM sodium oxalate, 50 mM succinic acid, 20% MeOH, pH 2.0) as previously described (65). In brief, equal volumes of bacterial culture supernatant and PRMM solution were thoroughly mixed and the pH was adjusted to 2.8 ± 0.1 with HCl. The samples were then precipitated overnight at 4 °C. The resulting precipitate was centrifuged at 3220 RCF, 4 °C for 1 h and the supernatant was discarded. The pellet was washed twice with ice-cold acetone and then allowed to air dry. The protein pellet was then solubilized in 50 mM ammonium bicarbonate and quantified using a Direct Detect Infrared Spectrometer (Millipore, Watford, UK).

SDS-PAGE and Immunoblotting—Proteins were separated using sodium dodecyl sulfate polyacrylamide gel electrophoresis (SDS-PAGE). Equal volumes of protein samples and Laemmli buffer were mixed and heated to 90 °C for 5 min. Samples were separated on Any kDa™ Mini-PROTEAN® TGX gels (Bio-Rad, Hemel Hempstead, UK) at 150V for 45 min in Tris-Glycine running buffer. Proteins were visualized by Coomassie staining. Western blots were used to identify particular proteins of interest. Proteins were transferred onto a nitrocellulose membrane using the Trans-Blot Turbo system (Bio-Rad, Hemel Hempstead, UK) at 2.5 A for 3 min. α-BopE (26), α-BipD (22), or α-cMyc (Insight Biotechnology, Wembley, UK) rabbit polyclonal antibodies were used at 1 μg/ml. For detection by infrared fluorescence, goat- α -rabbit IgG (H+L) (DyLight™ 800 Conjugate) was used at a 1:10,000 dilution (Cell Signaling Technology, Hitchin, UK). Blots were visualized using an Odyssey Infrared Imaging System (LI-COR Biosciences, Cambridge, UK) according to the manufacturer's instructions. Images were captured and analyzed using Image Studio Lite (LI-COR Biosciences, Cambridge, UK).

iTRAQ Experimental Design—Bacterial culture supernatants of *B. pseudomallei* 10276 WT, 10276 *bsaZ*::pDM4, 10276 *bipD*::pDM4, and 10276 Δ*bsaP* were generated in three independent experiments. Equal amounts of protein from each replicate were combined creating a single pooled sample for each strain. These samples were enzymatically digested, peptides were labeled using iTRAQ reagents, and then pooled and submitted to LC MS/MS in three technical replicates as follows:

(1) Protein Digestion and Peptide Fractionation—Protein samples were prepared for MS analysis using a protocol adapted from (66). Following protein quantification, samples were reduced in 10 mM DTT and alkylated in 50 mM Iodoacetamide prior to heating in Laemmli buffer, and then separated by one-dimensional SDS-PAGE (4–12% Bis-Tris Novex mini-gel, Life Technologies, Paisley, UK) and visualized by colloidal Coomassie staining (Life Technologies). The entire protein gel lanes were excised and cut into 10 slices each. Every gel slice was subjected to in-gel digestion with trypsin overnight at 37 °C. The resulting tryptic peptides were extracted by formic acid (1%) and acetonitrile, lyophilized in a speedvac, and resuspended in 1% formic acid.

ASBMB MOLECULAR & CELLULAR PROTEOMICS MCP

(2) Peptide Concentration—To determine the concentration of the peptides, the dried samples were resuspended in 100 mM TEAB 1 M ACN. To determine the volume of sample needed for an even protein load across all samples, 1 μl was injected onto an LTQ Velos Mass Spectrometer (Thermo Fisher Scientific, MA) and the TIC trace was used.

(3) iTRAQ Labeling—Samples were labeled according to the manufacturer's instructions using an iTRAQ Reagents Multiplex kit – fourplex (AB Sciex UK Ltd., Warrington, UK). To each vial of labeling reagent (labels- 114, 115, 116, and 117), 70 μl ethanol was added, after which they were vortexed and centrifuged. A single vial of label was added to a single vial of sample and mixed. The samples used with each label were: 10276 *bsaZ*::pDM4–114, 10276 WT-115, 10276 *bipD*::pDM4–116, and 10276 Δ*bsaP*-117. Samples were incubated with shaking at room temperature for 1 h, after which 100 μl of water was added and incubated for a further hour. The four vials of labels/samples were pooled into one vial and then dried under vacuum. Samples were desalted using a standard method.

(4) SCX Fractionation – Salt Cuts—To a Millipore (Watford, UK) C18 ziptip, 10 μl Poros HS resin (Life Technologies, Paisley, UK) was added and washed with 3 × 25 μl Buffer A (35% acetonitrile (ACN), 0.1% formic acid (FA)). Samples were resuspended in Buffer A and loaded onto the resin, washed with 3 × 25 μl Buffer A, and eluted with 2 × 25 μl of each of 11 salt cuts ranging from 5 mM to 800 mM NaCl. A final elution was performed using 2 × 25 μl 50% isopropanol, 0.4% ammonium hydroxide. Samples were centrifuged and speed vacuumed until dry. Samples were resuspended in 1% FA and pooled as six samples containing the salt cuts as follows: JS-1 (5 mM, 10 mM, 20 mM), JS-2 (50 mM), JS-3 (100 mM), JS-4 (150 mM), JS-5 (200 mM), and JS-6 (250 mM, 300 mM, 400 mM, 800 mM).

Mass Spectrometry—Peptides were separated using an Ultimate 3000 RSLC nanoflow LC system (Thermo Fisher Scientific, MA). With a constant flow of 5 μl/min, 15 μl of sample was loaded onto an Acclaim PepMap100 nanoViper C18 trap column (100 μm inner-diameter, 2 cm) (Thermo Fisher Scientific, MA). After trap enrichment, peptides were eluted onto an Acclaim PepMap RSLC nanoViper, C18 column (75 μm, 15 cm) (Thermo Fisher Scientific, MA) with a linear gradient of 2–45% solvent B (80% ACN with 0.08% FA) over 125 min with a constant flow of 300 nl/min. The HPLC system was coupled to a linear ion trap Orbitrap hybrid mass spectrometer (LTQ-Orbitrap Velos) (Thermo Fisher Scientific, MA) via a nanoelectrospray ion source (Thermo Fisher Scientific, MA). The spray voltage was set to 1.2kV and the temperature of the heated capillary was set to 250 °C. Full-scan MS survey spectra (*m/z* 335–1800) in profile mode were acquired in the Orbitrap with a resolution of 60,000 after accumulation of 1,000,000 ions. The ten most intense peptide ions from the preview scan in the Orbitrap were fragmented sequentially by higher-energy collisional dissociation (HCD) (two-step (6%) normalized collision energy (NCE), 40%; and activation time, 0.1 ms) prior to analysis in the Orbitrap after accumulation of 50,000 ions. Maximal filling times were 500 ms for the full scans and 200 ms for the MS/MS scans. Precursor ion charge state screening was enabled, and all unassigned charge states as well as singly charged species were rejected. The lock mass option was enabled for survey scans to improve mass accuracy (67). Data were acquired using Xcalibur software (Thermo Fisher Scientific, MA).

Quantification and Bioinformatic Analysis—The raw mass spectrometric data files obtained for each experiment were collated into a single data set using Proteome Discoverer version 2.0 (Thermo Fisher Scientific, MA) and the Mascot search engine version 2.4 (www.matrixscience.com) using a translated *B. pseudomallei* K96243 genome as a reference for protein identification. Enzyme specificity was set to that of trypsin, allowing for cleavage N-terminal to proline residues and between aspartic acid and proline residues. Other parameters used were: 1) variable modifications, methionine oxidation, protein N-acetylation, gln → pyro-glu; 2) fixed modifications, cysteine carbamidomethylation; 3) database: *B. pseudomallei* K96243_20120601 (compiled 01/06/2012, containing 5728 proteins); 4) iTRAQ labels: standard iTRAQ 4-plex quant method with labels 114–117; 5) MS/MS tolerance: FTMS- 10ppm, FTMS/MS- 0.06Da; 6) minimum peptide length, 6; 7) maximum missed cleavages, 2; and 8) false discovery rate, 1%. Peptide ratios were calculated for samples using the 10276 *bsaZ*::pDM4–114 label as the denominator. Data are available via ProteomeXchange with identifier PXD001656.

Protein ratios were normalized using the overall median ratio for all quantified proteins in each sample based on the assumption that the abundance of the majority of secreted proteins was identical in each condition. Proteins were selected as potential T3SS effector protein candidates if they had at least two unique peptides used in quantification with a MASCOT peptide score ≥21 (which corresponds to the threshold value for a 95% confidence level, a 1 in 20 chance that the match is random), and a "high" iTRAQ ratio in at least one strain, which we defined as a value greater than 1.5 × IQR. *IQR* is defined as $Q_3 = \left(\frac{3(n+1)}{4}\right)^{th} term - Q_1 = \left(\frac{(n+1)}{4}\right)^{th} term$; where *n* complete set of ratios over 10276 *bsaZ*::pDM4 for all quantified proteins in a given sample.

RESULTS

Construction and Characterization of Hypersecreting bsa Mutants—We hypothesized that BsaP may control the timing and magnitude of effector secretion based on homology to "gatekeeper" proteins from the T3SSs of other Gram-negative bacterial pathogens. BLAST analysis of available genomes indicated that BsaP shares 33% identity over 92% coverage (E-value 1e-41) with the *Shigella* MxiC "gatekeeper" protein and 34% identity over 88% coverage (E-value 4e-32) with the *Salmonella* InvE "gatekeeper" protein (supplemental Fig. S2). A nonpolar *bsaP* deletion mutant was therefore constructed in *B. pseudomallei* strain 10276 by double homologous recombination using a positive-selection suicide vector containing short regions of DNA flanking the *bpss1544* gene (62). The chromosomal deletion was confirmed by sequencing across the *bsaP* adjoining regions (data not shown). Because *bsaP* is predicted to reside in the middle of an operon, with seven genes upstream and two downstream, the deletion of *bsaP* was complemented using a constitutive expression vector encoding *bsaP* to confirm any phenotypes were not caused by polar effects. Alongside the *bsaP* mutant we also analyzed 10276 *bipD*::pDM4 lacking the BipD needle tip protein that has been previously reported to secrete elevated levels of the effector protein BopE (26).

Bacteria-free culture supernatants were collected from *B. pseudomallei* 10276 WT, 10276 *bsaZ*::pDM4, 10276 *bipD*::pDM4, 10276 Δ*bsaP*, and 10276 Δ*bsaP* (p*bsaP*) and analyzed by SDS-PAGE followed by Coomassie staining. The secreted protein profile of *B. pseudomallei* LB-culture supernatant is highly complex with few obvious differences between the strains (supplemental Fig. S3). The bacterial supernatants and whole cell lysates were also analyzed by Western blot using antibodies to detect the BopE effector protein and the BipD translocon protein (Fig. 1). The absence of both

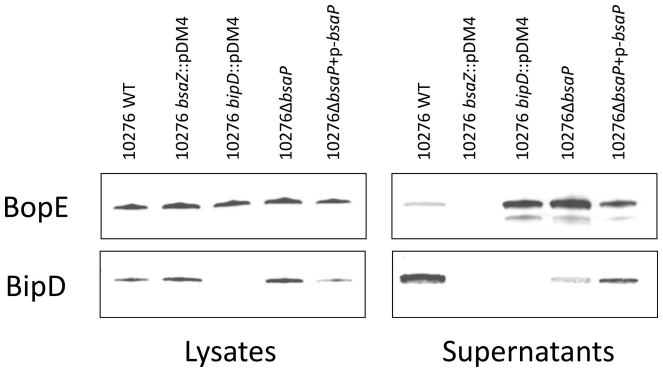


FIG. 1. **Western blot analysis of the expression and secretion of BopE and BipD proteins by wild-type and mutant *B. pseudomallei* strains.** 10276 WT, 10276 *bsaZ*::pDM4, 10276 *bipD*::pDM4, 10276 Δ*bsaP*, and 10276 Δ*bsaP* p*bsaP* were cultured for 6 h at 37 °C. Equal quantities of protein from the whole cell lysates or cell-free supernatants were separated by denaturing SDS-PAGE and proteins transferred to a nitrocellulose membrane for protein detection using polyclonal rabbit α-BopE or α-BipD (26) essentially as described under "Experimental Procedures."

BopE and BipD in the supernatants of the 10276 *bsaZ::*pDM4 insertion mutant indicates that there was no detectable cell lysis at the time when the secretome was sampled. When compared with the 10276 WT strain, both 10276 *bipD::*pDM4 and 10276 Δ*bsaP* strains demonstrated increased secretion of BopE. Interestingly, the levels of BipD secreted into the supernatant was reduced in 10276 Δ*bsaP* compared with 10276 WT. This pattern of increased levels of the effector BopE and reduced secretion of the translocator BipD provides the first evidence of a role for BsaP as a "gatekeeper" protein, controlling a switch between the secretion of translocators and effectors. In the case of both BopE and BipD, the phenotype of 10276 Δ*bsaP* was partially restored by plasmid-mediated complementation, indicating the effects are unlikely to be caused by polar or secondary defects. Differences in the levels of BopE and BipD across the different strains sampled are not caused by differences in the number of bacteria at six hours subculture, because the growth rates of all strains were shown to be identical by viable count assessment (data not shown).

Characterization of the total B. pseudomallei Secretome under Standard Laboratory Conditions—Having identified two *bsa* mutant strains with dysregulated BopE secretion profiles in bacterial culture supernatants, we then sought to identify the total secreted protein profile from these two strains in comparison to the isogenic parent strain (10276) and a *bsa*-null mutant strain. In three independent experiments, culture supernatants were prepared from the four test strains at 6 h post subculture. The strains used were *B. pseudomallei* 10276 WT, 10276 *bsaZ::*pDM4, 10276 *bipD::*pDM4, and 10276 Δ*bsaP* (supplemental Fig. S1). The samples were all assessed for a lack of cell lysis by immunoblotting for BopE. All 10276 *bsaZ::*pDM4 samples lacked BopE, indicating the samples were suitable for analysis (supplemental Fig. S4). After mixing equimolar amounts of each of the three biological replicates, the samples were subjected to iTRAQ labeling and MS/MS analysis as described under "Experimental Procedures." iTRAQ allowed the simultaneous identification and relative quantification of peptide fragments in all four separate samples, resulting in the positive identification of a total of 475 proteins in all samples (listed in supplemental Table S3). The data was expressed as ratios of relative protein abundance either in the 10276 WT, 10276 *bipD::*pDM4, or 10276 Δ*bsaP* samples over the 10276 *bsaZ::*pDM4 sample as a denominator (*i.e.* 10276 WT/10276 *bsaZ::*pDM4, 10276 *bipD::*pDM4/10276 *bsaZ::*pDM4, and 10276 Δ*bsaP*/10276 *bsaZ::*pDM4). The ratios were normalized to the median for each strain and a density plot showed that the majority of protein ratios cluster around the median of one, indicating that the mutations made did not radically change the secretion profile of the bulk of proteins (supplemental Fig. S5). From this analysis we identified a core set of 426 proteins, out of the predicted total proteome of *B. pseudomallei* K96243 of ~5900 proteins (68), that were present in all samples. These are listed in supplemental Table S4. Strikingly, the majority of these proteins (~80%) are encoded by Chromosome 1.

Of the proteins identified in the core secretome, 54 are annotated with reference to the K92643 genome as hypothetical (uncharacterized) proteins, several more are annotated with metabolic functions (supplemental Table S4). The core secretome also consisted of several elongation factors (Ts, G, P, Tu) and heat shock/chaperone proteins (GroES, GroEL), many of which have previously been reported to be present on the surface of *B. pseudomallei* or part of the outer membrane proteome and recognized by the sera of recovering melioidosis patients (35, 69–71). In addition to the presence of a collagenase, chitobiase, bacterioferritin, and Sec secretory pathway constituents, the secretome also harbored several proteases and lipoproteins. Several phage components, Type I fimbriae, and flagellar subunits were also present, although there was a notable lack of any of the predicted T6SS structural or effector proteins, Type V family of autotransporters or the Type IV pilus protein PilA.

Prediction of the Bsa Effector Repertoire—Putative T3SS effector proteins were identified in the data sets primarily on the calculated iTRAQ protein abundance ratios. The protein abundances obtained in each of the WT or mutant strain samples were each expressed as a ratio of the 10276 *bsaZ*::pDM4 sample and proteins with an iTRAQ ratio higher than the 1.5 × interquartile range (IQR), together with at least two unique peptides with a MASCOT peptide score ≥21, were taken to be T3SS effector protein candidates. The 1.5 × IQR values were calculated and the cut-offs set at 1.56 for the 10276 WT/10276 *bsaZ::*pDM4 data set, 1.79 for the 10276 *bipD::*pDM4/10276 *bsaZ::*pDM4 data set, and 1.46 for the 10276 Δ*bsaP*/10276 *bsaZ::*pDM4 data set, based on the calculation described under "Experimental Procedures." When

ASBMB MOLECULAR & CELLULAR PROTEOMICS MCP

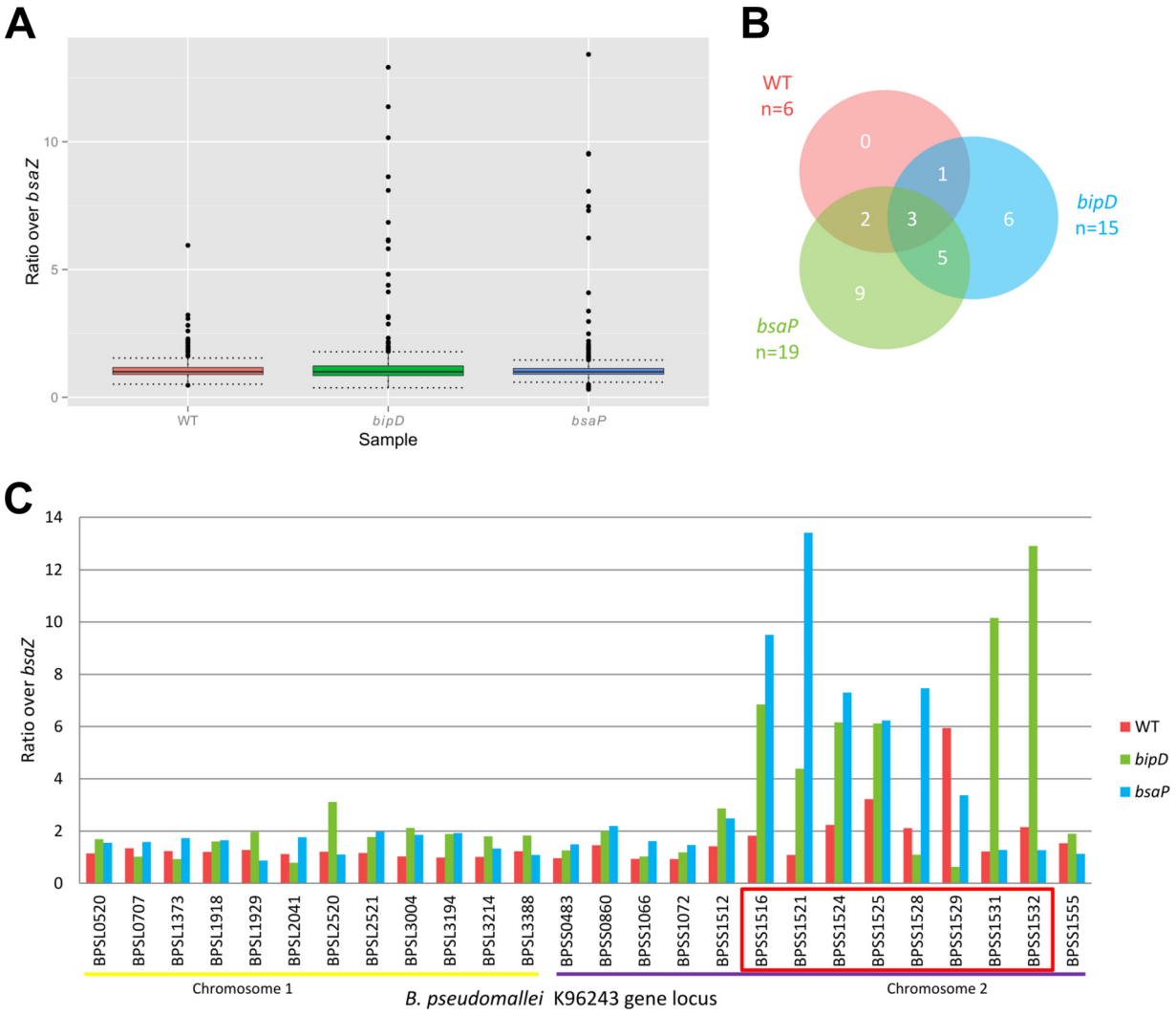


FIG. 2. **Proteins with high iTRAQ protein abundance ratios are enriched in hypersecreting *B. pseudomallei* strains and encoded within the *bsa* T3SS locus.** *A*, Boxplot generated by R software (www.r-project.org) showing the distribution and median values of the ratios of the protein abundances in the 10276 WT (WT), 10276 *bipD*::pDM4 (*bipD*), or 10276 Δ*bsaP* (*bsaP*) samples compared with the 10276 *bsaZ*::pDM4 (*bsaZ*) sample. The "cut-off" values (calculated using R software) are shown by the dotted lines. Points shown above the "cut-off" value are candidate T3SS effectors. *B*, A Venn diagram (constructed with Venny: www.bioinfogp.cnb.csic.es/tools/venny) depicting the number of strain-specific and shared candidate T3SS effector proteins identified in each of the strains 10276 WT (WT), 10276 *bipD*::pDM4 (*bipD*), and 10276 Δ*bsaP* (*bsaP*). *C*, Distribution of the candidate T3SS effector proteins plotted according to *B. pseudomallei* gene number across both Chromosomes and their ratios. Gene numbers refer to the *B. pseudomallei* K96243 reference strain. The *bsa* T3SS locus is indicated by the red box.

the data was plotted as a boxplot, the data showed a trend toward more proteins with larger ratios in the 10276 *bipD*::pDM4/10276 *bsaZ*::pDM4 and 10276 Δ*bsaP*/10276 *bsaZ*::pDM4 data sets when compared with the 10276 WT/10276 *bsaZ*::pDM4 data set (Fig. 2*A*). A total of 26 proteins met the selection criteria and can be considered putative effectors (Table I). Of the 26 proteins there were strain-specific subsets, with eight proteins with high ratios in two of the data sets and three proteins with high ratios in all three (Fig. 2*B*). The three proteins that displayed high ratios in all three data sets, BopC, BopA, and BopE, are all known *B. pseudomallei* Type III secreted (T3S) effector proteins or predicted to be T3S proteins based on their T3SS-dependent secretion in a surrogate host system (25, 26, 31) (Fig. 2*B*). Of the 26 proteins, 20 were only found in the hypersecreting mutant strain samples and would not have been identified had our study focused solely on the study of the secreted proteins of the 10276 WT strain (Fig. 2*B*). Plotting the iTRAQ ratios of the 26 putative effector proteins against their *B. pseudomallei* K96243 genetic locus number, it is clear that there is a concentration of eight proteins with especially high ratios encoded within the annotated *bsa* T3SS locus on Chromosome 2 compared with that of the rest of the genome (Table I, Fig. 2*C*).

TABLE I

Candidate Bsa T3SS effector proteins identified by iTRAQ. The table lists proteins in either the 10276 WT, 10276 bipD::pDM4 or 10276 ΔbsaP culture supernatant samples that displayed protein abundance ratios (compared to the 10276 bsaZ::pDM4 mutant) higher than the calculated cut-off values for each comparison. The cut-off values were set at 1.56 for the 10276 WT/10276 bsaZ::pDM4 dataset, 1.79 for the 10276 bipD::pDM4/10276 bsaZ::pDM4 data set, and 1.46 for the 10276 ΔbsaP/10276 bsaZ::pDM4 data set, as described in "Experimental Procedures." Additional criteria for protein identification included the presence of at least two unique peptides with a MASCOT peptide score of ≥21 corresponding to a 95% confidence level. The proteins are listed in order of gene number with genes from Chromosome one listed first. Those proteins fulfilling the criteria for selection as candidate T3SS effector proteins are highlighted in the gray shaded boxes. Protein score refers to the adjusted sum of scores of the individual peptide scores as calculated by MASCOT. Number of unique peptides refers to the number of significant peptides specific to a protein used in quantification

NCBI Accession number	*B. pseudomallei* Gene Number	Gene Name	WT/ *bsaZ* (protein abundance ratio)	*bipD*/ *bsaZ* (protein abundance ratio)	*bsaP*/ *bsaZ* (protein abundance ratio)	Protein Score	Number of Unique Peptides	Percent Coverage
YP_107146.2	BPSL0520		1.147	1.688	1.553	558	4	19.12%
YP_107336.1	BPSL0707		1.342	1.022	1.585	2106	16	32.94%
YP_107998.1	BPSL1373		1.235	0.926	1.731	586	5	41.18%
YP_108518.1	BPSL1918	*infB*	1.201	1.600	1.653	115	2	2.87%
YP_108528.1	BPSL1929		1.274	1.966	0.869	79	2	15.22%
YP_108638.1	BPSL2041		1.118	0.789	1.762	138	2	2.11%
YP_109116.1	BPSL2520		1.208	3.113	1.100	39	2	8.59%
YP_109117.1	BPSL2521	*gyrA*	1.163	1.772	1.975	105	2	3.58%
YP_109599.1	BPSL3004	*rpmA*	1.027	2.120	1.858	345	2	32.18%
YP_109788.1	BPSL3194	*rplO*	0.986	1.889	1.922	350	5	36.81%
YP_109808.1	BPSL3214	*rpsJ*	1.009	1.799	1.339	87	3	18.45%
YP_109980.1	BPSL3388		1.226	1.831	1.083	69	2	5.54%
YP_110505.1	BPSS04833		0.959	1.258	1.495	123	2	6.25%
YP_110870.1	BPSS0860		1.462	1.995	2.198	10865	29	81.07%
YP_111077.1	BPSS1066		0.939	1.027	1.620	2043	2	37.99%
YP_111083.1	BPSS1072		0.932	1.186	1.471	773	11	33.33%
YP_111519.1	BPSS1512	*tssM*	1.416	2.868	2.486	6008	11	81.24%
YP_111522.1	BPSS1516	*bopC*	1.826	6.846	9.512	14429	38	47.62%
YP_111527.1	BPSS1521	*bprD*	1.088	4.387	13.419	1826	12	64.45%
YP_111530.1	BPSS1524	*bopA*	2.240	6.164	7.301	14932	43	77.39%
YP_111531.1	BPSS1525	*bopE*	3.219	6.118	6.233	8631	24	28.86%
YP_111534.1	BPSS1528	*bapA*	2.111	1.098	7.471	4148	21	35.81%
YP_111535.1	BPSS1529	*bipD*	5.946	0.635	3.373	1505	9	68.02%
YP_111537.1	BPSS1531	*bipC*	1.222	10.159	1.280	8921	23	69.19%
YP_111538.1	BPSS1532	*bipB*	2.156	12.914	1.267	13376	44	64.78%
YP_111561.1	BPSS1555		1.534	1.897	1.127	7757	27	83.80%

As expected we observed Bsa-dependent secretion of BopE in the 10276 WT strain that increased in 10726 *bipD::*pDM4 and 10276Δ*bsaP* strains, in full agreement with Western blot data (Fig. 1). BopC and BopA, the latter of which has only been proven to be secreted in a T3SS-dependent manner in EPEC, followed a similar pattern of secretion to BopE. Although both of the two putative translocator proteins, BipB and BipC, were secreted at higher levels in 10276 WT than 10276 *bsaZ::*pDM4, only BipB was secreted at levels above the cut-off ratio of 1.56. Similar to the effect of *Shigella ipaD* mutation, the mutation of *bipD* in *B. pseudomallei* 10276 caused an increase in secretion of both BipB and BipC into the supernatant compared with 10276 WT. Where 10276 *bipD::*pDM4 had increased ratios of the translocators, 10276Δ*bsaP* showed a decrease in ratios below that of 10276 WT in agreement with Western blot data (Fig. 1). This is further evidence that BsaP plays a similar role in *B. pseudomallei* to its homolog InvE in *Salmonella* as a "gatekeeper" protein. The only proven effector missing from this screen was CHBP, however this is not surprising as we have recently reported that the gene encoding CHBP, *bpss1385*, is absent from the genome of the *B. pseudomallei* 10276 strain used here (27).

Besides the needle tip protein BipD, both putative translocators BipB and BipC, BopA, BopC, and BopE, there are also two hypothetical proteins encoded within the *bsa* T3SS locus identified by the screen that have high iTRAQ ratios. The first, BapA (BPSS1528), is a predicted 880 amino acid protein with no conserved domains and homologs only in the closely related species *B. mallei* and *B. thailandensis*. Unlike the

ASBMB MOLECULAR & CELLULAR PROTEOMICS MCP

known effector proteins in the iTRAQ screen, although secretion of BapA appears to be Bsa-dependent in 10276 WT and the ratio increases in the 10276 Δ*bsaP* data set, it does not appear to be secreted abundantly by the 10276 *bipD::*pDM4 mutant. Interestingly, under the conditions used we did not detect BapB or BapC, which are encoded downstream of BapA in the same operon and predicted to be substrates of the T3SS (21).

The other candidate effector protein encoded in the *bsa* T3SS locus is BprD (BPSS1521), which is annotated as a hypothetical regulator (48). Predicted to be much smaller than BapA at 147aa, BprD is another protein with no known conserved domains and homologs that exist only within closely related *Burkholderia* species. The iTRAQ ratios suggest that it is not secreted at detectable levels by 10276 WT *B. pseudomallei*, but secreted by both 10276 *bipD::*pDM4 and 10276Δ*bsaP*, with the ratio of 13.4 in the 10276 Δ*bsaP*/10276 *bsaZ::*pDM4 data set being the highest of any protein described in this iTRAQ study.

Outside of the Bsa T3SS locus the remaining 18 proteins with high ratios are distributed across both *B. pseudomallei* chromosomes. One of the proteins encoded by a gene closely flanking the *bsa* locus is the virulence factor TssM (BPSS1512), which is known to be coregulated with the Bsa T3SS as well as secreted in a Type II-dependent manner (72).

Validation of iTRAQ Data by Analysis of the Secretion of Epitope-Tagged Candidate Effector Proteins—To confirm a number of targets are secreted in a Bsa-dependent manner, a number of candidates were selected and cloned into an inducible expression vector as in-frame C-terminal c-Myc tagged fusion proteins. The targets chosen were BprD, BapA, BPSS0860, BPSS1512, BopE, and BopA, as well as BPSS1916, a protein with a very high iTRAQ ratio in all strains that did not meet the initial selection criteria because of being quantified with only a single unique peptide. Targets were chosen to represent proteins with both high and low protein scores, high and low numbers of peptides, and to be encoded inside and outside of the *bsa* T3SS locus. The plasmids were transformed into strains 10276 WT, 10276 *bsaZ::*pDM4, 10276 *bipD::*pDM4 and 10276Δ*bsaP*, and bacterial supernatants were collected and assessed by Western blot for the presence of the tagged proteins using a c-Myc tag-specific polyclonal antibody. Initial studies in which BopE was cloned as a c-Myc fusion in the widely used shuttle vector pBHR1 under a constitutive chloramphenicol resistance gene promoter indicated that BopE-c-Myc was secreted in a BsaZ-independent manner, possibly owing to the high level of expression (data not shown). We therefore elected to clone effector-c-Myc fusions under an IPTG-inducible promoter in pME6032 and select inducer levels at which strict BsaZ-dependent BopE-c-Myc secretion was observed (Fig. 3). BopA-c-Myc was absent in the supernatant of the 10276 *bsaZ::*pDM4 strain, but secreted by the parent strain and secreted at elevated levels by 10276Δ*bsaP* (Fig. 3), confirming for the first time in *B. pseudomallei* that it is a substrate

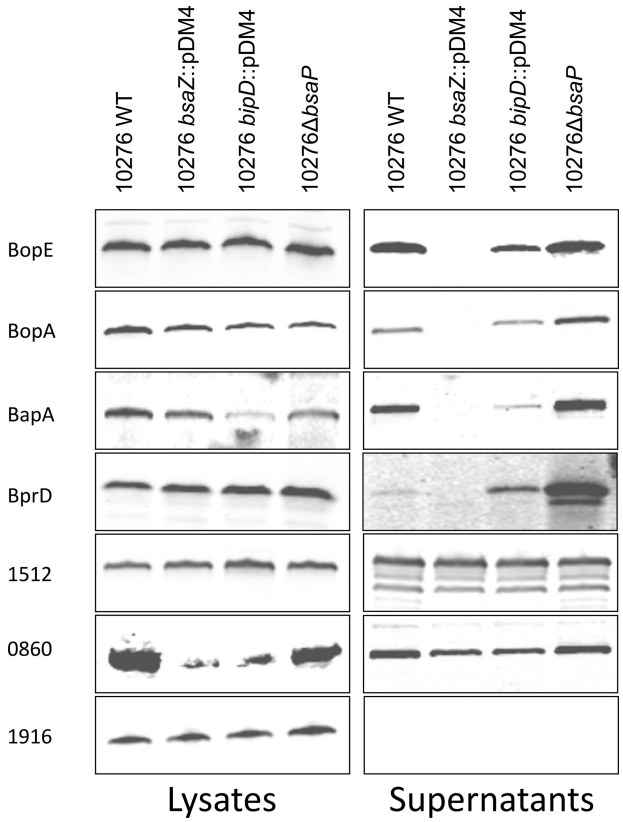


FIG. 3. **Western blot analysis of the expression and secretion of putative *B. pseudomallei* Bsa T3SS effector proteins expressed as c-Myc tagged fusion proteins.** The coding region of *bopE*, *bopA*, BPSS0860, BPSS1512, BPSS1916, *bprD*, and *bapA* were expressed with a c-terminal c-Myc tag in the IPTG-inducible expression vector pME6032 in *B. pseudomallei* strains 10276 WT, 10276 *bsaZ*::pDM4, 10276 *bipD*::pDM4 or 10276 Δ*bsaP*. Supernatant and whole cell fractions were collected after 6 h of incubation at 37 °C in the presence of 0.5 mM IPTG. Equal quantities of protein were separated by reducing SDS-PAGE, blotted onto nitrocellulose membranes and probed using polyclonal rabbit α-c-Myc antibody.

of the Bsa T3SS, not just the locus of enterocyte effacement-encoded T3SS in EPEC (31). Furthermore, both of the putative effector proteins located within the *bsa* locus, BprD-c-Myc and BapA-c-Myc, were secreted in a BsaZ-dependent manner (Fig. 3), confirming that these are novel effectors of the Bsa apparatus.

Interestingly, we were unable to validate Bsa-dependent secretion of proteins encoded outside of the Bsa T3SS locus. BPSS0860 and BPSS1512 appeared in the supernatants of all strains, including 10276 *bsaZ::*pDM4, indicating that although they are secreted, the Bsa system is not required for their secretion (Fig. 3). Secretion of the protein BPSS1916 could not be detected in any of the strains tested (Fig. 3). These examples highlight the need for independent validation of such data sets.

DISCUSSION

B. pseudomallei is an important cause of invasive clinical disease in South-East Asia and Northern Australia and its

potential as a bioterrorism agent is cause for concern. One of the known virulence factors that is important for invasion, intracellular net replication and virulence in mice is the Bsa T3SS (21–24), but the repertoire of effector proteins secreted by the system has not yet been fully characterized. To establish a better understanding of the Bsa T3SS, we made mutations in key structural components shown to dysregulate other T3SSs. We show these mutations lead to hypersecretion of known effector proteins. Using these mutants we have performed a quantitative proteomic analysis of the total secretome of the Bsa T3SS system. This iTRAQ analysis identified all known effector proteins and translocators present in *B. pseudomallei* 10276, as well as identifying a number of novel putative effector proteins, two of which were independently validated. Also, examining the changes in the abundance of effectors and translocators secreted by the different mutants provides insight into the role the proteins likely play in the temporal regulation of the Bsa T3SS compared with other T3SSs of other Gram-negative bacteria.

The inability of previous proteomics studies to identify known Bsa T3SS effectors highlights the need for the use of more sensitive techniques such as iTRAQ in combination with genetic dysregulation. The *B. pseudomallei* secretome is very complex (supplemental Table S4, supplemental Fig. S3). This is not surprising when taking into account the large 7.2 Mb genome (68), which encodes ~5900 proteins, of which over 55% are expressed in LB (73). This study produced one of the most comprehensive secretomes of *B. pseudomallei* to date, identifying a core secretome of 426 proteins secreted under standard laboratory conditions.

Although known effectors were absent from the secreted proteome of the *bsaZ* mutant by Western blotting (Fig. 1) and largely undetectable by iTRAQ (Table I) implying a lack of cell lysis, we detected a number of ribosomal proteins that are enriched in the supernatant when compared with the supernatant harvested from the 10276 *bsaZ::*pDM4 strain. This observation has been made in several other proteomic screens of T3SS effector repertoires (50, 74–76) and may be because of a combination of the high abundance of ribosomal proteins in the bacterial cell coupled with the sensitivity of iTRAQ.

Concurrent to this study, a proteome analysis investigating Type II secreted proteins of *B. pseudomallei* strain MSHR688 was published (72). From our screen, 27 of the 38 proteins identified as being substrates of Type II secretion in LB by Burtnick *et al.* (72) were also identified in our *B. pseudomallei* 10276 culture supernatants. Whether all 38 Type II secreted proteins identified in *B. pseudomallei* MSHR688 are encoded by *B. pseudomallei* 10276 is unknown because the genome sequence for *B. pseudomallei* 10726 is not yet available. Interestingly, three of the Type II secreted proteins were enriched in the supernatants of the hypersecreting mutants (BPSL0707, BPSS1512, BPSS1555) and two of the proteins are encoded by regions flanking the *bsa* T3SS locus, BPSS1512 and BPSS1555. The deubiquitinase BPSS1512 (TssM) has been shown to be secreted inside host cells where it suppresses the host innate immune response (77, 78). Although TssM is secreted independently of the Bsa T3SS, its expression appears to be coregulated with the Bsa T3SS and T6SS-5 (78, 79). This coregulation may explain the increased levels of TssM in the supernatants of the hypersecreting mutants in this study and again highlights the importance of validating candidate effector proteins.

The profile of secreted proteins encoded within the *bsa* T3SS locus provides a comprehensive picture of the secreted levels of the three known effector proteins. The profiles of both BopE and BopC in the iTRAQ screen correspond with previous studies in which they were shown to be secreted in a Bsa-dependent manner (25, 26). Although BopA has been shown to be Type 3 secreted in a surrogate host (31), we have confirmed its secretion to be dependent on the Bsa T3SS in *B. pseudomallei* and not one of the other T3SSs.

Two of the putative Bsa T3SS substrates encoded by the *bsa* T3SS locus (BapA and BprD) were validated as Bsa-dependent by Western blotting for a C-terminal c-Myc tag. Although the function of BapA is currently unknown, a *bapA* insertion mutation was not attenuated in a Syrian hamster model of acute melioidosis (23). BprD was previously annotated as a transcriptional regulator (48). In a previous study, when *bprD* was deleted along with *bprB* and *bprC*, there was no change in levels of transcription of other Bsa T3SS genes leaving the role of BprD as a regulator in doubt (48). More recently, a *bprD* mutant of *B. pseudomallei* K96243 was shown to have increased expression of *bprC* (80), a downstream gene in the same operon shown to be involved in regulation of the virulence-associated T6SS (81). The *bprD* mutant also showed decreased time to death in intraperitoneally inoculated BALB/c mice demonstrating its importance *in vivo* and indicating its possible role as a negative regulator of virulence (80). It is not without precedent that a regulator of the T3SS is also a substrate for secretion (*e.g.* LcrQ of *Yersinia*) (82).

Another candidate protein identified in this study, BPSS0860, appears to be a *fliD* homolog. There is a second copy of *fliD* (BPSL3320) located within the flagellar locus on Chromosome 1, which had protein abundance ratios that were similar between all strains. Interestingly, the expression of BPSL3320 was up-regulated, whereas the expression of BPSS0860 was down-regulated in the organs of hamsters infected by *B. pseudomallei* when compared with bacteria grown *in vitro* (83). Using our c-Myc expression system we were unable to establish Bsa-dependent secretion of BPSS0860; however, it is possible it may be coregulated with the Bsa T3SS in a similar manner to BPSS1512. One recent study has shown an effector protein may be secreted by more than one secretion system, thereby masking its secretion by the T3SS (84). This could also be the case for BPSS0860.

ASBMB MOLECULAR & CELLULAR PROTEOMICS MCP

At the time of writing, little is known about the post-translational control of the Bsa T3SS. Generally it is accepted that T3SSs are under tight temporal regulation to ensure substrates are secreted in the correct order (17). This starts with assembly of the membrane-associated structural components, assembly of the needle with needle tip, secretion of translocators to form a pore in the host cell membrane, followed by secretion of effector proteins. Changes in the patterns of secreted translocators and effector proteins in different mutant strains can inform us of the possible role these proteins play in the hierarchy of secretion.

Inactivation of the needle tip protein of *B. pseudomallei*, BipD, shows a large increase of levels of both translocators and effectors in the culture supernatant, in agreement with data published for the homologous *Shigella* protein IpaD (46, 52). IpaD is the needle cap protein, acting to block secretion of effector proteins until host cell contact has taken place (85). Because of its high similarity in both sequence and structure (53) it is perhaps unsurprising that BipD would have a similar effect on the levels of substrates secreted by the Bsa T3SS. Interestingly there was a high ratio of BipB, but not BipC in the WT *B. pseudomallei* 10276 strain culture supernatant compared with 10276 *bsaZ::*pDM4 (Table I). In *Shigella*, IpaB is present in the needle tip in complex with IpaD, whereas IpaC is secreted later, only upon host cell contact or activation (86). With this in mind it is possible that growth in LB lacks the stimuli required for BipC secretion in WT *B. pseudomallei* 10276.

Here we present evidence that BsaP functions as a "gatekeeper" protein for effectors in a manner similar to the homologous T3SS proteins InvE/SepL/MxiC/YopN-TyeA (54–60). Members of this family of proteins function differently from each other, but are all thought to be important in allowing effectors to be secreted by the mature T3SS. Here we show that deletion of *bsaP* creates a phenotype in which effector proteins are hypersecreted and levels of translocators decrease. To fully understand BsaP in the context of the other members of the "gatekeeper" family of proteins, more work would be required to determine the molecular interactions of BsaP with other components of the Bsa T3SS.

This study is another example of the power of a combination of classic targeted mutagenesis and a gel-free quantitative proteomics approach, such as iTRAQ, to study a complex secretion system, providing insights into the involvement of certain proteins on the regulation of the T3SS itself. Two new substrates of the Bsa T3SS were revealed by the study, confirming the effector repertoire is more complex than reported so far.

Acknowledgments—We thank, from Dundee Cell Products, Paul Ajuh for technical advice, Cristina Vazquez-Martin and Amy Wheat for help with MS. We would also like to thank Andy Gill and Dominic Kurian at The Roslin Institute for their kind advice. This work was supported by Institute Strategic Grant funding from the BBSRC. The mass spectrometry proteomics data have been deposited to the ProteomeXchange Consortium (87) via the PRIDE partner repository with the data set identifier PXD001656 and 10.6019/PXD001656.

[S] This article contains supplemental Figs. S1 to S5 and Tables S1 to S4.

¶ To whom correspondence should be addressed: Department of Infection and Immunity, The Roslin Institute, University of Edinburgh Easter Bush, Edinburgh, Midlothian EH25 9RG, United Kingdom. Tel.: 44-(0)131-6519100; Fax: +44 131 651 9105; E-mail: jo.stevens@roslin.ed.ac.uk.

REFERENCES

1. Strauss, J., Groves, M., Mariappan, M., and Ellison, D. W. (1969) Melioidosis in Malaysia II. Distribution of *Pseudomonas pseudomallei* in soil and surface water. *Am. J. Trop. Med. Hyg.* **18**, 698–702
2. Currie, B. J., Ward, L., and Cheng, A. C. (2010) The epidemiology and clinical spectrum of melioidosis: 540 cases from the 20 year Darwin prospective study. *PLoS Negl. Trop. Dis.* **4,** e900
3. Wiersinga, W. J., Currie, B. J., and Peacock, S. J. (2012) Melioidosis. *N. Engl. J. Med.* **367,** 1035–1044
4. Limmathurotsakul, D., Wongratanacheewin, S., Teerawattanasook, N., Wongsuvan, G., Chaisuksant, S., Chetchotisakd, P., Chaowagul, W., Day, N. P. J., and Peacock, S. J. (2010) Increasing incidence of human melioidosis in Northeast Thailand. *Am. J. Trop. Med. Hyg.* **82,** 1113–1117
5. Wiersinga, W. J., van der Poll, T., White, N. J., Day, N. P., and Peacock, S. J. (2006) Melioidosis: insights into the pathogenicity of *Burkholderia pseudomallei*. *Nat. Rev. Microbiol.* **4,** 272–282
6. Jones, A. L., Beveridge, T. J., and Woods, D. E. (1996) Intracellular survival of *Burkholderia pseudomallei*. *Infect. Immun.* **64,** 782–790
7. Stevens, M. P., Stevens, J. M., Jeng, R. L., Taylor, L. A., Wood, M. W., Hawes, P., Monaghan, P., Welch, M. D., and Galyov, E. E. (2005) Identification of a bacterial factor required for actin-based motility of *Burkholderia pseudomallei*. *Mol. Microbiol.* **56,** 40–53
8. Kespichayawattana, W., Rattanachetkul, S., Wanun, T., Utaisincharoen, P., and Sirisinha, S. (2000) *Burkholderia pseudomallei* induces cell fusion and actin-associated membrane protrusion: a possible mechanism for cell-to-cell spreading. *Infect. Immun.* **68,** 5377–5384
9. Schwarz, S., West, T. E., Boyer, F., Chiang, W.-C., Carl, M. A., Hood, R. D., Rohmer, L., Tolker-Nielsen, T., Skerrett, S. J., and Mougous, J. D. (2010) *Burkholderia* type VI secretion systems have distinct roles in eukaryotic and bacterial cell interactions. *PLoS Pathog.* **6**, e1001068
10. French, C. T., Toesca, I. J., Wu, T.-H., Teslaa, T., Beaty, S. M., Wong, W., Liu, M., Schröder, I., Chiou, P.-Y., Teitell, M. A., and Miller, J. F. (2011) Dissection of the *Burkholderia* intracellular life cycle using a photothermal nanoblade. *Proc. Natl. Acad. Sci. U.S.A.* **108,** 12095–12100
11. Schwarz, S., Singh, P., Robertson, J. D., LeRoux, M., Skerrett, S. J., Goodlett, D. R., West, T. E., and Mougous, J. D. (2014) VgrG-5 is a *Burkholderia* type VI secretion system-exported protein required for multinucleated giant cell formation and virulence. *Infect. Immun.* **82,** 1445–1452
12. Toesca, I. J., French, C. T., and Miller, J. F. (2014) The Type VI secretion system spike protein VgrG5 mediates membrane fusion during intercellular spread by *Pseudomallei* group *Burkholderia* species. *Infect. Immun.* **82,** 1436–1444
13. Galán, J. E., and Curtiss, R. (1989) Cloning and molecular characterization of genes whose products allow *Salmonella typhimurium* to penetrate tissue culture cells. *Proc. Natl. Acad. Sci. U.S.A.* **86,** 6383–6387
14. Maurelli, A. T., Baudry, B., D'Hautevil, H., Hale, T. L., and Sansonettil, P. J. (1985) Cloning of plasmid DNA sequences involved in invasion of HeLa cells by *Shigella flexneri*. *Infect. Immun.* **49,** 164–171
15. Gemski, P., Lazere, J. R., Casey, T., and Wohlhieter, J. A. (1980) Presence of a virulence-associated plasmid in *Yersinia pseudotuberculosis*. *Infect. Immun.* **28,** 1044–1047
16. Jarvis, K. G., Girón, J. a, Jerse, a E., McDaniel, T. K., Donnenberg, M. S., and Kaper, J. B. (1995) Enteropathogenic *Escherichia coli* contains a putative type III secretion system necessary for the export of proteins involved in attaching and effacing lesion formation. *Proc. Natl. Acad. Sci. U.S.A.* **92,** 7996–8000
17. Büttner, D. (2012) Protein export according to schedule: architecture, assembly, and regulation of type III secretion systems from plant- and

animal-pathogenic bacteria. *Microbiol. Mol. Biol. Rev.* **76,** 262–310
18. Dean, P. (2011) Functional domains and motifs of bacterial type III effector proteins and their roles in infection. *FEMS Microbiol. Rev.* **35,** 1100–1125
19. Rainbow, L., Hart, C. A., and Winstanley, C. (2002) Distribution of type III secretion gene clusters in *Burkholderia pseudomallei, B. thailandensis*, and *B. mallei. J. Med. Microbiol.* **51**, 374–384
20. Winstanley, C., Hales, B., and Hart, C. (1999) Evidence for the presence in *Burkholderia pseudomallei* of a type III secretion system-associated gene cluster. *J. Med. Microbiol.* **48,** 649–656
21. Stevens, M. P., Wood, M. W., Taylor, L. A., Monaghan, P., Hawes, P., Jones, P. W., Wallis, T. S., and Galyov, E. E. (2002) An Inv/Mxi-Spa-like type III protein secretion system in *Burkholderia pseudomallei* modulates intracellular behavior of the pathogen. *Mol. Microbiol.* **46,** 649–659
22. Stevens, M. P., Haque, A., Atkins, T., Hill, J., Wood, M. W., Easton, A., Nelson, M., Underwood-Fowler, C., Titball, R. W., Bancroft, G. J., and Galyov, E. E. (2004) Attenuated virulence and protective efficacy of a *Burkholderia pseudomallei bsa* type III secretion mutant in murine models of melioidosis. *Microbiology* **150,** 2669–2676
23. Warawa, J., and Woods, D. E. (2005) Type III secretion system cluster 3 is required for maximal virulence of *Burkholderia pseudomallei* in a hamster infection model. *FEMS Microbiol. Lett.* **242,** 101–108
24. Burtnick, M. N., Brett, P. J., Nair, V., Warawa, J. M., Woods, D. E., and Gherardini, F. C. (2008) *Burkholderia pseudomallei* type III secretion system mutants exhibit delayed vacuolar escape phenotypes in RAW 264.7 murine macrophages. *Infect. Immun.* **76,** 2991–3000
25. Muangman, S., Korbsrisate, S., Muangsombut, V., Srinon, V., Adler, N. L., Schroeder, G. N., Frankel, G., and Galyov, E. E. (2011) BopC is a type III secreted effector protein of *Burkholderia pseudomallei. FEMS Microbiol. Lett.* **323,** 75–82
26. Stevens, M. P., Friebel, A., Taylor, L. A., Wood, M. W., Brown, P. J., Hardt, W.-D., and Galyov, E. E. (2003) A *Burkholderia pseudomallei* type III secreted protein, BopE, facilitates bacterial invasion of epithelial cells and exhibits guanine nucleotide exchange factor activity. *J. Bacteriol.* **185**, 4992–4996
27. Pumirat, P., Broek, C. Vander, Juntawieng, N., Muangsombut, V., Kiratisin, P., Pattanapanyasat, K., Stevens, J. M., Stevens, M. P., and Korbsrisate, S. (2014) Analysis of the prevalence, secretion, and function of a cell cycle-inhibiting factor in the melioidosis pathogen *Burkholderia pseudomallei. PLoS One* **9,** e96298
28. Srinon, V., Muangman, S., Imyaem, N., Muangsombut, V., Lazar Adler, N. R., Galyov, E. E., and Korbsrisate, S. (2013) Comparative assessment of the intracellular survival of the *Burkholderia pseudomallei bopC* mutant. *J. Microbiol.* **51,** 522–526
29. Marchès, O., Ledger, T. N., Boury, M., Ohara, M., Tu, X., Goffaux, F., Mainil, J., Rosenshine, I., Sugai, M., De Rycke, J., and Oswald, E. (2003) Enteropathogenic and enterohaemorrhagic *Escherichia coli* deliver a novel effector called Cif, which blocks cell cycle G2/M transition. *Mol. Microbiol.* **50,** 1553–1567
30. Gong, L., Cullinane, M., Treerat, P., Ramm, G., Prescott, M., Adler, B., Boyce, J. D., and Devenish, R. J. (2011) The *Burkholderia pseudomallei* type III secretion system and BopA are required for evasion of LC3-associated phagocytosis. *PLoS One* **6,** e17852
31. Whitlock, G. C., Estes, D. M., Young, G. M., Young, B., and Torres, A. G. (2008) Construction of a reporter system to study *Burkholderia mallei* type III secretion and identification of the BopA effector protein function in intracellular survival. *Trans. R. Soc. Trop. Med. Hyg.* **102**, S127-S133
32. Dean, P., and Kenny, B. (2009) The effector repertoire of enteropathogenic E. coli: ganging up on the host cell. *Curr. Opin. Microbiol.* **12,** 101–109
33. Suwannasaen, D., Mahawantung, J., Chaowagul, W., Limmathurotsakul, D., Felgner, P. L., Davies, H., Bancroft, G. J., Titball, R. W., and Lertmemongkolchai, G. (2011) Human immune responses to *Burkholderia pseudomallei* characterized by protein microarray analysis. *J. Infect. Dis.* **203,** 1002–1011
34. Tippayawat, P., Pinsiri, M., Rinchai, D., Riyapa, D., Romphruk, A., Gan, Y.-H., Houghton, R. L., Felgner, P. L., Titball, R. W., Stevens, M. P., Galyov, E. E., Bancroft, G. J., and Lertmemongkolchai, G. (2011) *Burkholderia pseudomallei* proteins presented by monocyte-derived dendritic cells stimulate human memory T cells *in vitro*. *Infect. Immun.* **79,** 305–313
35. Felgner, P. L., Kayala, M. A., Vigil, A., Burk, C., Nakajima-Sasaki, R., Pablo, J., Molina, D. M., Hirst, S., Chew, J. S. W., Wang, D., Tan, G., Duffield, M., Yang, R., Neel, J., Chantratita, N., Bancroft, G., Lertmemongkolchai, G., Davies, D. H., Baldi, P., Peacock, S., and Titball, R. W. (2009) A *Burkholderia pseudomallei* protein microarray reveals serodiagnostic and cross-reactive antigens. *Proc. Natl. Acad. Sci. U.S.A.* **106,** 13499–13504
36. Tippayawat, P., Saenwongsa, W., Mahawantung, J., Suwannasaen, D., Chetchotisakd, P., Limmathurotsakul, D., Peacock, S. J., Felgner, P. L., Atkins, H. S., Titball, R. W., Bancroft, G. J., and Lertmemongkolchai, G. (2009) Phenotypic and functional characterization of human memory T cell responses to *Burkholderia pseudomallei. PLoS Negl. Trop. Dis.* **3,** e407
37. Heine, S. J., Diaz-McNair, J., Martinez-Becerra, F. J., Choudhari, S. P., Clements, J. D., Picking, W. L., and Pasetti, M. F. (2013) Evaluation of immunogenicity and protective efficacy of orally delivered *Shigella* type III secretion system proteins IpaB and IpaD. *Vaccine* **31,** 2919–2929
38. Martinez-Becerra, F. J., Kissmann, J. M., Diaz-McNair, J., Choudhari, S. P., Quick, A. M., Mellado-Sanchez, G., Clements, J. D., Pasetti, M. F., and Picking, W. L. (2012) Broadly protective *Shigella* vaccine based on type III secretion apparatus proteins. *Infect. Immun.* **80,** 1222–1231
39. Williamson, E. D., Eley, S. M., Stagg, A. J., Green, M., Russell, P., and Titball, R. W. (1997) A subunit vaccine elicits IgG in serum, spleen cell cultures and bronchial washings and protects immunized animals against pneumonic plague. *Vaccine* **15,** 1079–1084
40. Cornelius, C. A., Quenee, L. E., Overheim, K. A., Koster, F., Brasel, T. L., Elli, D., Ciletti, N. A., and Schneewind, O. (2008) Immunization with recombinant V10 protects cynomolgus macaques from lethal pneumonic plague. *Infect. Immun.* **76,** 5588–5597
41. Kurtz, J. R., Petersen, H. E., Frederick, D. R., Morici, L. A., and McLachlan, J. B. (2014) Vaccination with a single CD4 T cell peptide epitope from a *Salmonella* type III-secreted effector protein provides protection against lethal infection. *Infect. Immun.* **82,** 2424–2433
42. Lee, V. T., Mazmanian, S. K., and Schneewind, O. (2001) A program of *Yersinia enterocolitica* type III secretion reactions is activated by specific signals. *J. Bacteriol.* **183,** 4970–4978
43. Olive, A. J., Kenjale, R., Espina, M., Moore, D. S., Picking, W. L., and Picking, W. D. (2007) Bile salts stimulate recruitment of IpaB to the *Shigella flexneri* surface, where it colocalizes with IpaD at the tip of the type III secretion needle. *Infect. Immun.* **75,** 2626–2629
44. Michiels, T., Wattiau, P., Brasseur, R., Ruysschaert, J. M., and Cornelis, G. (1990) Secretion of Yop proteins by *Yersiniae. Infect. Immun.* **58,** 2840–2849
45. Forsberg, Å., and Wolf-Watz, H. (1988) The virulence protein Yop5 of *Yersinia pseudotuberculosis* is regulated at transcriptional level by plasmid-*pIB1*-encoded *trans*-acting elements controlled by temperature and calcium. *Mol. Microbiol.* **2,** 121–133
46. Parsot, C., Ménard, R., Gounon, P., and Sansonetti, P. J. (1995) Enhanced secretion through the *Shigella flexneri* Mxi-Spa translocon leads to assembly of extracellular proteins into macromolecular structures. *Mol. Microbiol.* **16,** 291–300
47. Jamison, W. P., and Hackstadt, T. (2008) Induction of type III secretion by cell-free *Chlamydia trachomatis* elementary bodies. *Microb. Pathog.* **45,** 435–440
48. Sun, G. W., Chen, Y., Liu, Y., Tan, G.-Y. G., Ong, C., Tan, P., and Gan, Y.-H. (2010) Identification of a regulatory cascade controlling Type III Secretion System 3 gene expression in *Burkholderia pseudomallei. Mol. Microbiol.* **76,** 677–689
49. Pumirat, P., Saetun, P., Sinchaikul, S., Chen, S.-T., Korbsrisate, S., and Thongboonkerd, V. (2009) Altered secretome of *Burkholderia pseudomallei* induced by salt stress. *Biochim. Biophys. Acta* **1794,** 898–904
50. Deng, W., Yu, H. B., de Hoog, C. L., Stoynov, N., Li, Y., Foster, L. J., and Finlay, B. B. (2012) Quantitative proteomic analysis of type III secretome of enteropathogenic *Escherichia coli* reveals an expanded effector repertoire for attaching/effacing bacterial pathogens. *Mol. Cell. Proteomics* **11,** 692–709
51. Deng, W., de Hoog, C. L., Yu, H. B., Li, Y., Croxen, M. A., Thomas, N. A., Puente, J. L., Foster, L. J., and Finlay, B. B. (2010) A comprehensive proteomic analysis of the type III secretome of *Citrobacter rodentium. J. Biol. Chem.* **285,** 6790–6800
52. Picking, W. L., Nishioka, H., Hearn, P. D., Baxter, M. A., Harrington, A. T., Blocker, A., and Picking, W. D. (2005) IpaD of *Shigella flexneri* is independently required for regulation of Ipa protein secretion and efficient insertion of IpaB and IpaC into host membranes. *Infect. Immun.* **73,** 1432–1440

53. Erskine, P. T., Knight, M. J., Ruaux, A., Mikolajek, H., Wong Fat Sang, N., Withers, J., Gill, R., Wood, S. P., Wood, M., Fox, G. C., and Cooper, J. B. (2006) High resolution structure of BipD: an invasion protein associated with the type III secretion system of *Burkholderia pseudomallei. J. Mol. Biol.* **363,** 125–136
54. Kubori, T., and Galán, J. E. J. (2002) *Salmonella* type III secretion-associated protein InvE controls translocation of effector proteins into host cells. *J. Bacteriol.* **184,** 4699–4708
55. Kresse, A., Beltrametti, F., and Müller, A. (2000) Characterization of SepL of enterohemorrhagic *Escherichia coli. J. Bacteriol.* **182,** 6490–6498
56. Deng, W., Puente, J. L., Gruenheid, S., Li, Y., Vallance, B. A., Vázquez, A., Barba, J., Ibarra, J. A., O'Donnell, P., Metalnikov, P., Ashman, K., Lee, S., Goode, D., Pawson, T., and Finlay, B. B. (2004) Dissecting virulence: systematic and functional analyses of a pathogenicity island. *Proc. Natl. Acad. Sci. U.S.A.* **101,** 3597–3602
57. Deng, W., Li, Y., Hardwidge, P. R., Elizabeth, A., Pfuetzner, R. A., Lee, S., Strynakda, N. C. J., Puente, J. L., Frey, E. A., Gruenheid, S., and Finlay, B. B. (2005) Regulation of type III secretion hierarchy of translocators and effectors in attaching and effacing bacterial pathogens. *Infect. Immun.* **73,** 2135–2146
58. Botteaux, A., Sory, M. P., Biskri, L., Parsot, C., and Allaoui, A. (2009) MxiC is secreted by and controls the substrate specificity of the *Shigella flexneri* type III secretion apparatus. *Mol. Microbiol.* **71,** 449–460
59. Forsberg, Å., Viitanen, A. M., Skurnik, M., and Wolf-Watz, H. (1991) The surface-located YopN protein is involved in calcium signal transduction in *Yersinia pseudotuberculosis. Mol. Microbiol.* **5,** 977–986
60. Iriarte, M., Sory, M. P., Boland, A., Boyd, A. P., Mills, S. D., Lambermont, I., and Cornelis, G. R. (1998) TyeA, a protein involved in control of Yop release and in translocation of *Yersinia* Yop effectors. *EMBO J.* **17,** 1907–1918
61. Allaoui, A., Woestyn, S., Sluiters, C., and Cornelis, G. R. (1994) YscU, a *Yersinia enterocolitica* inner membrane protein involved in Yop secretion. *J. Bacteriol.* **176,** 4534–4542
62. Logue, C.-A., Peak, I. R. A., and Beacham, I. R. (2009) Facile construction of unmarked deletion mutants in *Burkholderia pseudomallei* using *sacB* counter-selection in sucrose-resistant and sucrose-sensitive isolates. *J. Microbiol. Methods* **76,** 320–323
63. Ali, S., and Steinkasserer, A. (1995) PCR-ligation-PCR mutagenesis: a protocol for creating gene fusions and mutations. *BioTechniques* **18,** 746–750
64. Choi, K.-H., Kumar, A., and Schweizer, H. P. (2006) A 10-min method for preparation of highly electrocompetent *Pseudomonas aeruginosa* cells: application for DNA fragment transfer between chromosomes and plasmid transformation. *J. Microbiol. Methods* **64,** 391–397
65. Caldwell, R. B., and Lattemann, C. T. (2004) Simple and reliable method to precipitate proteins from bacterial culture supernatant. *Appl. Environ. Microbiol.* **70,** 610–612
66. Boisvert, F.-M., Lam, Y. W., Lamont, D., and Lamond, A. I. (2010) A quantitative proteomics analysis of subcellular proteome localization and changes induced by DNA damage. *Mol. Cell. Proteomics* **9,** 457–470
67. Olsen, J. V., de Godoy, L. M. F., Li, G., Macek, B., Mortensen, P., Pesch, R., Makarov, A., Lange, O., Horning, S., and Mann, M. (2005) Parts per million mass accuracy on an Orbitrap mass spectrometer via lock mass injection into a C-trap. *Mol. Cell. Proteomics* **4,** 2010–2021
68. Holden, M. T. G., Titball, R. W., Peacock, S. J., Cerdeño-Tárraga, A. M., Atkins, T., Crossman, L. C., Pitt, T., Churcher, C., Mungall, K., Bentley, S. D., Sebaihia, M., Thomson, N. R., Bason, N., Beacham, I. R., Brooks, K., Brown, K. A., Brown, N. F., Challis, G. L., Cherevach, I., Chillingworth, T., Cronin, A., Crossett, B., Davis, P., DeShazer, D., Feltwell, T., Fraser, A., Hance, Z., Hauser, H., Holroyd, S., Jagels, K., Keith, K. E., Maddison, M., Moule, S., Price, C., Quail, M. A., Rabbinowitsch, E., Rutherford, K., Sanders, M., Simmonds, M., Songsivilai, S., Stevens, K., Tumapa, S., Vesaratchavest, M., Whitehead, S., Yeats, C., Barrell, B. G., Oyston, P. C. F., and Parkhill, J. (2004) Genomic plasticity of the causative agent of melioidosis, *Burkholderia pseudomallei. Proc. Natl. Acad. Sci. U.S.A.* **101,** 14240–14245
69. Harding, S. V., Sarkar-Tyson, M., Smither, S. J., Atkins, T. P., Oyston, P. C. F., Brown, K. A., Liu, Y., Wait, R., and Titball, R. W. (2007) The identification of surface proteins of *Burkholderia pseudomallei. Vaccine* **25,** 2664–2672
70. Schell, M. a, Zhao, P., and Wells, L. (2011) Outer membrane proteome of *Burkholderia pseudomallei* and *Burkholderia mallei* from diverse growth conditions. *J. Proteome Res.* **10,** 2417–2424
71. Su, Y.-C., Wan, K.-L., Mohamed, R., and Nathan, S. (2008) A genome level survey of *Burkholderia pseudomallei* immunome expressed during human infection. *Microbes Infect.* **10,** 1335–1345
72. Burtnick, M. N., Brett, P. J., and DeShazer, D. (2014) Proteomic analysis of the *Burkholderia pseudomallei* type II secretome reveals hydrolytic enzymes, novel proteins, and the deubiquitinase TssM. *Infect. Immun.* **82,** 3214–3226
73. Ooi, W. F., Ong, C., Nandi, T., Kreisberg, J. F., Chua, H. H., Sun, G. W., Chen, Y., Mueller, C., Conejero, L., Eshaghi, M., Ang, R. M. L., Liu, J., Sobral, B. W., Korbsrisate, S., Gan, Y.-H., Titball, R. W., Bancroft, G. J., Valade, E., and Tan, P. (2013) The condition-dependent transcriptional landscape of *Burkholderia pseudomallei. PLoS Genet.* **9**, e1003795
74. Schumacher, J., Waite, C. J., Bennett, M. H., Perez, M. F., Shethi, K., and Buck, M. (2014) Differential secretome analysis of *Pseudomonas syringae pv tomato* using gel-free MS proteomics. *Front. Plant Sci.* **5,** 242
75. Kurushima, J., Kuwae, A., and Abe, A. (2012) The type III secreted protein BspR regulates the virulence genes in *Bordetella bronchiseptica. PLoS One* **7,** e38925
76. Vanden Bergh, P., Heller, M., Braga-Lagache, S., and Frey, J. (2013) The *Aeromonas salmonicida* subsp. *salmonicida* exoproteome: determination of the complete repertoire of Type-Three Secretion System effectors and identification of other virulence factors. *Proteome Sci.* **11,** 42
77. Shanks, J., Burtnick, M. N., Brett, P. J., Waag, D. M., Spurgers, K. B., Ribot, W. J., Schell, M. a, Panchal, R. G., Gherardini, F. C., Wilkinson, K. D., and Deshazer, D. (2009) *Burkholderia mallei* tssM encodes a putative deubiquitinase that is secreted and expressed inside infected RAW 264.7 murine macrophages. *Infect. Immun.* **77,** 1636–1648
78. Tan, K. S., Chen, Y., Lim, Y.-C., Tan, G.-Y. G., Liu, Y., Lim, Y.-T., Macary, P., and Gan, Y.-H. (2010) Suppression of host innate immune response by *Burkholderia pseudomallei* through the virulence factor TssM. *J. Immunol.* **184,** 5160–5171
79. Burtnick, M. N., Brett, P. J., Harding, S. V., Ngugi, S. A., Ribot, W. J., Chantratita, N., Scorpio, A., Milne, T. S., Dean, R. E., Fritz, D. L., Peacock, S. J., Prior, J. L., Atkins, T. P., and Deshazer, D. (2011) The cluster 1 type VI secretion system is a major virulence determinant in *Burkholderia pseudomallei. Infect. Immun.* **79,** 1512–1525
80. Chirakul, S., Bartpho, T., Wongsurawat, T., Taweechaisupapong, S., Karoonutaisiri, N., Talaat, A. M., Wongratanacheewin, S., Ernst, R. K., and Sermswan, R. W. (2014) Characterization of BPSS1521 (*bprD*), a regulator of *Burkholderia pseudomallei* virulence gene expression in the mouse model. *PLoS One* **9,** e104313
81. Chen, Y., Wong, J., Sun, G. W., Liu, Y., Tan, G.-Y. G., and Gan, Y.-H. (2011) Regulation of Type VI Secretion System during *Burkholderia pseudomallei* infection. *Infect. Immun.* **79,** 3064–3073
82. Cambronne, E. D., Cheng, L. W., and Schneewind, O. (2000) LcrQ/YscM1, regulators of the *Yersinia yop* virulon, are injected into host cells by a chaperone-dependent mechanism. *Mol. Microbiol.* **37,** 263–273
83. Tuanyok, A., Tom, M., Dunbar, J., and Woods, D. E. (2006) Genome-wide expression analysis of *Burkholderia pseudomallei* infection in a hamster model of acute melioidosis. *Infect. Immun.* **74,** 5465–5476
84. Neeld, D., Jin, Y., Bichsel, C., Jia, J., Guo, J., Bai, F., Wu, W., Ha, U.-H., Terada, N., and Jin, S. (2014) *Pseudomonas aeruginosa* injects NDK into host cells through a type III secretion system. *Microbiology* **160,** 1417–1426
85. Roehrich, A. D., Guillossou, E., Blocker, A. J., and Martinez-Argudo, I. (2013) *Shigella* IpaD has a dual role: signal transduction from the type III secretion system needle tip and intracellular secretion regulation. *Mol. Microbiol.* **87,** 690–706
86. Epler, C. R., Dickenson, N. E., Olive, A. J., Picking, W. L., and Picking, W. D. (2009) Liposomes recruit IpaC to the *Shigella flexneri* type III secretion apparatus needle as a final step in secretion induction. *Infect. Immun.* **77,** 2754–2761
87. Vizcaíno, J.A., Deutsch, E.W., Wang, R., Csordas, A., Reisinger, F., Ríos, D., Dianes, J.A., Sun, Z., Farrah, T., Bandeira, N., Binz, P.A., Xenarios, I., Eisenacher, M., Mayer, G., Gatto, L., Campos, A., Chalkley, R.J., Kraus, H.J., Albar, J.P., Martinez-Bartolomé, S., Apweiler, R., Omenn, G.S., Martens, L., Jones, A.R., Hermjakob, H. (2014) ProteomeXchange provides globally co-ordinated proteomics data submission and dissemination. *Nature Biotechnol.* **30,** 223–226

ASBMB MOLECULAR & CELLULAR PROTEOMICS MCP